ISOLATION OF BIOACTIVE CONSTITUENTS FROM SEEDS OF *SCHOTIA BRACHYPETALA* (FABACEAE) AND *COLOPHOSPERMUM MOPANE* (FABACEAE)

Kun Du

ISOLATION OF BIOACTIVE CONSTITUENTS FROM SEEDS OF *SCHOTIA BRACHYPETALA* (FABACEAE) AND *COLOPHOSPERMUM MOPANE* (FABACEAE)

Thesis submitted in fulfillment of the requirements for the degree of

MASTER OF SCIENCE

in the

Department of Chemistry

Faculty of Agricultural and Natural Science

at the

University of the Free State

Bloemfontein

by

Kun Du

Supervisor: Prof. Andrew Marston

Co-supervisor: Prof. Jan van der Westhuizen

November 2011

A part of this work has been published:

Marston A., Du K., Van Vuuren S.F., Van Zyl R.L., Zietsman P. (2011). Seeds from South African plants as a source of bioactive metabolites. *Planta Medica* **77**, 1336.

Parts of this work were reported at congresses as poster presentations:

1. Kun Du, Andrew Marston*, Sandy Van Vuuren, Robyn Van Zyl, Pieter Zietsman. (2011) Seeds from South African plants as a source of bioactive metabolites. IOCD Symposium, African Plants, Unique Sources of Drugs, Agrochemicals, Cosmetics and Food Supplements, 12th-15th January 2011, Cape Town, South Africa.

2. Kun Du, Andrew Marston*, Sandy Van Vuuren, Robyn Van Zyl, Pieter Zietsman. (2011) Seeds from South African plants as a source of bioactive metabolites. Indigenous Plant Use Forum, 4th-7th July 2011, St. Lucia, South Africa.

3. Kun Du, Andrew Marston*, Sandy Van Vuuren, Robyn Van Zyl, Pieter Zietsman. (2011) Seeds from South African plants as a source of bioactive metabolites. 59th International Congress and Annual Meeting of the Society for Medicinal Plant and Natural Product Research, 4th – 9th September 2011, Antalya, Turkey.

ACKNOWLEDGEMENTS

The present work was performed from January 2010 to August 2011 at the Department of Chemistry at the University of the Free State under the direction of Professor Andrew Marston. I wish to express my sincere gratitude to Prof. Andrew Marston as a supervisor for his guidance, assistance, patience, invaluable advice and supporting me during all the period of this thesis work.

I thank Prof. Jan van der Westhuizen (Organic Chemistry, University of the Free State) as a co-supervisor. I also thank Prof. Alvaro Viljoen (Department of Pharmaceutical Sciences, Tshwane University of Technology) and Prof. Liselotte Krenn (Department of Pharmacognosy, University of Vienna) for having accepted to be the examiners.

I am grateful to all my colleagues in the Chemistry Department for their help and kindness. In particular, I should thank Miss Rosinah Montsho for her help with NMR measurements and Mr. Pieter Venter for running mass spectra. My appreciation of other help I received and the friendship of all is just as profound

A number of persons have to be thanked for their precious help, without which this thesis would not have been possible.

First and foremost, thanks are due to Dr. Pieter Zietsman (National Museum, Bloemfontein, South Africa) for all his aid with collection and identification of plant material, and to Prof. Sandy Van Vuuren (Department of Pharmacy and Pharmacology, University of the Witwatersrand) for her considerable help in the running of antimicrobial tests. Prof. Robyn Van Zyl from the same department of the University of the Witwatersrand is also thanked for performing antimalarial testing.

High-resolution mass spectra of compounds **G** and **I** were kindly run by Dr. Paul Steenkamp at the CSIR in Pretoria.

The circular dichroism measurements for compound **F** were made by Prof. Daneel Ferreira and Dr. Christina Coleman at the Department of Pharmacognosy, University of Mississippi, USA.

The National Research Foundation is gratefully thanked for financing this research.

Finally, this work would not have been possible without the support of my family. They have always been the source of my motivation for work and study.

KUN DU

ABSTRACT

Natural products play an important role in drug discovery, as scaffolds and new skeletons. It is remarkable to note that in 2007, natural products were implicated in the development of 52% of all new drugs. These compounds give “smart structures” rather than a much larger random collection of assemblies, which results, for example, from combinatorial chemistry or computer modeling. As part of our natural heritage, higher plants are a potential source of millions of bioactive products with an almost infinite variety of different structural variations, and they represent an enormous store of valuable pharmacological molecules waiting to be discovered. South Africa is one of the richest centers of plant diversity in the world, thus providing a fantastic collection of natural products.

Of the different South African plant parts, seeds have been little studied from a chemical viewpoint but, in light of their function, may have interesting metabolites. Twenty-five species were collected based on a variety of information from traditional medicine, seed size and availability, and random collection. Seeds of trees were principally selected because these are often large and easier to handle. Extraction was with methanol, to minimize the quantity of oil in the sample. A total of 29 extracts were screened for biological activities.

The methanol extracts of the aril of *Schotia brachypetala* Sond. (Fabaceae) seeds, and the premature seeds of *Colophospermum mopane* (Kirk ex Benth.) J. Leonard (Fabaceae) were selected for further investigation since they had significant biological activities.

Fractionation and isolation were achieved mainly by using high-speed countercurrent chromatography. Biological assays, including free-radical scavenging activity, inhibition of acetylcholinesterase, antimicrobial and antimalarial testing, were used for activity-guided fractionation and for the activity assessment of extracts, fractions, and isolates. The structures of pure compounds were determined mainly by spectroscopic methods (UV, MS, NMR, CD) and some chemical methods. A total of 9 compounds were isolated from these two species, of which 2 were

new compounds. The principles responsible for the biological activities of the extracts were also identified.

From the methanol extract of the aril of *Schotia brachypetala*, 7 quercetin glucoside derivatives were isolated: 3-*O*-methylquercetin 7-*O*-*β*-glucopyranoside (**A**), 3,4′-di-*O*-methylquercetin 7-*O*-*β*-glucopyranoside (**B**), 3-*O*-methylquercetin 7-*O*-[*β*-D-6″(*E*-*p*-coumaroyl)glucopyranoside] (**C**), 3,4′-di-*O*-methylquercetin 7-*O*-[*β*-D-6″(*E*-*p*-coumaroyl)glucopyranoside] (**D**), quercetin 7-*O*-*β*-glucopyranoside (**E**), (*2R, 3R*)-dihydroquercetin 7-*O*-*β*-glucopyranoside (**F**) and quercetin 3-*O*-[2-*O*-*β*-xylopyranosyl-6-*O*-*α*-rhamnopyranosyl]-*β*-glucopyranoside (**G**). Five of them showed DPPH radical scavenging activity. One of the new compounds gave the strongest radical scavenging activity. The pure compounds **A** and **C** were also weakly active as antimalarials.

From the methanol extract of *Colophospermum mopane* premature seeds, two compounds were characterized. One was the sesquiterpene *β*-caryophyllene oxide (**I**) and one was a diterpenoid (**H**). The stereochemistry of the latter was analyzed with the help of NMR spectroscopy and, in particular, NOE experiments. The diterpenoid showed antimicrobial activity and potent acetylcholinesterase inhibition.

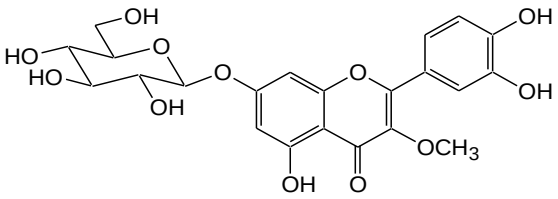

A

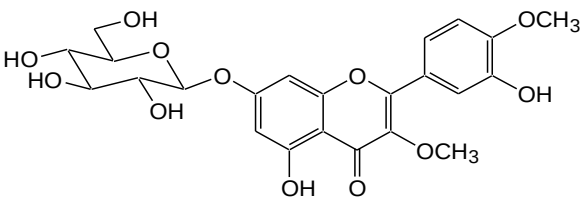

B

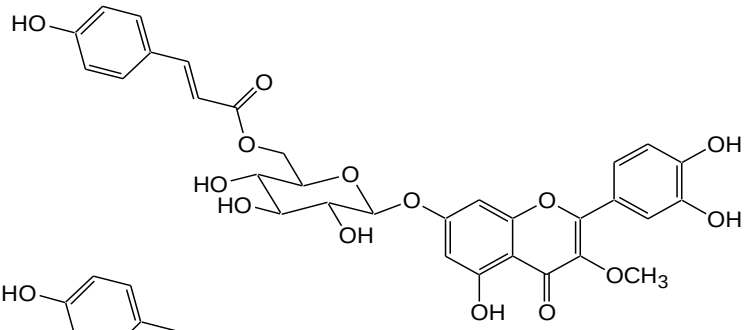

C

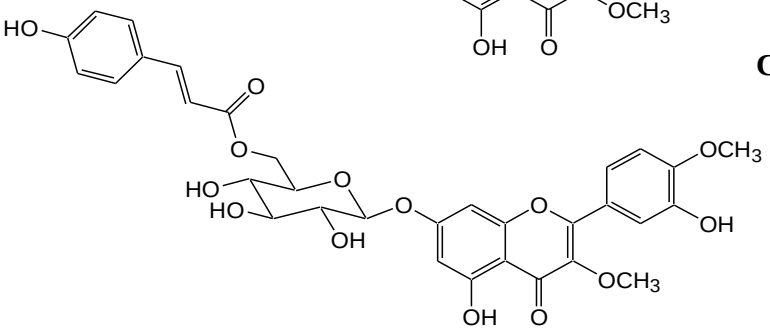

D

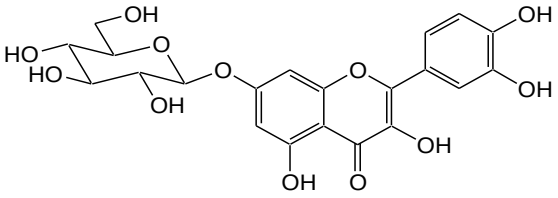

E

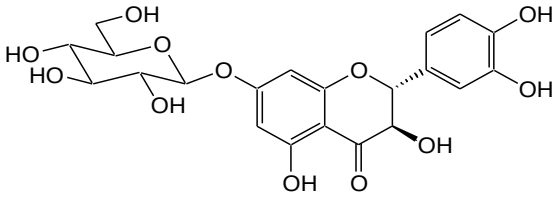

F

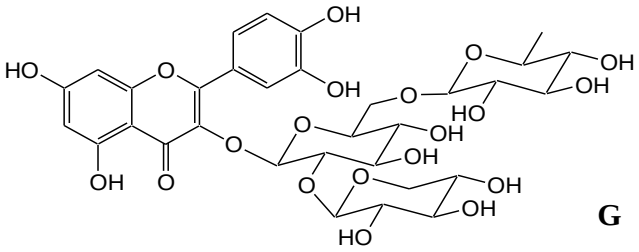

G

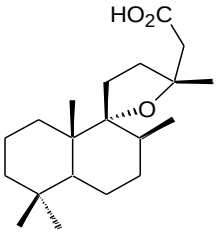

H

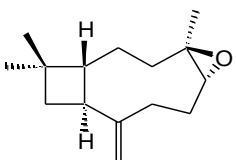

I

Key words: Seeds, *Schotia brachypetala*, *Colophospermum mopane*, Leguminosae, Fabaceae, Flavonol glycosides, Diterpene, Caryophyllene oxide, Antimalarials, Antimicrobials, Radical scavengers, Acetylcholinesterase inhibitors.

ABBREVIATIONS AND SYMBOLS

1, 2, 3, …	Symbols used for the compounds cited in the introduction
A, B, C, …	Symbols used for the isolates in this work
δ	Chemical Shift
ε	Molar Absorptivity (in UV spectrum)
λ	Wavelength
APT	Attached Proton Test
br s	Broad Singlet
CC	Column Chromatography
$CHCl_3$	Chloroform
COSY	^{1}H, ^{1}H Homonuclear Correlation Spectroscopy
d	Doublet
dd	Doublet of Doublets
DAD	Diode-Array Detector
DCM	Dichloromethane
DMSO	Dimethylsulphoxide
DPPH	1,1-Diphenyl-2-picrylhydrazyl
EtOAc	Ethyl Acetate
GHMBC	^{1}H, ^{13}C, Gradient Heteronuclear Multiple Bond Correlation
GHSQC	^{1}H, ^{13}C, Gradient Heteronuclear Single Quantum Coherence
Hz	Hertz
HPLC	High Performance Liquid Chromatography
HRAPCIMS	High Resolution Atmospheric Pressure Chemical Ionization Mass Spectrometry
HRESIMS	High Resolution Electrospray Ionization Mass Spectrometry
HSCCC	High-speed countercurrent chromatography
IR	Infrared Spectroscopy
J	Coupling Constant

LPLC	Low Pressure Liquid Chromatography
LRAPCIMS	Low Resolution Atmospheric Pressure Chemical Ionization Mass Spectrometry
LRESIMS	Low Resolution Electrospray Ionization Mass Spectrometry
m	Multiplets
MeCN	Acetonitrile
MeOH	Methanol
MIC	Minimal Inhibitory Concentration
m.p.	Melting Point
MS	Mass Spectrometry
MW	Molecular Weight
m/z	Mass per Electronic Charge
NOE	Nuclear Overhauser Effect
NOESY	Nuclear Overhauser Enhancement Spectroscopy
NMR	Nuclear Magnetic Resonance
ppm	Parts Per Million
sh	Shoulder (in UV spectrum)
sp.	Species (one)
spp.	Species (several)
subsp.	Subspecies
s	Singlet
t	Triplet
TBME	Tert-butylmethylether
TEAC	Trolox Equivalent Antioxidant Capacity
TFA	Trifluoroacetic Acid
TLC	Thin-Layer Chromatography
TMS	Tetramethylsilane
UV	Ultraviolet

TABLE OF CONTENTS

Table 1.1 The diagnostic characteristics of the three legume sub-families (Lewis *et al*., 2005).

Family LEGUMINOSAE		
CAESALPINIOIDEAE (4 TRIBES, 2,250 species)	MIMOSOIDEAE (4 TRIBES, 3,270 species)	PAPILIONOIDEAE (28 TRIBES, ca. 13,800 species)
Trees, shrubs, lianas	Trees, shrubs, lianas, rarely aquatic herbs	Herbs, shrubs, trees, lianas, twiners
Flowers relatively large	Small regular flowers aggregated into heads or spikes	Pea flowers,
Flowers generally zygomorphic	Flowers actinomorphic, radially symmetrical	Flowers zygomorphic
Petals imbricate in bud	Petals valvate in bud	Petals imbricate in bud
Median petal overlapped by others (when these present)	Median petal not overlapped by others, similar in shape and size	Median petal (standard, banner or vexilllum) overlaps others (these occationally absent)
Sepals generally free	Sepals (and petals) generally united at the base	Sepals united at base into a calyx tube
Seeds generally without pleurogram (if present this closed); also without a hilar groove	Seeds usually with open pleurogram	Seeds (if hard) with complex hilar valve (beans and peas); pleurogram absent
Embryo radicle usually straight	Embryo radicle usually straight	Embryo radicle usually curved
Leaves bipinnate or pinnate (rarely simple or 1-foliolate)	Leaves mainly bipinnate and often with specialized glands; Australian acacias have phyllodes	Leaves 1-foliolate to once pinnate (a few palmate); some with tendrils; only one rare species bipinnate
Stamens (1-) 10(-many); sometimes dimorphic or heteromorphic	Stamens (3-) 10-many (sometimes over 100); all the same	Stamens (9-) 10-many (sometimes dimorphic)
Petals most showy part	Stamens most showy part	Petals most showy part
Compound pollen (polyads) rare	Compound pollen (polyads) common	Pollen in single grains
Root nodules uncommon, but many associations with fungi	Root nodules generally present	Root nodules generally present

1. INTRODUCTION

1.1. Natural products as drug scaffolds

Natural products from plants, fungi, bacteria, protozoans, insects and animals have been used as biologically active pharmacophores (Strohl, 2000), which are applied extensively in the drug discovery and development process, particularly in the areas of cancer and infectious diseases (Cragg *et al*., 1997). As secondary metabolites are produced by organisms in response to external stimuli such as nutritional changes, infection and competition, the diversity of natural products is huge. In a review published in 2007 by Newman and Cragg, it is remarkable to note that natural products are implicated in the development of 52% of all new drugs. The authors introduce another sub-classification of drug origin called natural product mimics (NM), the compounds designed from the knowledge that is gained from natural products or discovered by using an assay in which a compound displaces the natural substrate in a competitive fashion (Figure 1.1). They also emphasized that although combinatorial chemistry techniques have succeeded as methods of optimizing structures, however, only one *de novo* combinatorial compound was approved as a drug between 1981 and 2006. The trend towards the synthesis of complex natural product-like libraries has continued (Newman and Cragg, 2007). A statistical analysis of compounds isolated from natural products and those derived by total synthesis employed in drug development has shown that a mere 90,000 known naturally occurring compounds contributed about 40% of the total possible new drug molecules, whereas the several millions of synthetic molecules accounted for the remaining 60%. (Muller, 2000) As was stated by Danishefsky in 2002, "*a small collection of smart compounds may be more valuable than a much larger hodgepodge collection mindlessly assembled*" (Borman, 2002).

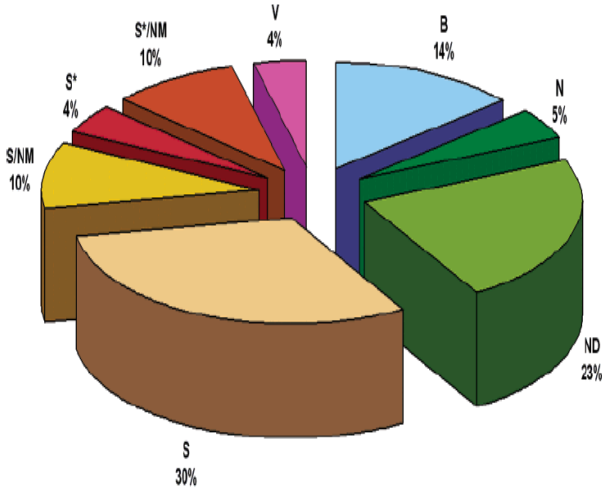

Figure 1.1 All new active substances (or new chemical entities), 01/1981- 06/2006, by source (N = 1184) "B" = Biological; usually a large (>45 residues) peptide or protein either isolated from an organism/cell line or produced by biotechnological means in a surrogate host. "N" = Natural product. "ND" derived from a natural product and is usually a semisynthetic modification. "S" = Totally synthetic drug, often found by random screening/modification of an existing agent. "S*" = made by total synthesis, but the pharmacophore is/was from a natural product. "V" = vaccine. "NM" = natural product mimic (Newman and Cragg, 2007).

1.2. Natural products derived from higher plants

Higher plants are a source of millions of natural products, with an almost infinite variety of different structural variations (Hostettmann *et al*., 2008). Among the ca. 400,000 plant species on the earth, only a small percentage has been phytochemically investigated and the fraction submitted to biological or pharmacological screening is even smaller. Moreover, a plant extract may contain several thousand different secondary metabolites and any phytochemical investigation of a given plant will reveal only a narrow spectrum of its constituents. The plant kingdom thus represents an enormous reservoir of pharmacologically valuable molecules to be discovered (Potterat and Hostettmann, 1995; Hamburger *et al*., 1991; Kinghorn *et al.*, 2011).

Classical examples of higher plant-derived drugs include the antimalarial agent quinine from the bark of *Cinchona officinalis* (Rubiaceae), the analgesic morphine and the well-known antitussive codeine from *Papaver somniferum* (Papaveraceae), atropine from *Atropa belladonna* and other Solanaceae species, and the cardiac glycoside digoxin from *Digitalis* spp.

(Scrophulariaceae) (Hostettmann and Marston, 2007).

Over the last few decades, there have also been remarkable examples of higher plant-derived drugs introduced in various therapeutic fields. The diterpenoid Paclitaxel (Figure 1.2), previously known as Taxol®, was isolated for the first time from the stem bark of the Pacific yew *Taxus brevifolia* (Taxaceae) in the late 1960s, and approved by the FDA in 1992. While Taxol® was initially used for the treatment of ovarian cancer resistant to chemotherapy, its therapeutic applications now include other gynecological cancers.

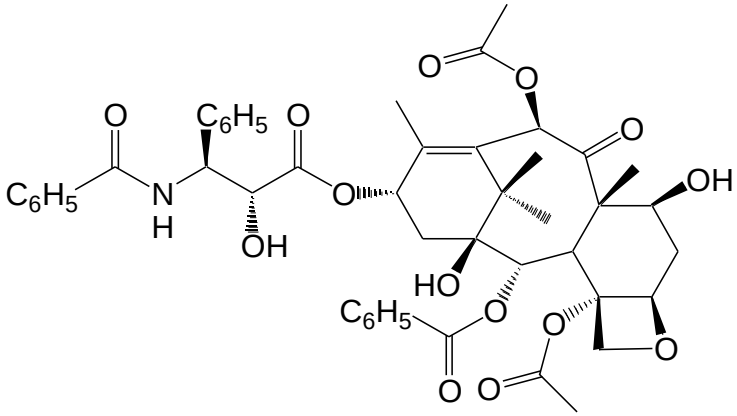

Figure 1.2 Paclitaxel.

Artemisinin (Figure 1.3), a sesquiterpene lactone containing an endoperoxide group, was isolated in 1972 from qinghao (*Artemisia annua*, Asteraceae) in China. It represents a completely new chemical class of antimalarial compounds and shows high activity against resistant *Plasmodium* strains. A series of derivatives including ethers and carbonates have been synthesized to overcome the lipophilic nature of artemisinin. Among them, artemether, arteether and sodium artesunate are being licensed as drugs in an increasing number of countries (Haynes, 2006; Klayman, 1985; Li *et al.*, 2006; Weina, 2008).

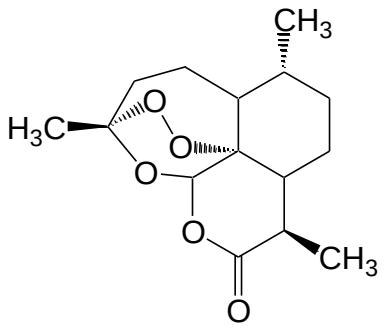

Qinghaosu (artemisinin)

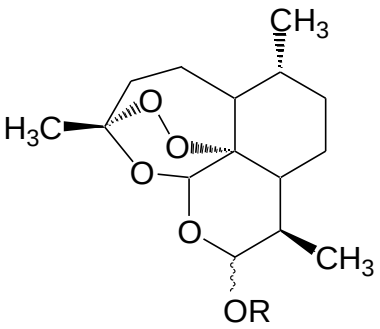

Artemether R = CH_3
Arteether R = C_2H_5
Sodium artesunate R = $COCH_2CH_2CO_2Na$

Figure 1.3 Artemisinin and derivatives.

Galanthamine (Figure 1.4), first isolated in the 1950s from *Galanthus nivalis* (Amaryllidaceae) (Shu, 1998), now is one of the few therapeutics used in the management of Alzeimer's disease, by a mechanism involving maintenance of acetylcholine levels in the brain.

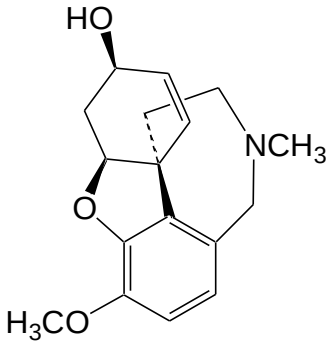

Figure 1.4 Galanthamine.

Some plant metabolites are also in the forefront of research for new drugs in the treatment of AIDS. These include the 'dimeric' naphthylisoquinoline alkaloid michellamine B from the West African liana *Ancistrocladus korupensis* (Ancistrocladaceae); the coumarin derivative calanolide A from the African tropical rainforest tree *Calophyllum lanigerum* (Guttiferae) (Rouhi, 2003); the phorbol ester prostratin from *Homolanthus nutans* (Euphorbiaceae) (Gustafson *et al*. 1992; Johnson *et al.* 2008); and the naphthoquinone trimer conocurvone from the Australian shrub *Conospermum incurvum* (Proteaceae) (Decosterd *et al*, 1993).

1.3. Higher plants from South Africa

South Africa is one of the richest centres of plant diversity in the world. Statistics show that about 25% of the total number of higher plants in the world is found in Africa south of the Sahara. The flora is not only extremely rich and diverse (Arnold and de Wet, 1993), but is also largely endemic in character, particularly in the Cape Floral Kingdom and the Succulent Karroo vegetation types. The region also has a rich cultural diversity. It has been found that about 3500 species of higher plants are used as medicines in South Africa (Gericke, 2002). Many of the indigenous plants have been investigated phytochemically (Mulholland and Drewes, 2004) and an issue of Journal of Ethnopharmacology has been devoted to the study of South African medicinal plants (Van Staden, 2008).

1.4. Seeds

Seeds of South African plants have been little studied from a chemical viewpoint and a survey of their constituents is of high interest. The source plants of these seeds may grow in areas with extreme climatic conditions, thus increasing the chances of finding original metabolites. Another advantage is that seeds can be collected without damaging the plants, unlike organs such as roots or stem bark, which may lead to the death of the plant when they are collected.

Seeds are the maturation products of the ovules, and contain the next generation. They are generally dispersed from the parent plant within the fruit, but may be dispersed individually. Each seed contains an embryo (which may be rudimentary at dispersal, as is the case in orchids and many parasitic plants) and possibly food-reserve material (endosperm or perisperm), wrapped inside the seed-coat or testa (Cullen, 2004).

Seeds vary in size from minute and dust-like (as in many orchids) to large and solid. The testa may be variously marked and coloured and the seed may be appendaged. Two kinds of appendages are important: the aril, which is an outgrowth from the funicle (the stalk of the ovule) and is often

fleshy or coloured and may partly or wholly envelop the seed, and the elaiosome (also known as the caruncle), which is an oily body formed at one end of the seed (Cullen, 2004).

1.4.1. Strategies in the collection of seed materials

Strategies in the collection of different species of seeds are mainly focused on three aspects: information from traditional medicine, size of the seeds and random collection.

Selection of seed materials based on the knowledge from traditional medicine may give a higher chance of discovering promising new molecules (Hostettmann *et al*., 2008).

The larger size of seeds is preferable since the subsequent phytochemical investigation might consume a lot of sample material, so mainly the seeds of trees were selected.

Random collection is also indispensable for phytochemical investigation of seeds which have not yet been studied. In the combat which has to be fought against diseases, many different avenues need to be taken for the discovery of novel therapeutic agents. Action needs to be taken quickly, notably against diseases for which there is not yet an effective remedy, e.g. Alzheimer's disease. Here random collection of plant material increases the number of sample that can be extracted.

There are some pitfalls of collecting seeds: they are difficult to collect, growing high up in trees –[or are of minute size in certain herbs, for example]; a collecting permit is needed [and landowners consent is needed]; snakes can be hidden in trees and bushes; competition with birds and monkeys; seeds ripen in different seasons; they are dependent on environmental and climatic factors; they may be found in isolated regions – long distances to be travelled for plant collection; reliable infrastructure and collaboration required for collecting; good weather needed for drying seeds.

1.5. General review of the family Leguminosae (Fabaceae)

1.5.1 Botanical classification

The Leguminosae or bean and pea family is the third largest flowering plant (ANGIOSPERMS) family after the orchids (Orchidaceae) and daisies (Asteraceae or Compositae). Legumes comprise 727 genera and ca. 19325 species. They vary in habit from ephemeral herbs to shrubs, vines, woody climbers (lianas), and giant emergent forest trees a few aquatic species (Lewis *et al*., 2005). They are to be found as major components of most of the world's vegetation types and many have the ability to colonise marginal or barren lands because of their capacity to fix atmospheric nitrogen through root nodules (Sprent, 2001).

The family is currently divided into three subfamilies, Caesalpinioideae, Mimosoideae and Papilionoideae (Lewis *et al*., 2005). The diagnostic characteristics of the three legume subfamilies are shown in Table 1.1.

The subfamily Caesalpinioideae comprises 4 tribes (CERCIDEAE, DETARIEAE, CASSIEAE and CAESALPINIESE) and ca. 2,250 species. The tribe *Detarieae sens. lat* are pantropical in distribution, with ca. 58% of the genera confined to Africa (incl. Madagascar), ca. 20% to the Neotropics, and ca. 12% to tropical Asia (Lewis *et al*., 2005).

The principle unifying feature of the family Leguminosae is the legume (Polhill, 1994). This (with a small number of exceptions) comprises a single superior carpel (a few species in tribe Ingeae have several free carpels per flower) with one locule (some species of *Astragalus* and *Oxytropis* have a septum intruding from one of the sutures rendering the carpel essential bilocular), parietal placentation along the adaxial suture, and ovules 2 – many, in two alternating rows on a single placenta. The most common type of fruit is a pod with two valves that separate and twist to expel the seeds, but this has been modified in many ways to facilitate dispersal by animals, wind and water. Sometimes the seeds are in hardened seed–chambers which do not open and are variously nut-like, winged, fleshy or buoyant. The legume seeds coat is also unique; the epidermis forms a distinct palisade with twisted walls and the hypodermis is almost always comprised of hourglass-shaped cells (Polhill, 1994).

1.5.2. Economic importance of the Legume family

Legumes have been gathered, cultivated, eaten and used in a multitude of other ways by humans for millennia and are arguably as important as grasses in global terms. The range of uses of legumes is certainly broader than that of the grass family (Doyle and Luckow, 2003). Legume products contribute enormously to the world's economy through food (for animals and humans) and drink, pharmaceuticals and medicine, biodiesel fuel, biotechnology (as industrial enzymes), building and construction, textiles, furniture and crafts, paper and pulp, mining, manufacturing processes, chemicals and fertilizers, waste recycling, horticulture, pest control, and ecotourism.(Lewis *et al*., 2005).

Ancient cultures were aware of the ability of many legumes to improve the soil, even if they did not then appreciate that this results from symbiotic nitrogen fixtion (Van den Bosch and Stacey, 2003). Some 40 to 60 million metric tons of nitrogen are fixed annually by agriculturally important legumes and a further 3 to 5 million metric tons by legumes in natural ecosystems (Graham and Vance, 2003). Many species are used as soil improvers, green manures and stabilizers and in reforestation programs. Natural accumulation of nitrogen has also resulted in predation of legumes

by a wide range of animals and insects. To combat this, the family has evolved a wide repertoire of chemical defenses based on secondary compounds, especially alkaloids. Humans have exploited the chemistry of legumes by utilizing many species as medicines, insecticides, molluscicides, abortifacients, purgatives, fish, arrow and ordeal poisons, anti-fungal agents, aphrodisiacs, hallucinogens, and antidotes to poisons. Several legumes are rich in gums used as glues and food thickeners (e.g. *Acacia*, *Astragalus*), resins used in paints, polishes and varbishes (e.g. *Hymenaea*, *Caopifera*, *Prioria*) and oils used in lubricants and cosmetics. Important dyes, such as brasil, indigo and dyer's greenweed all come from legumes, and several species are used as inks, and for tanning leather (Lewis *et al*., 2005).

Grain and forage legumes are grown on approximately 180 million hectares (12-15%) of the earth's arable surface and account for 27% of the world's primary crop production. Legumes alone contributing 33% of the dietary protein nitrogen needs of humans (Graham and Vance, 2003). Legumes (mainly soybean, *Glycine max* (L.) Merr. and peanut, *Arachis hypogaea* L.) also contribute more than 35% of the world's processed vegetable oil (Graham and Vance 2003). Forage legumes provide the protein, fibre and energy that have underpinned dairy and meat production for centuries (Graham and Vance, 2003).

1.5.3. The genus *Schotia* Jacq.

Schotia Jacq. is a small genus containing 4 species (Palmer, 1981). Distribution: E Zimbabwe, SW Mozambique, S Namibia, S Africa [excluding central regions] and Swaziland; dryland disjunctions occur between W and E Cape Provinces and NE Cape-Namibia (*S. afra* (L.) Thunb.) and between E Cape and the Sekhukhuneland Center of Endemism in Northern Province, S Africa (*S. latifolia* Jacq.) (Lewis *et al*., 2005).

According to Lewis *et al*., 2005, the genus *Schotia* is classified as follows:

Family LEGUMINOSAE

Subfamily CAESALPINIOIDEAE

Tribe DETARIEAE

Genus ***SCHOTIA***

Botanical characters of *Schotia* (Palgrave, 2002): Shrubs or trees. **Leaves**: paripinnate, with 3-8 pairs of leaflets; alternate. **Flowers**: in short, many-flowered panicles, terminal or lateral, often produced on the old wood; bracts small, falling early; flowers stalks (pedicels) short, producing compact heads; calyx lobes 4, joined at the base to form a tube, persistent, red or reddish brown; petals 5, sometimes long and narrow, red or pink, arising from the mouth of the calyx tube, falling early; stamens 10, arising with the petals, free or joined at the base; ovary oblong, with a short stalk. **Fruit**: a flattened, woody pod, often curved, beaked, with a hard, persistent rim which often remains on the tree after the tardily dehiscent valves have eventually split away. **Seeds**: smooth and brown, 1-2 cm in diameter, with or without a yellow aril, may remain attached to the rim of the pod.

1.5.3.1. *Schotia brachypetala* Sond.

Figure 1.5 *Schotia brachypetala* trees in Manyeleti Nature Reserve, Mpumalanga.

Figure 1.6 Fruit pod of *Schotia brachypetala*, showing the yellow aril.

Figure 1.7 Flower of *Schotia brachypetela*.

Previously known as *S. rogersii* Burtt Davy; *S. semireduxta* Merxm. Common name: Weeping Boer-bean, Huilboerboon. Distribution: Eastern Cape northwards to KwaZulu Natal, Swaziland, Limpopo, Mozambique, Zimbabwe (Palmer, 1981).

Botanical characters of *Schotia brachypetala* Sond. (Palgrave, 2002): Briefly deciduous, a tree up to 16 m in height, with a rounded crown and branches that hang down and turn upwards at the end; occurring in open deciduous bushveld, drier types of woodland and scrub forest, frequently associated with termite mounds and also along riverbanks. Bark: brown or brownish grey and rough. Leaves: rachis flattened and can be grooved above or slightly winged, with 4-7 (occasionally 8) pair of opposite or sub-opposite leaflets oblong to ovate-oblong or more or less rectangular, with or without sparse hairs, 2.5-8.5 x 1.2-4.5 cm, the end leaflets being the largest; apex rounded or abruptly finely pointed; base rounded, asymmetric; margin entire, wavy; petiolules short, up to 2 mm or absent; petioles up to 2.5 cm long. Flowers: deep red, with slender, pink petals up to 1.5 cm long that are sometimes reduced or absent; stamens joined at the base; in dense, branched heads or panicles, 6-13 cm long; copious nectar is produced (Sept./Oct). Fruit: a flattened, woody pod,

usually 6-10 cm long; with the characteristic persistent rim (Feb.-May). Seeds: ovoid, flattened, pale brown, about 2 cm in diameter, with a large, conspicuous yellow aril.

The copious nectar which drips from the flowers – and thus gives the tree its common name- attracts both insects and birds. The seeds are roasted and then eaten, and the wood, with sapwood yellowish grey, and heartwood dark brown to nearly blackish, hard and moderately heavy, is used for all types of furniture, especially benches and chairs. The bark contains tannin and is used for tanning leather (Venter and Venter, 1996).

This plant has a wide range of traditional uses. A decoction of the bark is reported to be taken (presumably as an emetic) to treat heartburn and the effects of too much drinking (Watt and Breyer-Brandwijk, 1962). Bark mixtures are also used to strengthen the body and for a facial sauna (Pujol, 1993). The bark and root may be used to treat diarrhoea (Watt and Breyer-Brandwijk, 1962; Hutchings *et al*., 1996) or, in Venda, nervous heart conditions (Netshiungani, 1981). Leaves are burnt and the smoke is inhaled to stop a bleeding nose. Powdered leaves are applied to topical ulcers to speed up the healing process (Venter and Venter, 1996).

The chemical compounds of *Schotia* species are poorly known (Dictionary of Natural Products, 2008). Two polyhydroxystilbenes have been isolated from the water : methanol extract of heartwood of *S. brachypetala*, of which *trans*-3,3′,4,5,5′-pentahydroxystilbene is the major compound, and *trans*-3, 3′, 4, 5′-tetrahydroxystilbene, a minor one (Drewes and Fletcher, 1974). Two fatty acids were isolated from the ethanol extract of leaves: linolenic acid and methyl-5,11,14,17-eicosatetraenoic acid (McGaw *et al*., 2002). Crude extracts from the roots (Mathabe *et al*., 2006; Masika and Afolayan, 2002) as well as the two fatty acids that were isolated from the roots (McGaw *et al*., 2002) displayed moderate antibacterial activity. The antidiarrhoeal activity may also be due to the presence of astringent tannins in the bark (Bruneton, 1995). Many stilbenes are known to have antibiotic properties but the biological activity of the *Schotia* stilbenes appears to be unknown. Water and ethanol bark extracts inhibit monoamine oxidase (MAO) but this activity was not selective. These enzymes catalyse the oxidation of monoamines and they are

employed in the treatment of neurodegenerative related illness such as Parkinson's and Alzheimer's disease. The water extracts, which resemble those prepared traditionally, were more active than the ethanol extracts (Stafford *et al*., 2007). Extracts of *Schotia brachypetala* root and bark showed antioxidant activity (Adewusi *et al.*, 2011) and weak acetylcholinesterase inhibitory activity (Adewusi *et al.*, 2011). The wood dust and roots are believed to contain tannins (Watt and Breyer-Brandwijk, 1962).

1.5.4. The genus *Colophospermum* J. Leonard

Figure 1.8 Leaves of *Colophospermum mopane*, showing the characteristic bilobe morphology.

Figure 1.9 Mature seeds of *Colophospermum mopane*.

Colophospermum J. Leonard is a monotypic genus with only one species, *Colophospermum mopane* (J. Kirk ex Benth.) J. Kirk ex J. Leonard, previously known as *Copaifera mopane* Kirk ex Benth. (Palmer, 1981). Distribution: south tropical and southern Africa (in lower altitude river valleys from S Angola, N Namibia, Zimabwe, S Zambia, S Malawi, N South Africa and Mozambique) (Lewis *et al*., 2005).

According to Lewis *et al*., 2005, the genus *Colophospermum* is classified as follows:

Family LEGUMINOSAE

Subfamily CAESALPINIOIDEAE

Tribe DETARIEAE

Genus ***COLOPHOSPERMUM***

Botanical characteristics (Palgrave, 2002): A medium-sized to large tree 4-18 m in height, usually about 10 m high; dominant over great areas of southern tropical Africa in hot, low-lying

areas, often on alluvial soils, and also on alkaline and poorly drained soils which it tolerates better than many other species do. **Bark**: dark grey to blackish, characteristically deeply, vertically fissured and flaking in narrow strips. **Leaves**: bifoliolate, with 2 leaflets without stalks, resembling a pair of butterflywings, and the vestigial remains of a third, terminal leaflet forming a very small appendage between the pair of leaflets; 5 alternate; leaflets ovate, 4.5-10 x 1.5-5 cm, with several veins from the base, with transparent gland dots (10 x lens); apex tapering; base markedly asymmetric and slightly lobed on 1 side; margin entire; petiole 2-4 cm long. **Flower**: greenish, small and inconspicuous, in short axillary racemes or sprays; hermaphrodite; sepals 4, greenish; petals absent; stamens 20-25, hanging out of the flowers to facilitate wind pollination; stigma enlarged, style on the side of the ovary (Oct-Mar, but flowering can be erratic; sometimes the trees in a whole area produce no flowers for several years). **Fruit**: a flattened pod, kidney-shaped or almost semi-circular, leathery but not woody, indehiscent (Mar-Jun). **Seeds**: distinctive, flat, conspicuously convoluted, sticky, copiously dotted with resin glands.

Mopane is one of the dominant tree species of the hot, low-lying areas of southern tropical Africa. It is one of the most distinctive species, often forming pure stands. These have given rise to now accepted term ‘mopane woodland’ or ‘colophospermum woodland’, a type of vegetation that has an atmosphere entirely of its own. (Palgrave, 1983).

The leaves and pods provide an important food source for many animals, while the roasted caterpillars of the mopane moth—commonly known as ‘mopane worms’—are an important delicacy and protein source in the diet of local Africans. In addition, plant infusions are used in traditional medicine to treat syphilis, dysentery, diarrhea and inflamed eyes (Watt and Breyer-Brandwijk, 1962).

The polyphenolic pool of the heartwood of the mopane, *Colophospermum mopane* Kirk ex J. Leonard, exhibits extreme diversity and complexity. It comprises a variety of monomeric flavonoids, dimeric proanthocyanidins, and a variety of profisetinidin-type triflavanoids. (Ferreira *et al.*, 2003). Initial chemical investigation of the heartwood extract of *C. mopane* was prompted by indications

of 'an association of interrelated flavonoid compounds of potential interest in the study of the biogenesis of tannins, their stereochemistry, and their reddening on exposure to sunlight' (Drewes and Roux, 1965, 1966, 1967). These preliminary investigations focused mainly on the presence of di- and trimeric flavanoids (Du Preez, 1971; Du Preez *et al.*, 1971; Botha *et al.*, 1982). The aerial parts of the mopane are rich in essential oils that comprise mainly α-pinene and limonene, as well as at least 36 compounds in lesser quantities according to GC and GC/MS analyses (Chagonda *et al.*, 1999; Brophy *et al.*, 1992). These compounds are presumably responsible for the strong turpentine odor of the pods. The leaves also contain significant concentrations of *β*-sitosterol and stigmasterol which are apparently the source of sterols in various organs of the mopane moth, *Gonimbrasia belina* (Cmelik, 1970).

Mopaneol A (**1**) and mopaneol B (**2**) were identified in hexane extracts from mopane leaves and seed husks, respectively (Reiter *et al.*, 2003). The corresponding aldehydes **3** and **4** were obtained as an inseparable mixture from the hexane extract of mopane roots. These compounds represent primitive diterpenes that are regarded as the 'missing links' in the biosynthesis of the 9,13-epoxylabdanes. The proposed genesis from geraniol pyrophosphate also attempted to explain the unusual C-3-*α* hydroxyl and C-8-*β* methyl groups in compounds **1**-**8**, as well as the highly variable configurations at C-9 and C-13. Three diterpenes, dihydrogrindelic acid (**5**), dihydrogrindealdehyde (**6**) and methyl labd-13*E*-en-15-oate (**7**) are present in the bark and seeds. Dihydrogrindelaldehyde (**6**) exhibits significant cytotoxicity against a human breast cancer cell line (Mebe, 2001). A new diterpene, 8(*S*),13(*S*)-dihydrogrindelic acid (**8)** was isolated from the seeds of *Colophospermum mopane* along with its previously described C-13 epimer (Englund *et al.*, 2009).

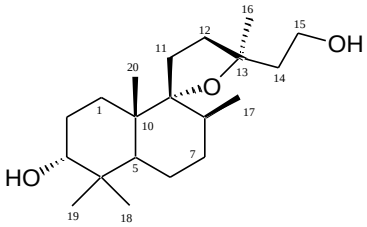

Mopaneol A

1

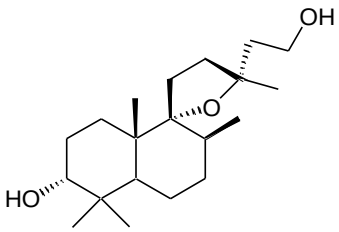

Mopaneol B

2

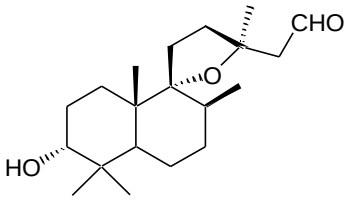

3

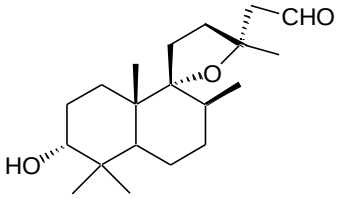

4

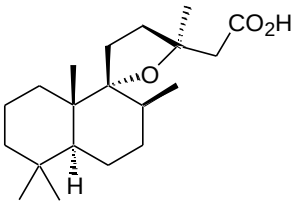

5

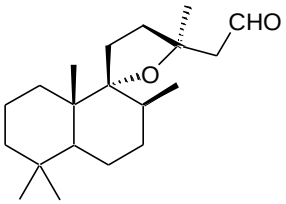

6

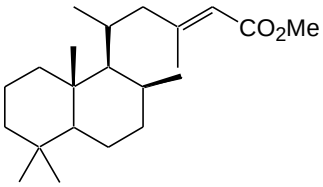

7

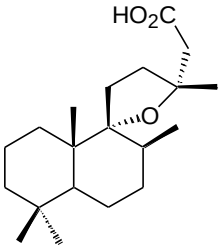

8

1.6. The main biological assays used in this study

1.6.1. Test for free-radical scavenging activity (TLC)

Oxidation is well known to be a major cause of food and materials degradation. More recently, reactive oxygen species, in particular free radicals, have been recognized to be involved in several diseases including the two major causes of death: cancer and atherosclerosis. Aging also may be the sum of the deleterious free-radical reactions which occur continuously throughout cells and tissues (Muller, 1992). In this context, natural antioxidants and radical scavenging are receiving increasing attention. They can be an alternative to the use of synthetic compounds in food and pharmaceutical technology or serve as lead compounds for the development of new drugs with the prospect of improving the treatment of various disorders (Cuendet *et al*., 1997).

In the radical scavenging assay, a solution of DPPH, a stable radical with a violet colour, is sprayed on the developed TLC plate. If there are any antiradical substances present, they will capture and reduce the DPPH radicals and the colour will disappear (Figure 1.10). The active zone is exhibited as pale yellow spots against a violet background (Cuendet *et al*., 1997).

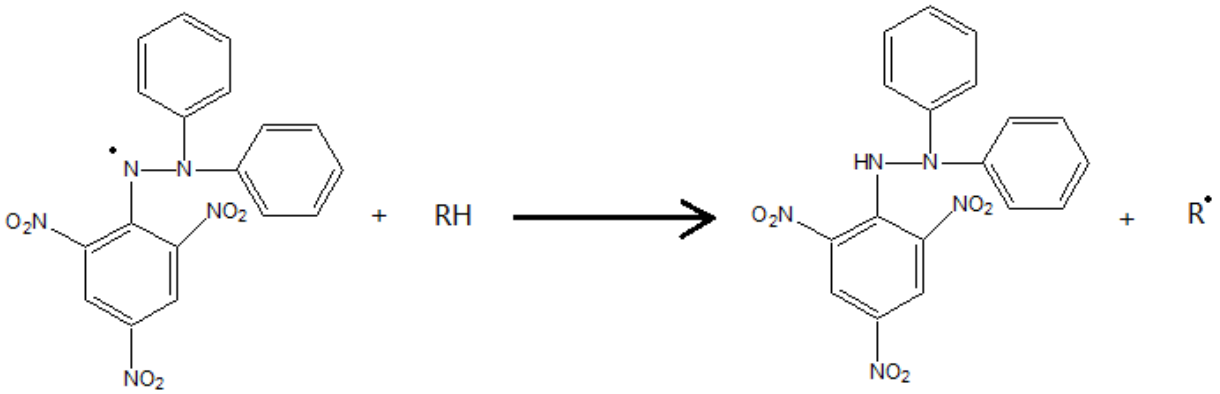

Stable radical
2,2′-Diphenyl-1-picrylhydrazyl (DPPH)
Purple coloration

Colourless / Pale yellow

Figure 1.10 TLC assay for the detection of radical scavengers. The TLC plate is sprayed with a 0.3% solution of DPPH in methanol and radical scavengers appear as yellow-white spots on a purple background.

1.6.2. Test for inhibition of acetylcholinesterase (TLC) (Marston *et al*., 2002)

Alzheimer's disease is the most common cause of senile dementia in later life of humans. It is estimated that up to 4 million people are affected in the USA. Inhibitors of acetylcholinesterase currently form the basis of the newest drugs available for the management of this disease. They function by correcting a deficiency of the neurotransmitter acetylcholine in the synapses of the cerebral cortex. A TLC bioautographic assay has been introduced to screen plant extracts and other samples for inhibition of acetylcholinesterase activity and to aid in the search for new potential drugs. The test relies on the cleavage reaction of acetylcholinesterase on α-naphthyl acetate, to form α-naphthol, which in turn reacts with Fast Blue B salts to give a purple-colored diazonium dye (Figure 1.11), except in regions containing acetylcholinesterase inhibitors which show up as white spots.

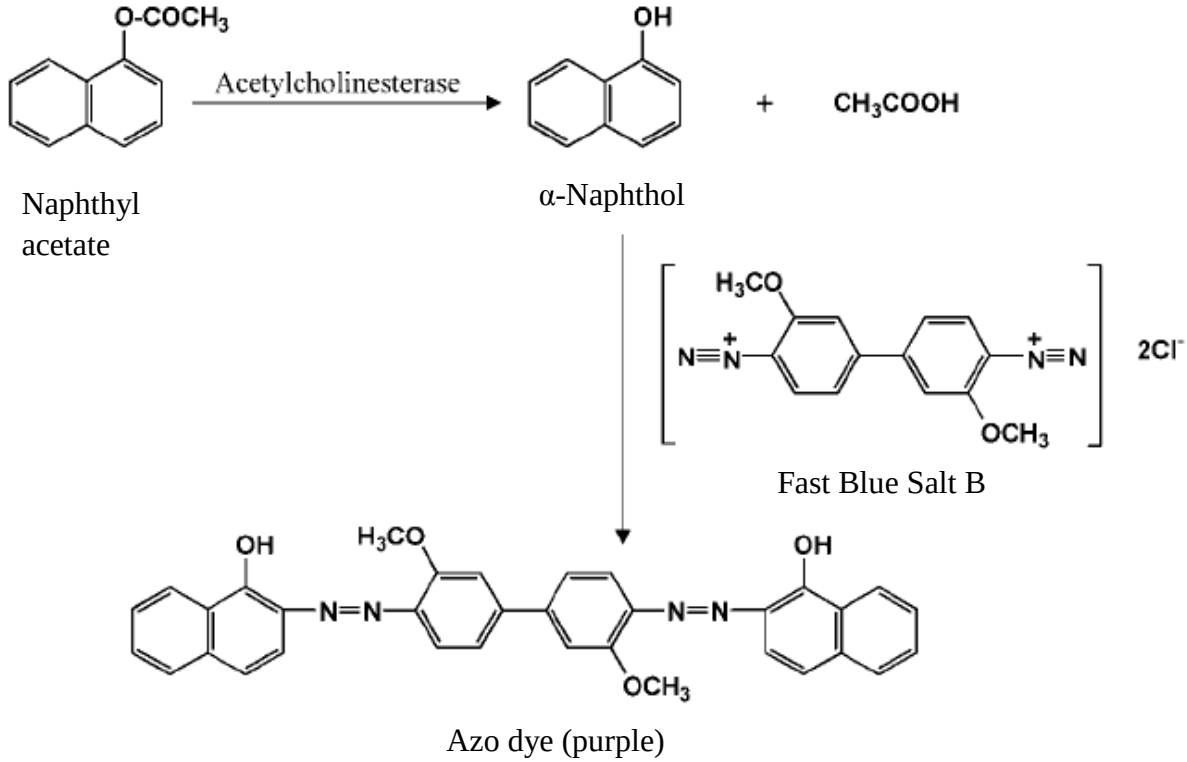

Figure 1.11 Reaction of acetylcholinesterase with naphthyl acetate and the subsequent formation of the purple dye in the TLC bioassay.

1.6.3. Antimicrobial testing

The fight against bacterial infections over the last 70 years has been one of the great success stories of medicinal chemistry, yet it remains to be seen whether this positive situation will last. Bacteria such as *Staphylococcus aureus* have the worrying ability to gain resistance to known drugs, so the search for new drugs is never ending. Although deaths from bacterial infection have dropped in the developed world, bacterial infection is still a major cause of death in the developing world. For example, the World Health Organization estimated that tuberculosis was responsible for about 2 million deaths in 2002 and that one in three of the world's population was infected. The same organization estimated that, in the year 2000, 1.9 million children died worldwide of respiratory infections with 70% of these deaths occurring in Africa and Asia. They also estimated that each year 1.4 million children died from gut infections and the diarrhea resulting from these infections. In the developed world, deaths from food poisoning due to virulent strains of *Escherichia coli* have attracted widespread publicity, and tuberculosis has returned as a result of the AIDS epidemic (Patrick, 2005).

Four representative strains were used in this work for antimicrobial testing: *Escherichia coli* (ATCC 8739), *Staphylococcus aureus* (ATCC 25923), *Enterococcus faecalis* (ATCC 29212) and *Klebsiella pneumoniae* (ATCC 13883).

1.6.4. Antimalarial testing

Malaria is one of the oldest and important parasitic diseases in humans with more than 3 billion people at risk of *Plasmodium falciparum* infection. It is estimated that the disease afflicts 515 million people and kills 1.5-2.7 million people each year, most of these being children under 5 years old in sub-Saharan Africa (Guerin *et. al.*, 2002, Snow *et. al.* 2005). *P. falciparum,* the most dangerous of the four human malaria parasites [*P. falciparum, P. vivax*, *P. ovalae*, *P. malariae*], is responsible for the majority of deaths (Krungkrai *et. al.*, 2010).

Since malaria chemotherapy has relied on a limited number of drugs, the acquisition and

spread of drug resistance has led to an increase in morbidity and mortality rates in malaria endemic countries in recent years (World Health Organization, 2008). In view of this situation, the World Health Organization has recommended the use of artemisinin-based combination therapy (ACT) as the first-line drug for the treatment of uncomplicated *P. falciparum* malaria since 2001 (World Health Organization, 2001). Up to now, falciparum parasite resistance to artemisinin and derivative drugs in human patients has not been clearly documented (Krungkrai *et. al.*, 2010**)**. Artemisinin has been used as monotherapy in the Thai-Cambodian border for over 30 years; artemisinin-based combination therapies (i.e., artesunate-mefloquine combination) were introduced there in 2001 as the first-line treatment for falciparum malaria (World Health Organization, 2001). Until very recently, Dondorp *et. al.* reported a decrease in clinical efficacy of the artemisinin derivative in artesunate-mefloquine treatment in the falciparum malaria patients at the Thai Cambodian border in 2009, showing that the parasites clear slowly from the patients' blood after the ACT treatment without a corresponding reduction on *in vitro* susceptibility testing (Dondorp *et. al.*, 2009).

The prevalence of malaria in tropical zones worldwide, together with the lack of a vaccine and the appearance of a strain of malaria parasite resistant to commercially available anti-malaria drugs, makes the search for new anti-malarials a global requirement (Butler *et. al.*, 1997).

Table 2.1 Extraction of collected seeds

Family	Species	Weights of seeds extracted	MeOH extract weight
Anacardiaceae	*Lannea edulis* ripe seeds	40 g	1.573 g
Anacardiaceae	*Searsia dentata*	40 g	5.246 g
Anacardiaceae	*Searsia pyroides*	40 g	3.854 g
Burseraceae	*Commiphora glandulosa* unripe fruits	40 g	1.973 g
Burseraceae	*Commiphora glandulosa* ripe fruits	23 g	1.435 g
Burseraceae	*Commiphora* cf *pyracanthoides*	40 g	2.663 g
Combretaceae	*Combretum apiculatum*	40 g	26.929 g
Combretaceae	*Terminalia prunioides*	40 g	3.017 g
Cucurbitaceae	*Acanthosicyos naudinianus*	40 g	1.767 g
Cucurbitaceae	*Citrillus lanatus*	40 g	1.729 g
Cucurbitaceae	*Cucumis africanus*	40 g	3.708 g
Ebenaceae	*Diospyros lycioides*	40 g	0.998 g
Ebenaceae	*Diospyros mespiliformis*	43 g	3.542 g
Ebenaceae	*Euclea divinorum*	40 g	6.093 g
Fabaceae	*Acacia erioloba*	40 g	4.843 g
Fabaceae	*Acacia haematoxylon*	40 g	3.957 g
Fabaceae	*Afzelia quanzensis* aril	9 g	0.934 g
Fabaceae	*Cassia abbreviata* subsp. *beareana*	40 g	4.173 g
Fabaceae	*Colophospermum mopane* premature (green) seeds	40 g	16.844 g
Fabaceae	*Colophospermum mopane* mature (red) seeds	36 g	9.377 g
Fabaceae	*Peltophorum africanum*	8.1 g	1.223 g
Fabaceae	*Schotia brachypetala* aril	40 g	39.708 g
Fabaceae	*Schotia brachypetala* rest of seed	40 g	9.929 g
Fabaceae	*Tylosema fassoglense* pitts	40 g	4.341 g
Fabaceae	*Tylosema fassoglense* hulls	40 g	9.749 g
Fabaceae	*Xanthocercis zambesiaca*	40 g	10.191 g
Meliaceae	*Trichilia emetica*	40 g	4.050 g

Family	Species	Weights of seeds extracted	MeOH extract weight
Rhamnaceae	*Berchemia discolor*	40 g	13.405 g
Sapotaceae	*Englerophytum magalismontanum* *	40 g	4.700 g

*****Fresh seed material used. Otherwise, dried seeds were extracted.

Table 2.2 Antimicrobial activities of the extracts

Family	Species	*E. coli* ATCC 8739 (mg/ml)	*S. aureus* ATCC 25923 (mg/ml)	*K. pneumoniae* ATCC 13883 (mg/ml)	*E. faecalis* ATCC 29212 (mg/ml)
Anacardiaceae	*Lannea edulis* ripe seeds	4.0	4.0	2.0	4.0
Anacardiaceae	*Searsia dentata*	2.0	2.0	2.0	2.0
Anacardiaceae	*Searsia pyroides*	0.5	0.5	2.0	0.5
Burseraceae	*Commiphora glandulosa* unripe seeds	6.0	8.0	2.0	8.0
Burseraceae	*Commiphora glandulosa* ripe seeds	16.0	>16.0	13.3	16.0
Burseraceae	*Commiphora* cf *pyracanthoides.*	>16.0	>16.0	>16.0	>16.0
Combretaceae	*Combretum apiculatum*	0.5	1.3	0.5	1.0
Combretaceae	*Terminalia prunioides*	>16.0	16.0	>16.0	16.0
Cucurbitaceae	*Acanthosicyos naudinianus*	>16.0	>16.0	>16.0	>16.0
Cucurbitaceae	*Citrillus lanatus*	>16.0	>16.0	>16.0	>16.0
Cucurbitaceae	*Cucumis africanus*	4.0	16.0	4.0	12.0
Ebenaceae	*Diospyros lycioides*	2.0	2.0	2.0	2.0
Ebenaceae	*Diospyros mespiliformis*	0.7	1.7	2.0	2.0
Ebenaceae	*Euclea divinorum*	3.1	1.6	3.1	0.8
Fabaceae	*Acacia erioloba*	12.0	16.0	4.0	16.0
Fabaceae	*Acacia haematoxylon*	>16.0	>16.0	>16.0	>16.0
Fabaceae	*Afzelia quanzensis* aril	6.25	>12.5	6.2	0.63
Fabaceae	*Cassia abbreviata* subsp. *beareana*	>16.0	>16.0	3.3	>16.0
Fabaceae	*Colophospermum mopane* premature (green) seeds	4.0	0.1	4.0	0.04
Fabaceae	*Colophospermum mopane* mature (red) seeds	2.0	0.3	3.0	0.5
Fabaceae	*Peltophorum africanum*	12.5	12.5	6.3	9.5
Fabaceae	*Schotia brachypetala* aril	0.5	16.0	8.0	8.0
Fabaceae	*Schotia brachypetala* rest of seed	1.0	2.0	2.0	1.0
Fabaceae	*Tylosema fassoglense* pitts	9.5	12.5	9.5	9.5
Fabaceae	*Tylosema fassoglense* hulls	0.8	0.4	3.1	0.8

Family	Species	*E. coli* ATCC 8739 (mg/ml)	*S. aureus* ATCC 25923 (mg/ml)	*K. pneumoniae* ATCC 13883 (mg/ml)	*E. faecalis* ATCC 29212 (mg/ml)
Fabaceae	*Xanthocercis zambesiaca*	>16.0	>16.0	>16.0	>16.0
Meliaceae	*Trichilia emetica* subsp. *emetica*	3.3	0.2	4.0	0.16
Rhamnaceae	*Berchemia discolor*	8.0	10.7	2.0	8.0
Sapotaceae	*Englerophytum magalismontanum*	12.0	16.0	8.0	16.0
	culture control	>16.0	>16.0	>16.0	>16.0
	negative control	>16.0	>16.0	>16.0	>16.0
	ciprofloxacin control (µg/ml)	0.63	0.30	0.12	0.63

Table 2.3 Antimalarial activities of the extracts

Family	Species	Final mean % parasite growth at 50 µg/ml			IC_{50} (µg/ml)		
		%	s.d.[a]	n[b]	IC_{50} (µg/ml)	s.d.[a]	n[b]
Anacardiaceae	*Lannea edulis* ripe seeds	1.0	0.9		18.03	1.10	
Anacardiaceae	*Searsia dentata*	104.3	8.9				
Anacardiaceae	*Searsia pyroides*	97.6	10.0				
Burseraceae	*Commiphora glandulosa* unripe seeds	112.5	7.5				
Burseraceae	*Commiphora glandulosa* ripe seeds	109.5	1.3				
Burseraceae	*Commiphora* cf *pyracanthoides*	109.6	3.9				
Combretaceae	*Combretum apiculatum*				17.47	5.41	5
Combretaceae	*Terminalia prunioides*	4.4	3.4		23.83	1.05	
Cucurbitaceae	*Acanthosicyos naudinianus*	107.4	6.3				
Cucurbitaceae	*Citrillus lanatus*	101.7	1.7				
Cucurbitaceae	*Cucumis africanus*	97.5	3.1				
Ebenaceae	*Diospyros lycioides*	74.2	15.0				
Ebenaceae	*Diospyros mespiliformis*	86.5	7.6				
Ebenaceae	*Euclea divinorum*	N.T.					
Fabaceae	*Acacia erioloba*	89.4	9.8				
Fabaceae	*Acacia haematoxylon*	100.4	6.4				
Fabaceae	*Afzelia quanzensis* aril	101.43	6.11	5			
Fabaceae	*Cassia abbreviata* subsp. *beareana*	86.4	1.7				
Fabaceae	*Colophospermum mopane* premature (green) seeds	66.69	8.64	5			
Fabaceae	*Colophospermum mopane* mature (red) seeds				40.98	8.78	2
Fabaceae	*Peltophorum africanum*	79.26	7.71	4			
Fabaceae	*Schotia brachypetala* aril	2.3	1.0		17.58	2.06	5
Fabaceae	*Schotia brachypetala* rest of seed	82.6	4.5				
Fabaceae	*Tylosema fassoglense* pitts	101.02	5.73	4			
Fabaceae	*Tylosema fassoglense* hulls	93.99	4.71	5			

Family	Species	Final mean % parasite growth at 50 µg/ml			IC_{50} (µg/ml)		
		%	s.d.[a]	n[b]	IC_{50} (µg/ml)	s.d.[a]	n[b]
Fabaceae	*Xanthocercis zambesiaca*	109.8	7.7				
Meliaceae	*Trichilia emetica* subsp. *emetica*	105.7	7.9				
Rhamnaceae	*Berchemia discolor*	97.7	10.6				
Sapotaceae	*Englerophytum magalismontanum*	99.9	8.7				

a, standard deviation; b, number of times tested; N.T.: Not tested.

Table 2.4 Radical scavenging activities with DPPH and acetylcholinesterase inhibition test of the extracts.

Family	Species	Radical scavenging	Acetylcholinesterase inhibition
Anacardiaceae	*Lannea edulis* ripe seeds	++	+
Anacardiaceae	*Searsia dentata*	-	+
Anacardiaceae	*Searsia pyroides*	-	+
Burseraceae	*Commiphora glandulosa* unripe fruits	-	+
Burseraceae	*Commiphora glandulosa* ripe fruits	-	+
Burseraceae	*Commiphora* cf *pyracanthoides*	-	+
Combretaceae	*Combretum apiculatum*	++	+
Combretaceae	*Terminalia prunioides*	+	-
Cucurbitaceae	*Acanthosicyos naudinianus*	-	-
Cucurbitaceae	*Citrillus lanatus*	-	-
Cucurbitaceae	*Cucumis africanus*	+	-
Ebenaceae	*Diospyros lycioides*	-	-
Ebenaceae	*Diospyros mespiliformis*	+	-
Ebenaceae	*Euclea divinorum*	+	-
Fabaceae	*Acacia erioloba*	-	+
Fabaceae	*Acacia haematoxylon*	-	+
Fabaceae	*Afzelia quanzensis* aril	-	N.T.
Fabaceae	*Cassia abbreviata* subsp. *beareana*	+	-
Fabaceae	*Colophospermum mopane* premature (green) seeds	+	++
Fabaceae	*Colophospermum mopane* mature (red) seeds	+	++
Fabaceae	*Peltophorum africanum*	-	+
Fabaceae	*Schotia brachypetala* aril	+++	-
Fabaceae	*Schotia brachypetala* rest of seed	+	-
Fabaceae	*Tylosema fassoglense* pitts	-	-
Fabaceae	*Tylosema fassoglense* hulls	++	-
Fabaceae	*Xanthocercis zambesiaca*	-	++
Meliaceae	*Trichilia emetica* subsp. *emetica*	++	-

Family	Species	Radical scavenging	Acetylcholinesterase inhibition
Rhamnaceae	*Berchemia discolor*	-	-
Sapotaceae	*Englerophytum magalismontanum*	-	-

-: No activity; +: Weak activity; ++: Moderate activity; +++: Strong activity; N.T.: Not tested.

2. RESULTS AND DISCUSSIONS

2.1. Extraction and preliminary screening

2.1.1. Extraction

Seeds from 25 species of plants (mainly trees) from South Africa were collected by Dr. P. Zietsman (National Museum, Bloemfontein). In the case of *Colophospermum mopane* and *Commiphora glandulosa*, both green seeds and ripe seeds were extracted. The arils and seeds of *Schotia brachypetala* were extracted, as were the pits and hulls of *Tylosema fassoglense*.

Methanol was chosen as the solvent for extraction, because it gives a large spectrum of apolar and polar material, and little oil. Solvents such as dichloromethane were not used because they also extract the fats and oils. The yields of the extractions are shown in Table 2.1.

2.1.2. Biological screening

All methanol extracts were subjected to different biological tests in order to evaluate their biological activities and potential for further investigation. The tests were performed according to protocols (see Experimental part) so that results from different extracts, fractions and compounds were coherent and comparable. The tests used in this study were as follows:

- ✓ Antimicrobial tests (*Escherichia coli* (ATCC 8739), *Staphylococcus aureus* (ATCC 25923), *Enterococcus faecalis* (ATCC 29212) and *Klebsiella pneumoniae* (ATCC 13883).
- ✓ Anti-malaria test
- ✓ Radical scavenging test with DPPH
- ✓ Acetylcholinesterase inhibition test

The results of the extracts tested are listed in Tables 2.2, 2.3 and 2.4.

2.1.2.1. Antimicrobial activity

Some methanol extracts showed good antimicrobial activity (Table. 2.2). Among them, the methanol extract of *Colophospermum mopane* immature seeds was the best inhibitor of *E. faecalis* ATCC 29212 (0.04 mg/ml).

2.1.2.2. Antimalarial activity

In the anti-malaria test, only 4 extracts were of interest, i.e. methanol extracts of *Lannea edulis* var. *edulis* ripe seeds, *Schotia brachypetala* aril, *Terminalia prunioides* and *Colophospermum mopane* mature seeds (Table. 2.3).

In a preliminary analysis of the chemical constituents of the methanol extracts of premature and mature seeds of *Colophospermum mopane* by TLC, the methanol extract of premature seeds contained more polar constituents than the ripe seeds, with the polar constituents contributing to the radical scavenging activity. Both methanol extracts of premature and mature seeds of *Colophospermum mopane* were further fractionated into heptane fractions and methanol fractions through partition (first dissolve in methanol, then extract 3 x with heptane), then the fractions were subjected to the anti-malaria test again. Both heptane fractions showed interesting anti-malarial activity, while the methanol fractions lacked such activity (Table 2.5).

Table 2.5 Results of antimalaria test for heptane and methanol fractions of premature and mature seeds of *Colophospermum mopane*.

	IC_{50} (µg/ml)	s. d.[a]	n[b]
Colophospermum mopane premature seeds MeOH extract	>50		
Colophospermum mopane premature seeds MeOH extract – methanol fraction of methanol-heptane partition	>50		
Colophospermum mopane premature seeds MeOH extract – heptane fraction of methanol-heptane partition	26.85	3.08	3
Colophospermum mopane mature seeds MeOH extract	40.98	8.78	2
Colophospermum mopane mature seeds MeOH extract – methanol fraction of methanol-heptane partition	>50		
Colophospermum mopane mature seeds MeOH extract - heptane fraction of methanol-heptane partition	35.37	4.02	3
Quinine	0.023	0.004	5
Chloroquine	0.057	0.001	5
Pyrimethamine	0.023	0.004	4

a, standard deviation; b, number of tests.

2.1.2.3. Radical scavenging activity and acetylcholinesterase inhibition activity

Both radical scavenging activity and acetylcholinesterase inhibition were measured in-house as TLC bioassays, in which a known amount of crude extract or fraction was deposited on a thin-layer chromatography (TLC) plate and eluted with a suitable solvent system prior to the respective assays. This allowed separation of the compounds in the extract or fraction, leading to easy localization of active zones and tracing of active compounds in a complex matrix. The method can thus be employed for the target-directed isolation of these constituents. The number of active zones on TLC together with the intensities of the active zones gave a measure of how active the extract was. In the radical scavenging test with DPPH, the methanol extract of *Schotia brachypetala* aril was the most active one, and gave the most intensive active zones on TLC. In the acetylcholinesterase inhibition test, methanol extracts of premature and mature seeds of *Colophospermum mopane* were the most active ones, and gave the most intensive active zones on TLC.

Since the methanol extract of *Schotia brachypetala* aril showed distinct activities in the radical

scavenging test with DPPH and anti-malaria test (IC_{50} 11.12 μg/ml), and the methanol extract of *Colophospermum mopane* immature seeds showed distinct activities in antimicrobial testing (*E. faecalis* ATCC 29212), and acetylcholinesterase inhibition, together with an interesting activity in the antimalarial test, these two methanol extracts were selected for further study.

2.2. Isolation strategy

The strategy of isolation in this work can be described as "semi-bioguided", and consisted of two parts: First, the active fractions, not necessarily the active compounds, were localized; second, the compounds (not necessarily the active ones), localized in the active fractions, were isolated with an effective preparative strategy. The isolated compounds were then evaluated for their biological activities. The whole process was monitored by TLC. The advantage of this "semi-bioguided" method is to minimize the isolation steps, since a long procedure may result in the formation of artifacts, loss of biological activity (by modification of the active principle on the chromatographic supports, for example), or loss of sample. Preparative isolation for each pure compound is not only for the structure determination, but also for the comprehensive biological testing in this work. For this reason, a good selection of different approaches is essential. The disadvantage is the limitation of the TLC analysis, with a relatively low resolution, which usually has to be compensated by HPLC analysis. With HPLC a convenient detection method is required; for example, coupling with mass spectrometry usually is suggested.

There are a number of preparative separation techniques, such as CC (open-column chromatography), VLC (vacuum liquid chromatography), PTLC (preparative thin-layer chromatography), flash chromatography, LPLC (low-pressure liquid chromatography), MPLC (medium-pressure liquid chromatography), each with their own characteristics (Hostettmann *et al*, 1998). In this work, high-speed counter-current chromatography (HSCCC) was chosen as the major separation technique. This technique is an all-liquid method, without solid phases, which relies on the partition of a sample between two immiscible solvents to achieve separation. The relative proportions of solute passing into each of the two phases is determined by the respective partition

coefficients (Marston and Hostettmann, 2006).

Modern countercurrent chromatography (CCC) has split into two basic directions. The first, which is called "CCC", mainly involves apparatus with a variable gravity field produced by a double axis gyratory motion and a seal-free arrangement for the column (generally tubing wrapped around bobbins). The second has been termed "centrifugal partition chromatography", or CPC, and employs a constant gravity field produced by a single axis rotation, together with rotatory seals for supply of solvent. Separation takes place in cartridges or disks. CPC with cartridges or disks is a hydrostatic equilibrium system and can be likened to a static coil. If the coil is filled with stationary phase of a biphasic solvent system and then the other phase is pumped through the coil at a suitable speed, a point is reached at which no further displacement of the stationary phase occurs and the apparatus contains approximately 50% of each of the two phases. Steady pumping-in of mobile phase results in elution of mobile phase alone (Marston and Hostettmann, 2006). This basic system uses only 50% of the efficient column space for actual mixing of the two phases. A more effective way of using the column space is to rotate the coil around its central axis while eluting the mobile phase. A hydrodynamic equilibrium is rapidly established between the two phases and almost 100% of the column space can be used for their mixing. CCC with rotating coil instruments is an example of this latter mechanism (Mandava and Ito, 1988).

The *type-J synchronous planetary motion* of a *multilayer coil* separation column in high-speed countercurrent chromatography (HSCCC) is illustrated in Figure 2.1. The planetary motion is produced by engaging a planetary gear mounted on the column holder axis to an identical stationary sun gear rigidly fixed to the centrifuge framework. This 1:1 gear coupling produces a particular type of planetary motion of the column holder, i.e., the holder rotates about its own axis while revolving around the centrifuge axis at the same angular velocity (synchronous) in the same direction. This planetary motion provides two major functions for performing CCC separation: a rotary-seal-free elution system so that the *mobile phase* is continuously eluted through the rotating separation column. The second and more important function is that it produces a unique hydrodynamic motion of two solvent phases within the rotating multilayer coiled column mainly due to the *Archimedean*

screw effect. When two immiscible solvent phases are introduced in an end-closed coiled column, the rotation separates the two phases completely along the length of the tube where the lighter phase occupies one end called the head and the heavier phase, the other end called the tail. In Figure 2.2 A, the coil at the top shows bilateral hydrodynamic distribution of the two phases in the coil where the white phase (head phase) occupies the head half and the black phase (tail phase) the tail half. This condition clearly indicates that white phase introduced at the tail end will move toward the head and similarly the black phase introduced at the head will move toward the tail. This hydrodynamic trend is effectively used for performing CCC as shown in Figure 2.2 B. The coil is first entirely filled with the white phase followed by pumping the black phase from the head end (Figure 2.2 B, upper diagram). Similarly, the coil is filled with the black phase followed by pumping the white phase from the tail (Figure 2.2 B, lower diagram). In either case, the mobile phase quickly moves through the coil, leaving a large volume of the other phase stationary in the coil (Ito, 2005).

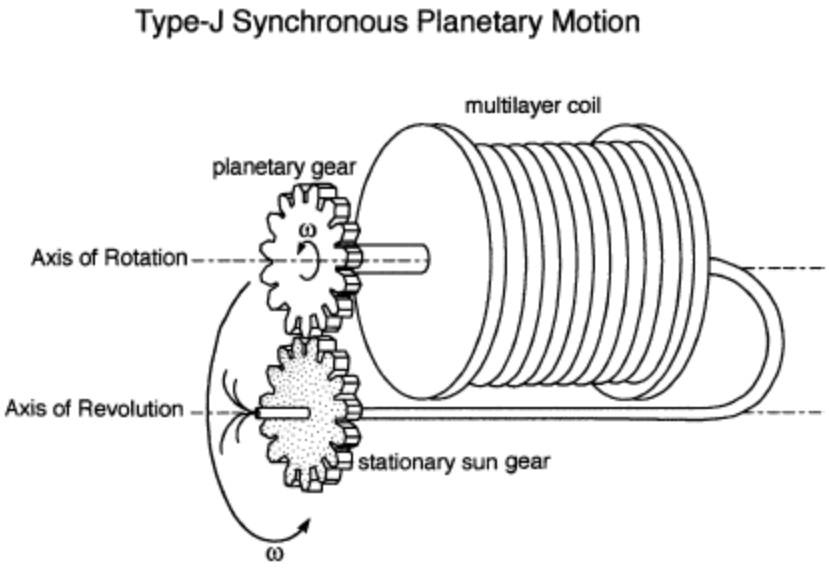

Figure 2.1 Type-J planetary motion of a multilayer coil separation column. The column holder rotates about its own axis and revolves around the centrifuge axis at the same angular velocity (ω) in the same direction. This planetary motion prevents twisting the bundle of flow tubes allowing continuous elution through a rotating column without risk of leakage and contamination (Ito, 2005).

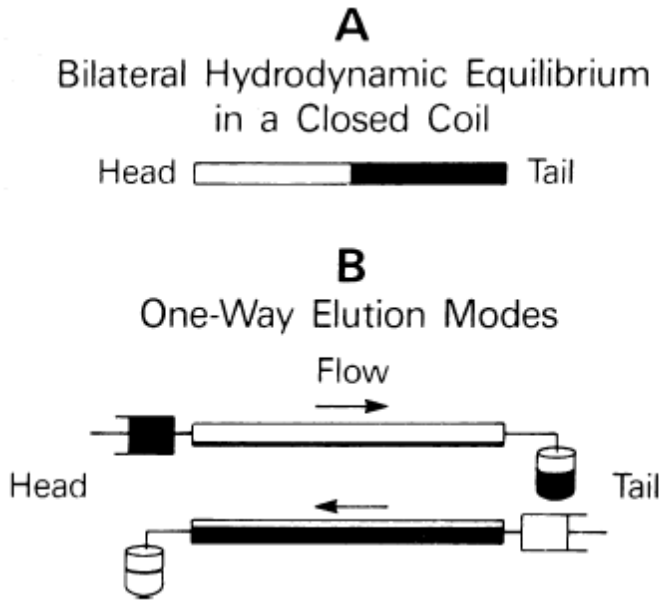

Figure 2.2 Mechanism of HSCCC. (A) Bilateral hydrodynamic distribution of two phases in the coiled column. (B) Elution mode of both lighter and heavier phases through the rotating coiled column (Ito, 2005).

HSCCC benefits from a number of advantages when compared with the more traditional liquid solid separation methods: (i) no irreversible adsorption; (ii) total recovery of injected sample; (iii) tailing minimized; (iv) low risk of sample denaturation; (v) low solvent consumption; and (vi) favourable economics (once the initial investment in an instrument has been made, no expensive columns are required and only common solvents are consumed). Although the efficiency (as represented by the number of theoretical plates) cannot match that of HPLC, the high selectivity and the high stationary to mobile phase ratio more than compensate. In HPLC, around 20% of the volume of the column is stationary (bonded) phase around the silica support, available for interaction with solute, while in CCC the figure for stationary phase content can be as high as 80%. Another advantage of CCC is the ability to reverse the flow direction and interchange the mobile and stationary phases ("reversed-phase" operation) (Marston and Hostettmann, 2006).

2.3. *Schotia brachypetala*

2.3.1. Fractionation of the methanol extract of the aril

Since the methanol extract of *Schotia brachypetala* aril showed distinct activities in the radical scavenging test with DPPH and the antimalarial test (IC_{50} 11.12 µg/ml), a bioactivity-guided fractionation was performed.

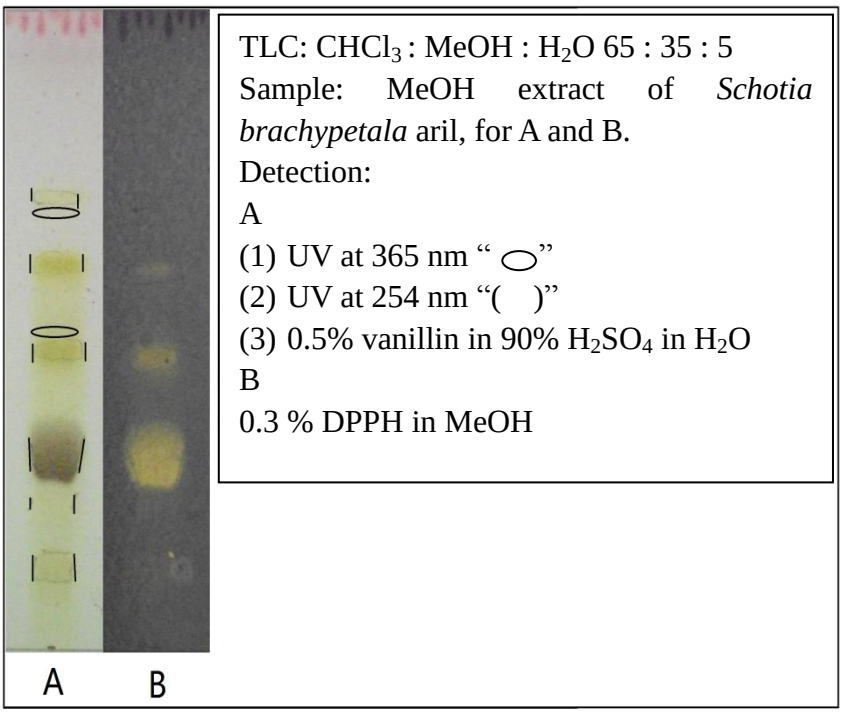

Figure 2.3 TLC Radical scavenging activity of the methanol extract of *Schotia brachypetala* aril.

The methanol extract of *Schotia brachypetala* aril was analyzed by HPLC (Figure 2.4).

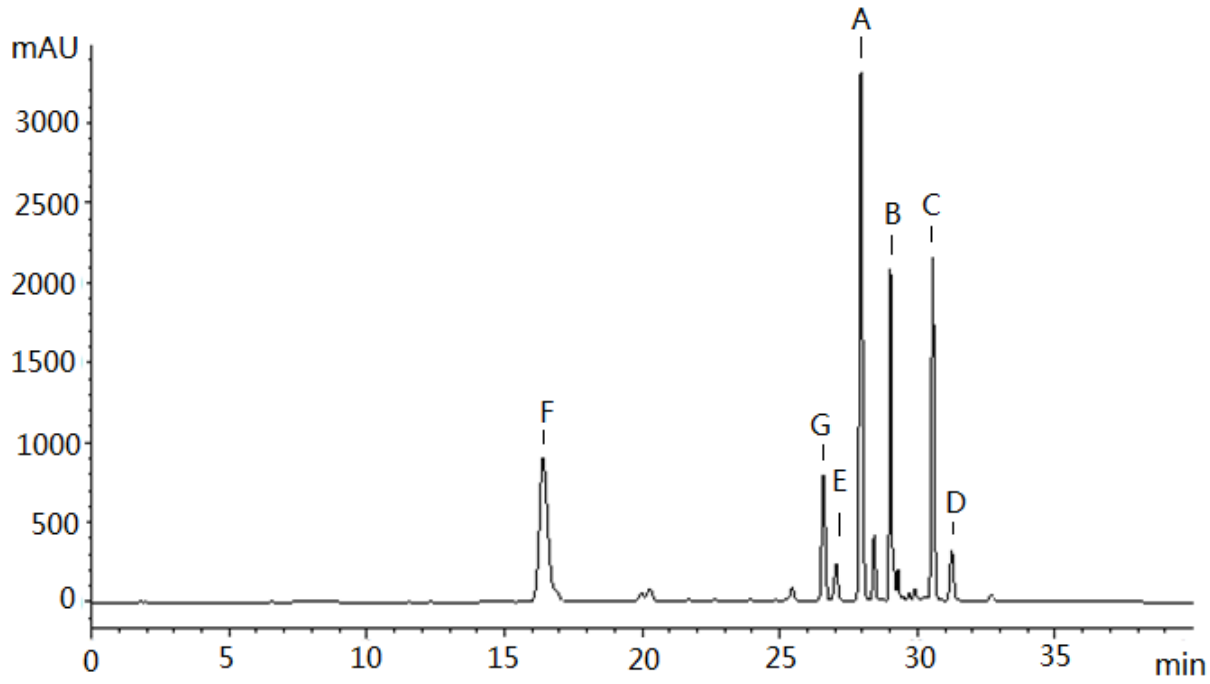

Figure 2.4 HPLC chromatogram of the methanol extract of *Schotia brachypetala* aril (detection: 254 nm). The subsequent isolates **A**-**G** are labeled. Conditions: column: Phenomenex C18 reverse phase column (150 x 4.6 mm, 5 micron); solvents: A: distilled H_2O + 0.1% formic acid, B: 70% MeOH/H_2O + 0.1% formic acid, gradient: 0-15 min, 10-30% B; 15-25 min, 30-70% B; 25-27 min, 70-100% B; 27-35 min, 100% B; 35-35.01 min, 100%-10% B; 35.01-45 min, 10% B; flow rate: 1 ml/min; sample: 10 µl of a solution of *Schotia brachypetala* aril MeOH extract at a concentration of 10 mg/ml in pure MeOH.

The methanol extract (200 mg) was fractionated by HSCCC into fractions I-VII, and each fraction was subjected to the antimalarial test again. The results are shown in Table 2.6. Fraction I had the highest activity.

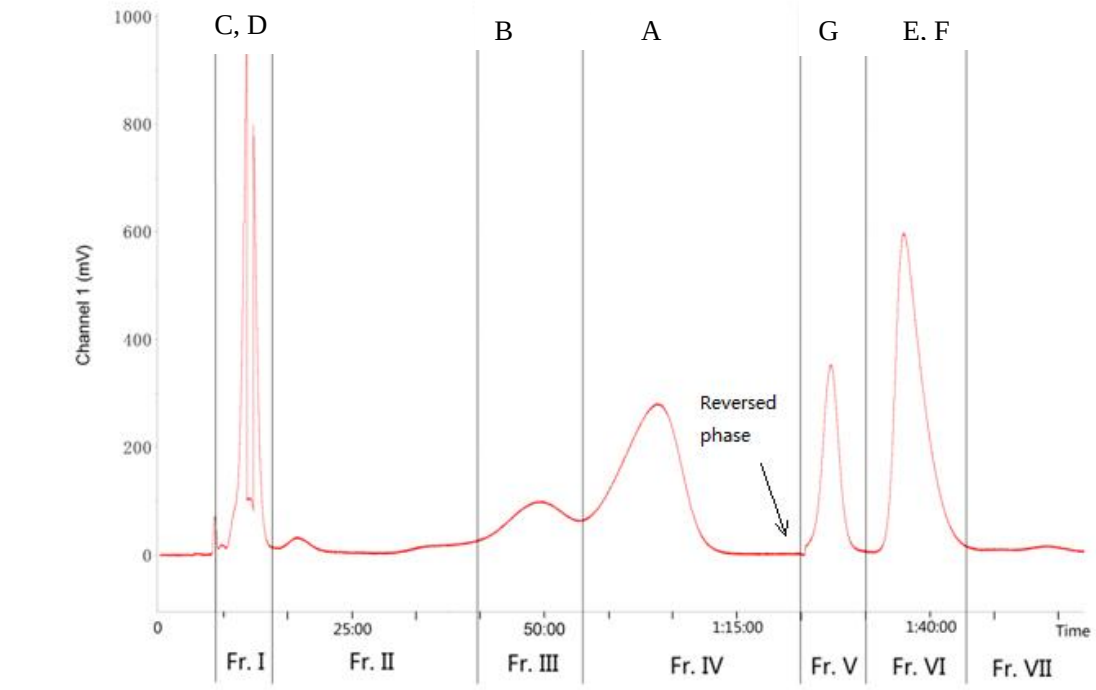

(a)

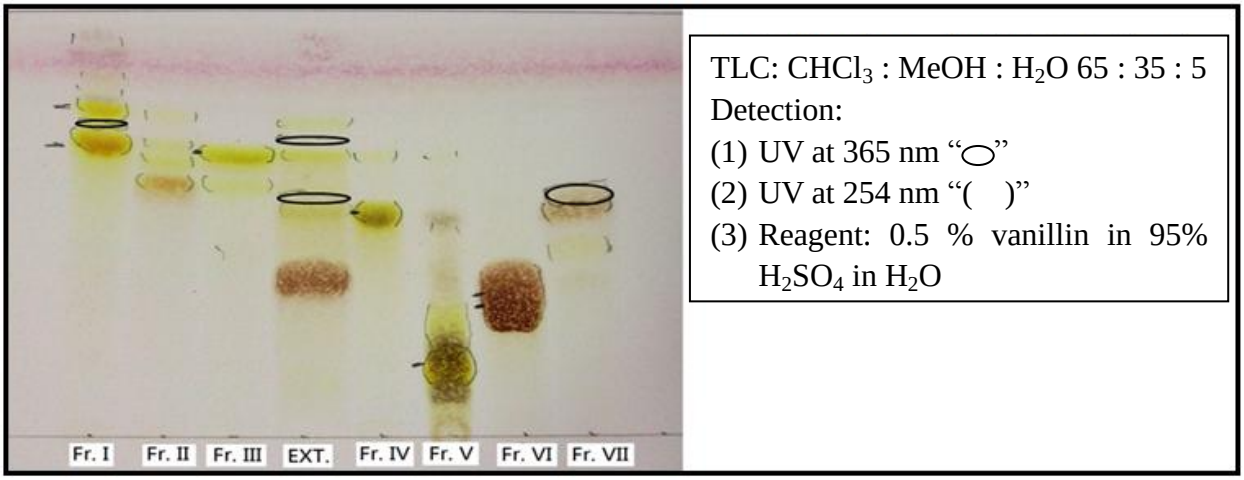

(b)

Figure 2.5 (a) HSCCC chromatogram of the MeOH extract of *S. brachypetala* aril. Solvent system: TBME : MeCN : 1% TFA in H_2O 2 : 2 : 3 (mobile phase: upper phase); 1500 rpm; flow rate: 3 ml/min; sample amount: 200 mg; UV detection: 254 nm. (b) TLC chromatogram of the fractions.

Table 2.6 Antimalarial activities of the HSCCC fractions I-VII from the methanol extract of *S. brachypetala* aril.

	IC_{50} (µg/ml)	s.d.[a]	n[b]
Methanol extract of *Schotia brachypetala* aril	17.58	2.06	5
Fr. I	10.15	3.10	3
Fr. II	26.27	3.00	3
Fr. III	>50		
Fr. IV	14.47	0.45	3
Fr. V	>50		
Fr. VI	15.89	2.58	3
Fr. VII	>50		
Quinine	0.023	0.004	5
Chloroquine	0.057	0.001	5
Pyrimethamine	0.023	0.004	4

a, standard deviation; b, number of tests.

2.3.2. Isolation of pure compounds

In order to have sufficient material for isolation of pure compounds (Figure 2.6), HSCCC was repeated with 1g of methanol extract (Figure 2.7). For gel filtration, the compounds were dissolved in MeCN or mixtures of MeCN and MeOH; elution was with either MeOH or MeOH and MeCN.

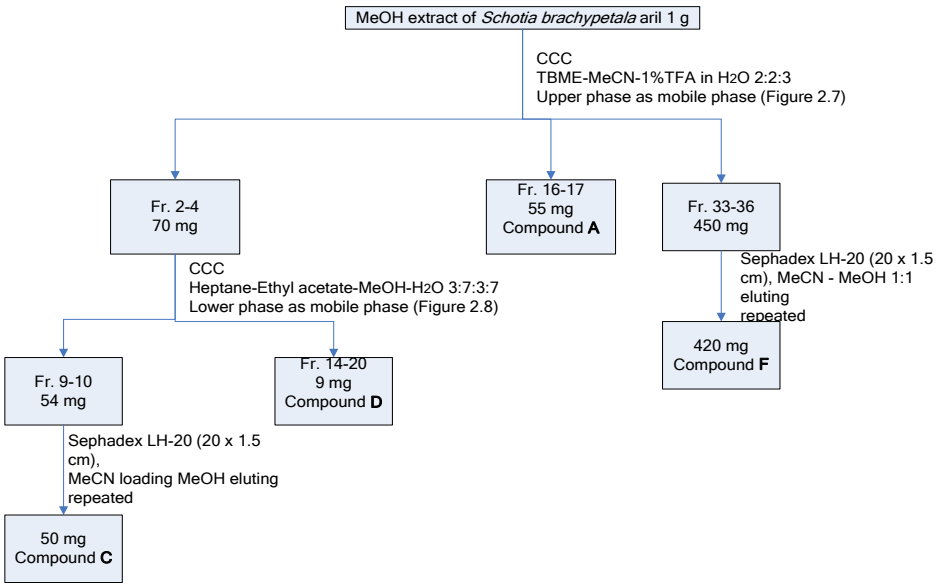

Figure 2.6 Isolation scheme of compounds **A, C**, **D**, **F** from the MeOH extract of *Schotia brachypetala* aril.

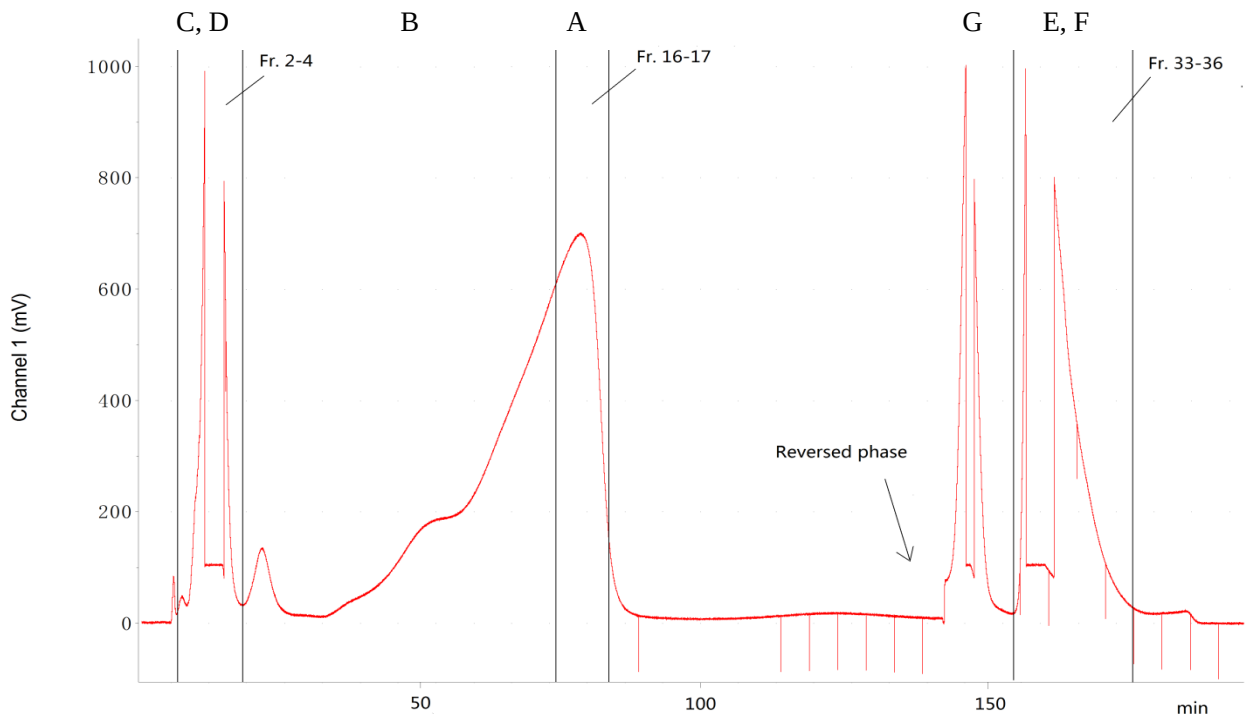

Figure 2.7 HSCCC chromatogram of the MeOH extract of *S. brachypetala* aril. Solvent system: TBME : MeCN : 1% TFA in H_2O 2 : 2 : 3 (mobile phase: upper phase); 1500 rpm, flow rate: 3 ml/min; sample amount: 1 g; UV detection: 254 nm.

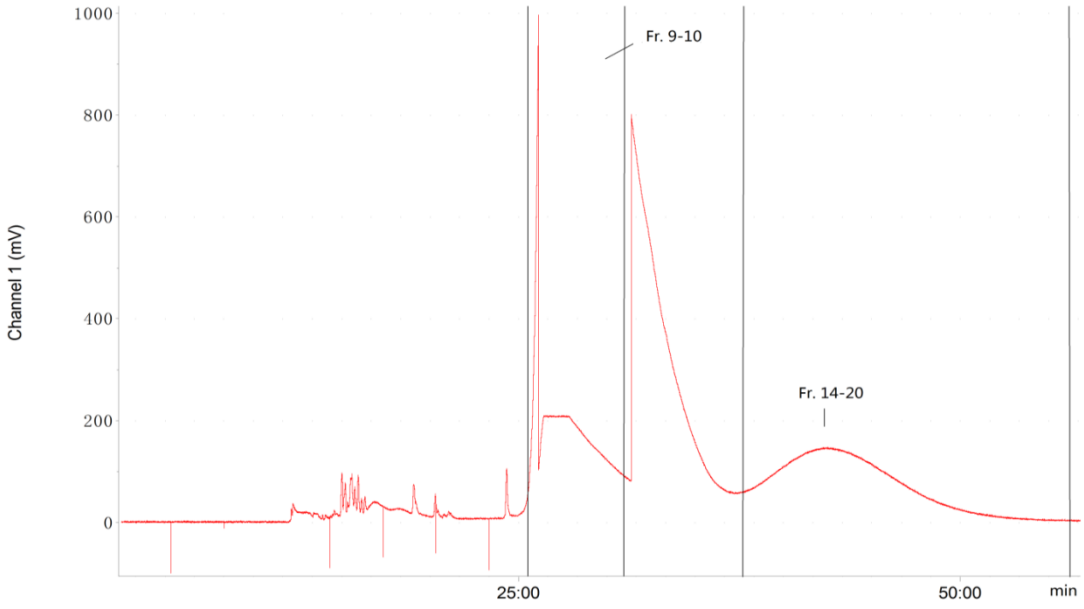

Figure 2.8 HSCCC chromatogram of Fr. 2-4 of the MeOH extract of *S. brachypetala* aril. Solvent system: Heptane : EtOAc : MeOH : H_2O 3 : 7 : 3 : 7 (mobile phase: lower phase); 1500 rpm, flow rate: 3 ml/min; sample amount: 70 mg; UV detection: 254 nm.

Repetition of HSCCC with the MeOH extract using TBME-MeCN-H_2O 2:2:3 led to the isolation of compounds **A-F** (Figure 2.9). Compounds **C** and **D** can be obtained from fractions 4-5, the same procedure as Figure 2.6.

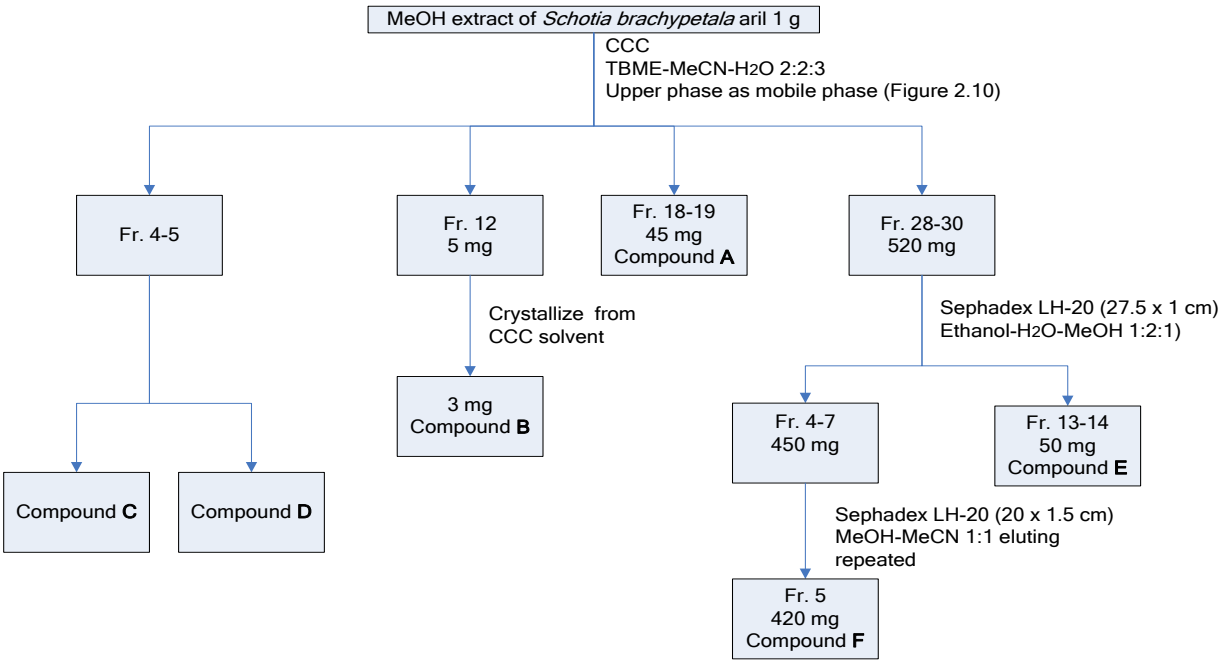

Figure 2.9 Isolation scheme of compounds **A-F** from the MeOH extract of *Schotia brachypetala* aril.

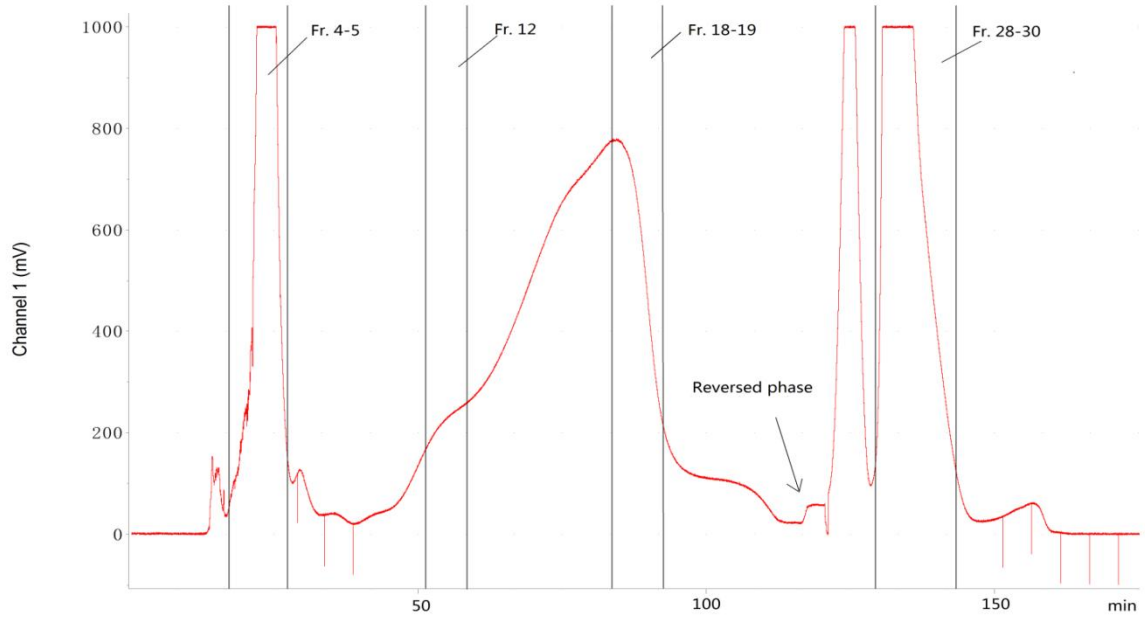

Figure 2.10 HSCCC chromatogram of the MeOH extract of *S. brachypetala* aril. Solvent system: TBME : MeCN : H_2O 2 : 2 : 3 (mobile phase: upper phase); 1500 rpm; flow rate: 3 ml/min; sample amount: 1 g; UV detection: 254 nm.

Compound **G** was isolated by the procedure shown in Figure 2.11.

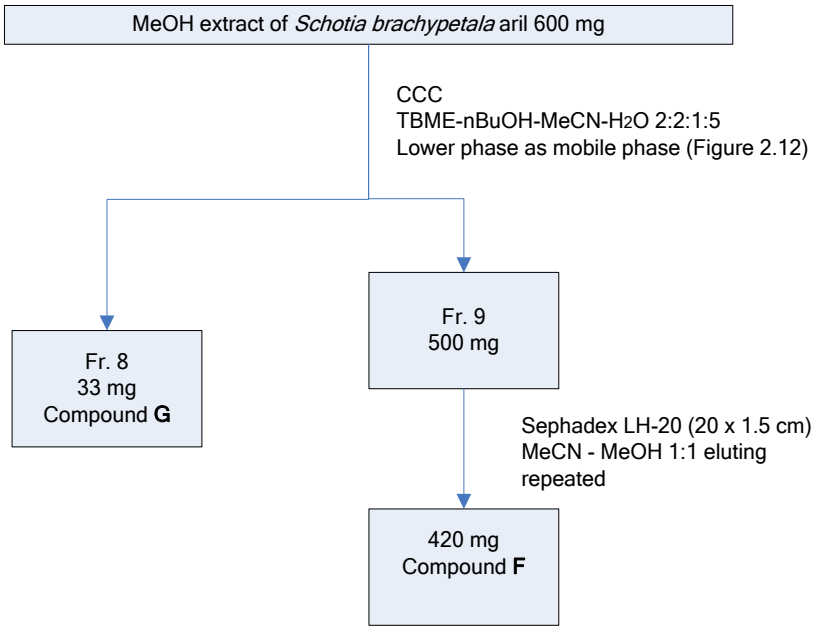

Figure 2.11 Isolation scheme of compounds **G** and **F** from the MeOH extract of *Schotia brachypetala* aril.

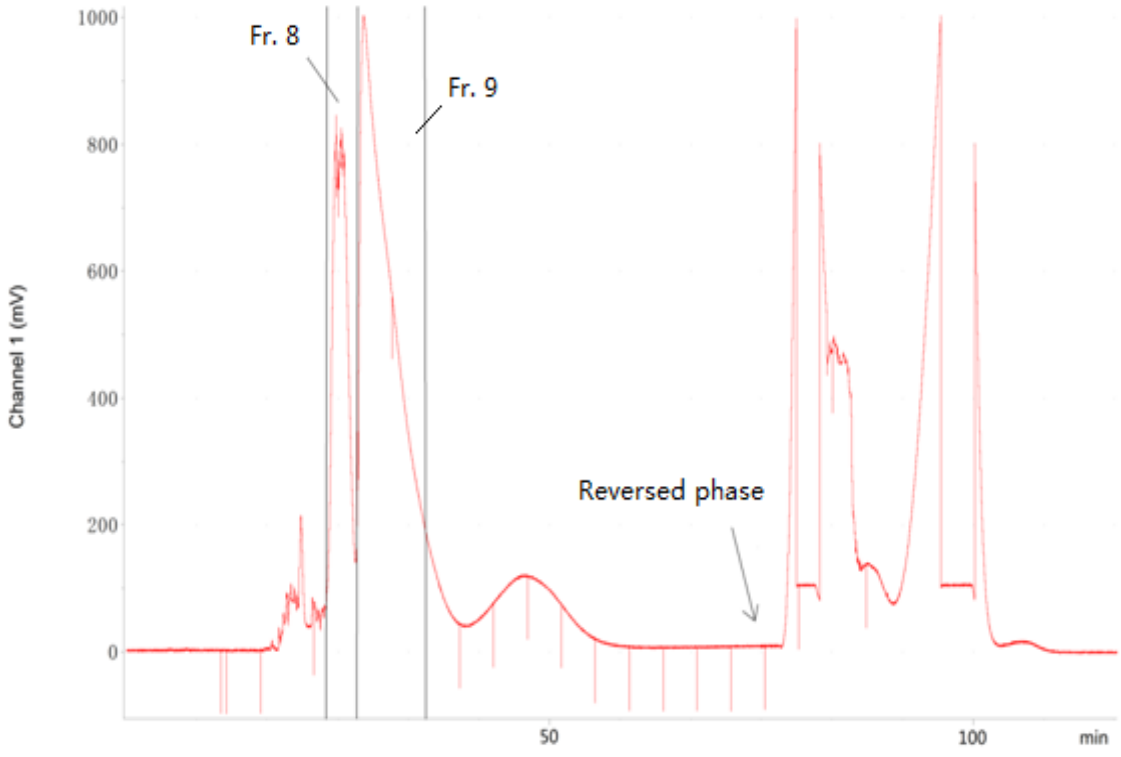

Figure 2.12 HSCCC chromatogram of the MeOH extract of *S. brachypetala* aril. Solvent system: TBME : nBuOH : $CHCl_3$: H_2O 2 : 2 : 1 : 5 (mobile phase: lower phase); 1500 rpm; flow rate: 3 ml/min; sample amount: 600 mg; UV detection: 254 nm.

2.3.3. Structure elucidation of pure compounds

2.3.3.1. Compound **A**

Compound **A** was isolated as fine yellow needle crystals. The positive LRESIMS showed a pseudomolecular ion at *m/z* 479 $[M + H]^+$ and the negative LRESIMS showed one at *m/z* 477 $[M - H]^-$; the former ion analyzed for $C_{22}H_{23}O_{12}$. Information from the ^1H NMR and ^{13}C NMR spectra, confirmed the molecular formula as $C_{22}H_{22}O_{12}$. Unambiguous NMR assignments were determined by Homonuclear Correlation Spectroscopy (^1H-^1H COSY), Gradient Heteronuclear Single Quantum Coherence (^1H-^{13}C HSQC), and Gradient Heteronuclear Multiple Bond Correlation (^1H-^{13}C HMBC) experiments. The UV-vis absorption spectra indicated a flavonol derivative, and the spectra after addition of different shift reagents suggested the 3, 7-hydroxyl groups to be substituted and the presence of a *o*-diOH system on the B ring. Two proton doublets at δ 6.75 (1H, *d*, *J* = 2.1 Hz) and δ 6.48 (1H, *d*, *J* = 2.1 Hz) correlating with the carbons at δ 93.76 and 98.76 respectively in the HSQC spectrum, were assigned to the H-8 and H-6 protons of ring A. From the HMBC experiment, ring B was assigned as a 1, 3, 4-trisubstituted benzene ring. The ^1H NMR spectrum showed an ABX coupling system, with chemical shifts of δ 7.65 (1H, *d*, *J* = 2.1 Hz), δ 7.56 (1H, *dd*, ^3J = 8.5 Hz, ^4J = 2.1 Hz) and δ 6.91 (1H, *d*, *J* = 8.5 Hz), which were assigned to H-2′, H-6′ and H-5′ respectively. The three proton singlet at δ 3.80 correlated with the carbon at δ 59.10 in the HSQC spectrum and suggested a methoxy group. The HMBC experiment displayed a long-range correlation between the three protons of the methoxy group and C-3 (δ 137.72), revealing the site of the methoxy group. Collectively, these data indicated that the aglycone moiety was 3-*O*-methylquercetin. In the ^{13}C NMR spectrum, one anomeric resonance at δ 99.62 and 5 oxygenated carbon resonances in the δ 60-80 region suggested the presence of a sugar, which was in accordance with the supplementary proton signals in the ^1H NMR spectrum. The sugar was hydrolyzed by acid and identified as *β*-glucose based on TLC elution with a reference standard (Figure 2.20) and the coupling constant (*J* = 7.2 Hz) of the anomeric H-1″ in the ^1H NMR spectrum. The HMBC experiment displayed a long-range correlation between C-7 (δ 162.73) and the anomeric proton (δ 5.07, *d*, *J* = 7.2 Hz), revealing the site of glycosylation as the 7-OH of 3-*O*-methylquercetin. Thus the structure of

compound **A** was determined as transilin (3-*O*-methylquercetin 7-*O*-*β*-glucopyranoside).

Compound **A** has been isolated from several sources, including *Lepisorus contortus* (Yang *et al.*, 2011), *Conyza discoridis* (Alqasoumi, 2009), *Paulownia fortunei* (Zhang and Li, 2008), *Opuntia* (Chen *et al.*, 2003), *Parodia sanguiniflora* (Iwashina *et al.*, 1984), *Trifolium pratense* (Jain and Saxena, 1986), *Nicotiana* species (Jurzysta *et al.*, 1983), *Carthamus glaucus* (Khafagy *et al.*, 1978) and *Inula viscose* (Oksuz, 1977).

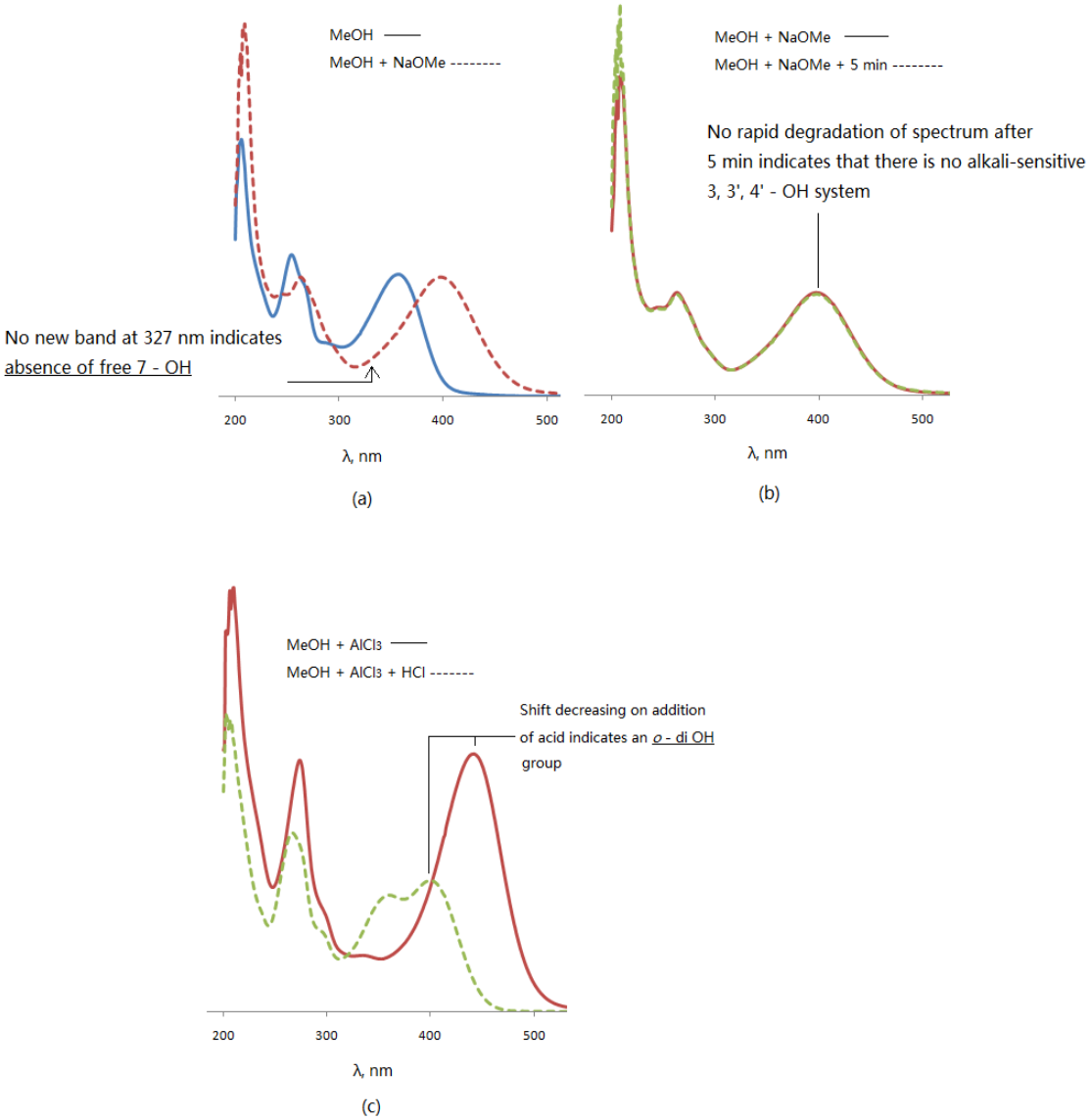

Figure 2.13 UV-vis spectra of compound **A** obtained after the addition of different shift reagents.

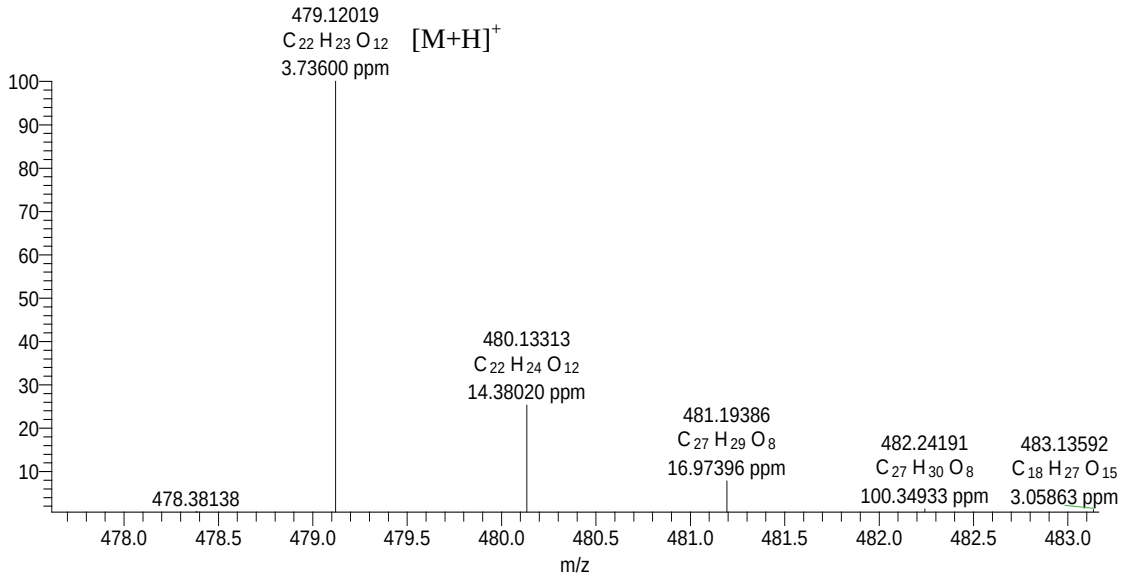

Figure 2.14 HRESIMS spectrum of compound **A**

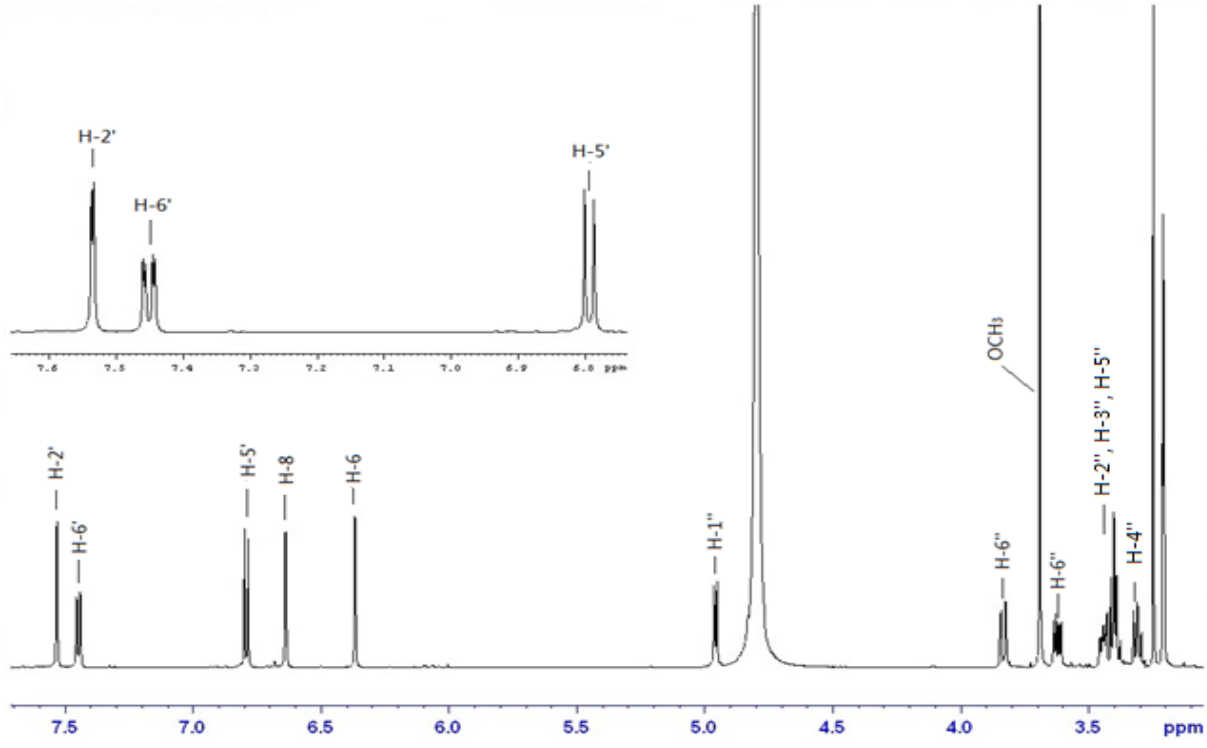

Figure 2.15 ^{1}H NMR spectrum (600 MHz, CD_3OD) of compound **A**

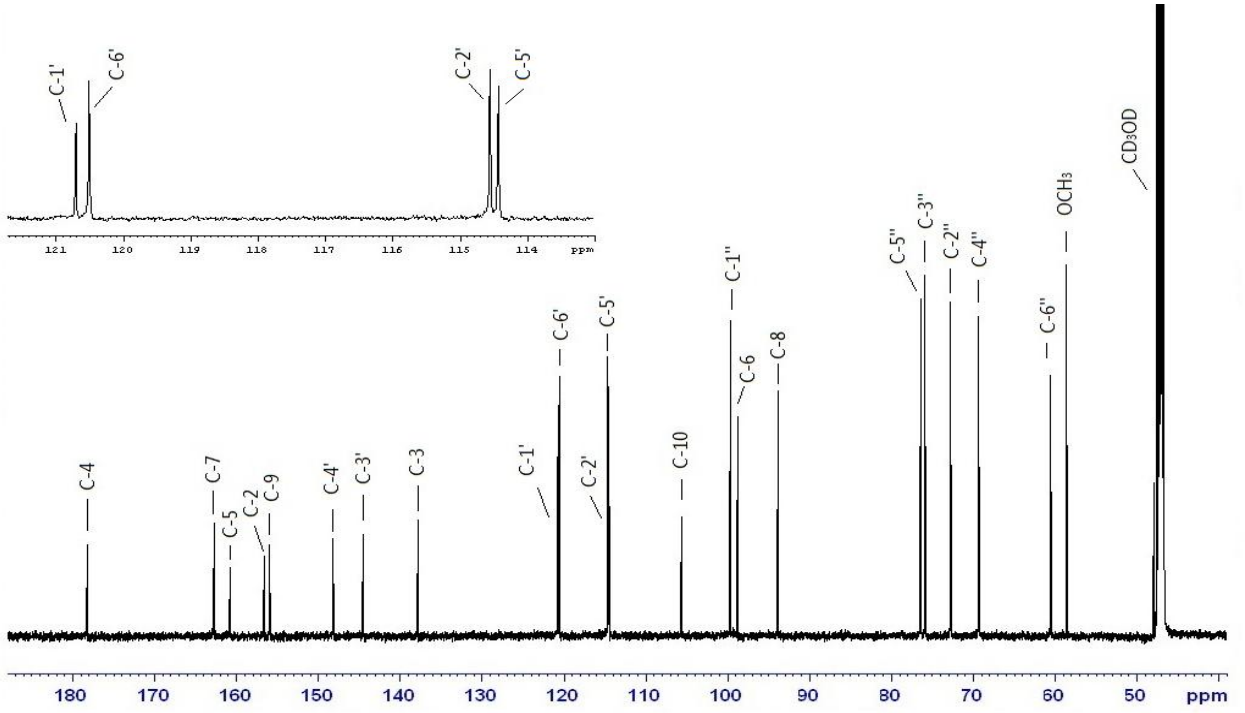

Figure 2.16 ^{13}C NMR spectrum (150 MHz, CD_3OD) of compound **A**

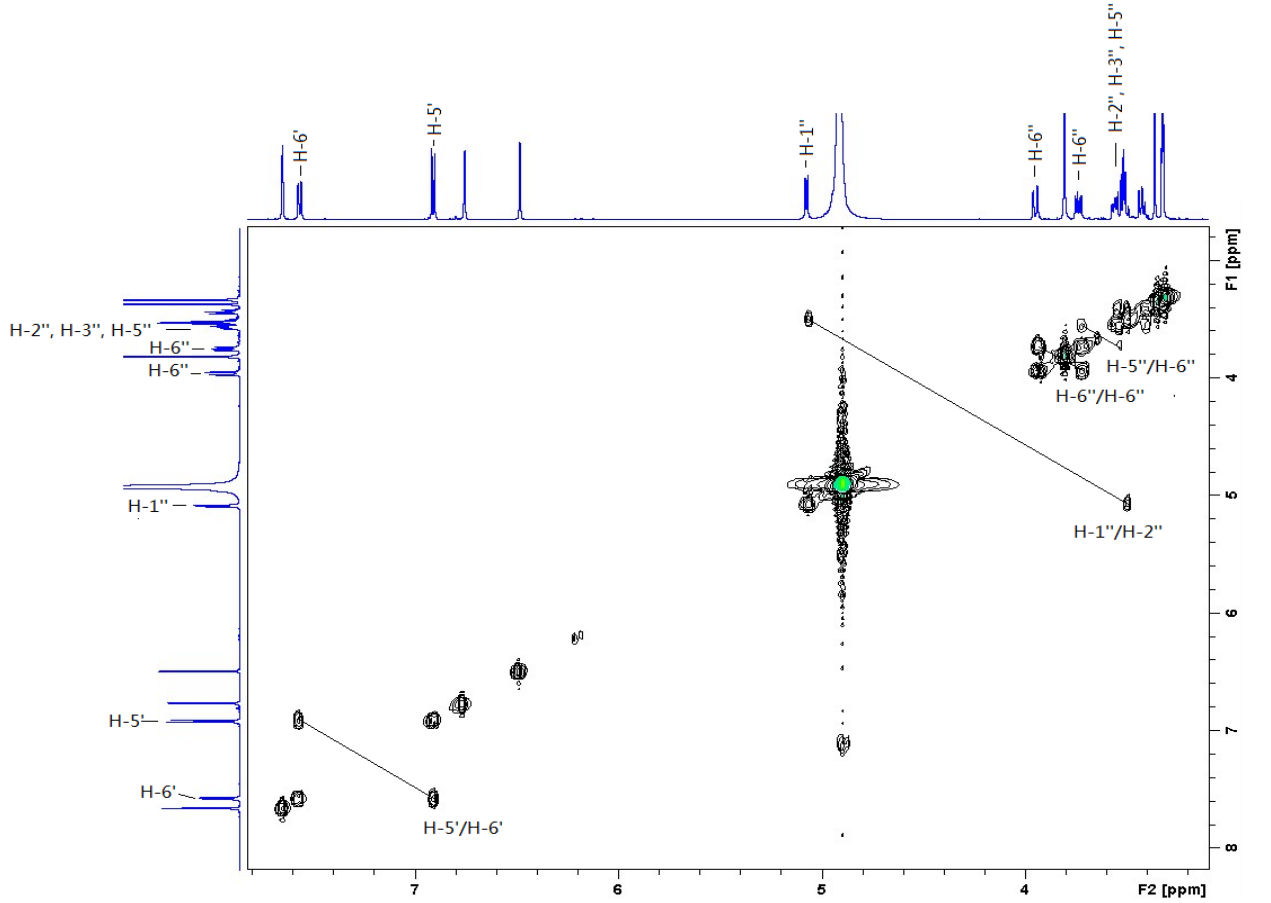

Figure 2.17 COSY spectrum of compound **A**.

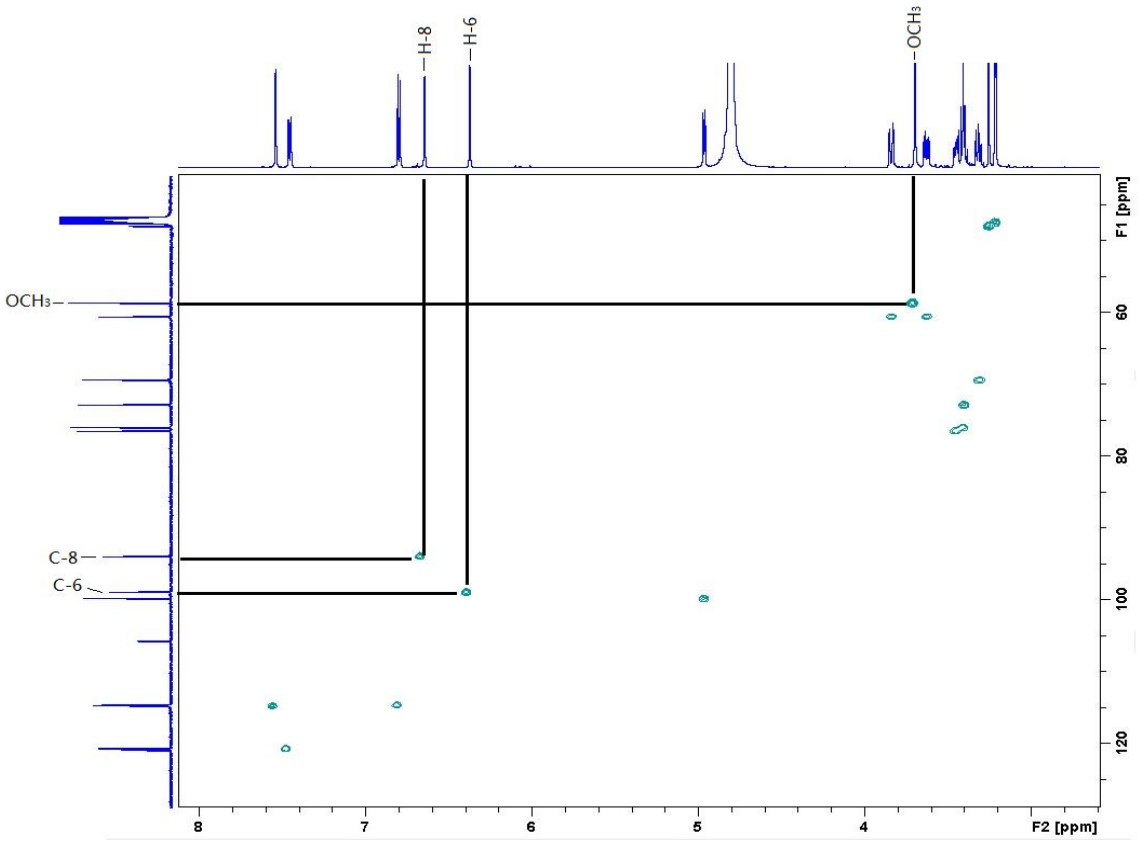

Figure 2.18 HSQC spectrum of compound **A**.

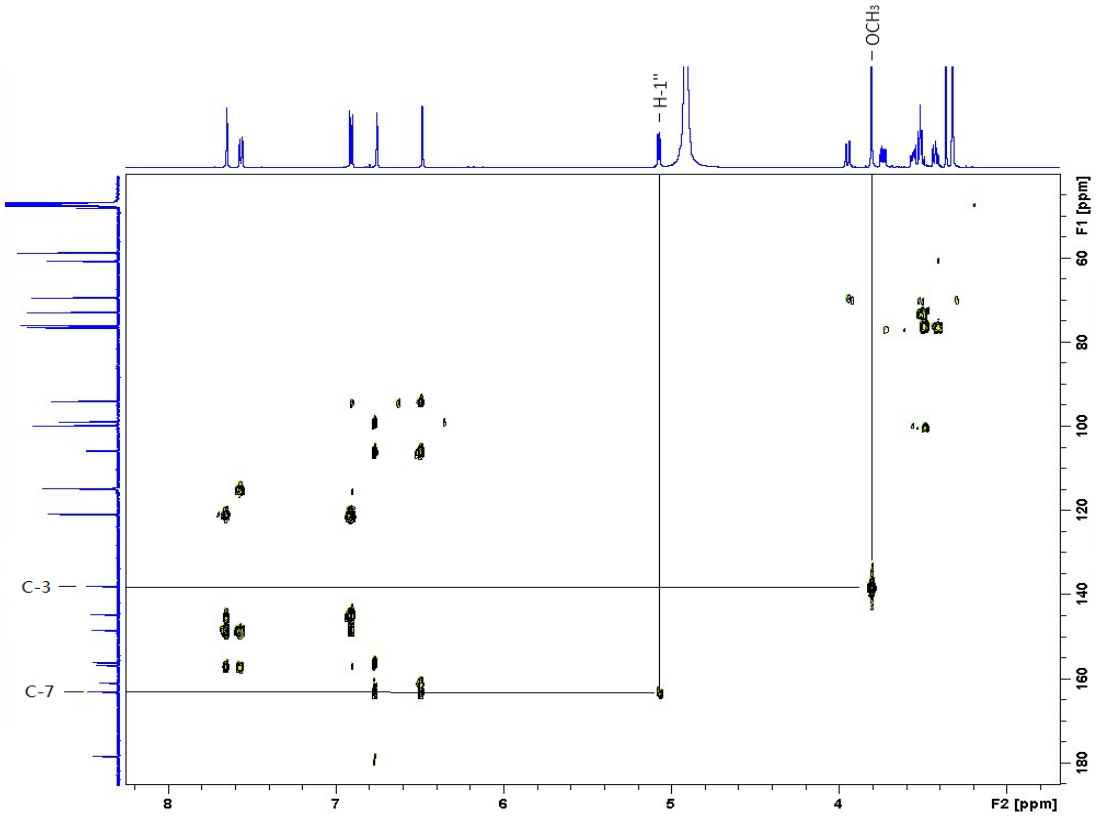

Figure 2.19 HMBC spectrum of compound **A**.

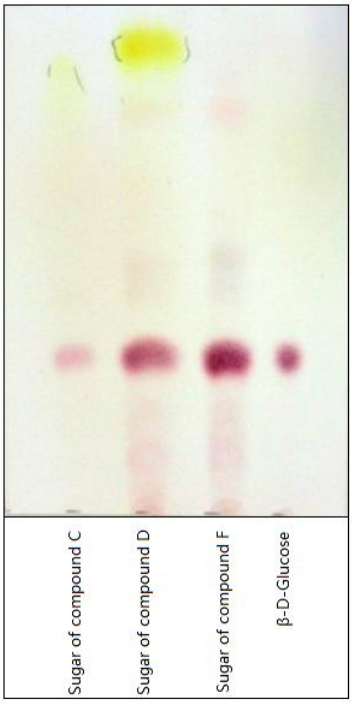

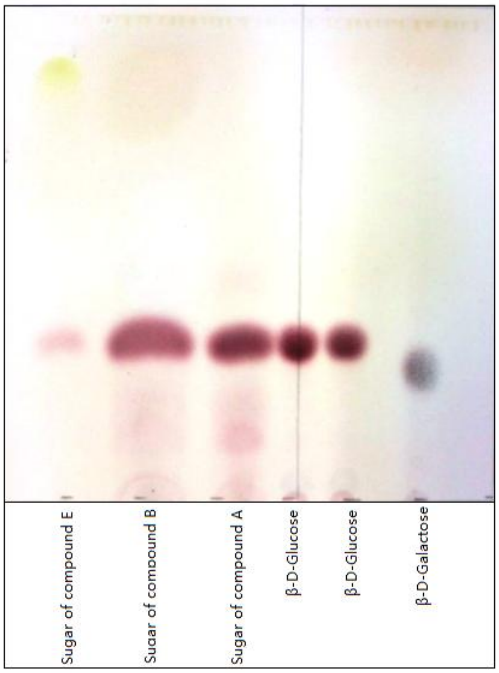

TLC:
$CHCl_3$: *n*-BuOH : MeOH : H_2O : CH_3COOH 9 : 25 :10 :3 :3
Detection:
0.05 g naphthoresorcinol
0.1 g diphenylamine
1 ml conc. H_2SO_4
25 ml Ethanol

Figure 2.20 Sugars of compounds **A**, **B**, **C**, **D**, **E** and **F** were acid hydrolyzed and co-eluted with the reference standards β-D-glucose and β-D-galactcose. With the detection reagent, β-D-glucose showed a pink color and β-D-galactose showed a purple color on TLC.

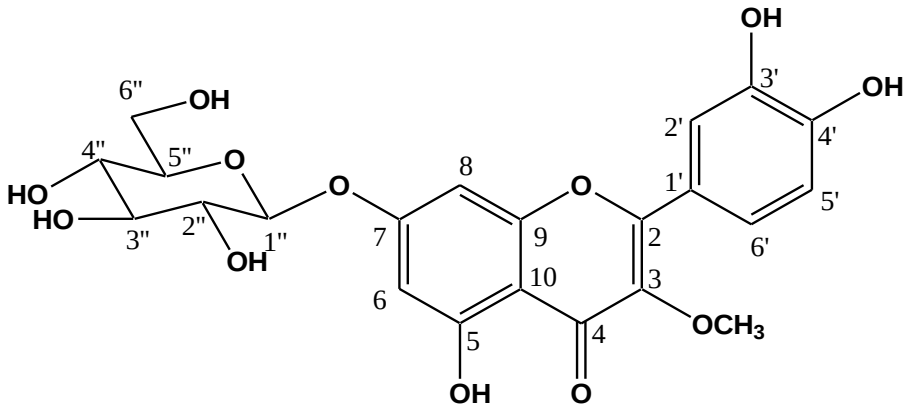

Structure of compound A

2.3.3.2. Compound **B**

Compound **B** was obtained as pale green crystals. The UV-vis absorption spectra indicated a flavonol derivative, and the spectra after addition of different shift reagents suggested the 3, 7,

4′-hydroxyl groups to be substituted. The positive HRESIMS showed a pseudomolecular ion at *m/z* 493 $[M+H]^+$, which analyzed for the molecular formula $C_{23}H_{25}O_{12}$. This was confirmed by ^1H and ^{13}C NMR spectra and an APT experiment. ^1H and ^{13}C NMR spectra of the sample were recorded in methanol-d_4 for comparison with the spectrum of compound **A**. However, because of the poor solubility in methanol-d_4, more comprehensive 2D NMR spectra were run in DSMO-d_6 for complete structure investigation. In the ^1H spectrum in methanol-d_4 compared with compound **A**, two proton doublets at δ 6.77 (1H, *d*, *J* = 2.0 Hz) and 6.49 (1H, *d*, *J* = 2.0 Hz) were assigned to H-8 and H-6 protons of ring A, an ABX coupling system was present, i.e., δ 7.67 (1H, *dd*, ^3J = 8.6 Hz, ^4J = 2.1 Hz), 7.63 (1H, *d*, *J* = 2.1 Hz), 7.08 (1H, *d*, *J* = 8.6 Hz), which was assigned to H-2′, H-6′, H-5′ respectively, and two three-proton singlets at δ 3.81 and 3.94 suggested the presence of two methoxyl groups. The sites of the two methoxy groups were suggested to be at C-3 and C-4′ by HSQC and HMBC experiments. Collectively, these data indicated that the aglycone moiety was 3,4′ di-*O*-methylquercetin. The sugar was hydrolyzed by acid and identified as a *β*-glucose based on the elution with a reference standard (Figure 2.20) and the coupling constant (*J* = 7.2 Hz) of the anomeric proton in the ^1H NMR spectrum. The HMBC experiment (recorded in DMSO-d_6) displayed a long-range correlation between C-7 (δ 162.84) and the anomeric proton (δ *ca*. 5.1, *d*, *J* = 7.2 Hz), revealing the site of glycosylation as the 7-OH of 3,4′-di-*O*-methylquercetin. Thus the structure of compound **B** was determined as 3,4′-di-*O*-methylquercetin 7-*O*-*β*-glucopyranoside. Complete assignment of the ^1H and ^{13}C NMR signals was achieved with the help of the two dimensional COSY, HSQC and HMBC spectra.

Compound **B** was firstly isolated and reported from *Dillenia indica* by Tiwari *et al*., 1979. Since the NMR spectra data was not complete in the literature, full assignment was achieved with the help of two-dimensional NMR experiments in this work.

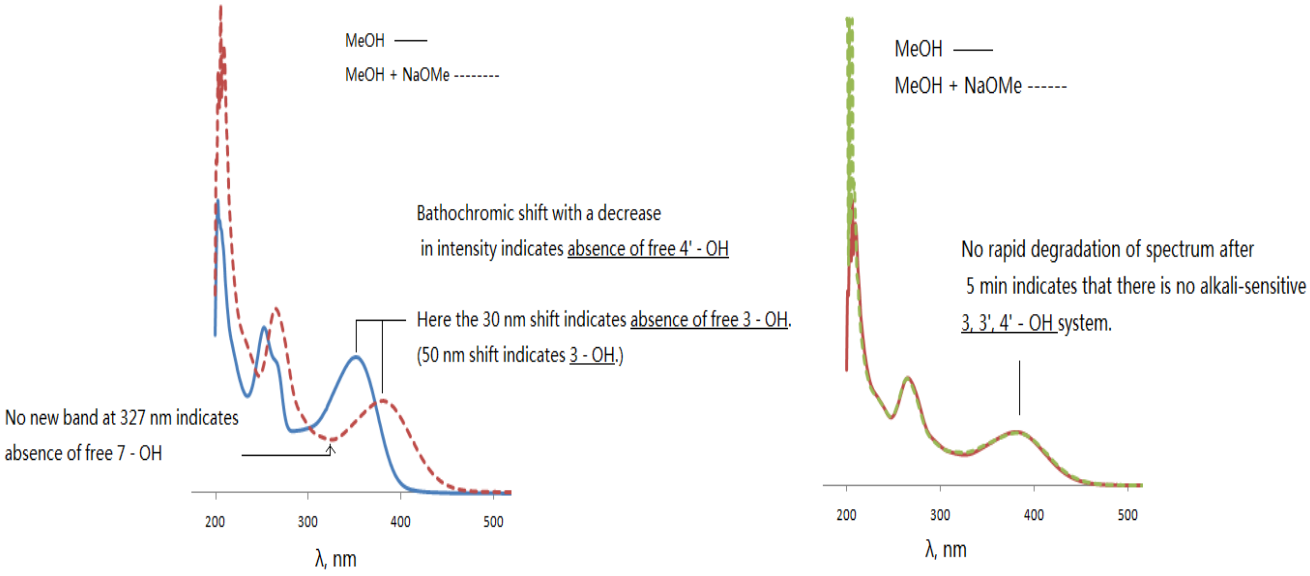

Figure 2.21 UV-vis spectra of compound **B** obtained after the addition of different shift reagents.

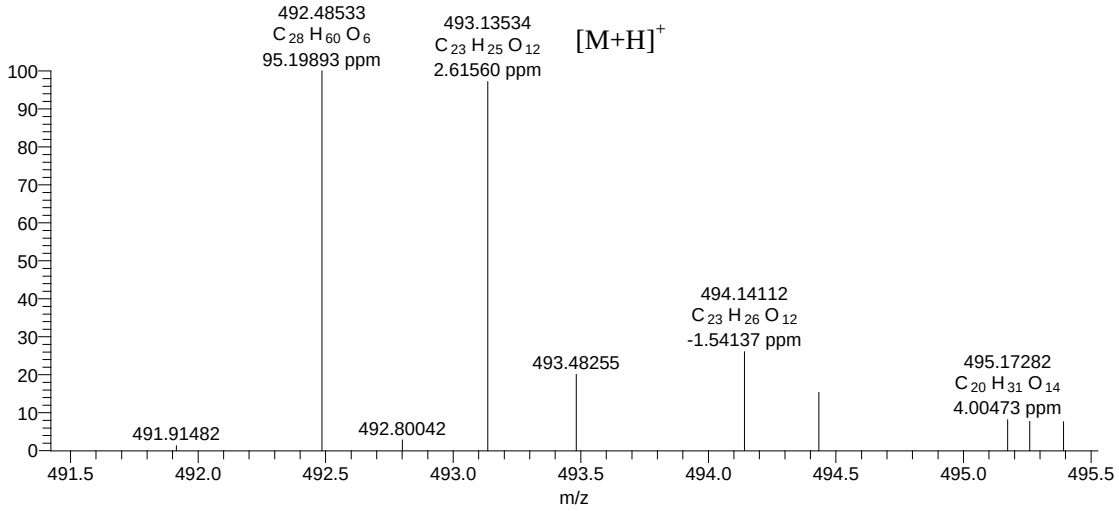

Figure 2.22 HRESIMS spectrum of compound **B**.

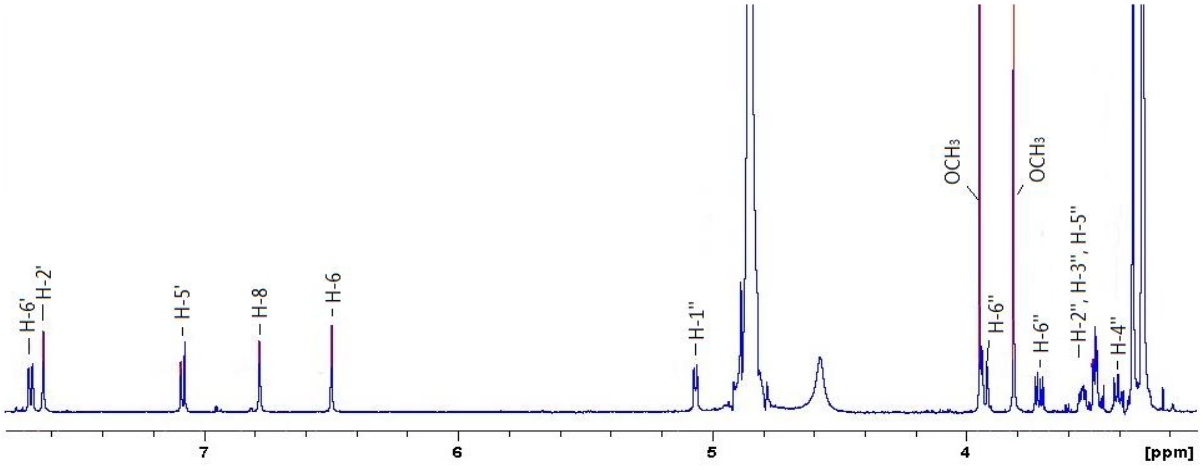

Figure 2.23 ^{1}H NMR spectrum (600 MHz, CD_3OD) of compound **B**.

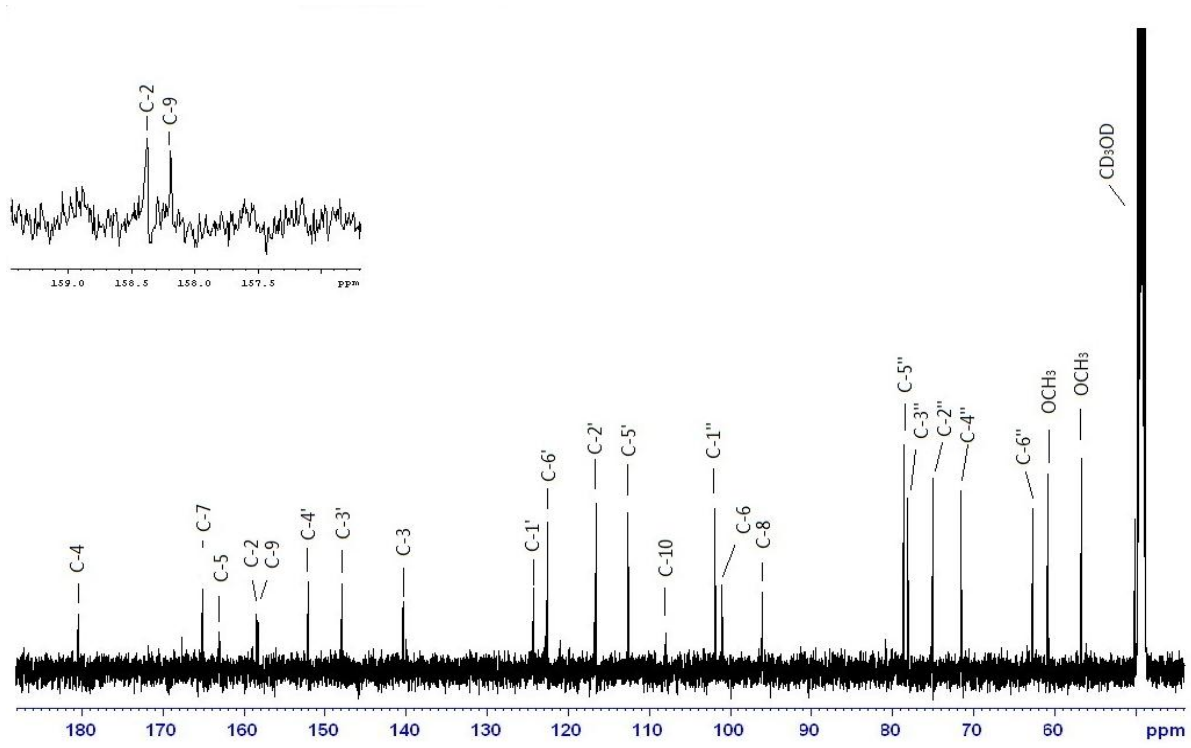

Figure 2.24 ^{13}C NMR spectrum (150 MHz, CD_3OD) of compound **B**

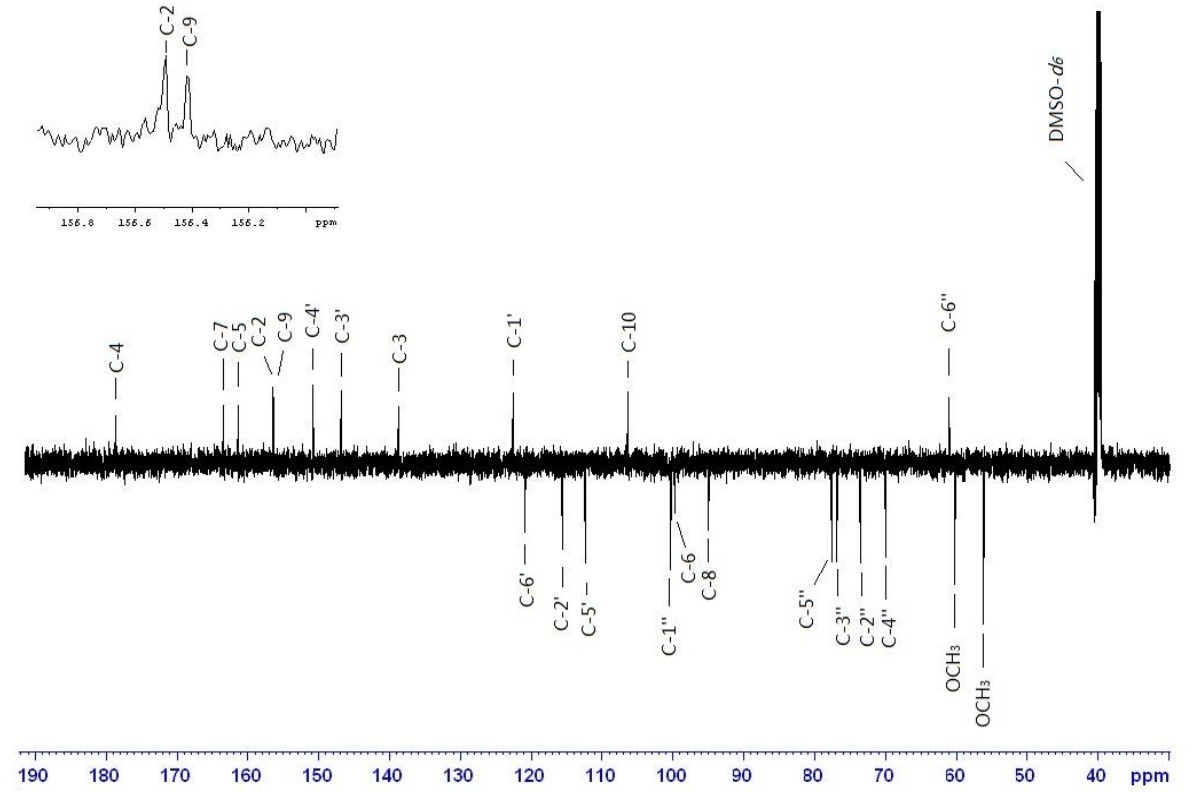

Figure 2.25 APT experiment (150 MHz, DMSO-d_6) of compound **B**.

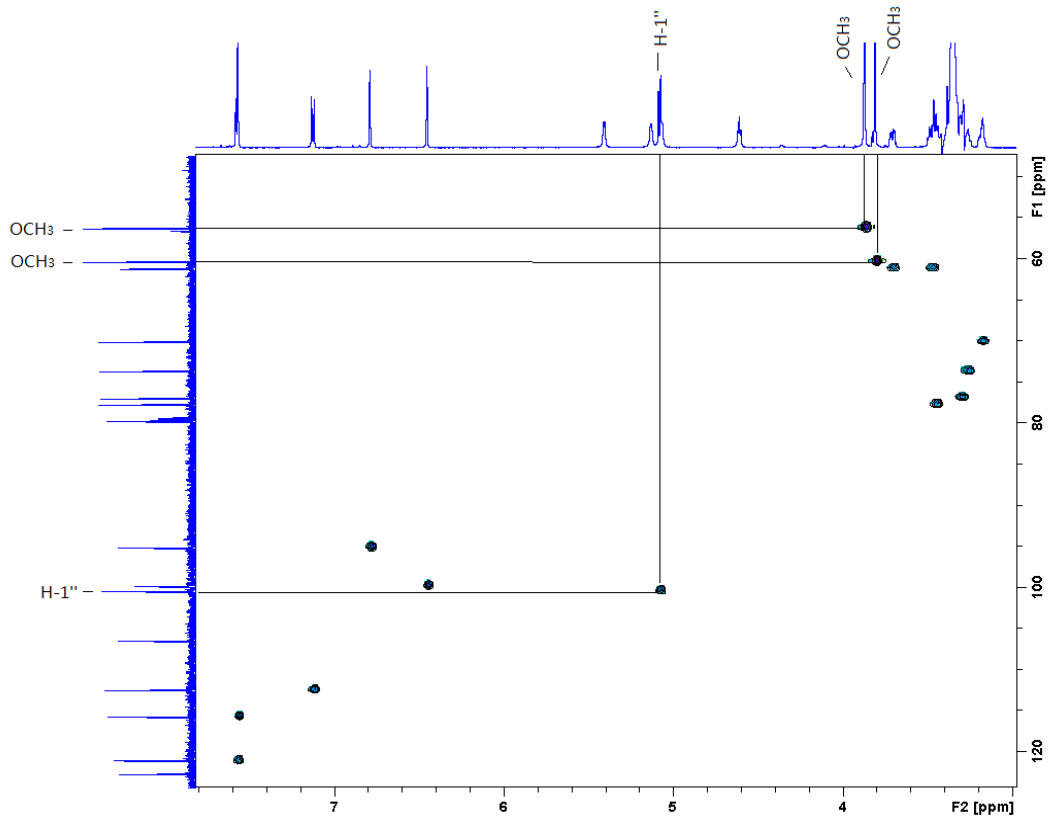

Figure 2.26 HSQC (DMSO-d_6) spectrum of compound **B**.

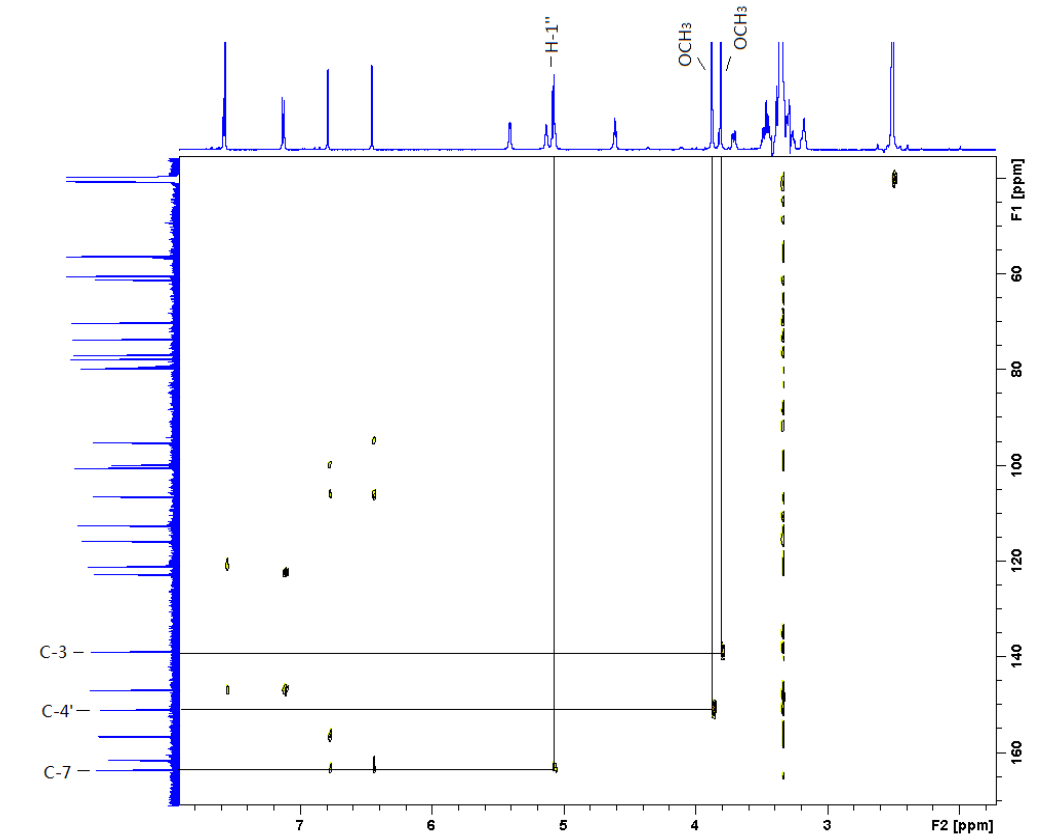

Figure 2.27 HMBC (DMSO-d_6) spectrum of compound **B**.

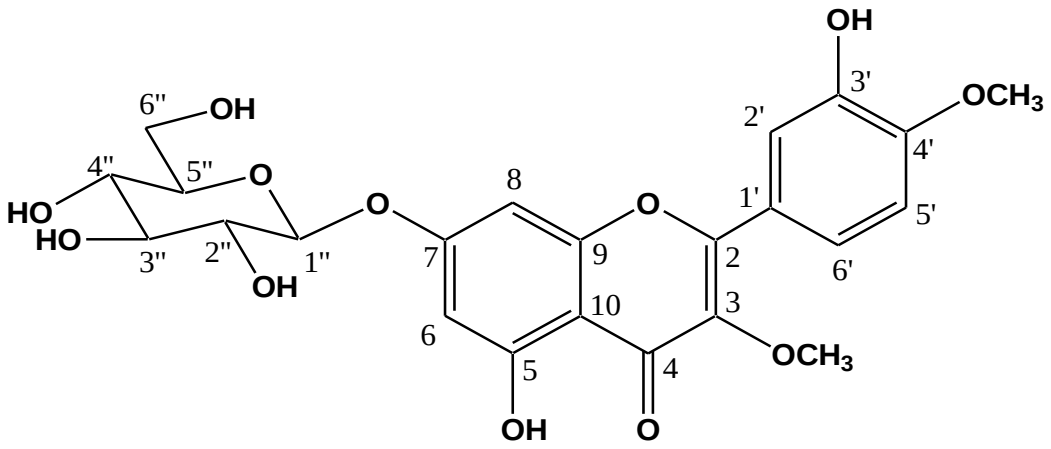

Structure of compound B

2.3.3.3 Compound **C**

Compound **C** was obtained as yellow amorphous product. The positive LRESIMS showed a pseudomolecular ion at *m/z* 625 $[M + H]^+$ and the negative LRESIMS gave a pseudomolecular ion at *m/z* 623 $[M - H]^-$; the former ion analyzed for $C_{31}H_{29}O_{14}$ in the HRESIMS, and together with the ^1H NMR spectrum and APT experiment, confirmed the molecular formula to be $C_{31}H_{28}O_{14}$.

In the ^{13}C NMR spectrum (Figure 2.31), among the 6 oxygenated carbon resonances in the δ 60-80 region, one at δ 59.01correlated with a three-proton singlet at δ 3.74 in the HSQC spectrum (Figure 2.37), suggesting a methoxy group; the other five oxygenated carbon resonances, together with one anomeric carbon resonance at δ 99.78 correlating with a doublet at δ 5.08 (1H, *d*, *J* = 7.2 Hz), suggested the presence of a sugar. Complete acid hydrolysis of compound C gave *β*-glucose, determined by eluting with a reference standard on TLC (Figure 2.20) and the coupling constant (*J* = 7.2 Hz) of the anomeric proton in the ^1H NMR spectrum. The absolute configuration of glucose was determined as D-glucose by GC analysis of its thiazolidine derivative (Figure 2.40). Of the 29 signals present in the ^{13}C NMR spectra of compound **C**, 21 corresponded to those of compound **A** (3-*O*-methylquercetin 7-*O*-*β*-glucopyranoside). The remaining signals were attributed to an acyl moiety comprised of nine carbons, including an ester carbonyl (δ 167.64). The presence of an absorption band at 314 nm in the UV-vis spectrum suggested another type of phenolic compound

since flavonoids lack significant absorptions in this region. The ^{1}H NMR spectrum showed two doublets at δ 6.27 (J = 15.6 Hz) and 7.53 (J = 15.9 Hz) characteristic of a *trans*-double bond and an AA′BB′ coupling system, i.e., δ 6.64 (2H, *d*, J = 8.5 Hz), 7.19 (2H, *d*, J = 8.5 Hz). Consequently, with the help of two dimensional HSQC, HMBC and COSY experiments, this fragment was identified to be a *p*-coumaryl ester. The linkage of this fragment to the 6''-OH was established by the significant downfield shift of glucose H_2-6'' (δ 4.62, 1H, *dd*, ^{2}J = 12.2, ^{3}J = 2 Hz; δ 4.29, 1H. *dd*, ^{2}J = 12.2 Hz, ^{3}J = 8.1 Hz). The HMBC spectrum, in which the ester carbonyl carbon at δ 167.64 was correlated to H-6'', further substantiated these findings.

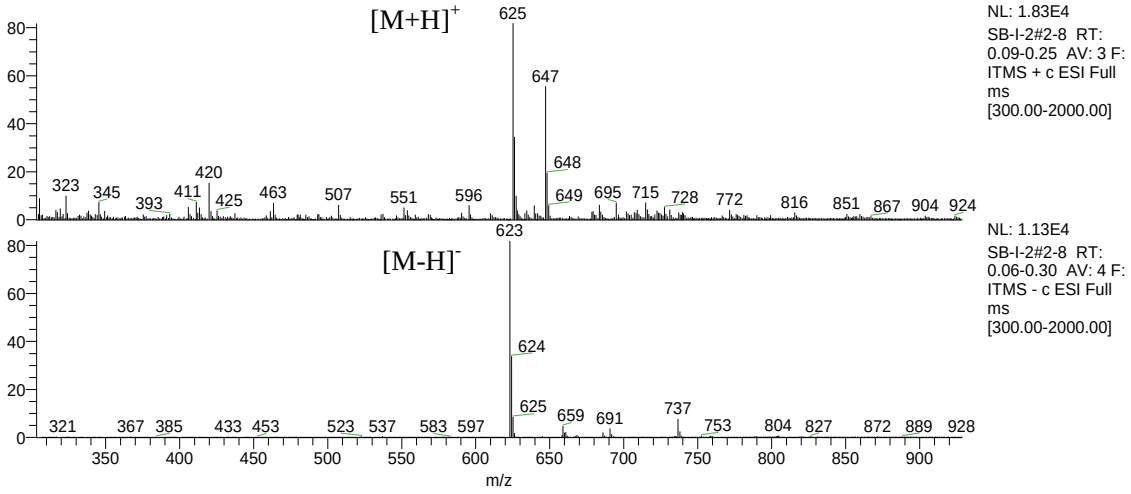

Figure 2.28 LRESIMS spectrum of compound **C**, a) positive mode; b) negative mode.

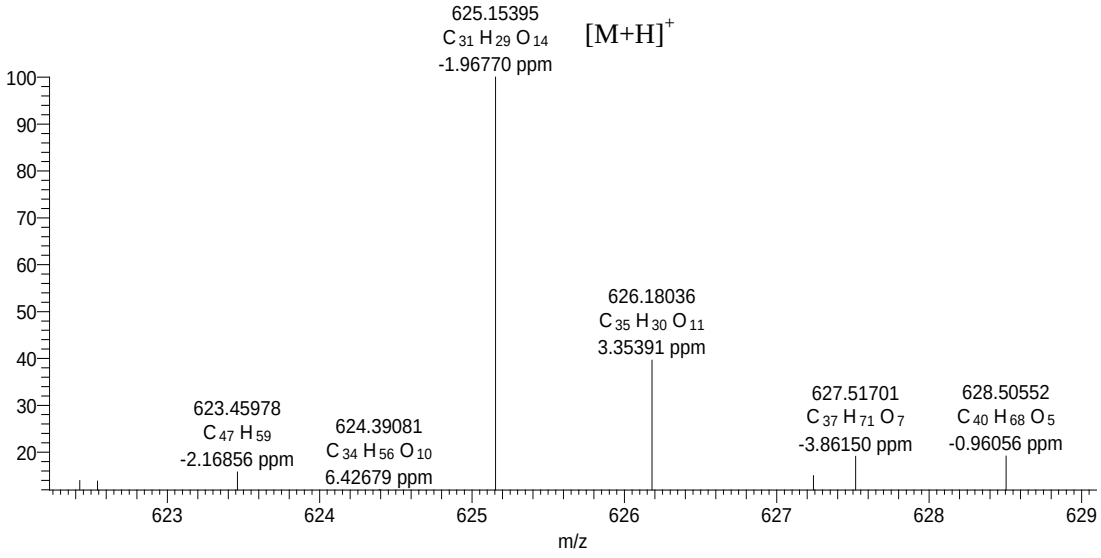

Figure 2.29 HRESIMS spectrum of compound **C**.

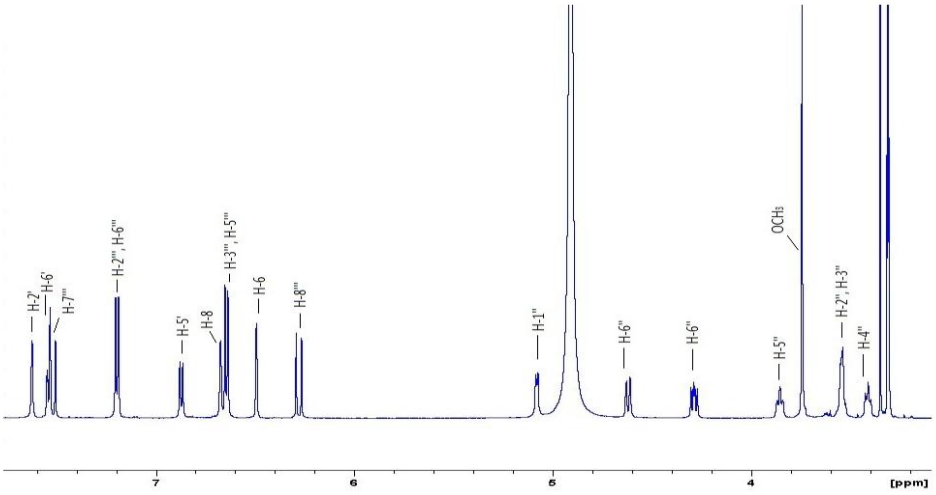

Figure 2.30 ^{1}H NMR spectrum (600 MHz, CD_3OD) of compound **C**

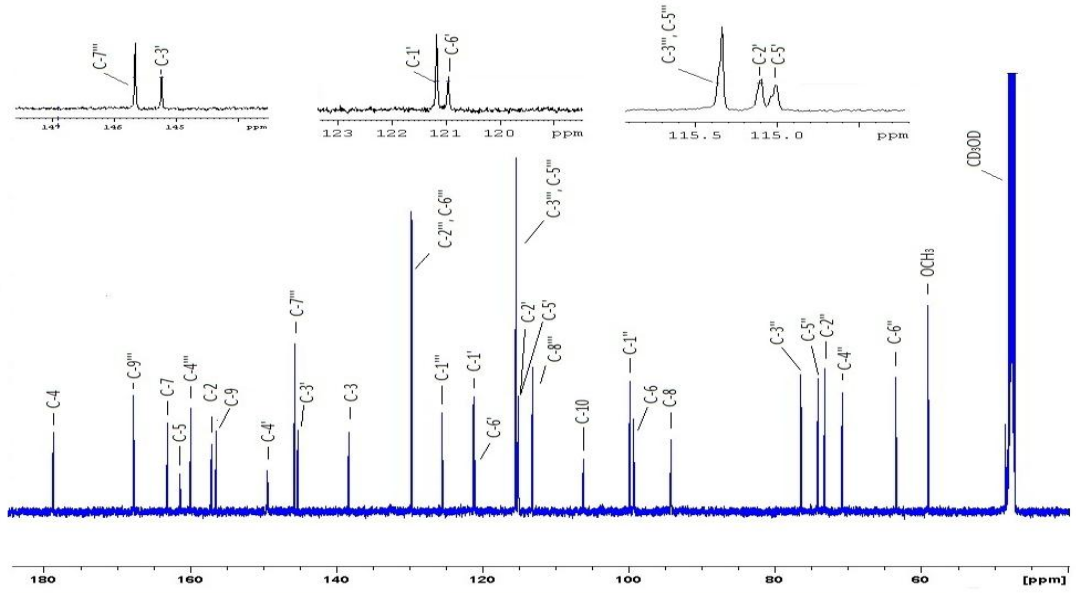

Figure 2.31 ^{13}C NMR spectrum (150 MHz, CD_3OD) of compound **C**.

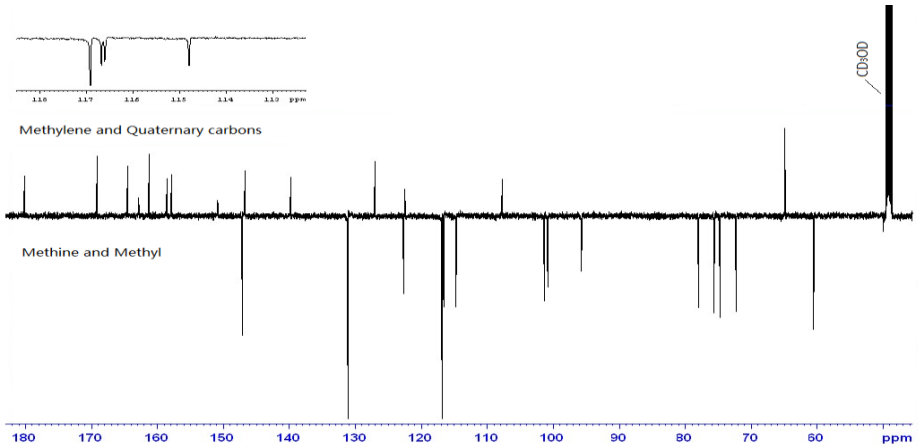

Figure 2.32 APT experiment (150 MHz, CD_3OD) of compound **C**.

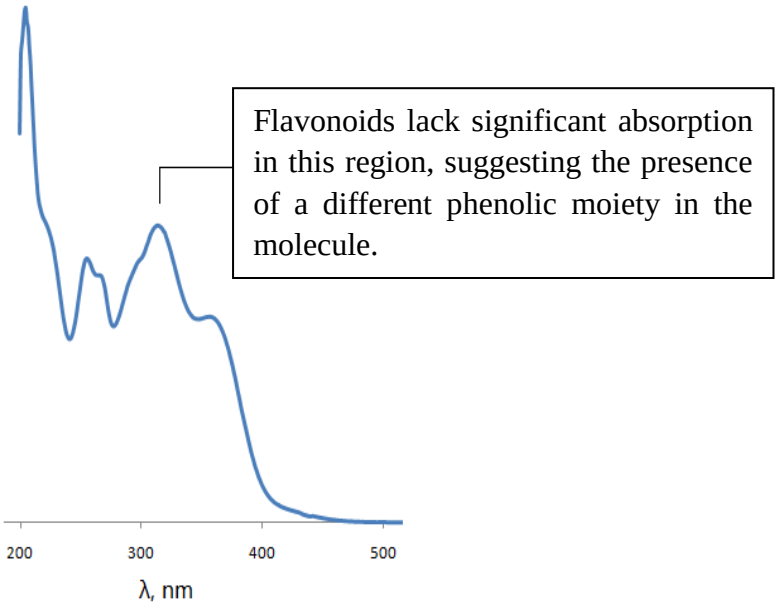

Figure 2.33 UV-vis spectrum of compound **C** in MeOH.

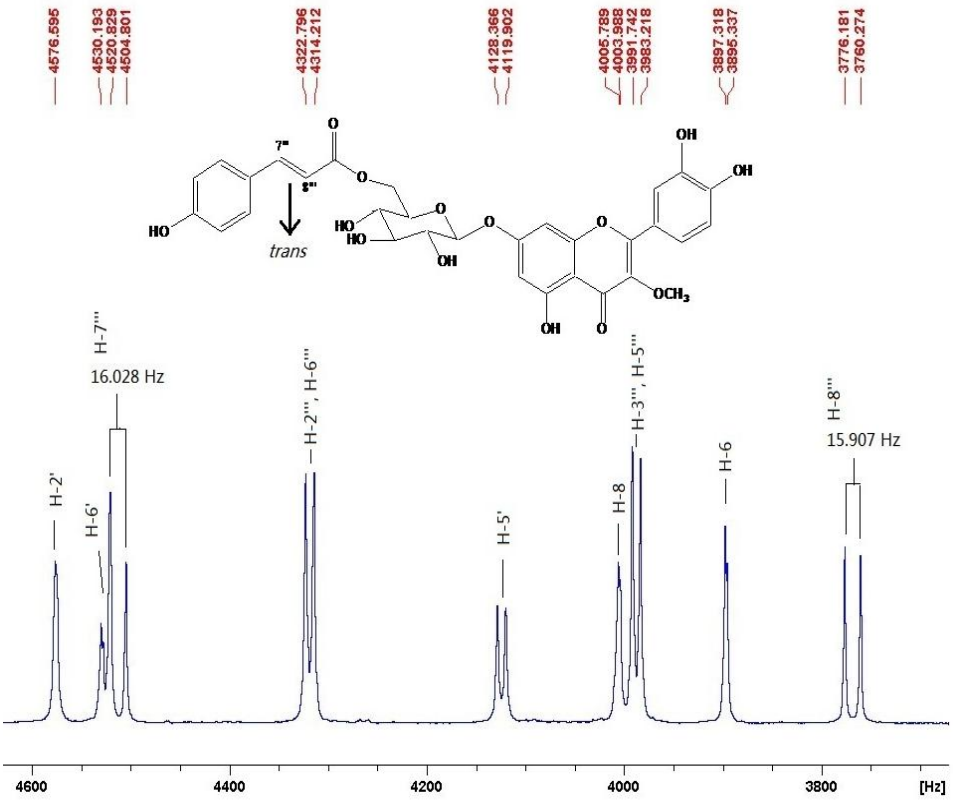

Figure 2.34 Expanded ^{1}H NMR spectrum (600 MHz, CD_3OD) of compound **C**; the coupling constant of H-7‴/H-8‴(^{3}J = 15.9 Hz) suggested a *trans* configuration.

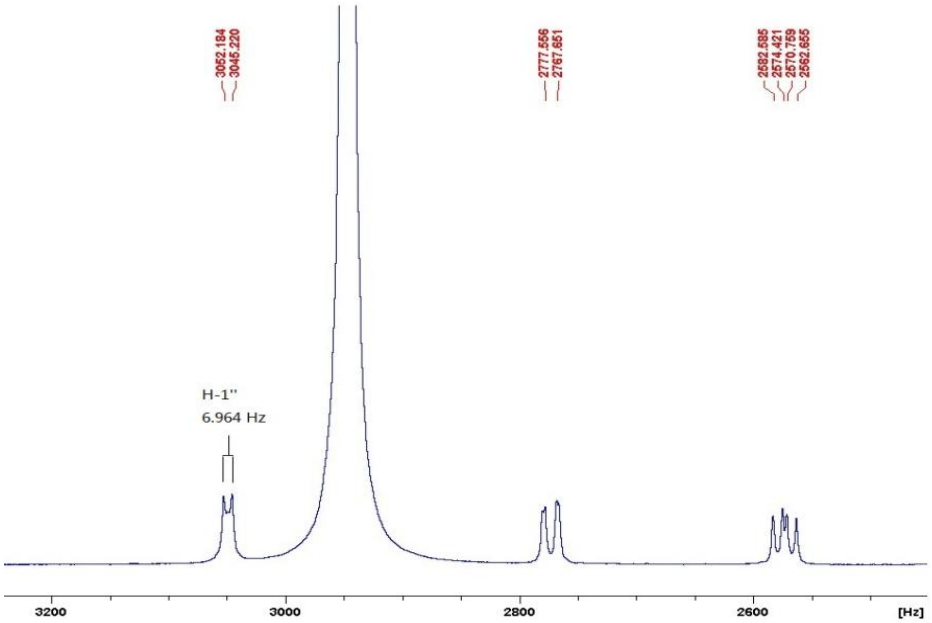

Figure 2.35 Expanded ^{1}H NMR spectrum (600 MHz, CD_3OD) of compound **C**; the coupling constant of H-1‴ (*J* = 7 Hz) suggested a β configuration of the glucose.

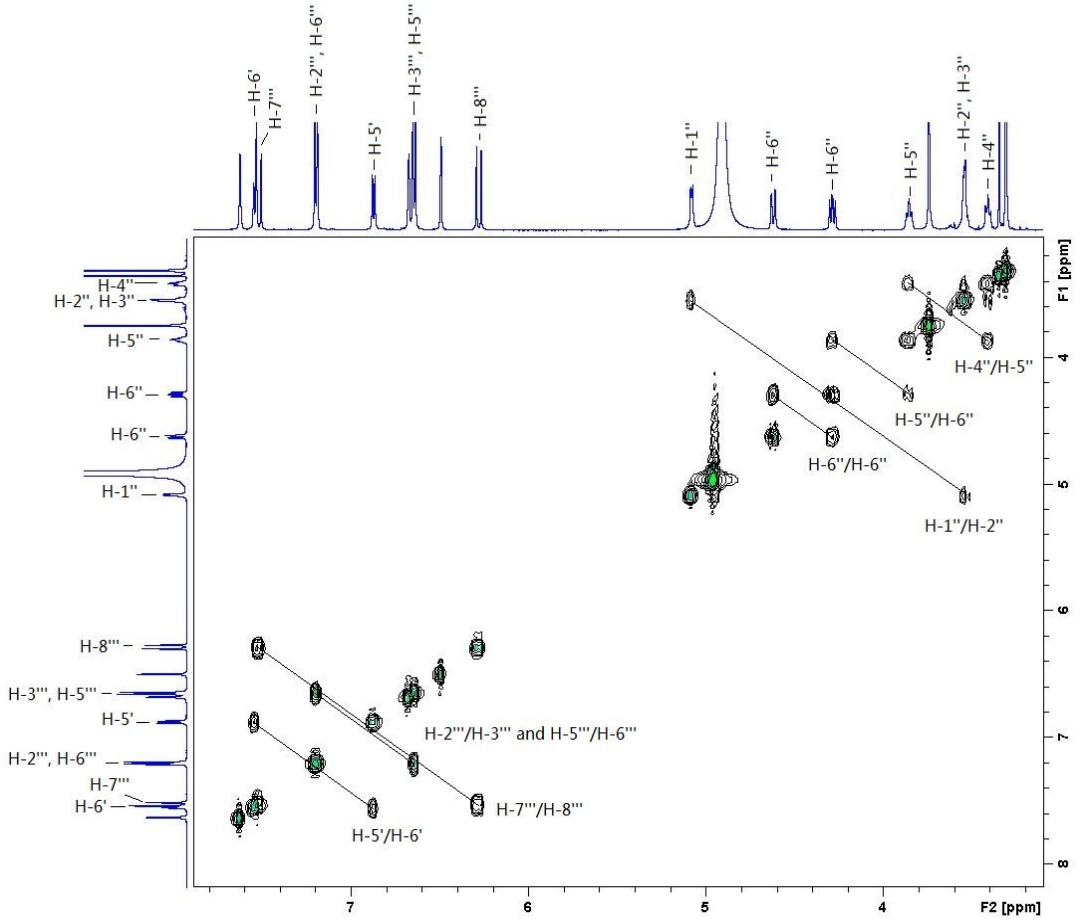

Figure 2.36 ^{1}H-^{1}H COSY spectrum of compound **C**.

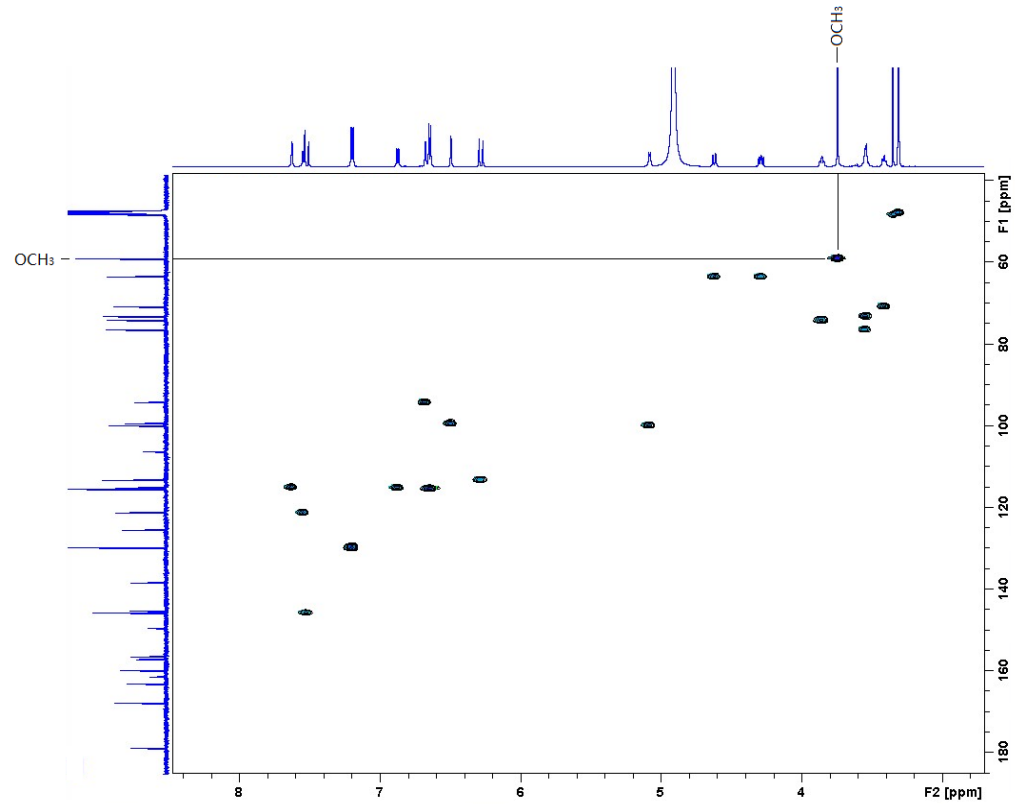

Figure 2.37 HSQC spectrum of compound **C**.

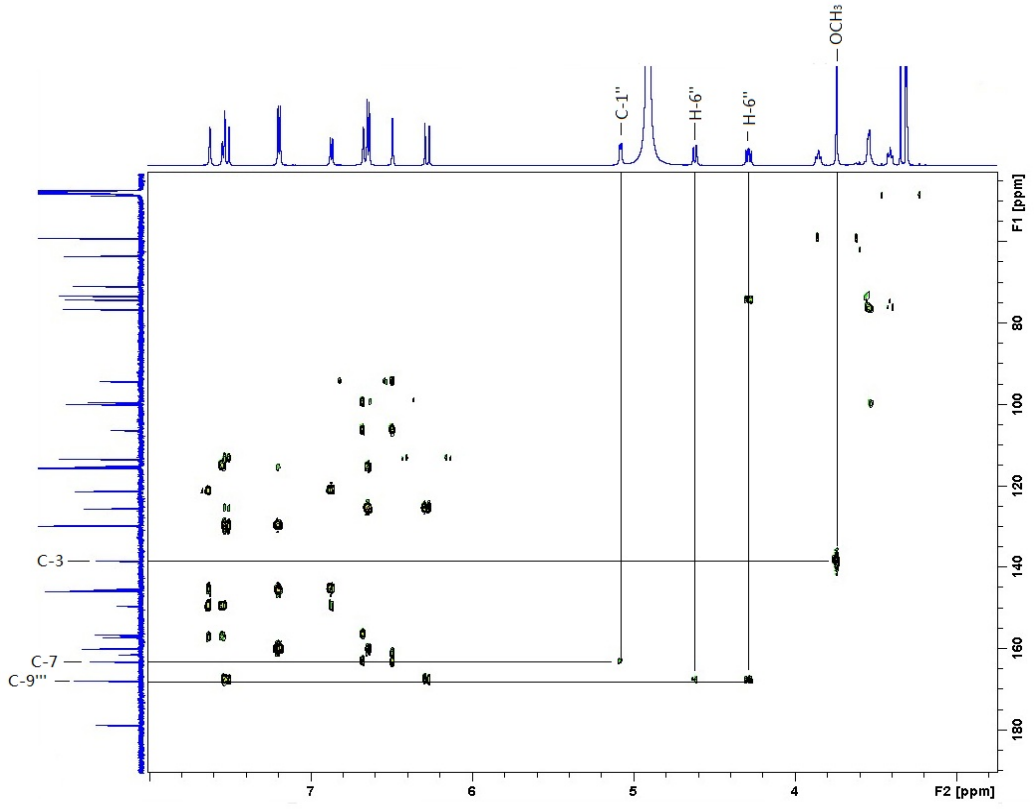

Figure 2.38 HMBC spectrum of compound **C**.

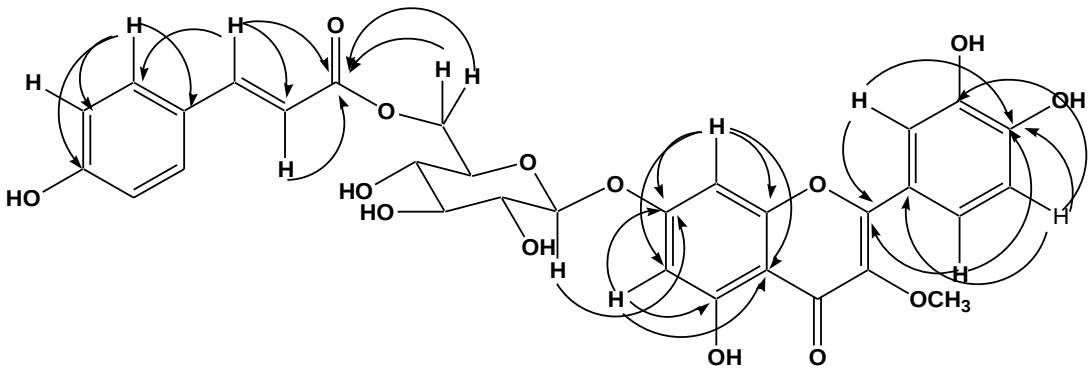

Figure 2.39 Selected long-range ^{1}H-^{13}C couplings observed for compound **C** in a HMBC experiment.

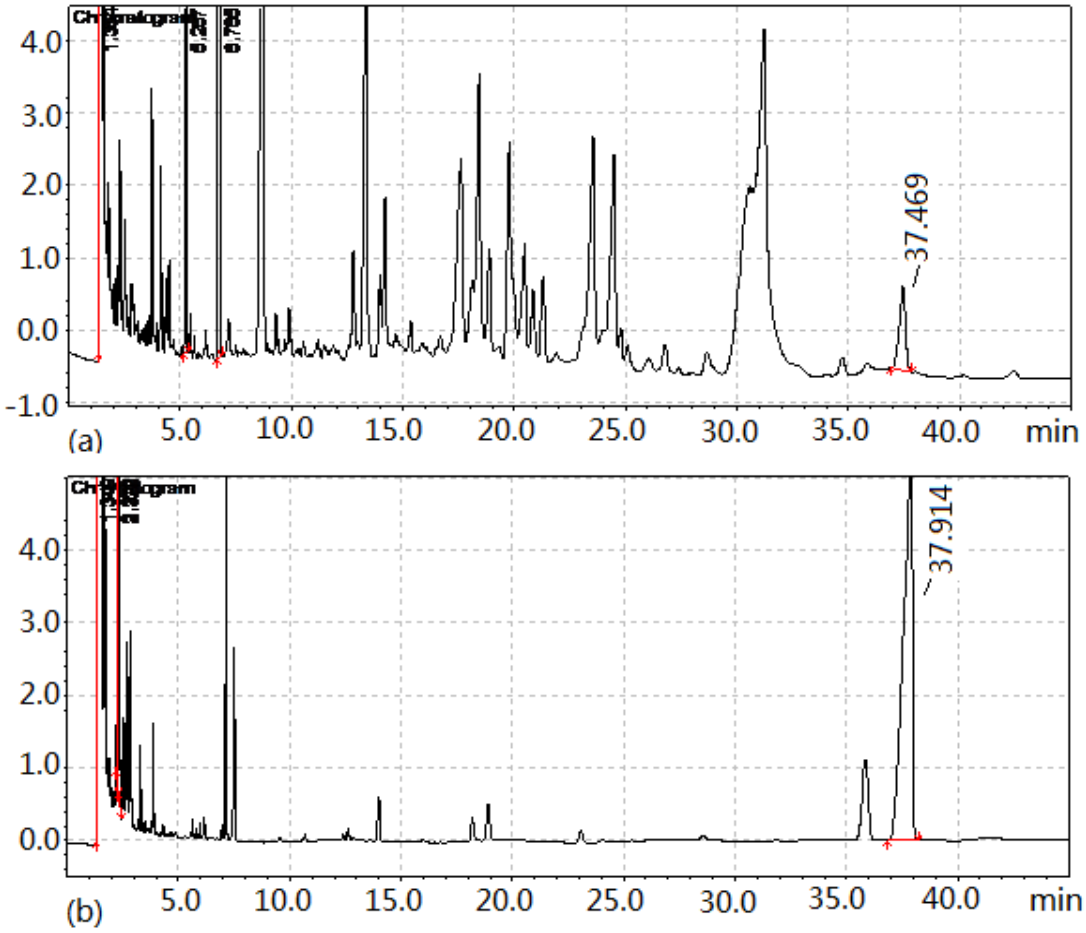

Figure 2.40 a) GC chromatogram of thiazolidine derivatives of D-glucose, b) GC chromatogram of thiazolidine derivatives of the base hydrolyzed sugars from compound **C**.

Basic hydrolysis of compound **C** was performed to cleave the ester. Since *p*-coumaric acid was relatively unstable in the reaction mixture and only a small quantity of compound was used as the

starting material for this basic hydrolysis, confirmation of *p*-coumaric acid with reference standards by TLC-UV or HPLC-UV was inefficient. Thus LC-MS employing direct injection and multiple reaction monitoring (MRM) (Figure 2.41) was used for the identification of *p*-coumaric acid in the hydrolyzed reaction mixture. For this scan mode, the first mass analyzer (Q2) was set at a specific *m/z* value to allow only ions of that *m/z* value to pass through into the collision cell. After fragmentation by collision induced dissociation (CID), the fragment ions moved into the second mass analyzer which was set at a specified *m/z* value, to allow only this fragment ion through to the ion detector. This fragment ion thus represented the original molecule and the presence of only that one fragment ion was registered by the ion detector. Comparing the product ion scan of the reference standard (*p*-coumaric acid) (Figure 2.42) with the product ion scans of hydrolyzed mixture (Figure 2.43), indicated that the sample contains *p*-coumaric acid. Further evidence is provided by the retention times for the reference standard (*p*-coumaric acid) and the hydrolyzed product when injected into a HPLC column. Figure 2.44 is the chromatogram of the reference standard (*p*-coumaric acid) at a retention time of 1.92 minutes which has the same retention time as the product produced by hydrolysis, indicated by Figure 2.45.

Thus the final structure of compound **C** was determined as 3-*O*-methylquercetin 7-*O*-[*β*-D-6″(*E*-*p*-coumaroyl)glucopyranoside]. Compound **C** is a new natural product.

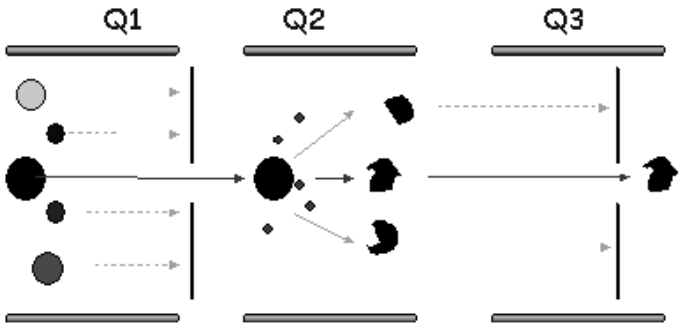

Figure 2.41 MRM (Multiple Reaction Monitoring) scan of the hydrolyzed product for compounds **C** and **D**.

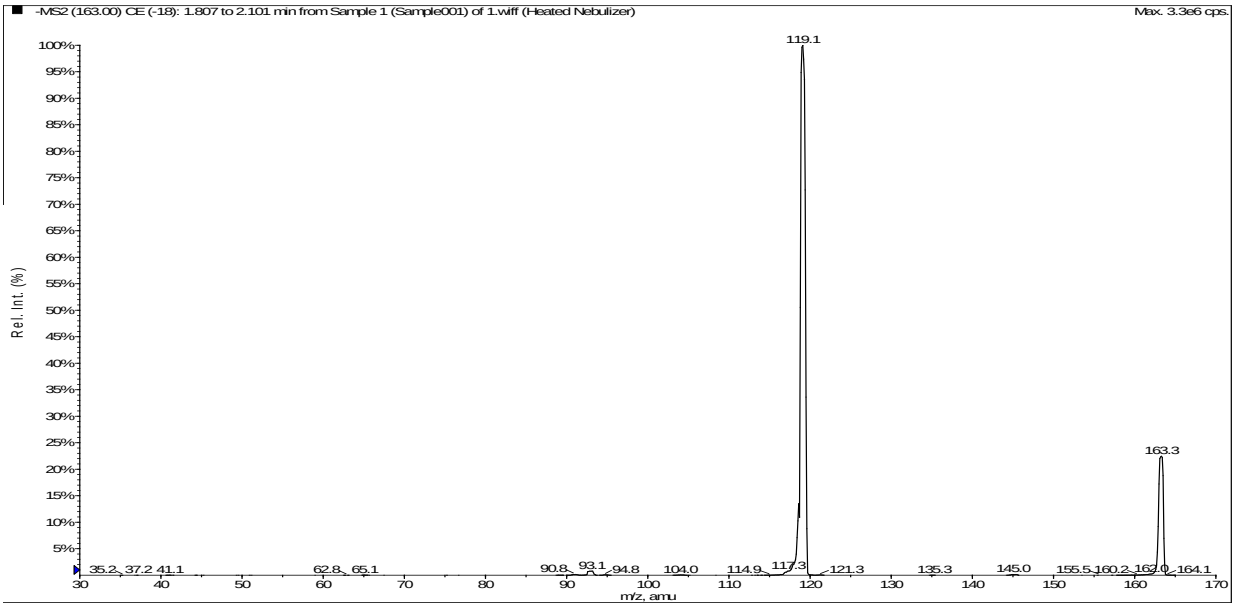

Figure 2.42 Product ion scan of coumaric acid showing the precursor ion $[M - H]^-$ at *m/z* 163 and the product ions produced during fragmentation by collision induced dissociation.

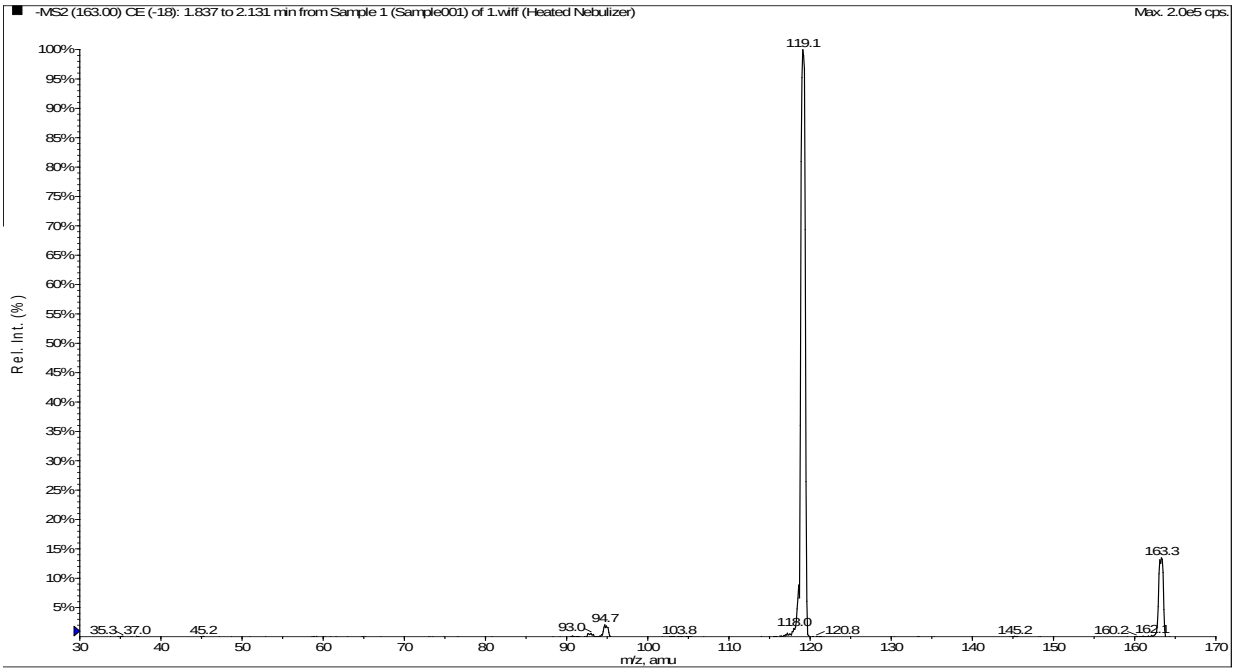

Figure 2.43 Product ion scan of *m/z* 163 (compound **C**).

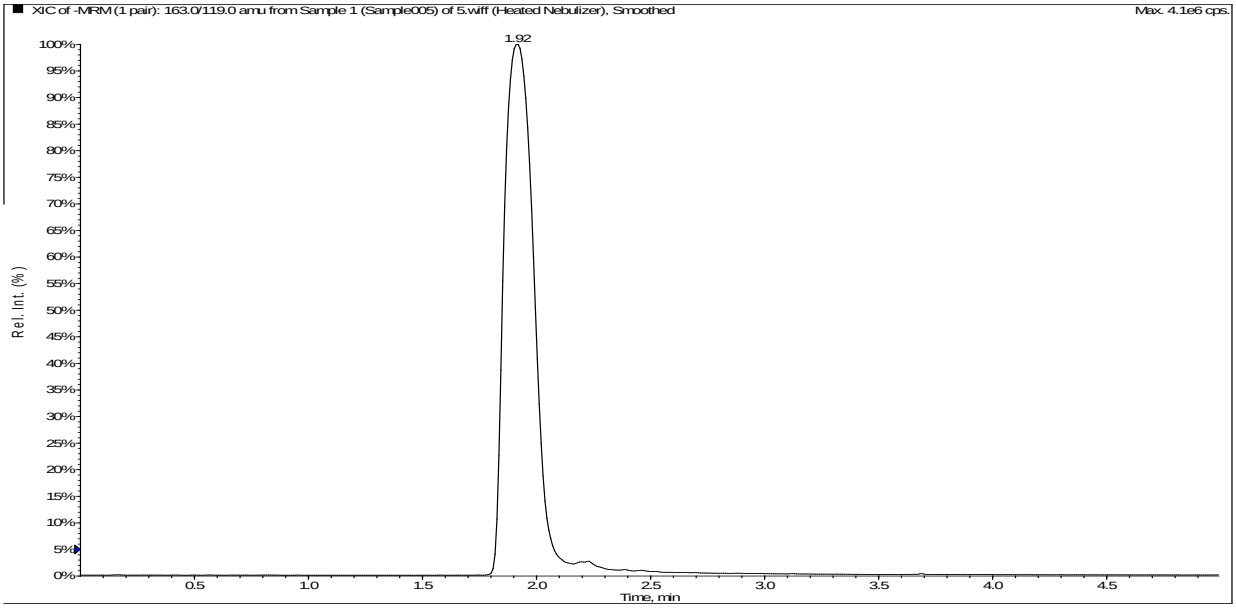

Figure 2.44 HPLC chromatogram of *p*-coumaric acid (reference standard) at a retention time of 1.92 minutes. Column: Phenomenex® C_{18} (15cm × 2.0mm, 5µm); the injection solvent and mobile phase consisted of water : methanol (10:90, v/v) acidified with formic acid (0.05%) and 20µL was loaded onto the column; the flow rate of the mobile phase through the analytical column was 200 µL/min.

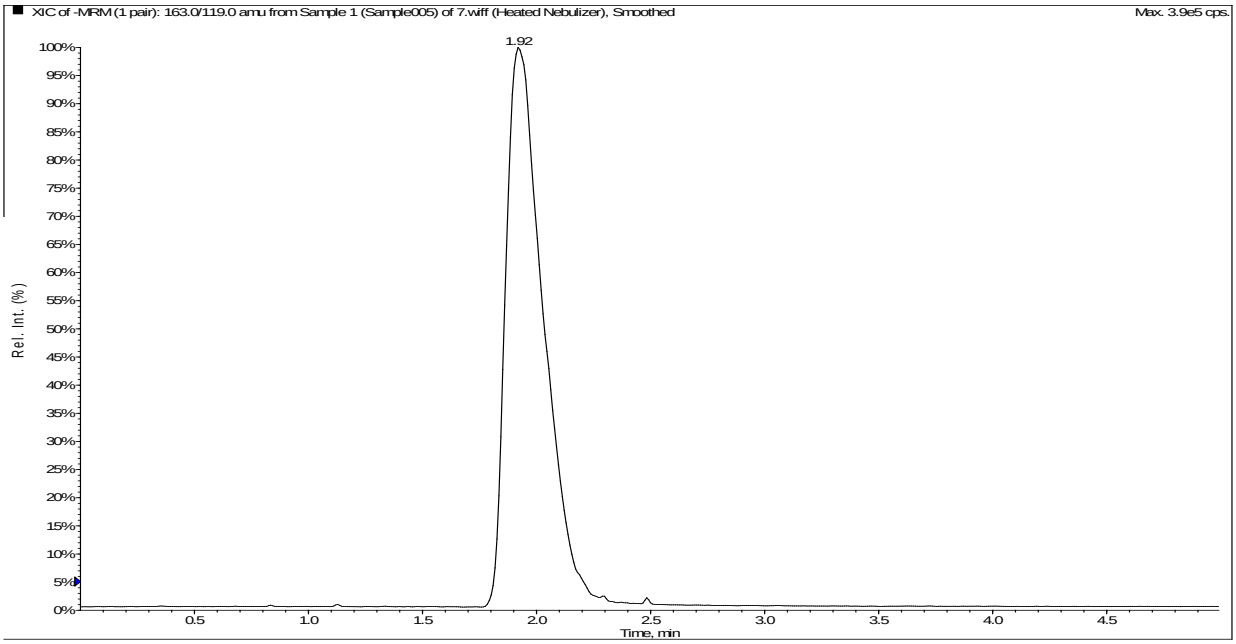

Figure 2.45 HPLC chromatogram of *p*-coumaric acid in sample (compound **C)** at a retention time of 1.92 minutes. Column: Phenomenex® C_{18} (15cm × 2.0mm, 5µm); the injection solvent and mobile phase consisted of water : methanol (10:90, v/v) acidified with formic acid (0.05%) and 20µL was loaded onto the column; the flow rate of the mobile phase through the analytical column was 200 µL/min.

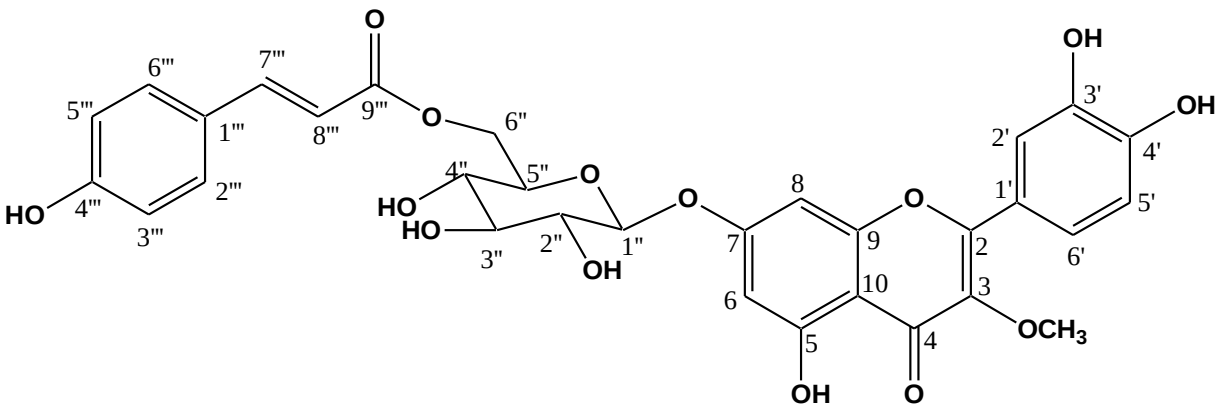

Structure of compound C

2.3.3.4. Compound **D**

Compound **D** was obtained as pale green amorphous product. The positive LRESIMS showed a pseudomolecular ion at *m/z* 639 $[M + H]^+$ and the negative LRESIMS a pseudomolecular ion at *m/z* 637 $[M - H]^-$; the former ion analyzed for $C_{32}H_{31}O_{14}$ in the HRESIMS (Figure 2.47). Together with the ^1H and ^{13}C NMR spectra and the APT experiment, this suggested a molecular formula of $C_{32}H_{30}O_{14}$. An absorption band at 314 nm present in the UV-vis absorption spectrum, indicated a cinnamic acid derivative in addition to a flavonoid moiety, as found in compound **C**. The ^1H NMR spectrum displayed typical resonances for *p*-coumaric acid: two doublets at δ 6.27 (*J* = 15.8 Hz) and 7.54 (*J* = 15.8 Hz) characteristic of the *trans*-double bond; and an AA′BB′ coupling system of the benzene ring, i.e., 6.62 (2H, *d*, *J* = 8.6 Hz), 7.19 (2H, *d*, *J* = 8.6 Hz). In the ^{13}C NMR spectrum, 22 out of 30 signals corresponded to those of 3,4′-*O*-methylquercetin 7-*O*-*β*-glucopyranoside (compound **B**). Complete acid hydrolysis of compound **D** gave *β*-glucose, determined by eluting with the standard compound on TLC (Figure 2.20) and the coupling constant (*J* = 7.2 Hz) of the anomeric sugar proton in the ^1H NMR spectrum. The absolute configuration of the glucose was determined as D-glucose by GC analysis of its thiazolidine derivative (Figure 2.58). The HMBC experiment (Figure 2.56) displayed a long-range correlation between C-7 (δ 163.15) and the anomeric proton (δ 5.10, *d*, *J* = 7.2 Hz), confirming the site of glycosylation as the 7-OH of 3,4′-methoxyquercetin. The linkage of the *p*-coumaric ester to the 6″-OH was established by the significant downfield shift of glucose H_2-6″ (δ 4.66, 1H, *dd*, ^2J = 11.9 Hz, ^3J = 2.2 Hz; δ 4.27, 1H,

dd, ^2J = 11.9 Hz, ^3J = 8.2 Hz). The HMBC spectrum, in which the ester carbonyl carbon at δ 167.62 was correlated to H-6″, further substantiated these findings. The *p*-coumaryl ester was hydrolyzed by base, and the *p*-coumaric acid in the reaction mixture was identified in the same way as compound **C**, with the same pattern in the product ion scan of *m/z* 163 (Figure 2.59 and 2.60) and the same HPLC retention time (Figures 2.61 and 2.62) as the reference standard. Thus the final structure of compound **D** was determined as 3,4′-di-*O*-methylquercetin 7-*O*-[*β*-D-6″(*E*-*p*-coumaroyl)glucopyranoside]. Compound **D** is a new natural product.

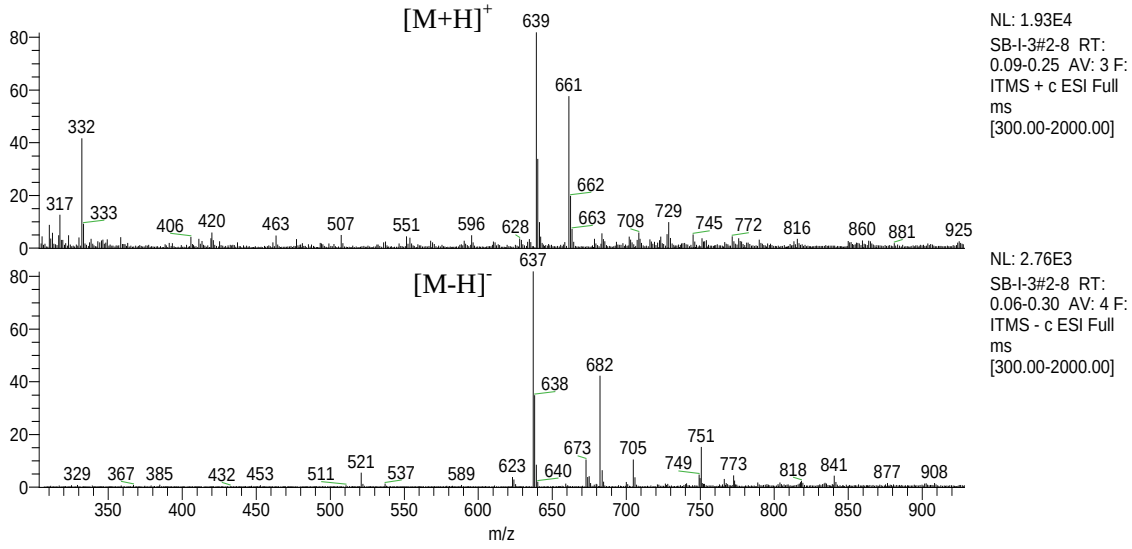

Figure 2.46 LRESIMS spectrum of compound **D**, a) positive mode; b) negative mode.

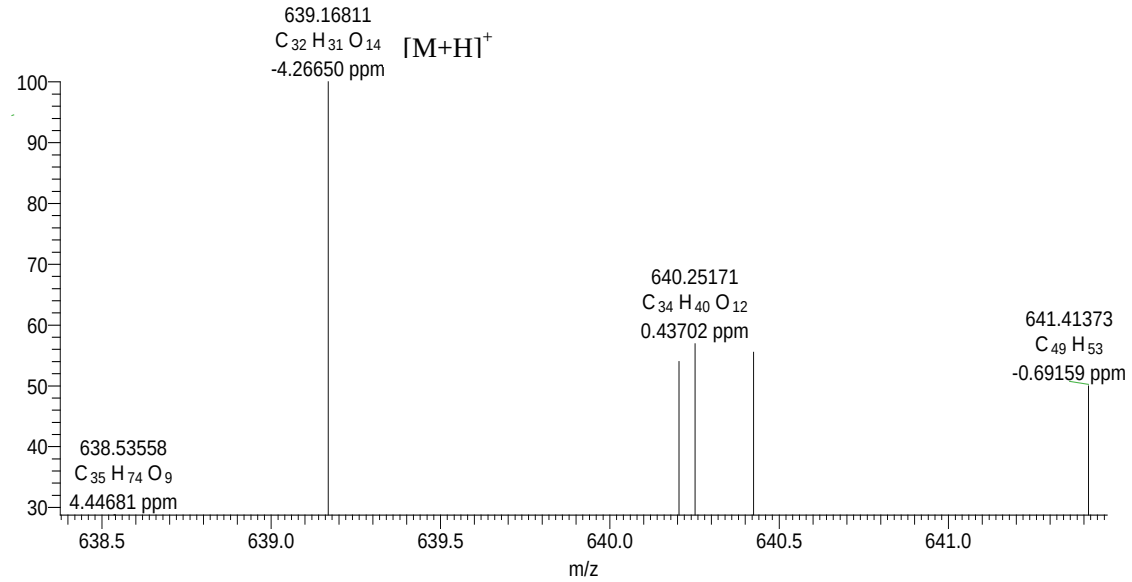

Figure 2.47 HRESIMS spectrum of compound **D**

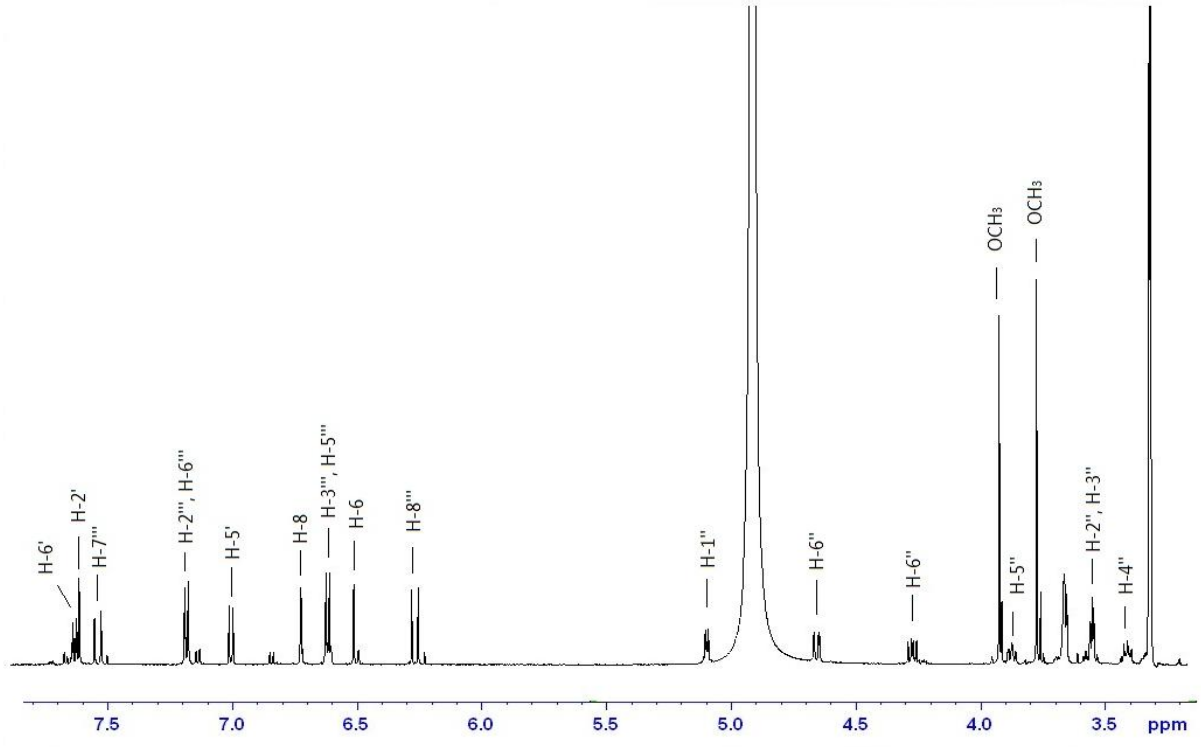

Figure 2.48 ^{1}H NMR spectrum (600 MHz, CD_3OD) of compound **D**

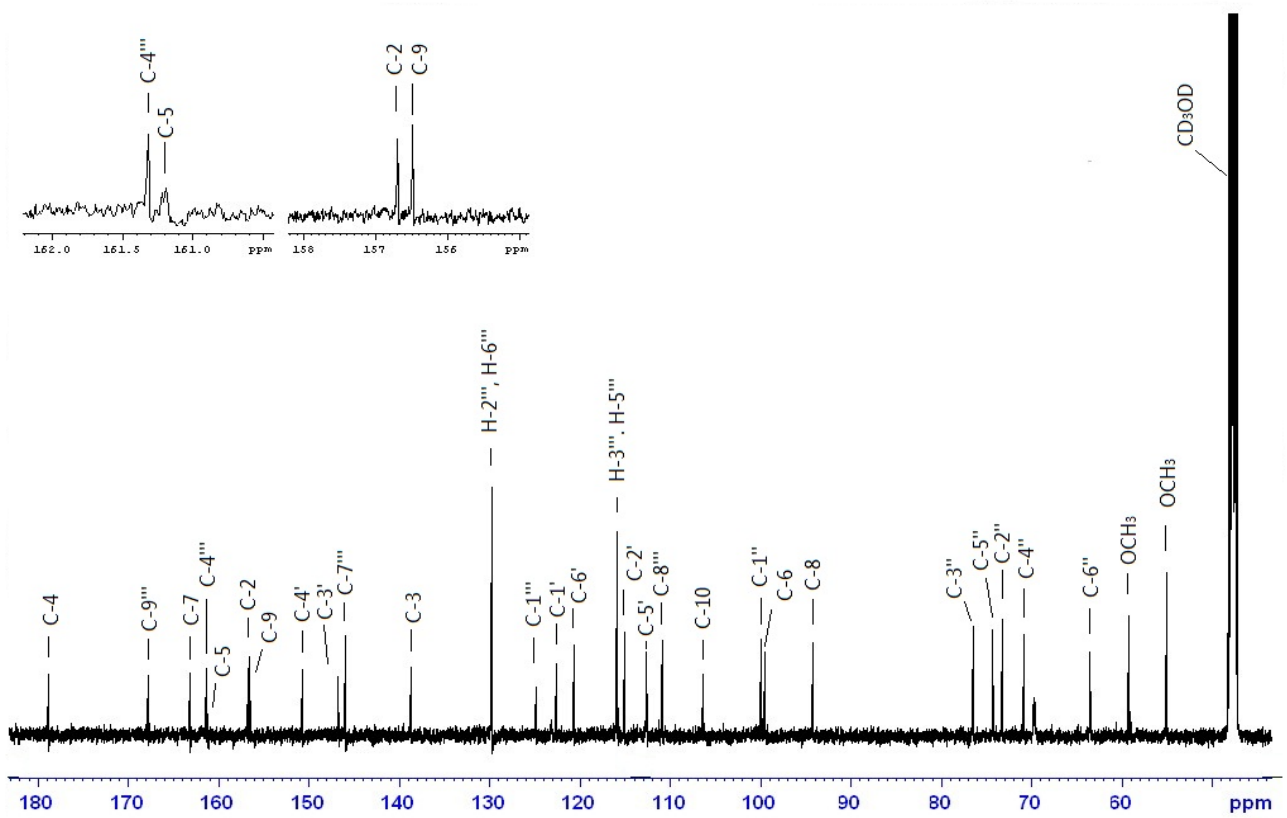

Figure 2.49 ^{13}C NMR spectrum (150 MHz, CD_3OD) of compound **D**.

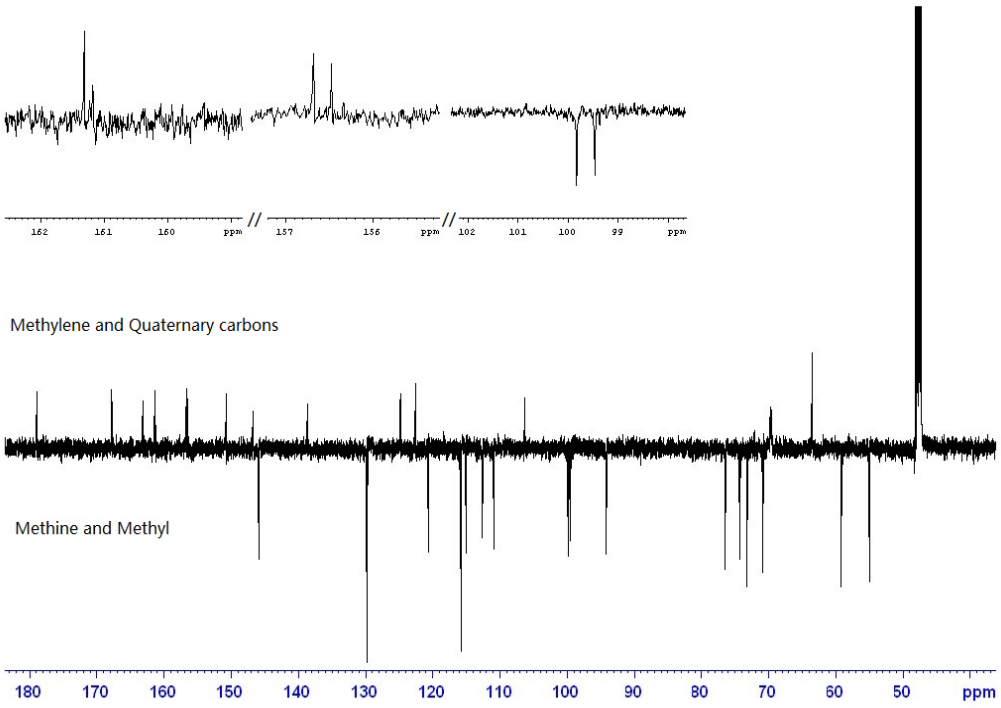

Figure 2.50 APT experiment (150 MHz, CD_3OD) of compound **D**.

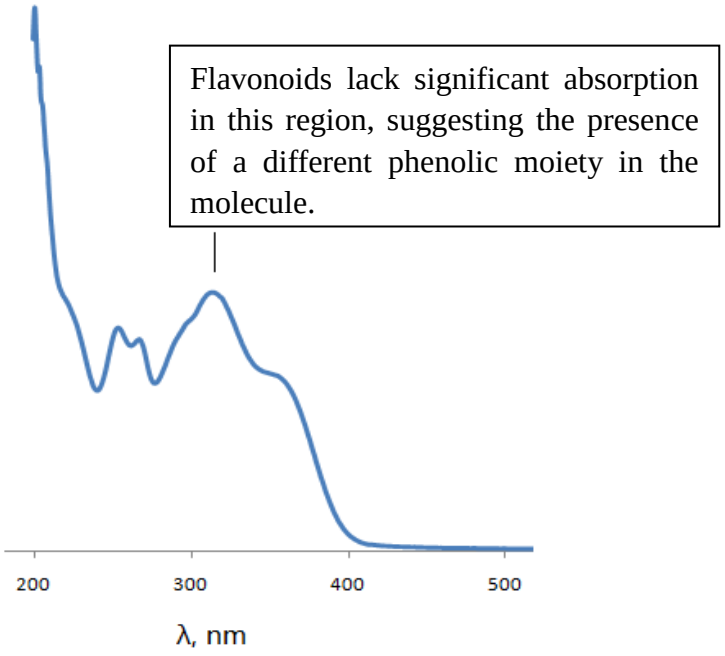

Figure 2.51 UV-vis spectrum of compound **D** in MeOH.

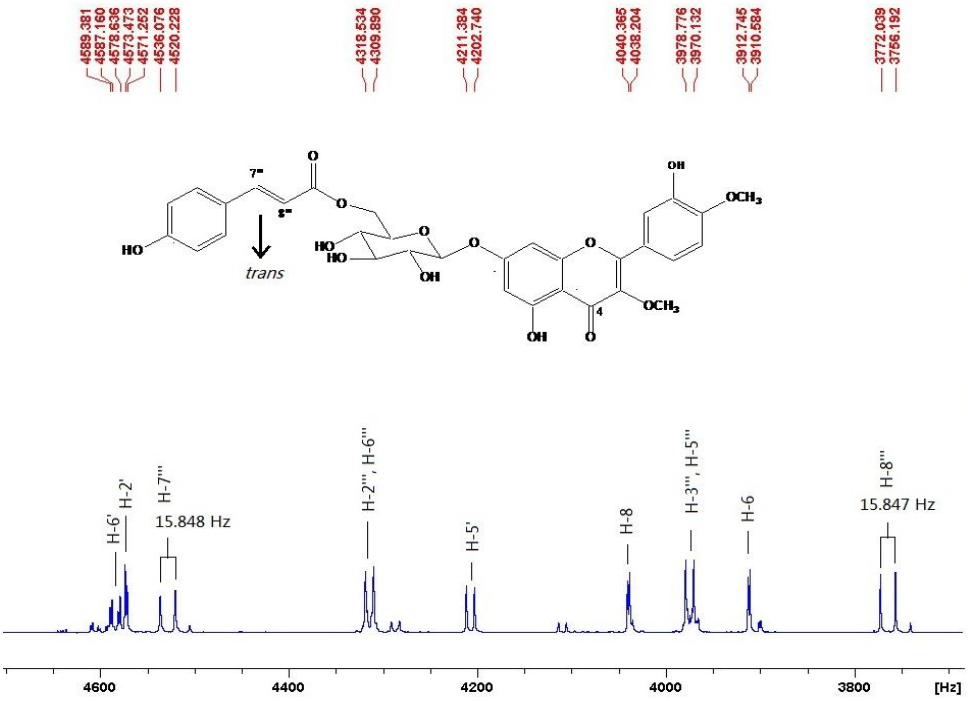

Figure 2.52 Expanded ^{1}H NMR spectrum (600 MHz, CD_3OD) of compound **D**; the coupling constant of H-7‴/H-8‴ (^{3}J = 15.8 Hz) suggested a *trans* configuration.

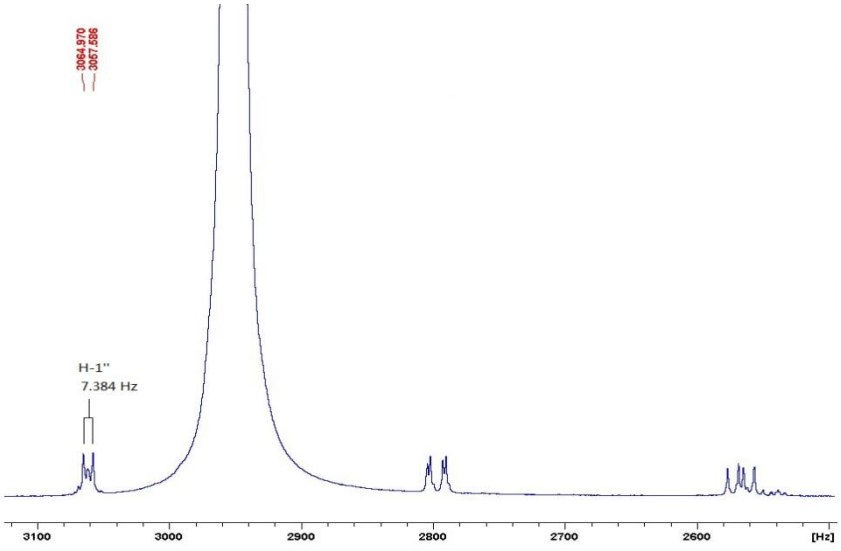

Figure 2.53 Expanded ^{1}H NMR spectrum (600 MHz, CD_3OD) of compound **D**; the coupling constant of H-1‴ (J = 7 Hz) suggested a β configuration of the glucose.

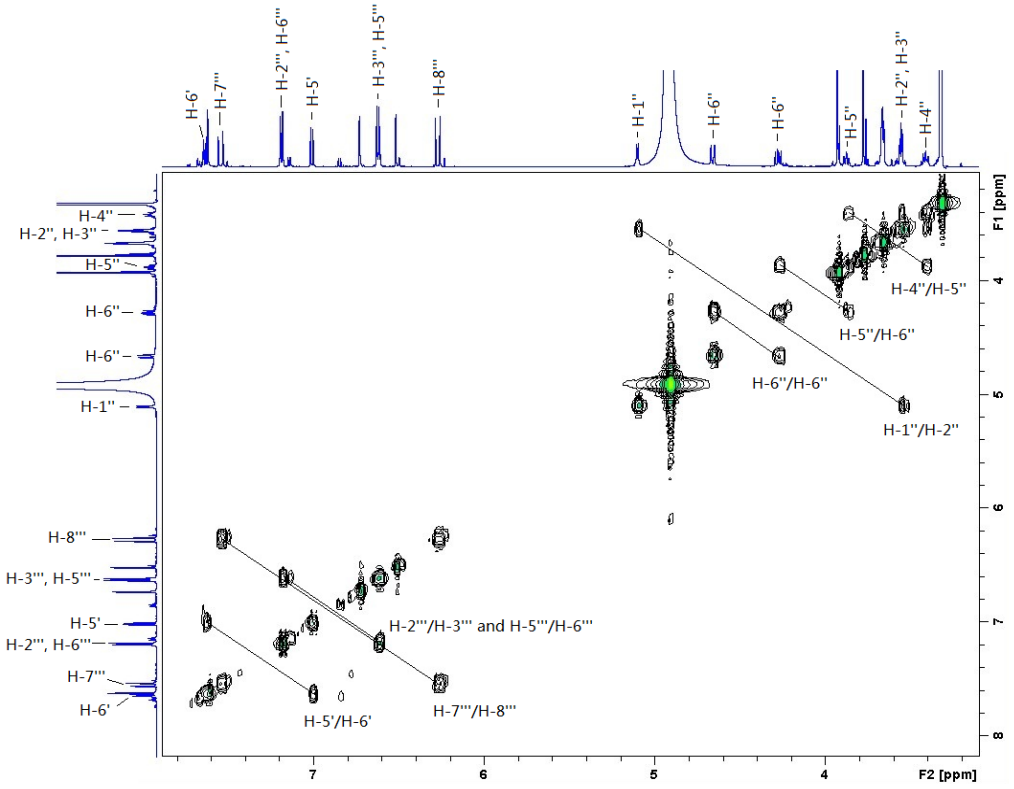

Figure 2.54 COSY spectrum of compound **D**.

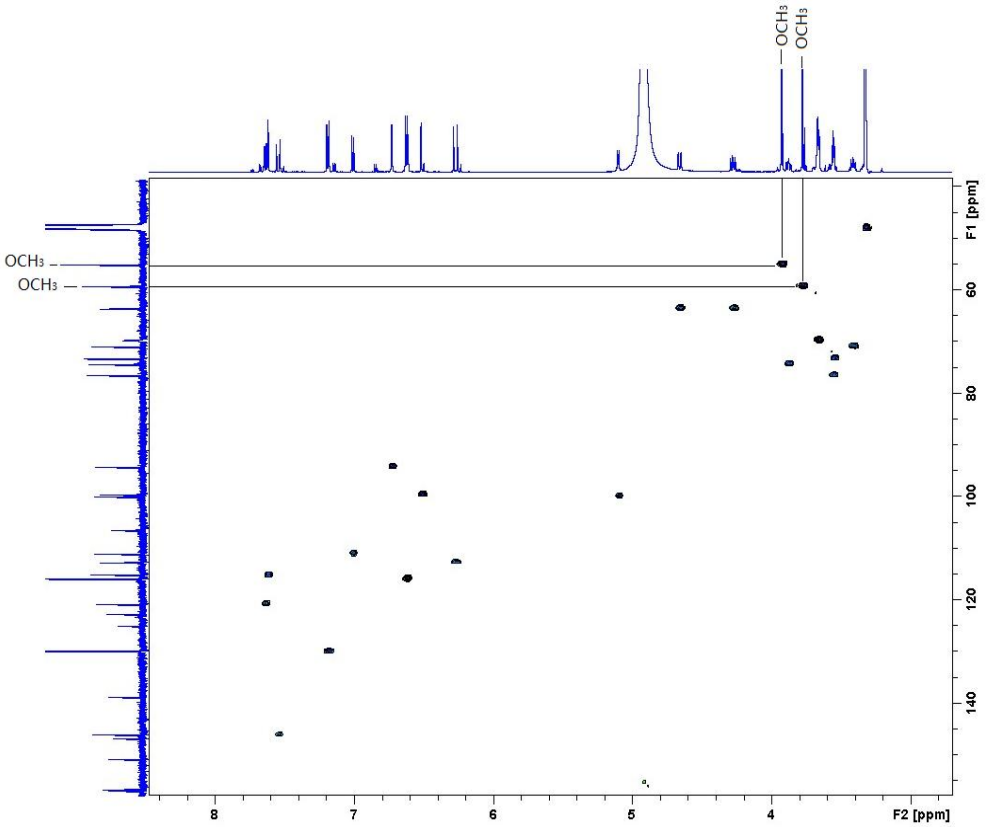

Figure 2.55 HSQC spectrum of compound **D**.

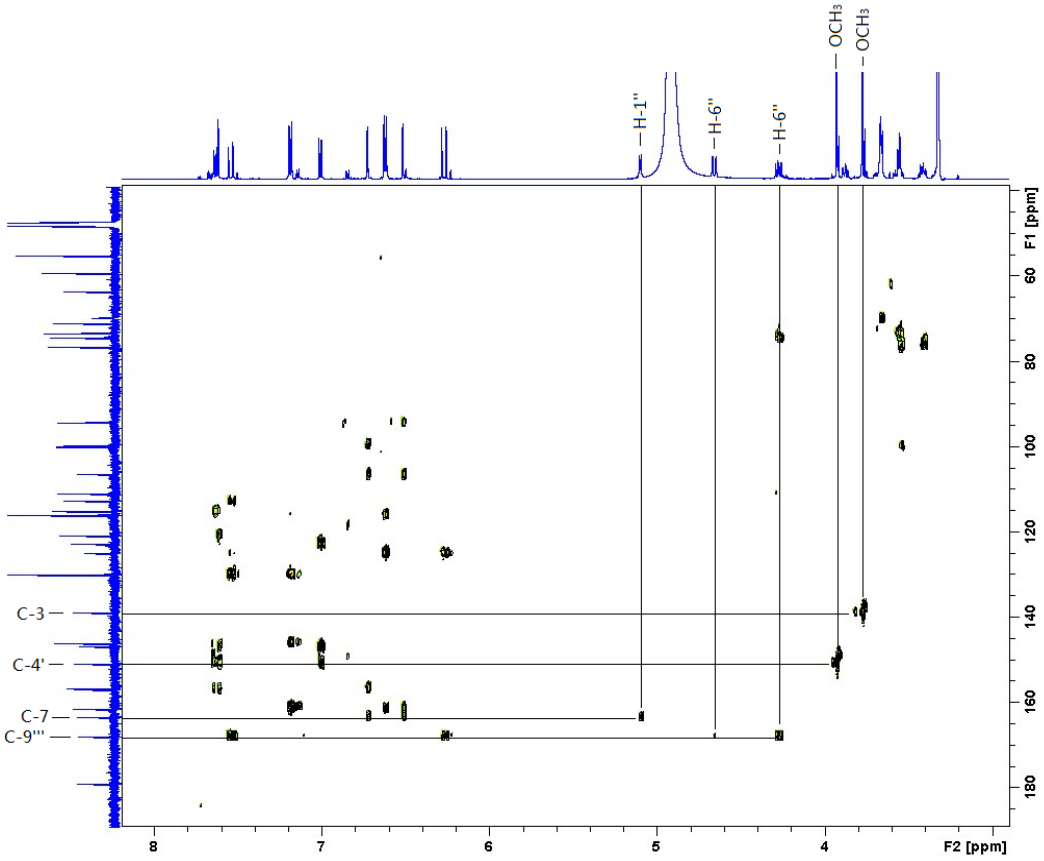

Figure 2.56 HMBC spectrum of compound **D**.

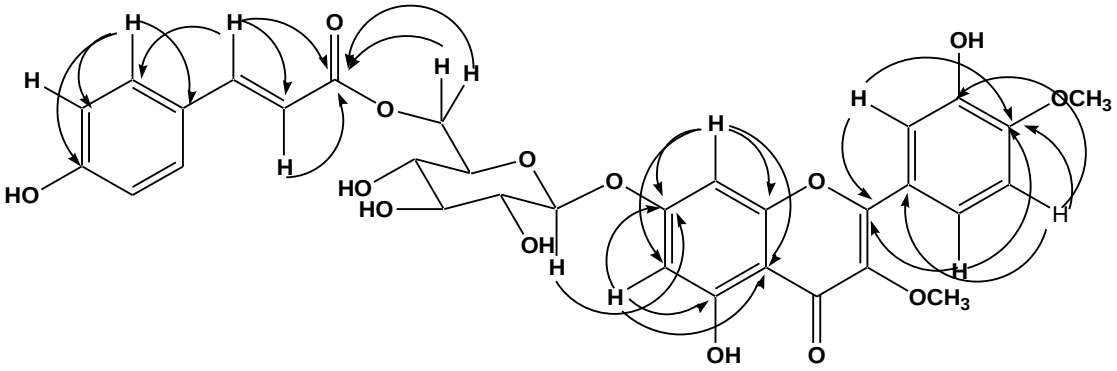

Figure 2.57 Selected long-range ^{1}H-^{13}C couplings observed for compound **D** in a HMBC experiment.

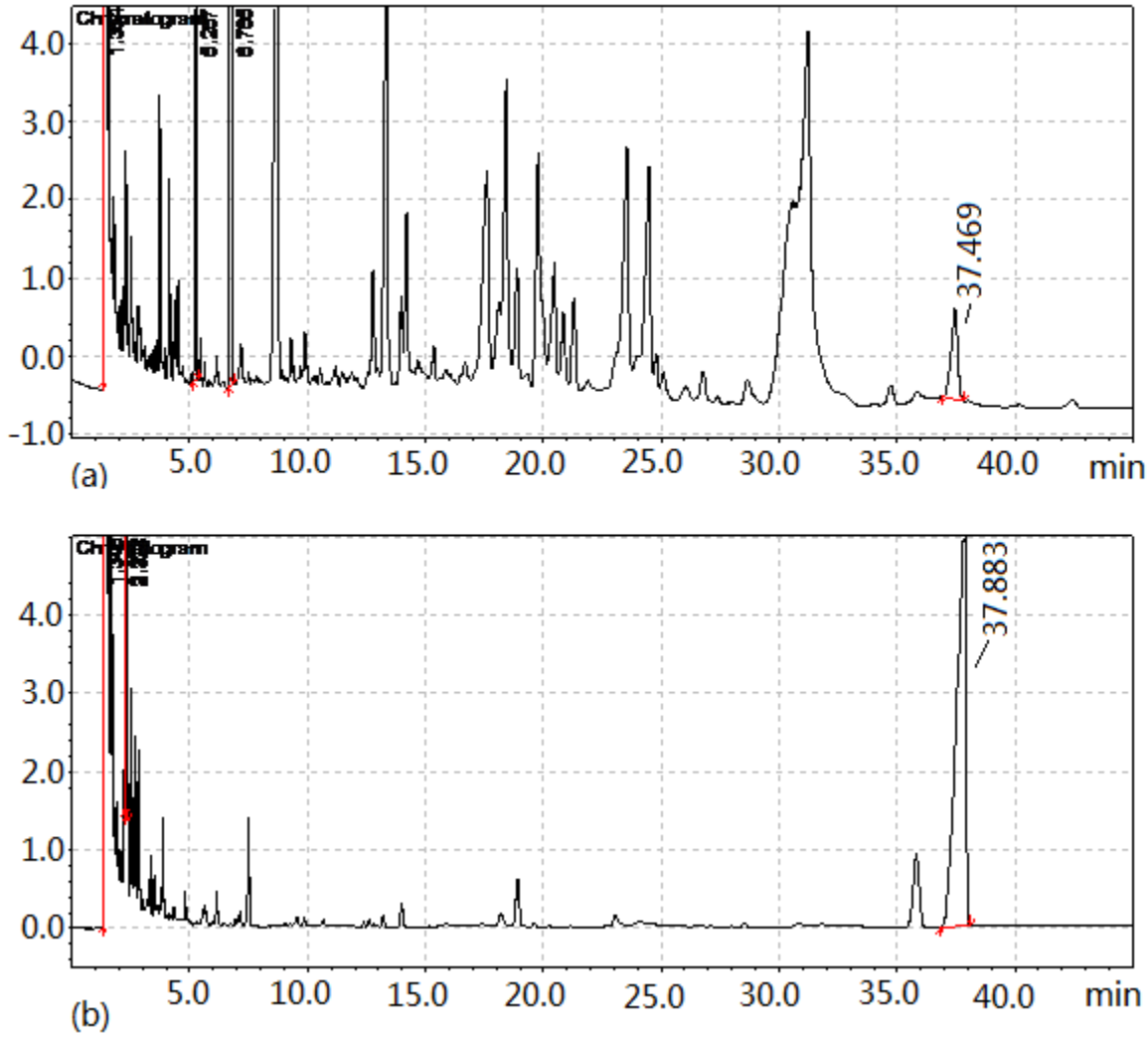

Figure 2.58 a) GC chromatogram of thiazolidine derivatives of D-glucose, b) GC chromatogram of thiazolidine derivatives of the base hydrolyzed sugars from compound **D**.

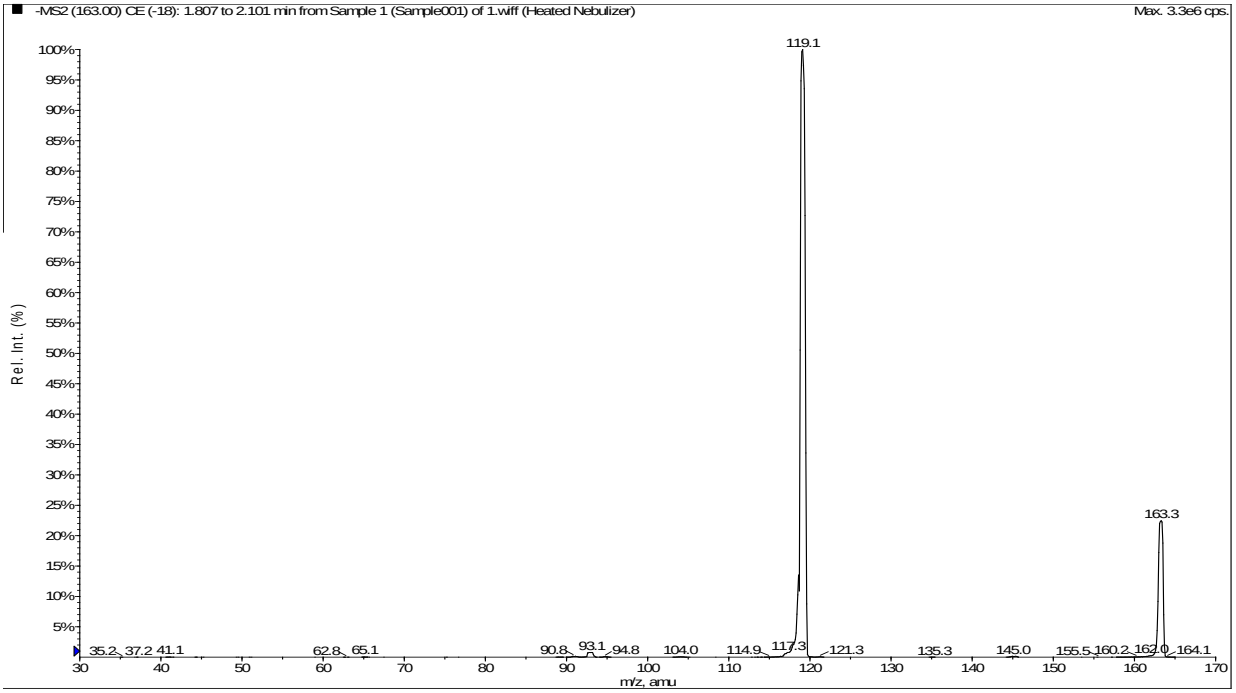

Figure 2.59 Product ion scan of coumaric acid showing the precursor ion $[M - H]^-$ at *m/z* 163 and the product ions produced during fragmentation by collision induced dissociation.

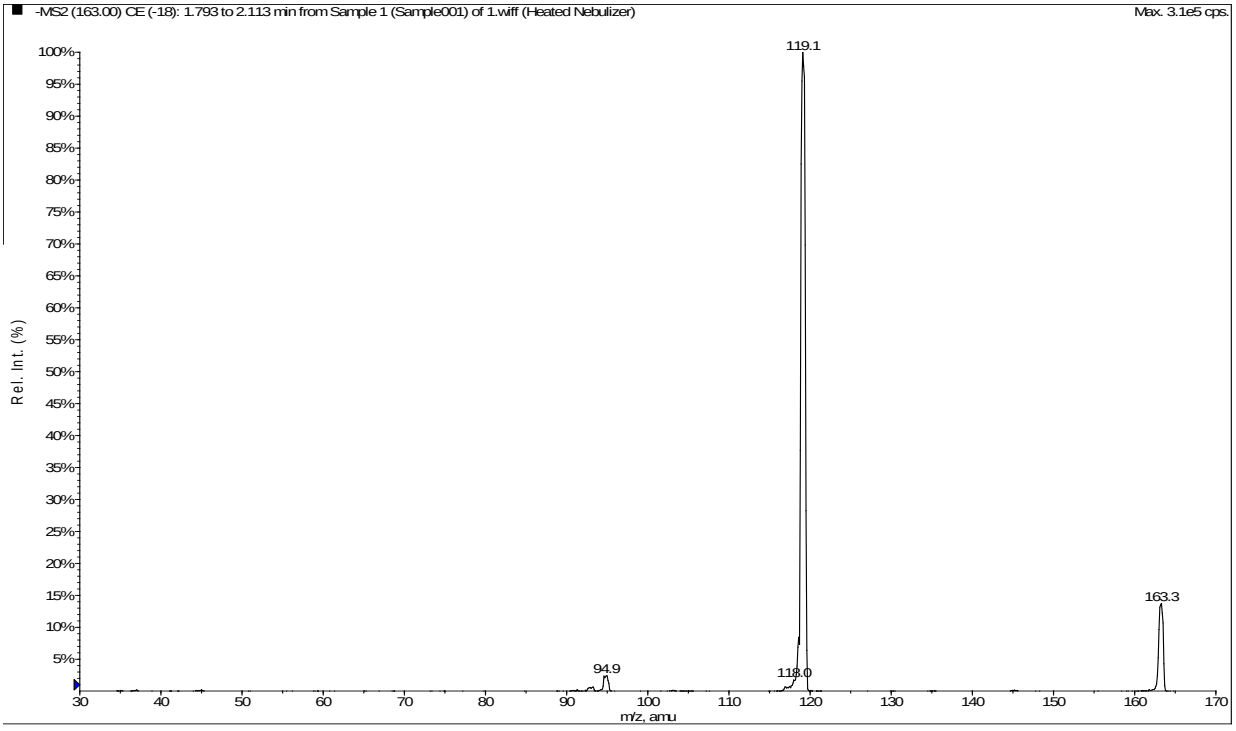

Figure 2.60 Product ion scan of *m/z* 163 (compound **D**).

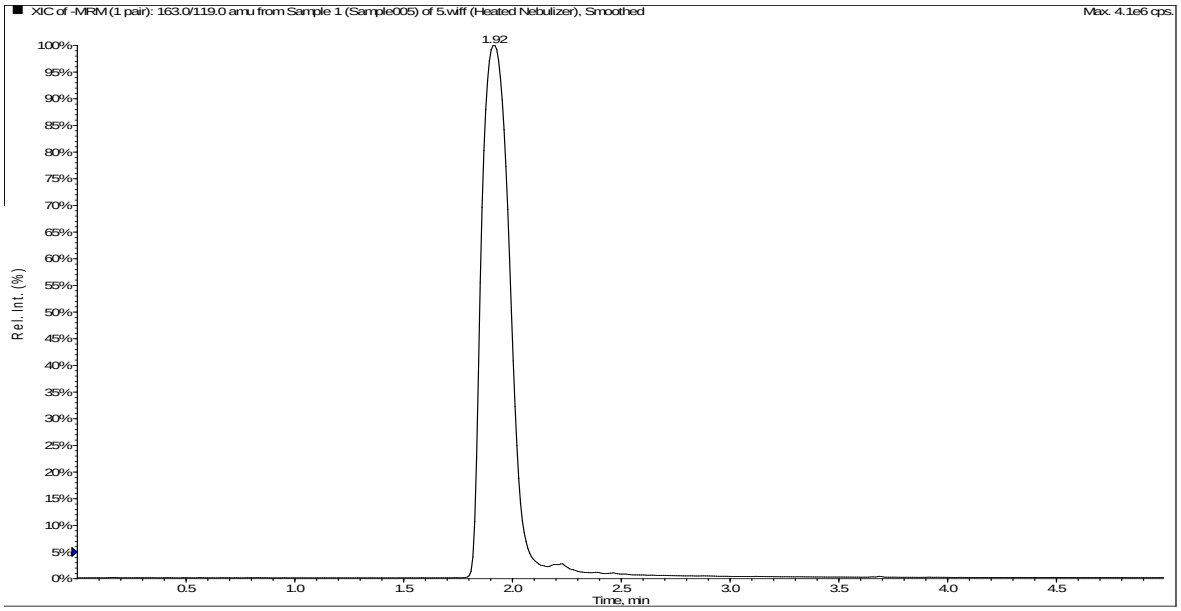

Figure 2.61 HPLC chromatogram of *p*-coumaric acid (reference standard) at a retention time of 1.92 minutes. Column: Phenomenex® C_{18} (15cm × 2.0mm, 5µm); the injection solvent and mobile phase consisted of water : methanol (10:90, v/v) acidified with formic acid (0.05%) and 20µL was loaded onto the column; the flow rate of the mobile phase through the analytical column was 200 µL/min.

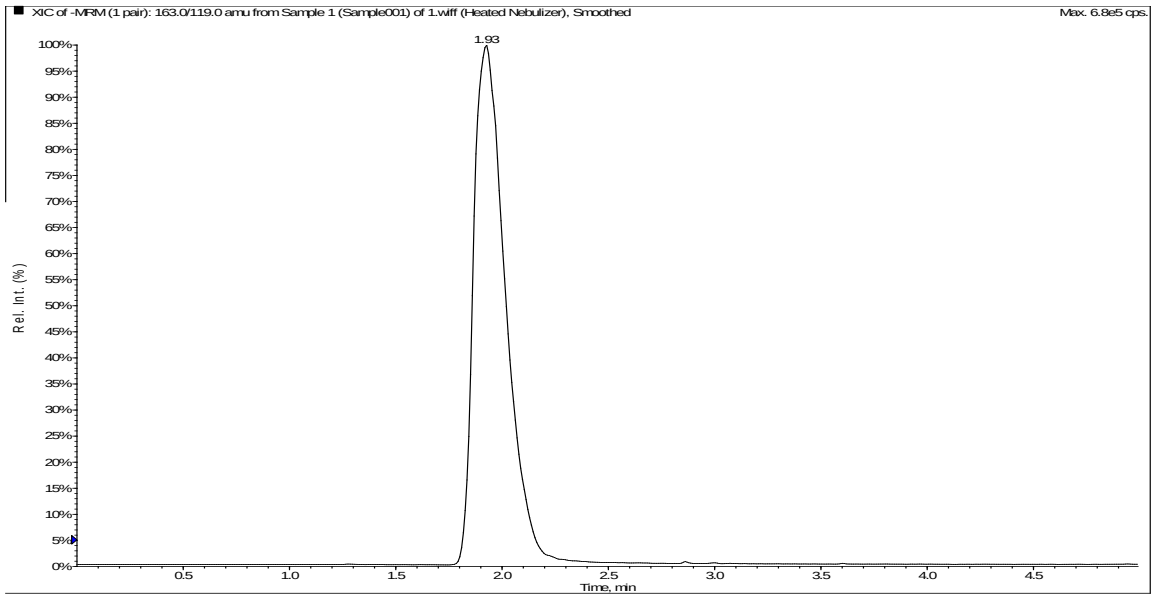

Figure 2.62 HPLC chromatogram of *p*-coumaric acid in sample compound **D** at a retention time of 1.93 minutes. Column: Phenomenex® C_{18} (15cm × 2.0mm, 5µm); the injection solvent and mobile phase consisted of water : methanol (10:90, v/v) acidified with formic acid (0.05%) and 20µL was loaded onto the column; the flow rate of the mobile phase through the analytical column was 200 µL/min.

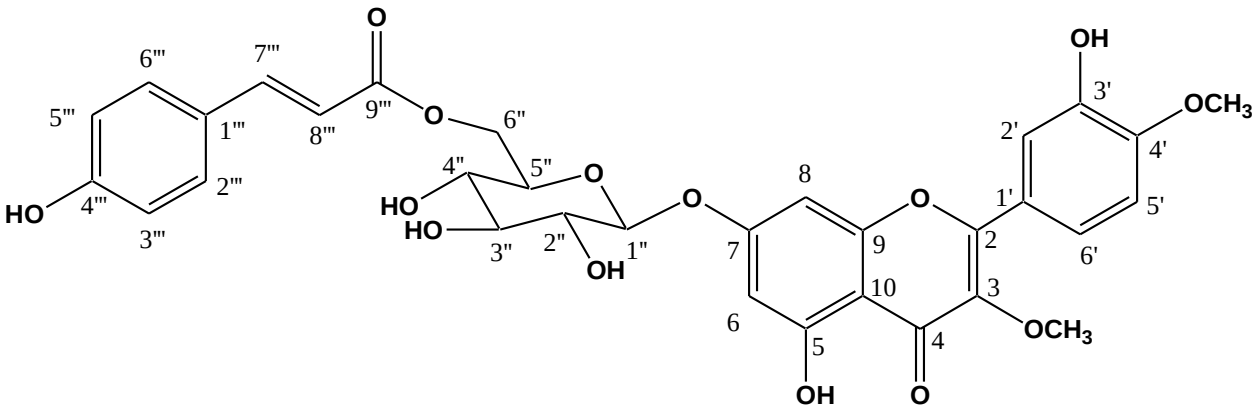

Structure of compound D

2.3.3.5 Compound **E**

Compound **E** was isolated as a buff-coloured amorphous product. The negative LRAPCIMS showed a pseudomolecular ion at *m/z* 463.1 $[M - H]^-$. The signal at *m/z* 301.2 in the APCI mass spectrum (Figure 2.63a) corresponded to the loss of a hexose moiety from the parent compound. Together with the ^1H spectrum and APT experiment, this suggested a molecular formula of $C_{21}H_{20}O_{12}$. The UV-vis absorption spectra indicated a flavonol derivative; the observed shift and degradation in alkali suggested the 7-hydroxyl group to be substituted and an alkali-sensitive 3, 3′, 4′-OH system to be present (Figure 2.64). Complete acid hydrolysis of compound **E** gave quercetin and *β*-glucose. Co-elution with reference standards on TLC (Figure 2.20) confirmed the sugar to be *β*-glucose. The HMBC experiment displayed a long-range correlation between C-7 (δ 163.02) and the anomeric proton (δ 5.05), revealing the site of glycosylation as the 7-OH of quercetin. Thus the structure of compound **E** was determined as quercetin 7-*O*-*β*-glucopyranoside. Complete assignment of the ^1H and ^{13}C NMR signals were achieved with the help of two dimensional COSY, HSQC and HMBC spectra.

Compound **E** was found, for example, in *Vigna sinensis* beans (Chang and Wong, 2004), and was recently isolated by HSCCC from *Flos gossypii* (Yang *et al.*, 2008).

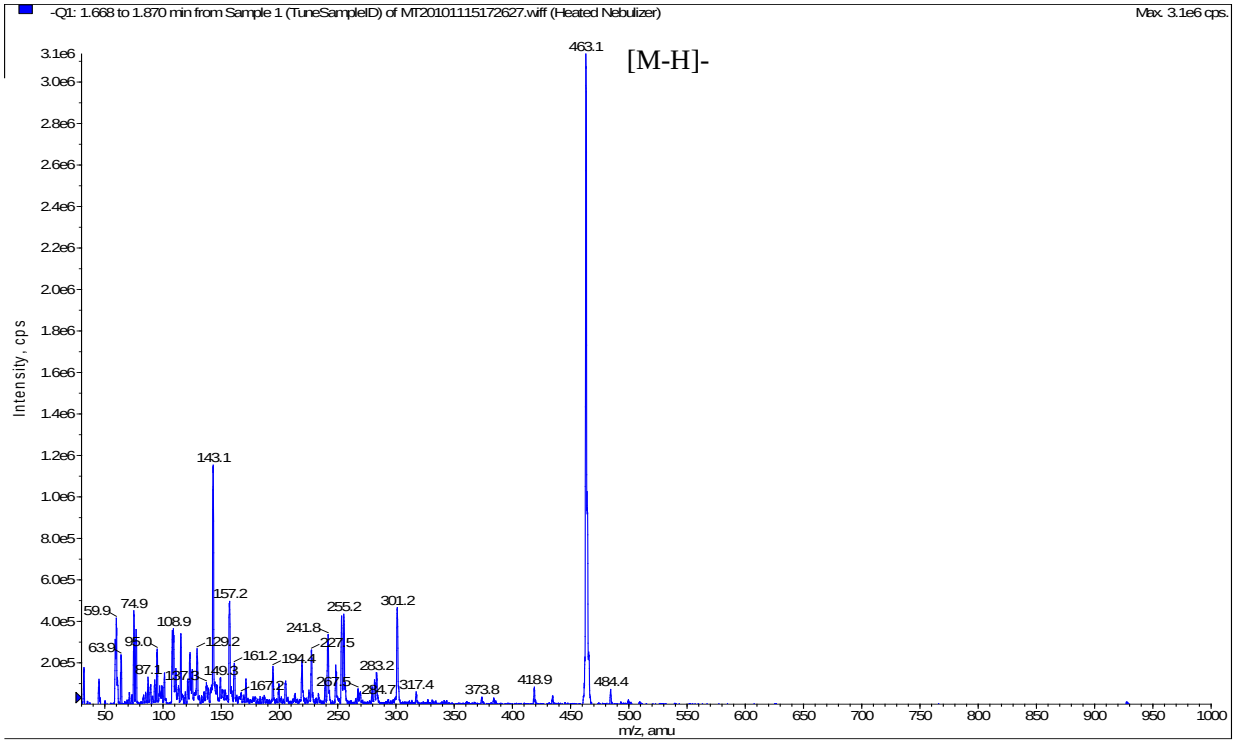

(a)

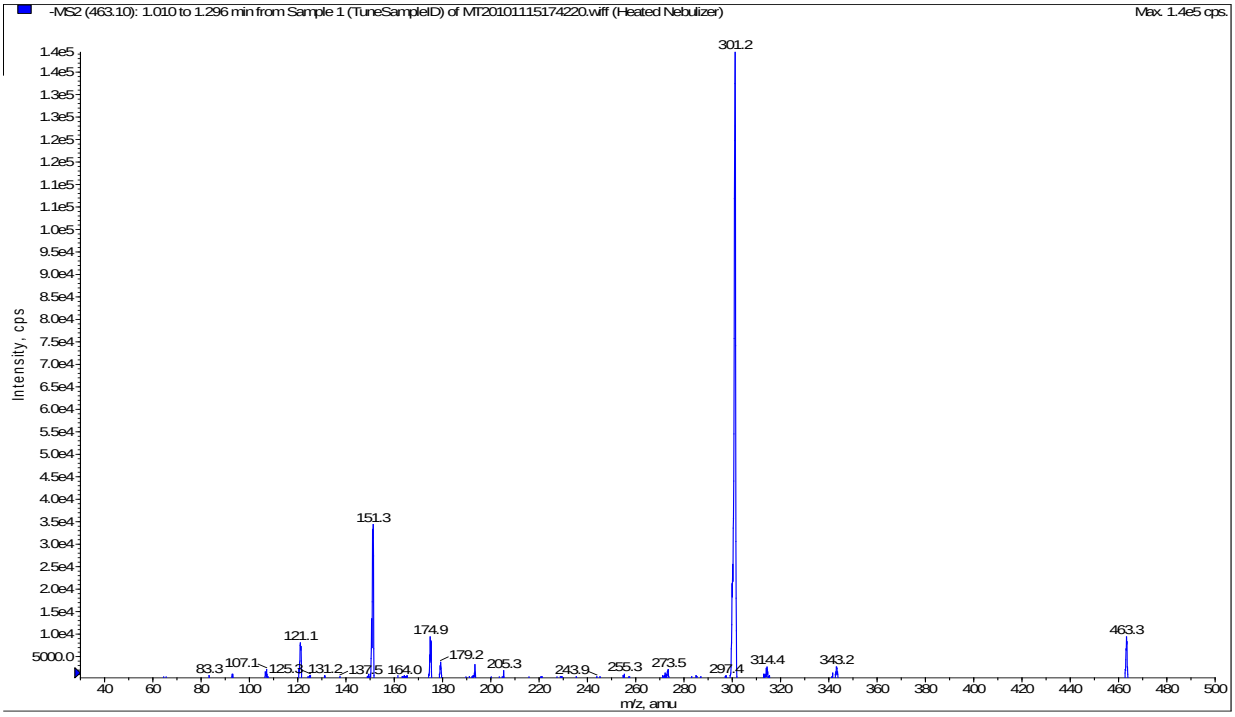

(b)

Figure 2.63 a) Q1mass scan in the negative ion mode of compound **E** obtained by APCI. b) Product ion scan of m/z 463.3.

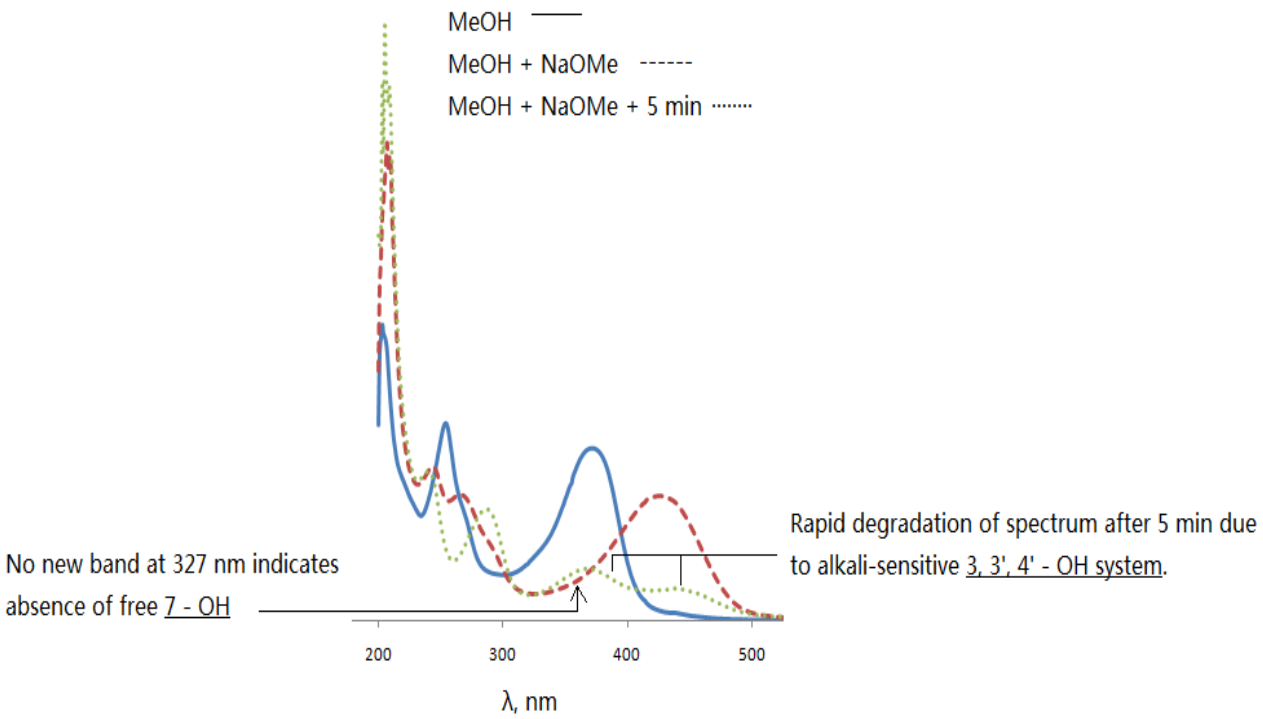

Figure 2.64 UV-vis spectra of compound **E** obtained after the addition of shift reagent NaOMe.

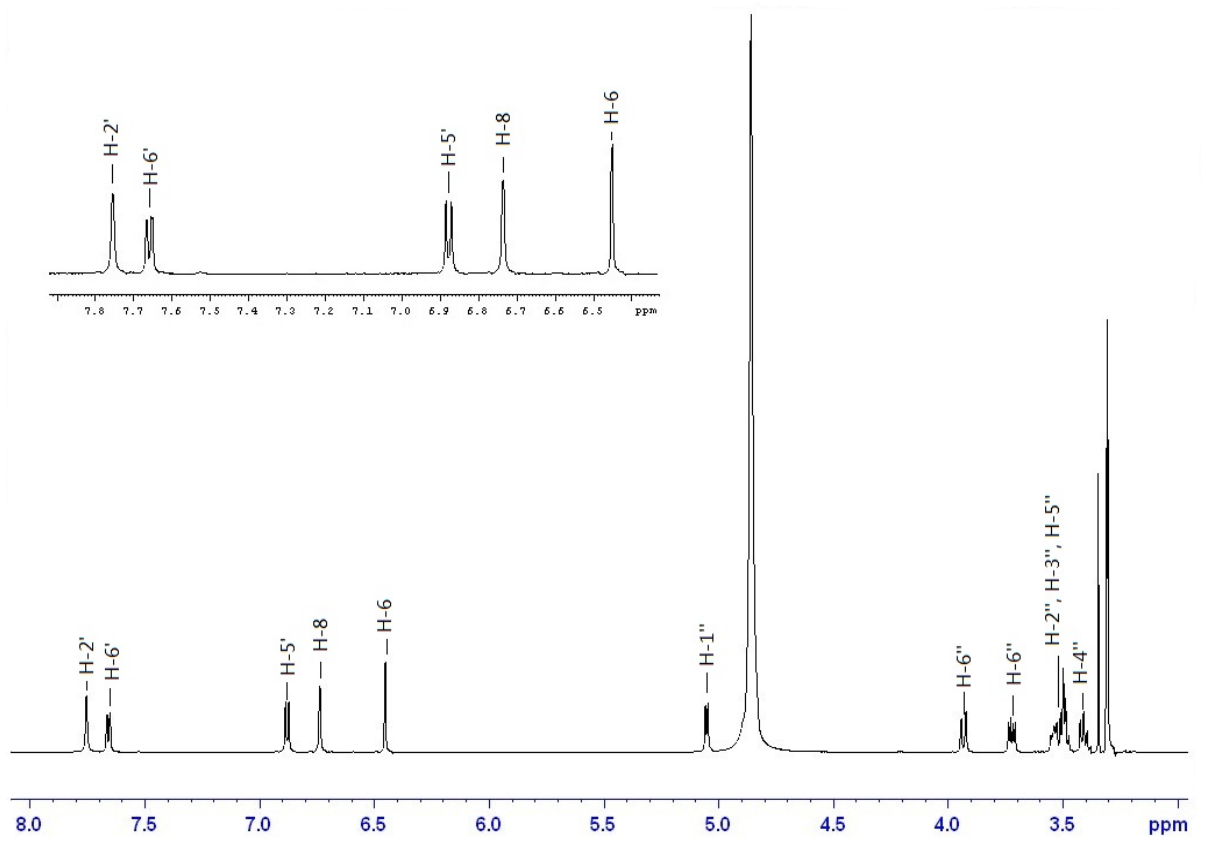

Figure 2.65 ^{1}H NMR spectrum (600 MHz, CD_3OD) of compound **E**.

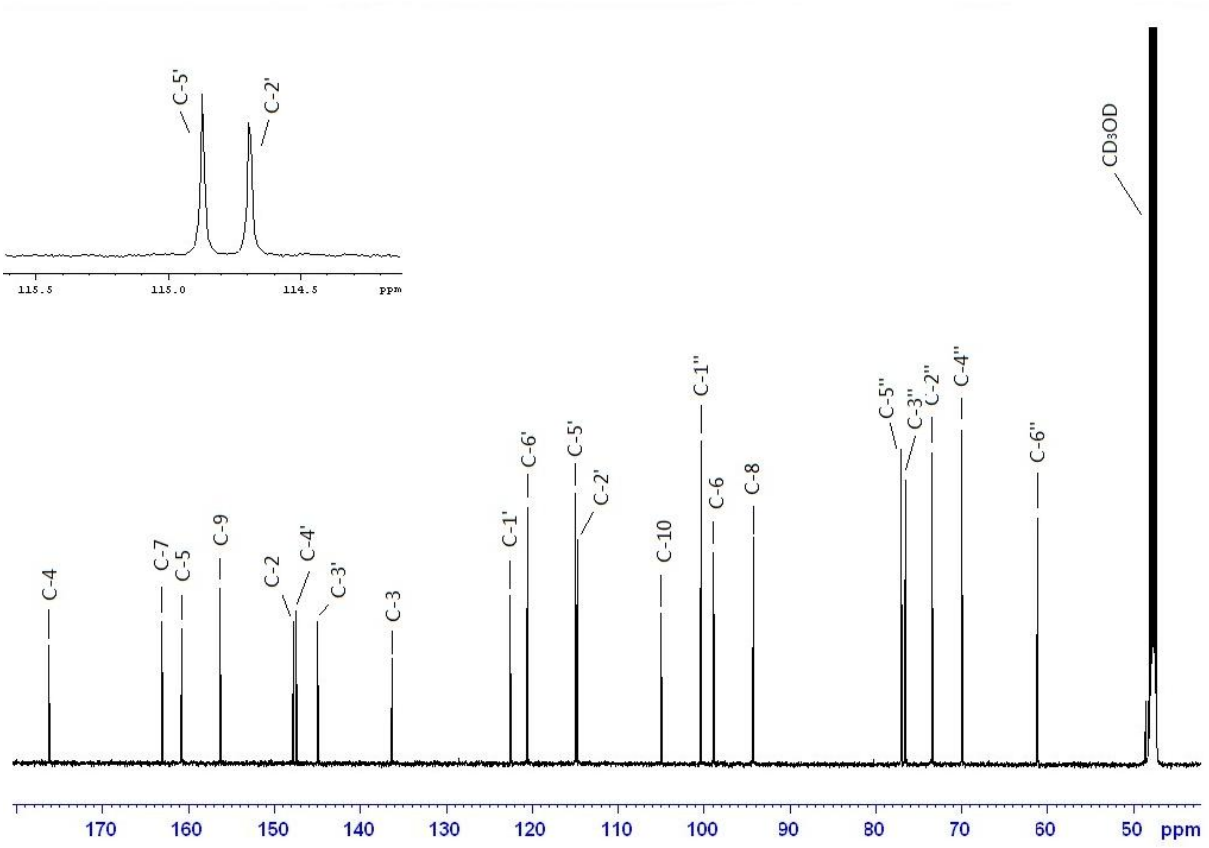

Figure 2.66 ^{13}C NMR spectrum (150 MHz, CD_3OD) of compound **E**

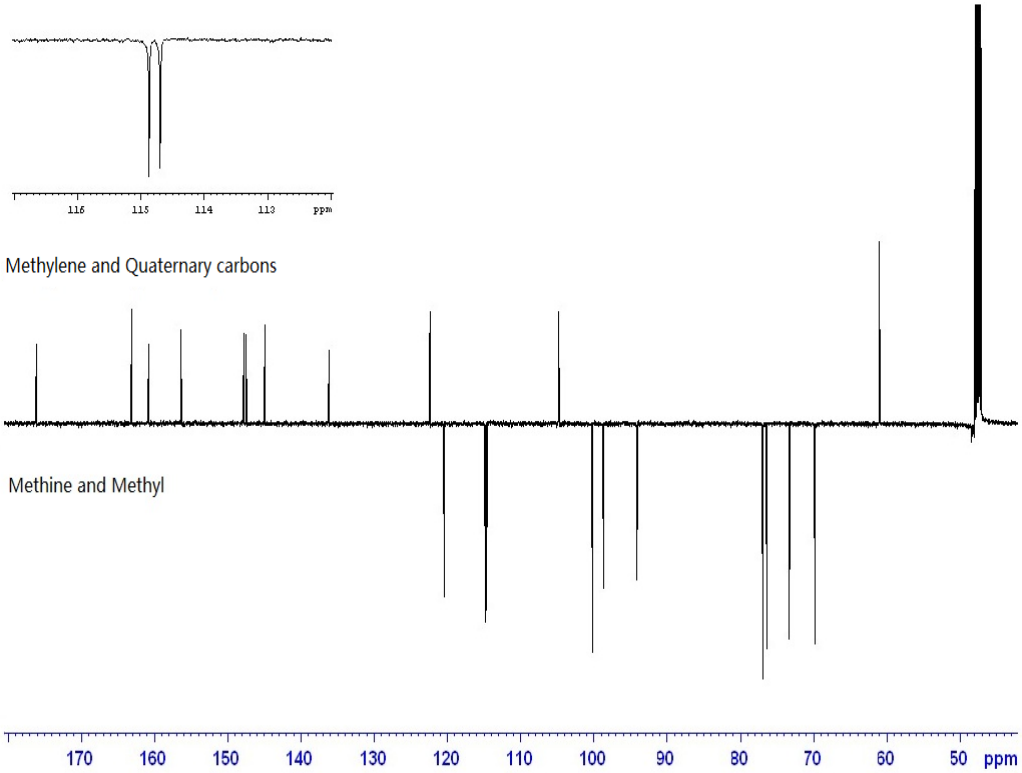

Figure 2.67 APT experiment (150 MHz, CD_3OD) of compound **E**.

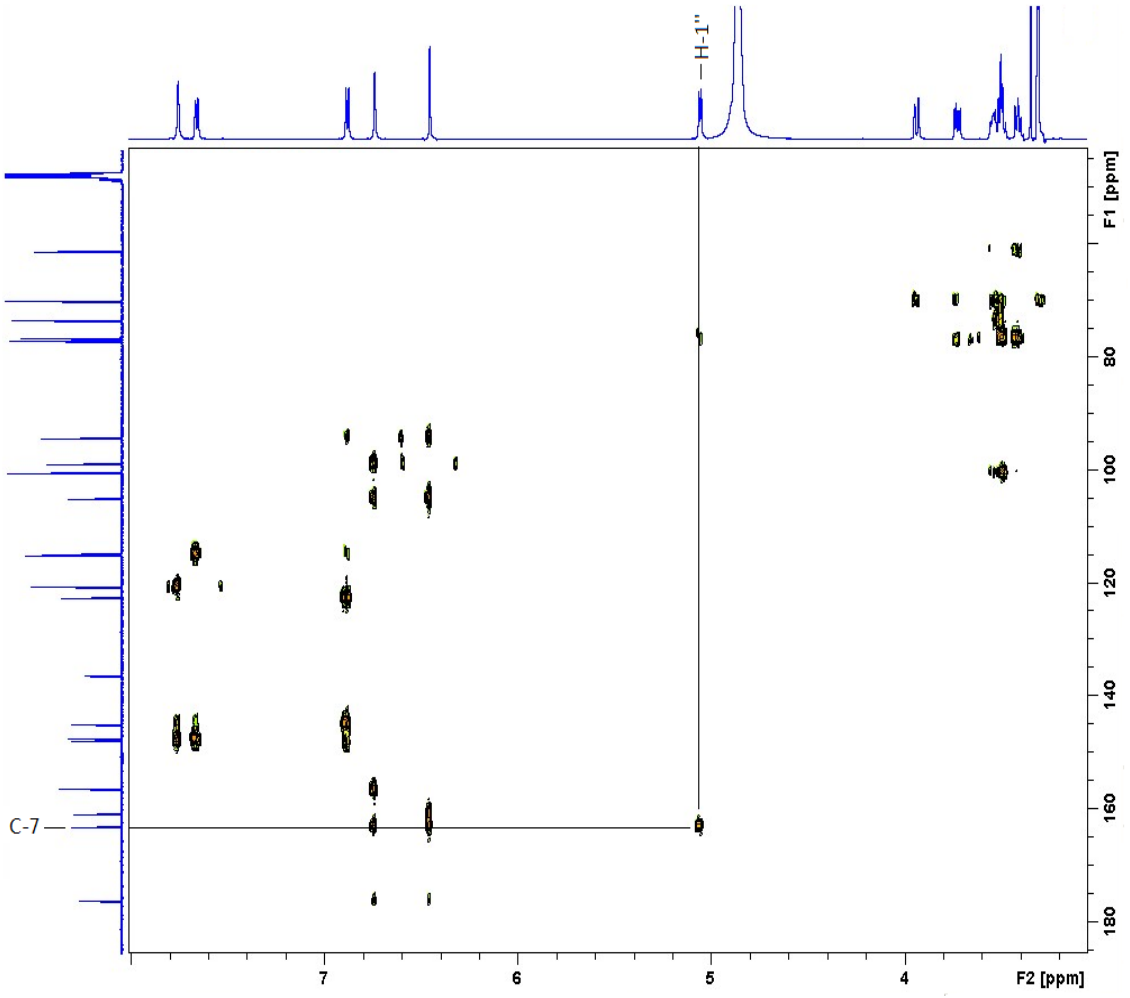

Figure 2.68 HMBC spectrum of compound **E**.

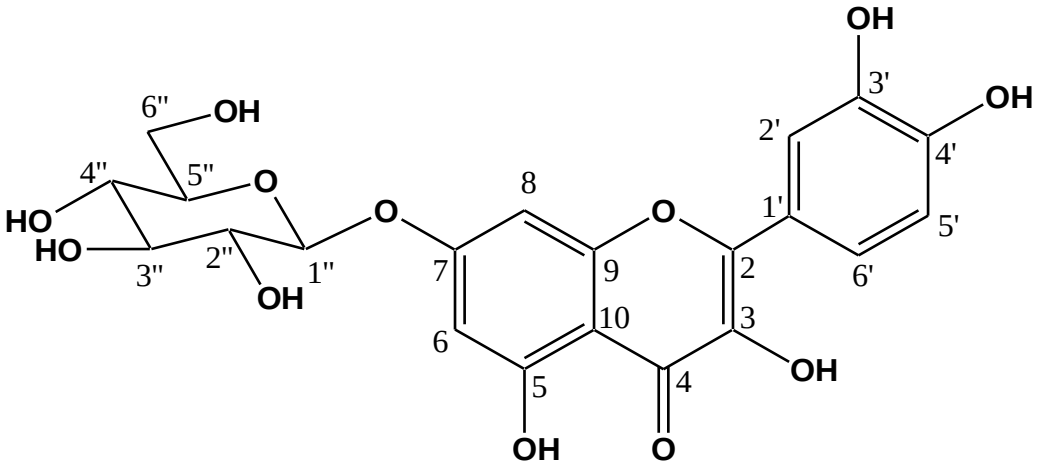

Structure of compound E

2.3.3.6 Compound **F**

Compound **F** was obtained as light beige amorphous product. The positive LRAPCIMS showed a pseudomolecular ion at *m/z* 467.2 $[M + H]^+$, which together with the ^{1}H NMR spectrum and APT experiment, suggested a molecular formula of $C_{21}H_{22}O_{12}$. The UV-vis absorption spectra of compound **F** indicated a dihydroflavonol or a flavanone derivative, because of the lack of strong absorption around 350 nm. The observed shift and degradation in alkali suggested the 7-hydroxyl group to be substituted and an alkali-sensitive 3, 3′, 4′-OH system to be present. The ^{1}H NMR spectrum showed two doublets at δ 4.97 (*J* = 11.5 Hz, H-2) and 4.57 (*J* = 11.5 Hz, H-3) characteristic of *trans* H-2/H-3 protons in a dihydroflavonol. The two proton doublets at δ 6.24 (*J* = 2.1 Hz) and 6.21 (*J* = 2.1 Hz) correlated with the carbons at δ 96.88 and 95.61 in the HSQC spectrum (Figure 2.77) and were assigned to the H-8 and H-6 protons of ring A. From the HMBC experiment, ring B was assigned as a 1, 3, 4-trisubstitued benzene ring. The ^{1}H NMR spectrum showed an ABX coupling system, i.e., δ 6.98 (1H, *d*, *J* = 1.6 Hz, H-2′), δ 6.86 (1H, *dd*, ^3J = 8.2 Hz, ^4J = 1.6 Hz, H-6′) and δ 6.81 (1H, *d*, *J* = 8.1 Hz, H-5′). Collectively, these data indicated that the aglycone moiety was dihydroquercetin. The sugar was hydrolyzed by acid and identified as a *β*-glucose based on co-elution with standard (Figure 2.20) and the coupling constant (*J* = 7 Hz) of the anomeric proton in the ^{1}H NMR spectrum. The HMBC experiment displayed a long-range correlation between C-7 (δ 165.89) and the anomeric proton (δ 4.98, *d*, *J* = 7 Hz), revealing the site of glycosylation as the 7-OH of dihydroquercetin. Dihydroflavonols have chiral centers at C-2 and C-3, which translate into four possible isomers. The vicinal spin-spin coupling constant for H-2 and H-3 ($J_{2,3}$) is 11.5 Hz. According to the Karplus equation, the dihedral angles between the planes accommodating the H^2-C^2-C^3-H^3 bond should be close to 180^o. Hence, the H-2 and H-3 protons were in the *trans*-diaxial position (Nifant'ev *et al*., 2006), and a *trans*-dihydroquercetin 7-*O*-*β*-D-glucopyranoside was present, with two possible orientations, i.e, (*2R,3R*)-*trans*-dihydroquercetin 7-*O*-*β*-D-glucopyranoside or (*2R,3S*)- *trans*-dihydroquercetin 7-*O*-*β*-D-gluco pyranoside. The smooth circular dichroism spectra of compound **F** are shown in Figure 2.79; a negative Cotton effect at 223 nm and positive Cotton effects at 330 nm and 296 nm unequivocally defined the 2*R*, 3*R* absolute configuration of the dihydroflavonol (Slade *et. al.*, 2005, Gaffield,

1970). Thus the structure of compound **F** was determined as (*2R, 3R*)-dihydroquercetin 7-*O*-*β*-glucopyranoside.

Compound **F** was the major compound from the methanol extract of *Schotia brachypetala* aril, which is not surprising since dihydroflavonols have been proposed as the biosynthetic precursors of flavonols (Markham, 1982).

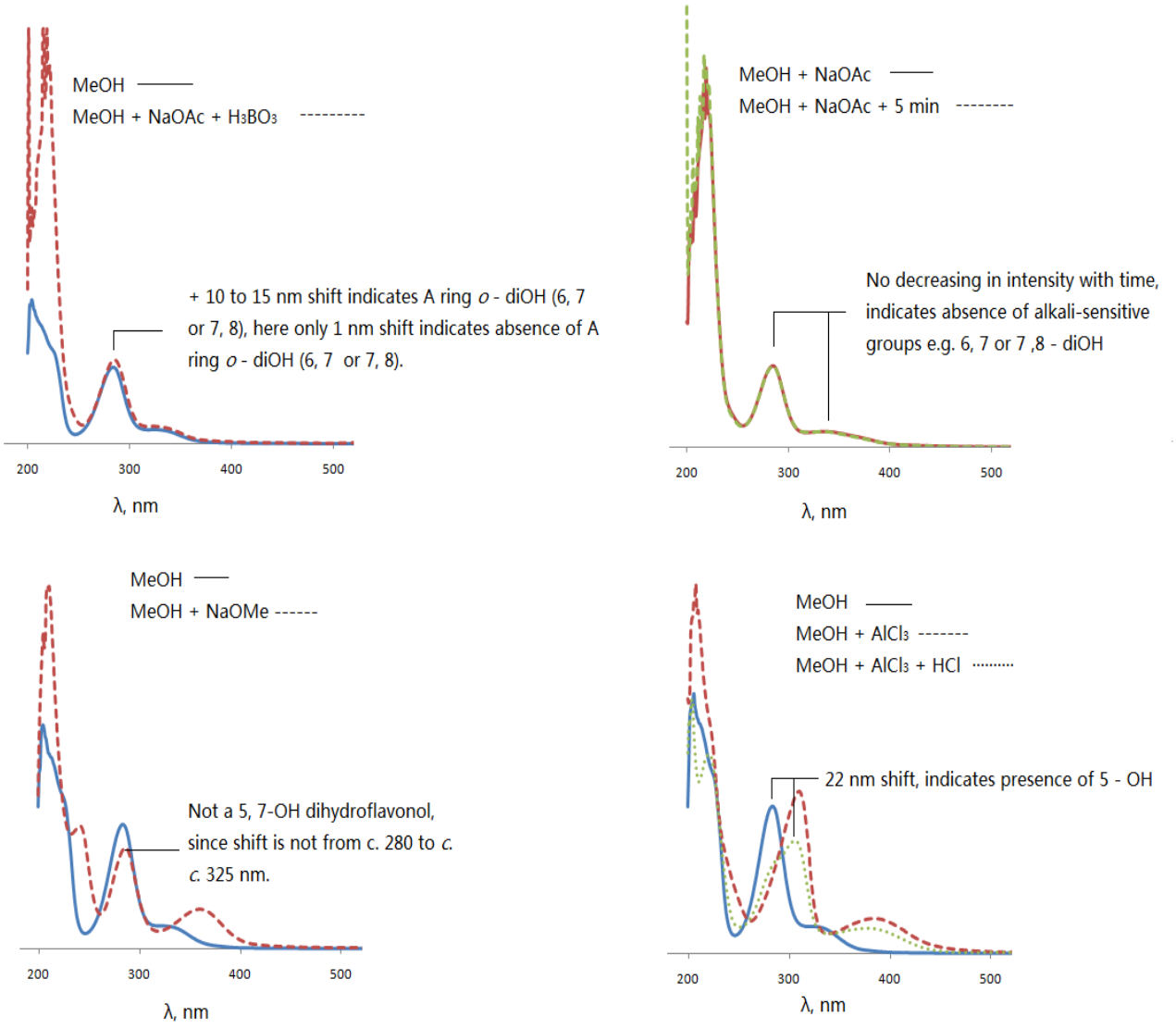

Figure 2.69 UV-vis spectra of compound **F** obtained after the addition of different shift reagents.

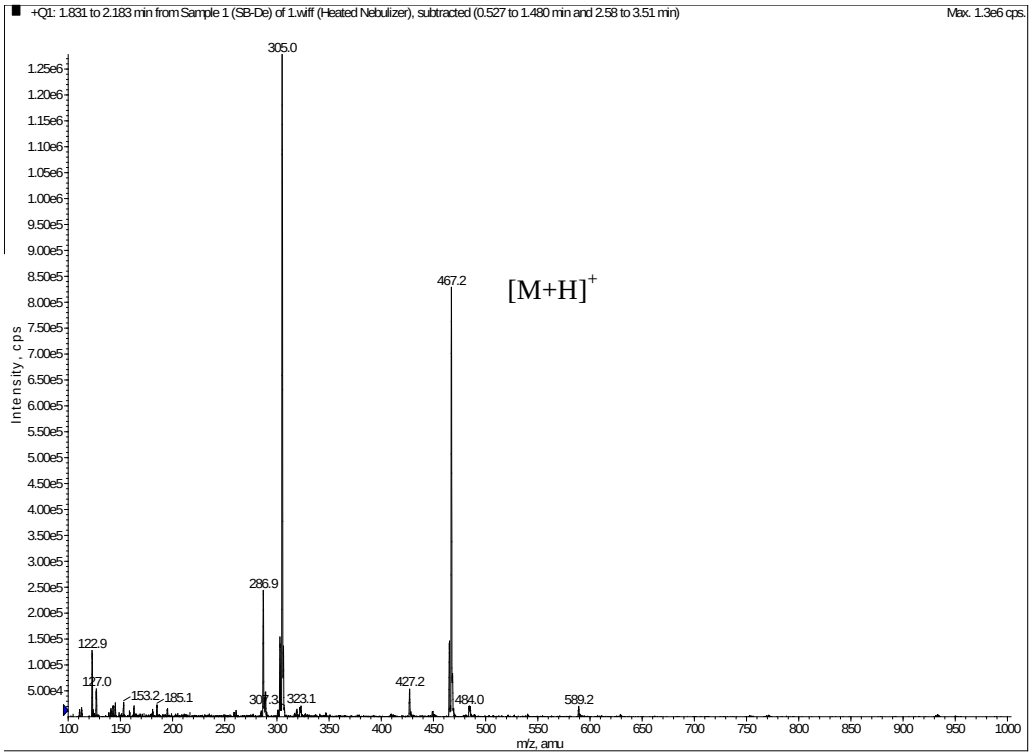

Figure 2.70 LRAPCIMS spectrum of compound **F**

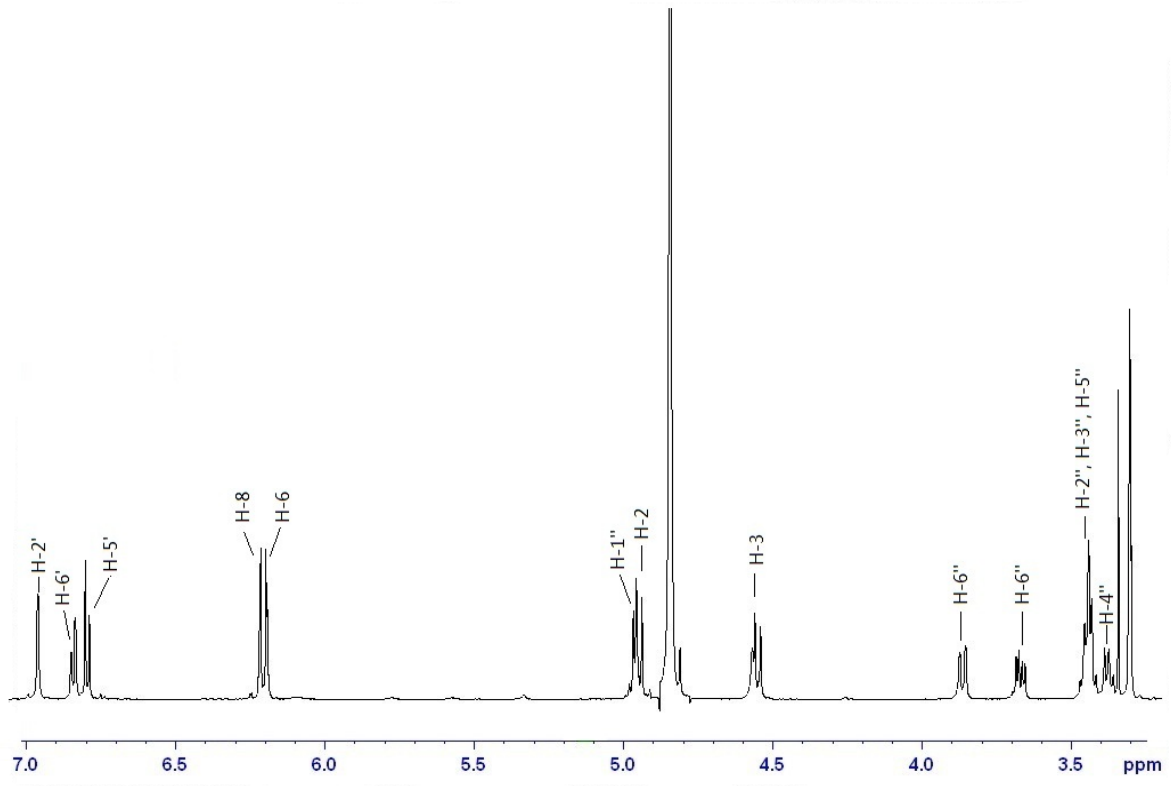

Figure 2.71 ^{1}H NMR spectrum (600 MHz, CD_3OD) of compound **F**

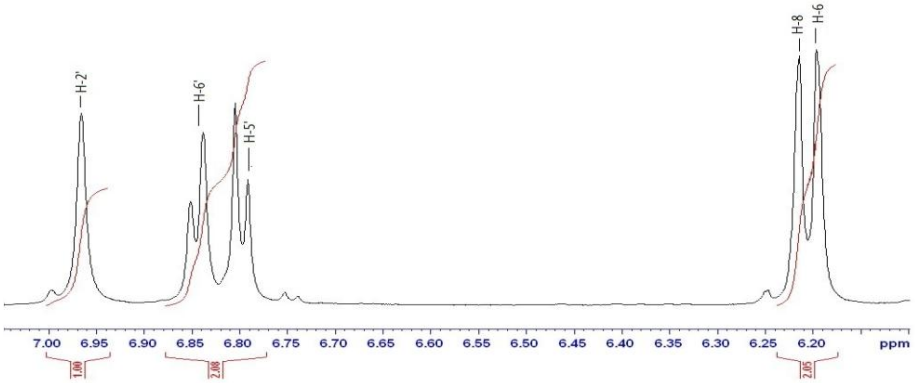

Figure 2.72 Expanded ^{1}H NMR spectrum (600 MHz, CD_3OD) of compound **F**

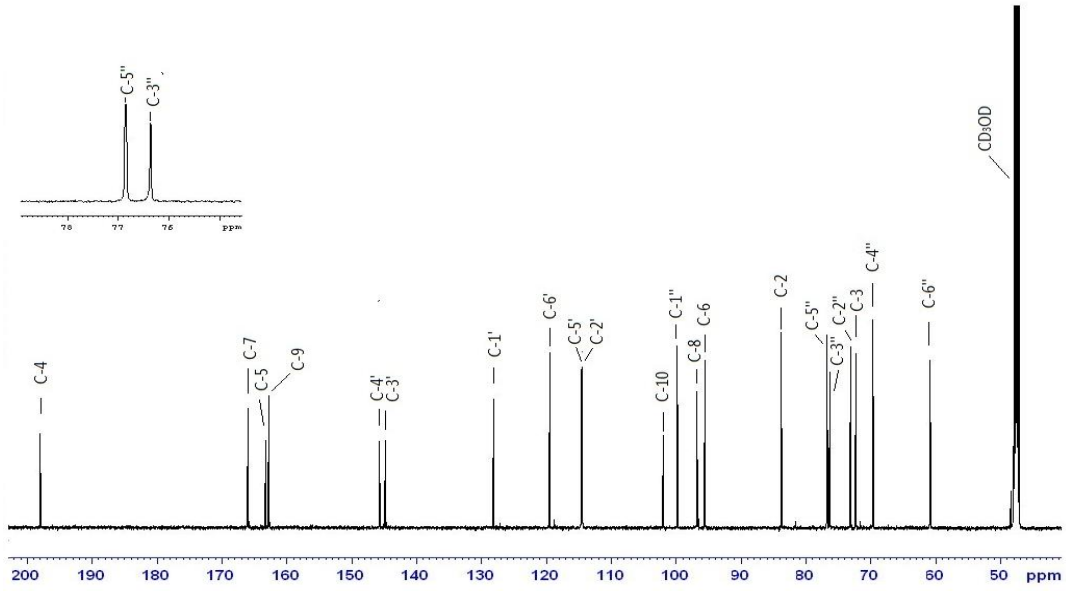

Figure 2.73 ^{13}C NMR spectrum (150 MHz, CD_3OD) of compound **F**

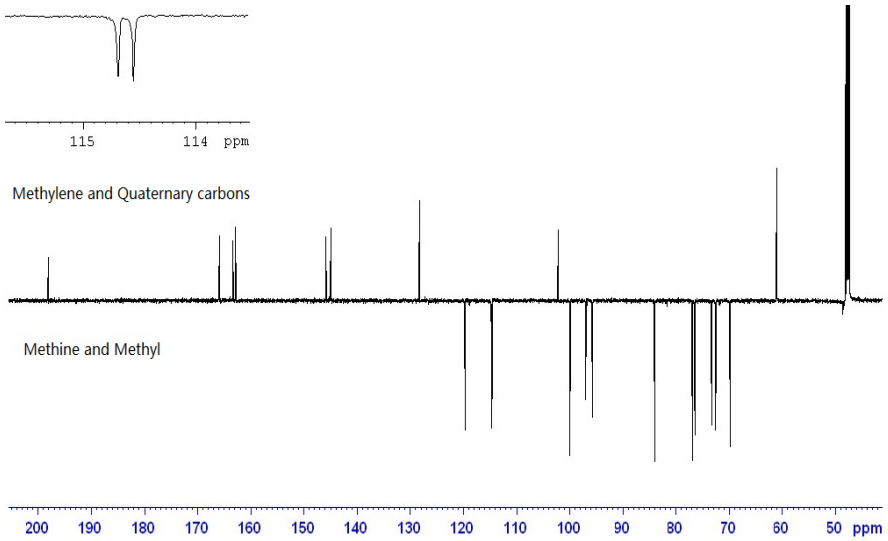

Figure 2.74 ^{13}C NMR spectrum of APT experiment (150 MHz, CD_3OD) of compound **F**.

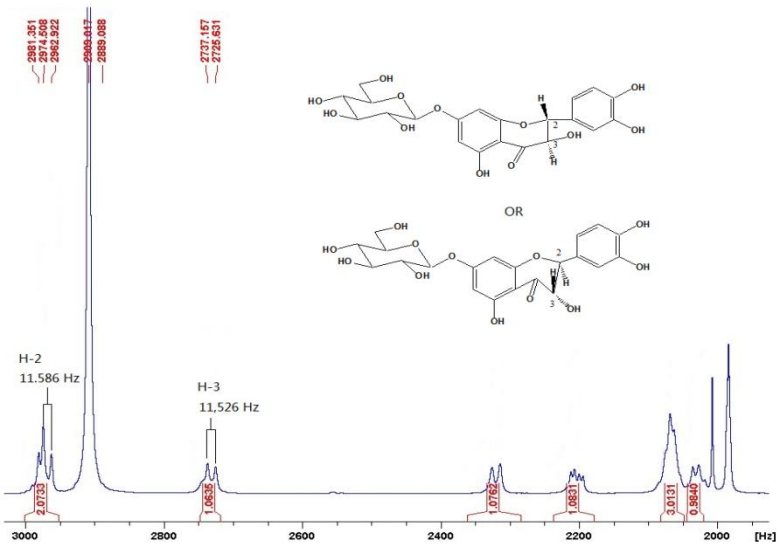

Figure 2.75 Expanded ^{1}H NMR; the coupling constant (J = 11.5 Hz) of H-2/H-3 suggested a *trans* configuration.

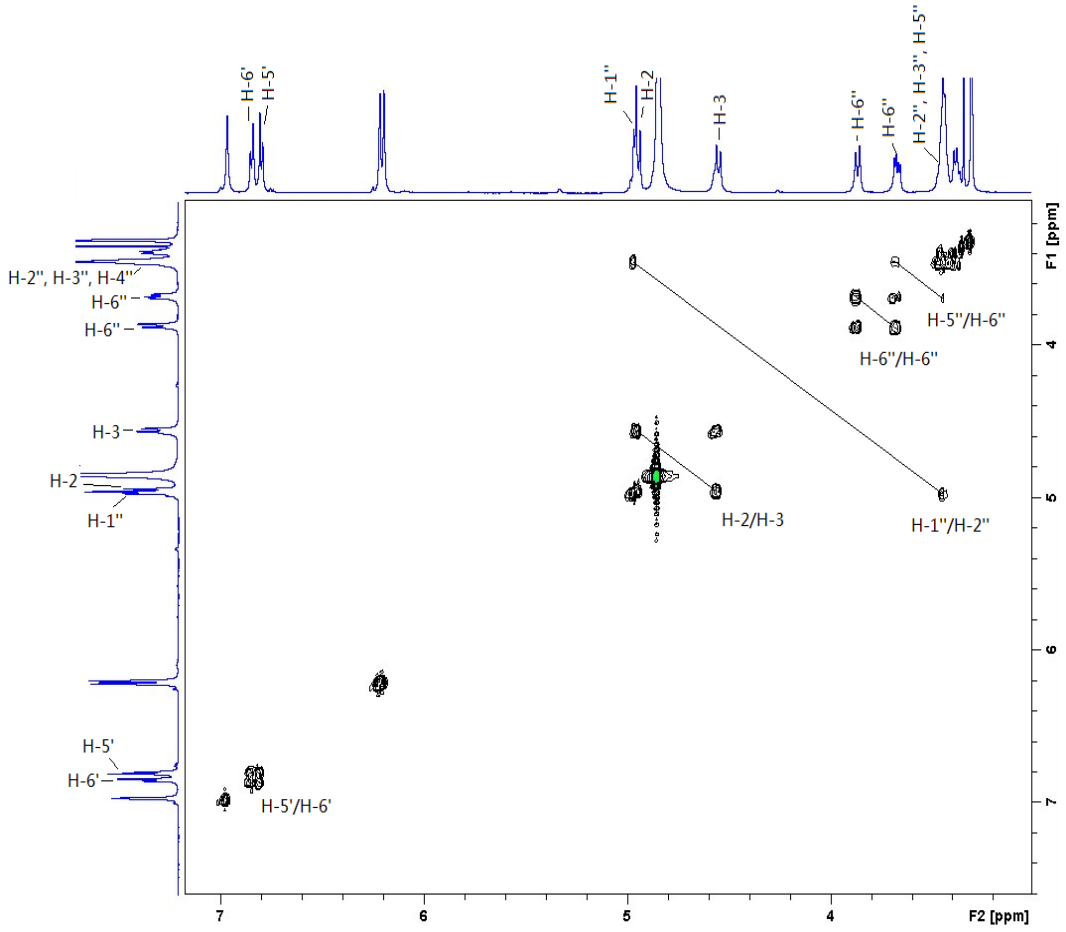

Figure 2.76 COSY spectrum of compound **F**.

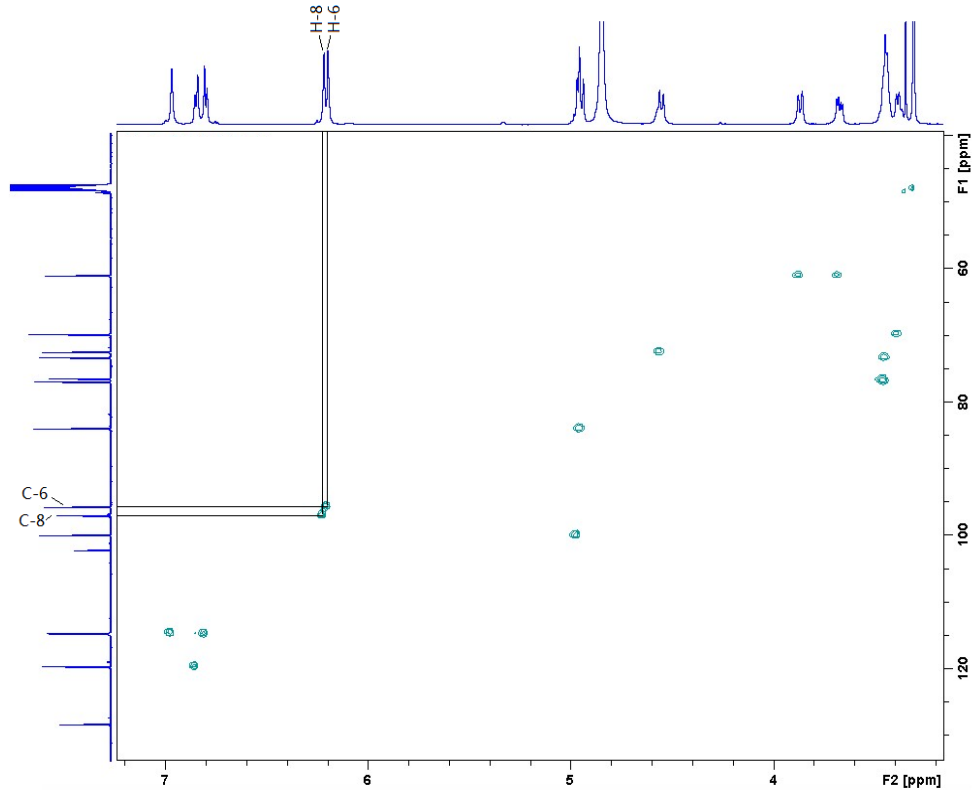

Figure 2.77 HSQC spectrum of compound **F**.

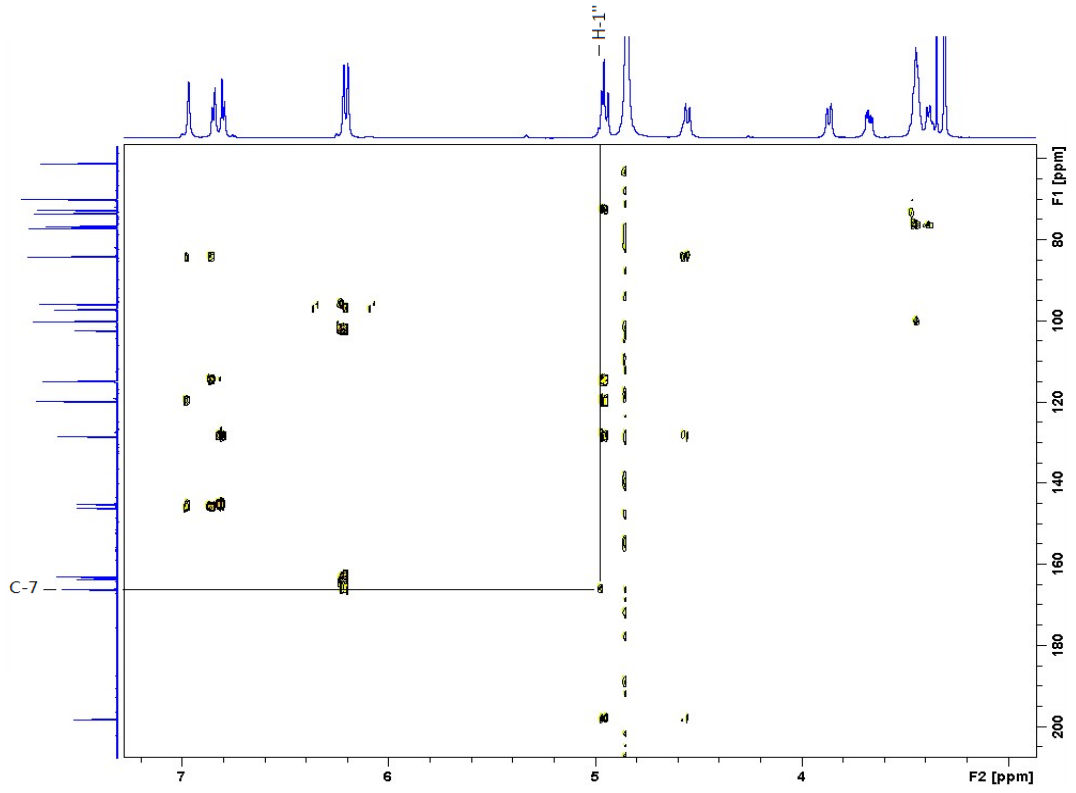

Figure 2.78 HMBC spectrum of compound **F**.

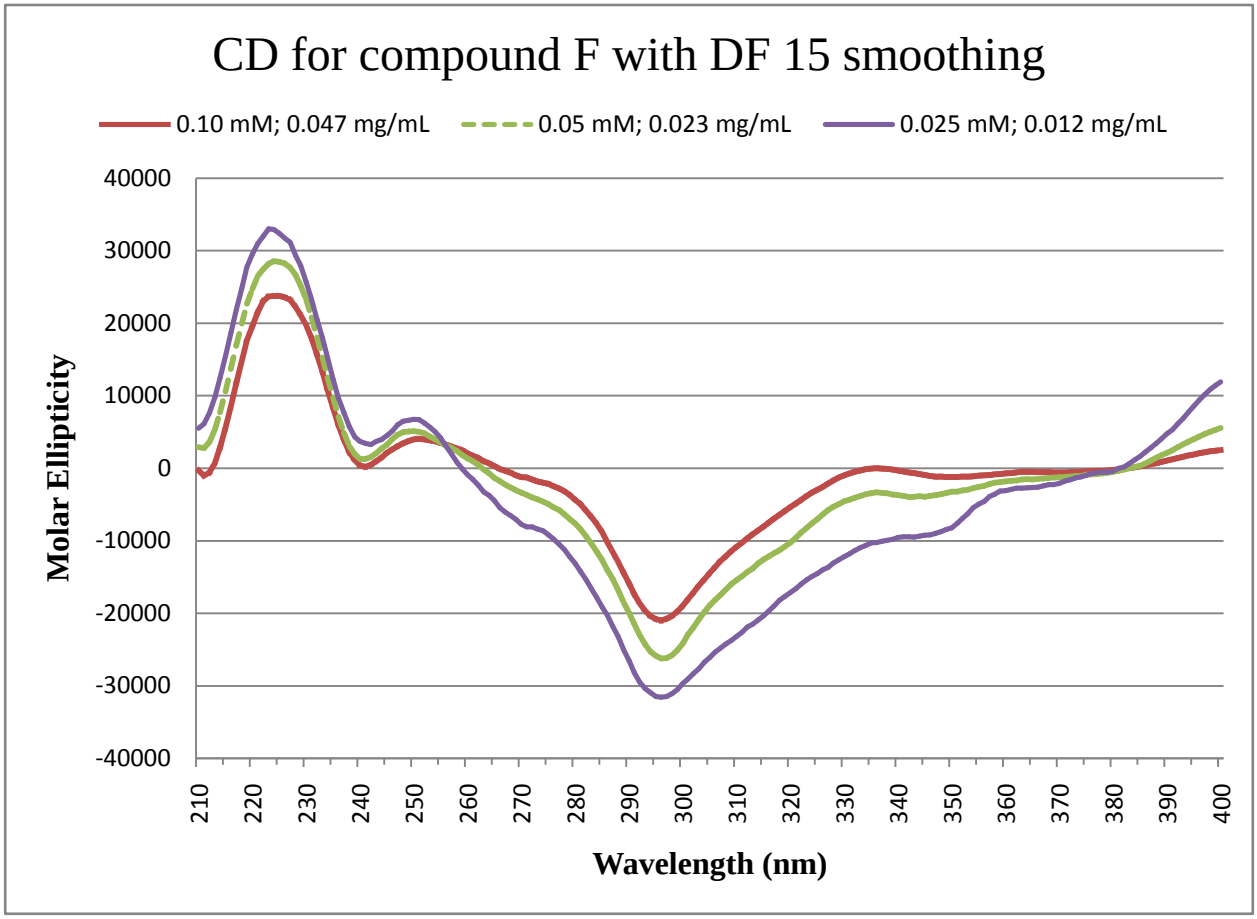

Figure 2.79 Circular dichroism spectra of compound **F**.

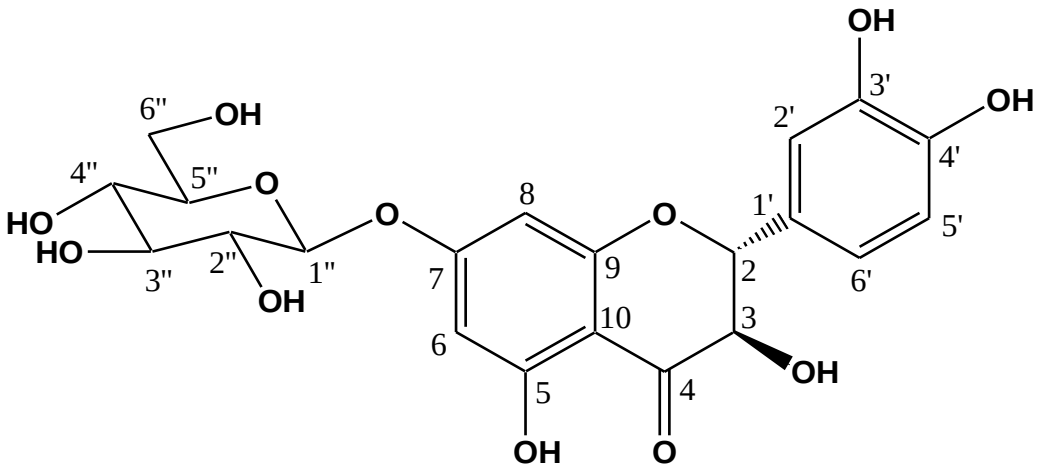

Structure of compound F

2.3.3.7 Compound **G**

Compound **G** was isolated as an amber-coloured amorphous product. The elemental composition $C_{32}H_{38}O_{20}$ was determined from its HRESIMS and ^{13}C NMR spectral data. The UV-vis absorption spectra indicated a flavonol derivative, and the spectra after addition of the shift reagents suggested the 3-OH to be substituted, and free 5,7-OH and *o*-diOH on the B ring. The sugar composition was determined by TLC to be glucose, xylose and rhamnose, after a microscale acid hydrolysis with 10% HCl in H_2O. Also obtained on acid hydrolysis was the aglycone, which was determined to be quercetin by co-TLC with an authentic sample. The presence of a number of oxymethylene and oxymethine signals in the ^{13}C NMR and signals attributable to three anomeric protons in ^{1}H NMR and the relevant carbons in ^{13}C NMR confirmed the number of sugars and the structure of the aglycone moiety. Their linkage of sugar moieties and the linkage between quercetin and the sugar chain were unequivocally decided by two dimensional COSY, HSQC, HMBC experiments. This compound **G** was identified as quercetin 3-*O*-[2-*O*-*β*-xylopyranosyl-6-*O*-*α*-rhamnopyranosyl]-*β*-glucopyranoside. It was previously isolated from *Actinidia arguta* var. *giraldii* (Webby, 1991) and *Arachis hypogaea L.* (Lou *et al.*, 2001)

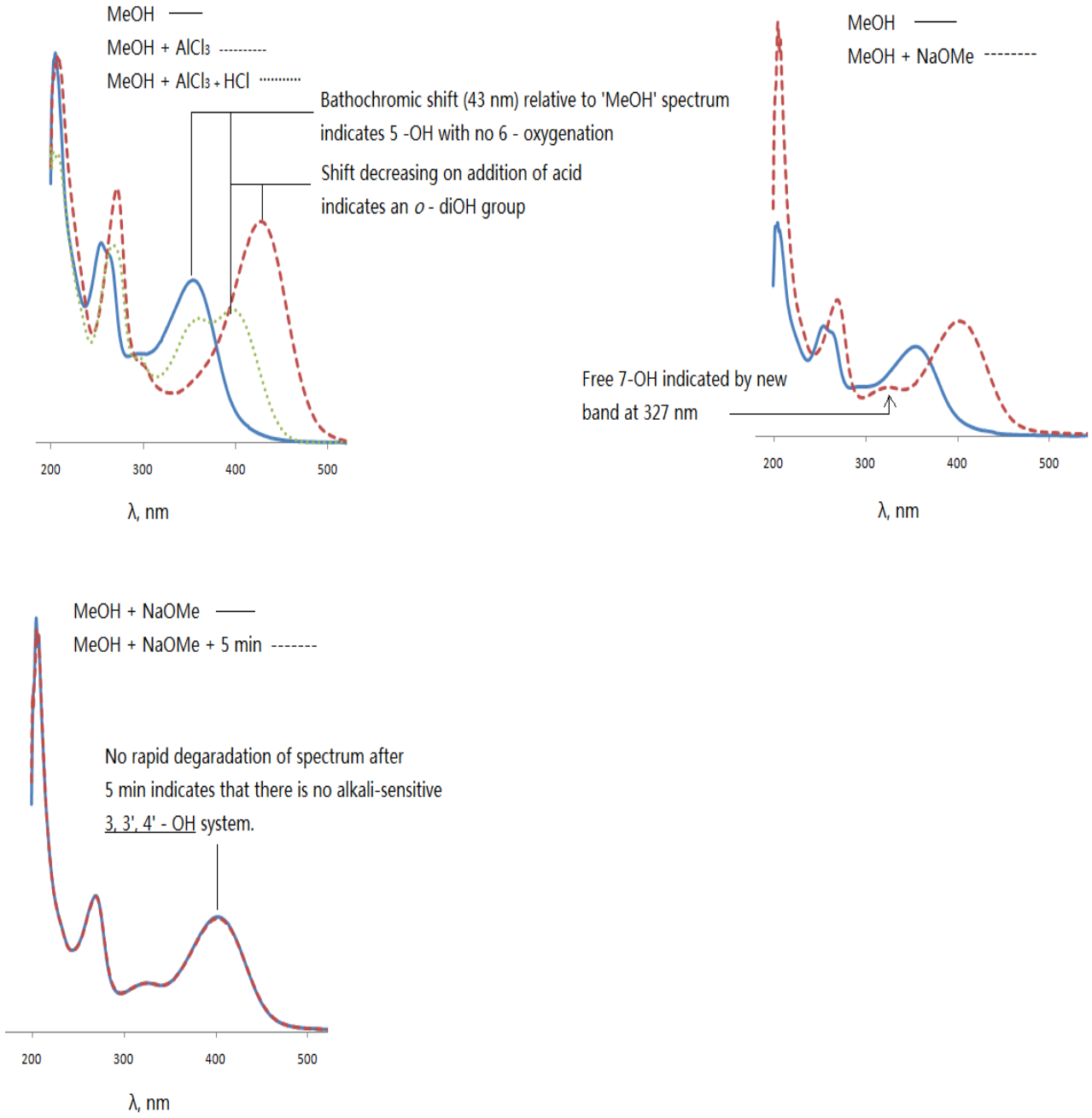

Figure 2.80 UV-vis spectra of compound **G** obtained after the addition of different shift reagents.

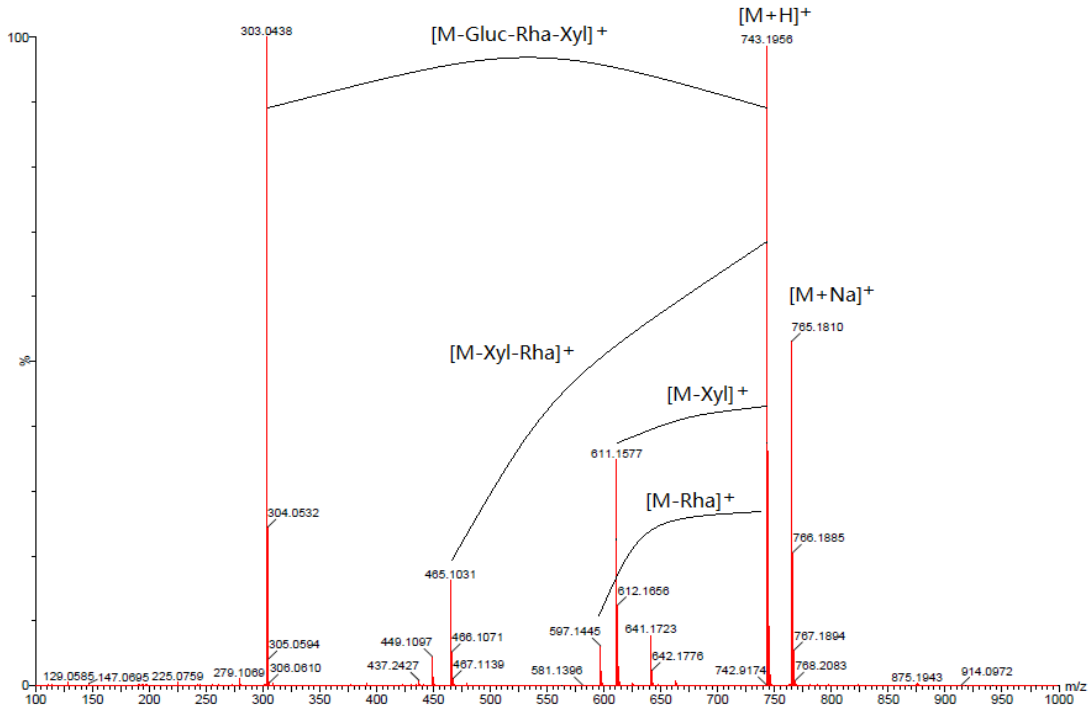

(a)

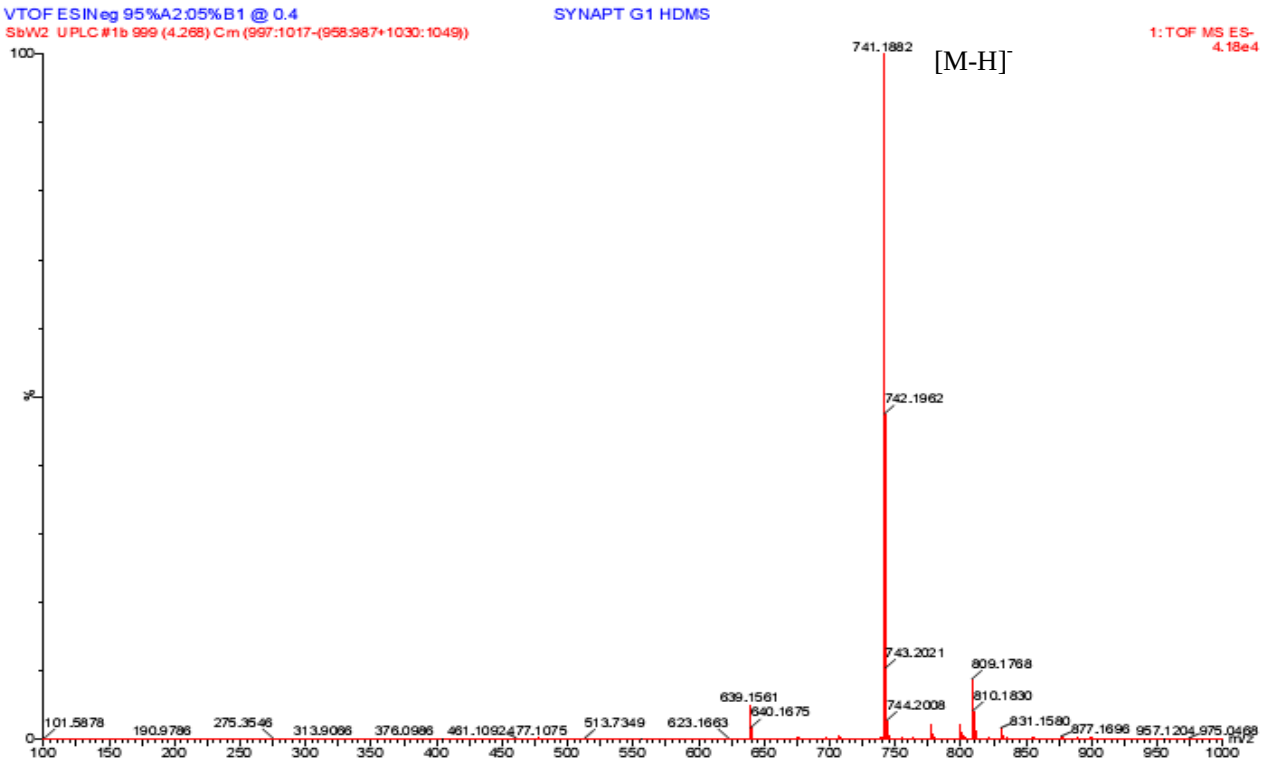

(b)

Figure 2.81 HRESIMS of compound **G**, (a) positive mode; (b) negative mode.

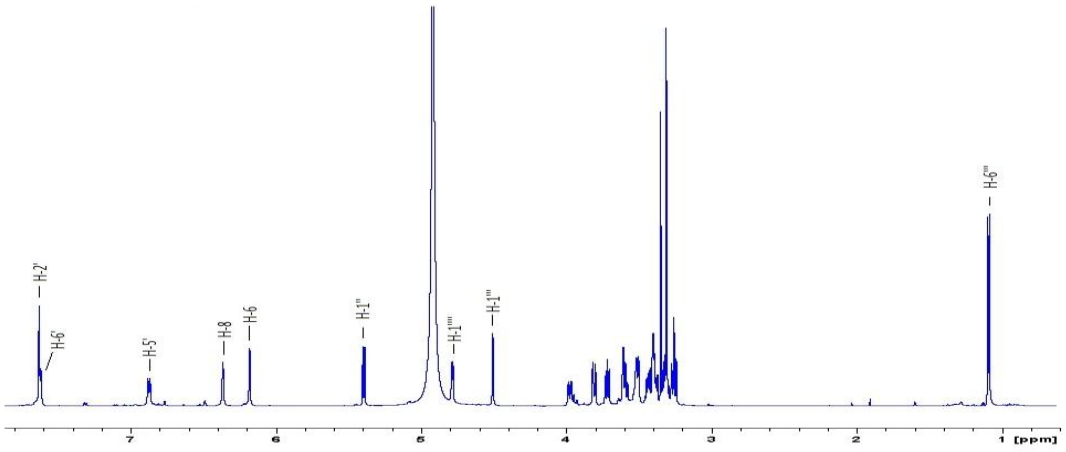

Figure 2.82 ^{1}H NMR spectrum (600 MHz, CD_3OD) of compound **G**

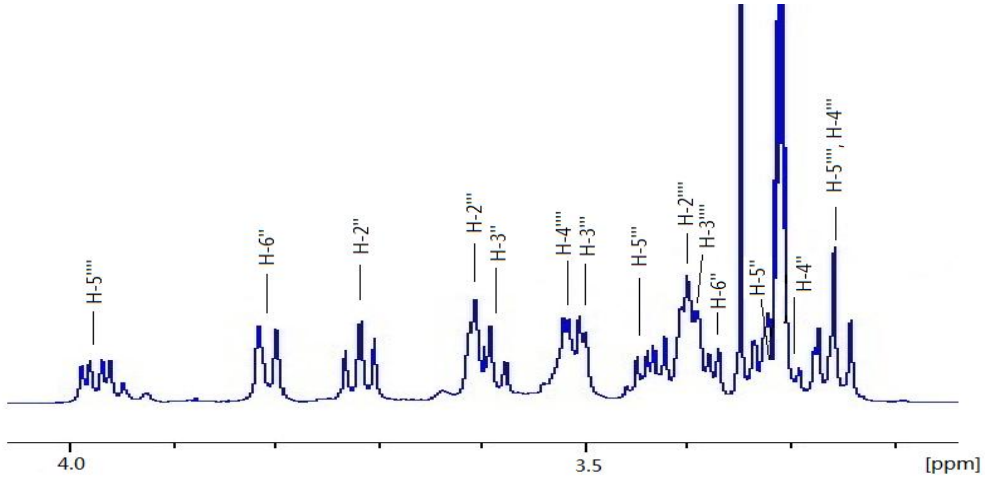

Figure 2.83 Expanded ^{1}H NMR spectrum (600 MHz, CD_3OD) of compound **G**

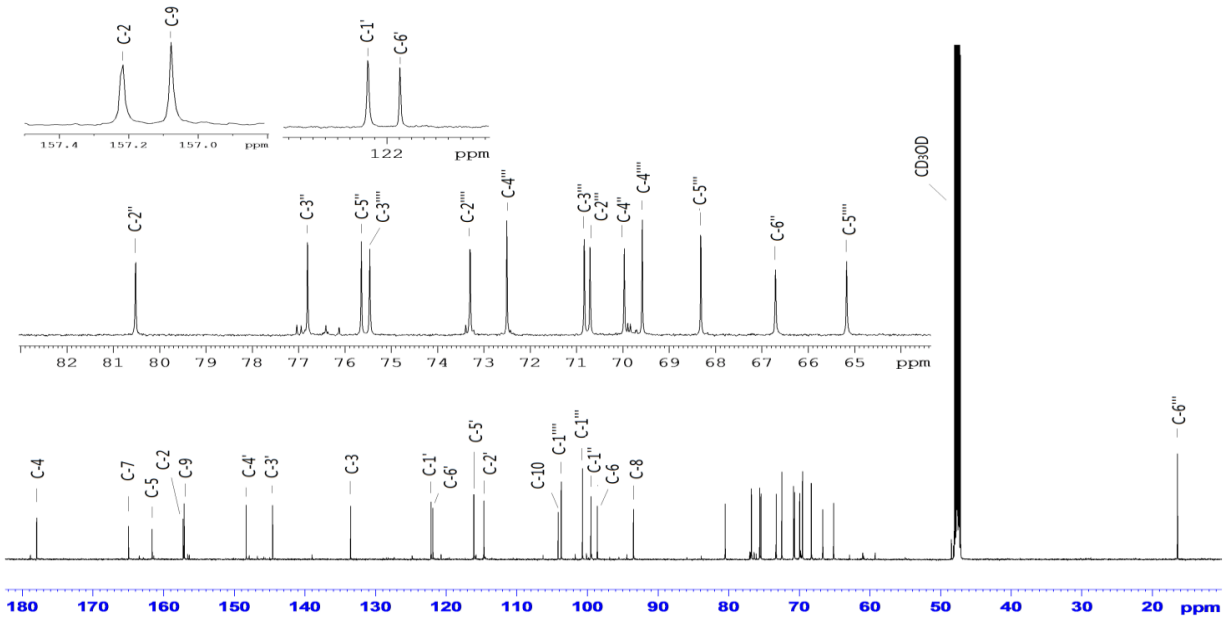

Figure 2.84 ^{13}C NMR spectrum (150 MHz, CD_3OD) of compound **G**

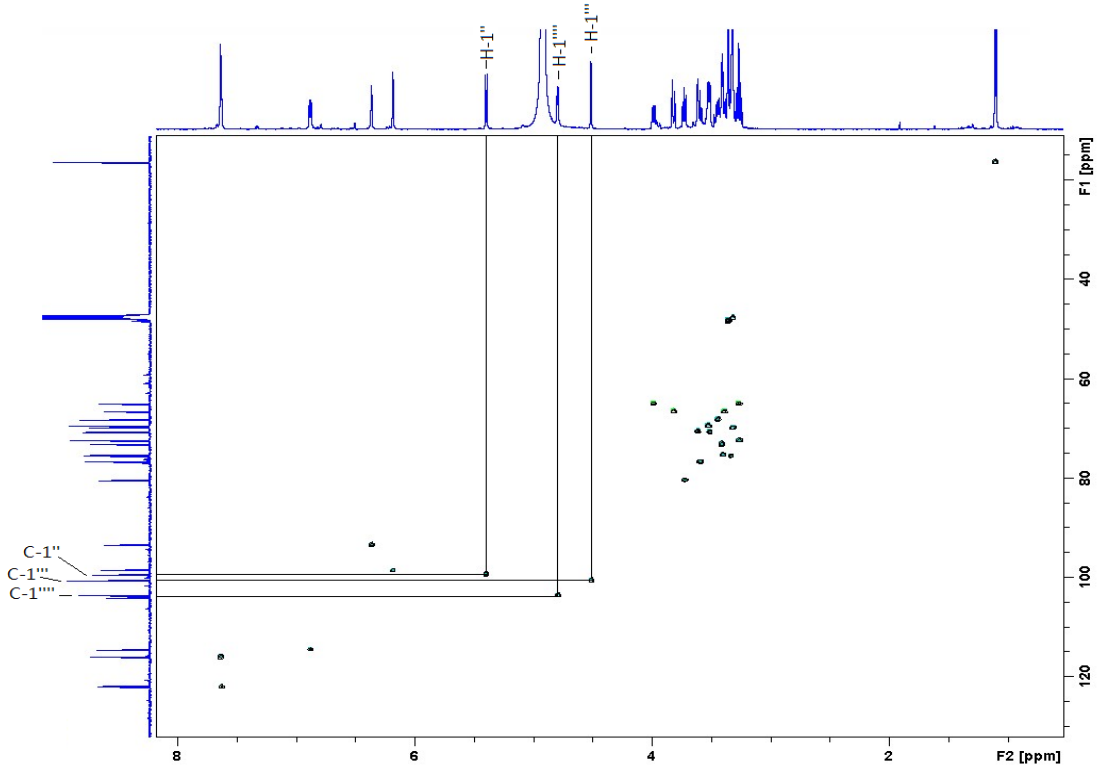

Figure 2.85 HSQC spectrum of compound **G**.

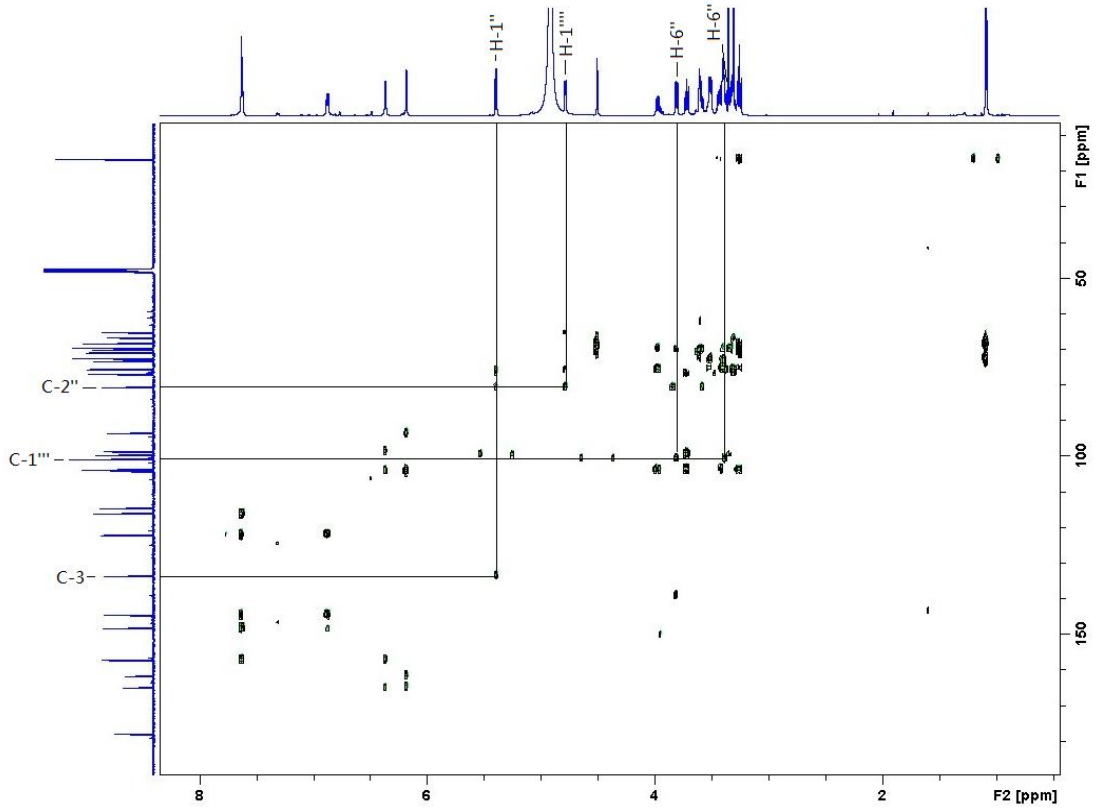

Figure 2.86 HMBC spectrum of compound **G**.

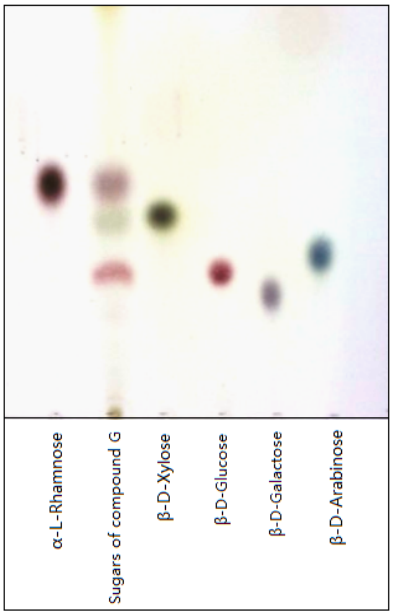

TLC:
$CHCl_3$: *n*-BuOH : MeOH : H_2O : Acetic acid 9 : 25 :10 : 3 : 3
Detection:
0.05 g naphthoresorcinol
0.1 g diphenylamine
1 ml conc. H_2SO_4
25 ml 95% ethanol

Figure 2.87 Identification of sugar moieties of compound **G**. Compounds **G** was acid hydrolyzed and sugars were co-eluted with the reference standards *β*-D-glucose, *β*-D-galactcose, *β*-D-arabinose, *β*-D-xylose and *α*-L-rhamnose. With the detection reagent, *β*-D-glucose showed a pink color, *β*-D-galactcose showed a purple color, *β*-D-arabinose showed a blue color, *β*-D-xylose showed a green colour and *α*-L-rhamnose showed a dark red color.

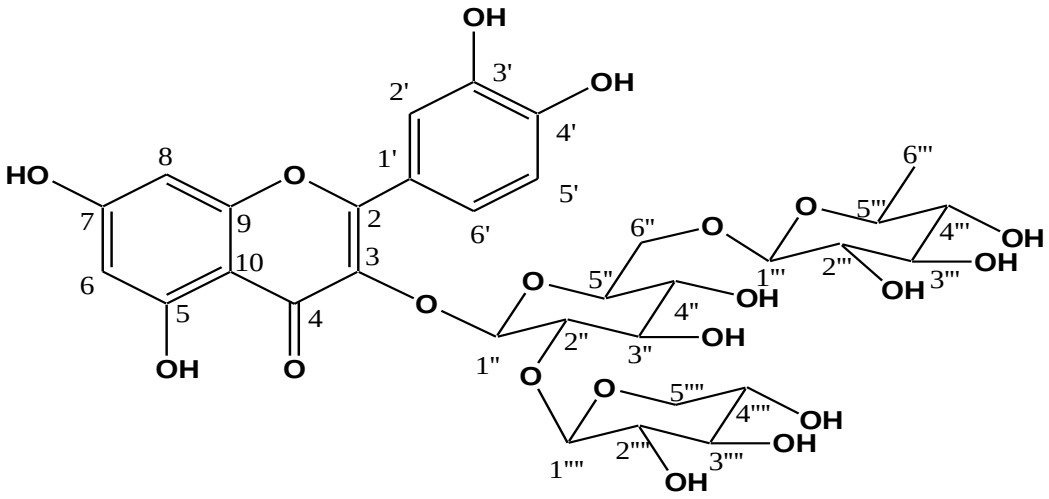

Structure of compound G

2.3.4. The radical scavenging activities of compounds **A**-**G**

Compounds **A**–**G** were tested against the DPPH radical in a spectrophotometric assay using quercetin as a reference compound. Compounds **B** and **D** were inactive (Figure 2.89 a), Compounds **C** and **F** had almost the same activity as quercetin, while the others were weakly active (Figure 2.89 b and c).

Research investigating relationships between the structure and antioxidant activity of phenolic compounds has been conducted for many years. Results obtained so far have established general relationships, e.g. it has been shown that the antioxidant activity of a compound is determined by the presence of free hydroxyl groups and their mutual location (Rice-Evans *et al*., 1997; Wang *et al*., 2006). In addition, analyses carried out in various model systems have led to the determination of functional groups in flavonoid molecules responsible for the activity in the investigated system (Wang *et al*., 2006). Regarding the reaction of quercetin with DPPH radical, its high antiradical activity has been shown to be determined by the presence of a 1,2 dihydroxybenzene moiety (catechol) in the B ring (Burda & Oleszek, 2001; Goupy *et al.,* 2003). This was supported by research comparing the antiradical activity of quercetin and its C(3)-OH and C(4′)-OH glycoside derivatives. In reaction with DPPH, quercetin donates two hydrogen atoms and is transformed into a quinone intermediate (Figure 2.88). In the case of quercetin derivatives, glycosylation at C(4′)-OH markedly decreased the H-donating ability (Goupy *et al.*, 2003), while C(3)-OH derivatives of quercetin showed reducing potential comparable with that of free aglycone (Burda and Oleszek, 2001; Materska and Perucka, 2005).

Wang *et al.* (2006), investigating the antioxidant activity of flavonoid aglycones, including fisetin, kaempferol, morin, myricetin and quercetin, concluded that with reference to superoxide radicals, the highest reduction potential is demonstrated by the 4′-OH group in the B-ring. On the other hand, research investigating the scavenging activity of quercetin derivatives in relation to radicals does not fully support the theory that 4′-OH in the B ring is mainly responsible for high scavenging power. The lower antioxidant activity of quercetin derivatives is mainly due to the blocking of

hydroxyl groups by sugar or alkoxyl substituents. In addition, the increased hydrophilicity of quercetin glycosides modifies the coefficients of distribution between the aqueous and lipid phase, which is of great significance in lipid systems such as TEAC or *β*-carotene emulsion (Burda and Oleszek, 2001).

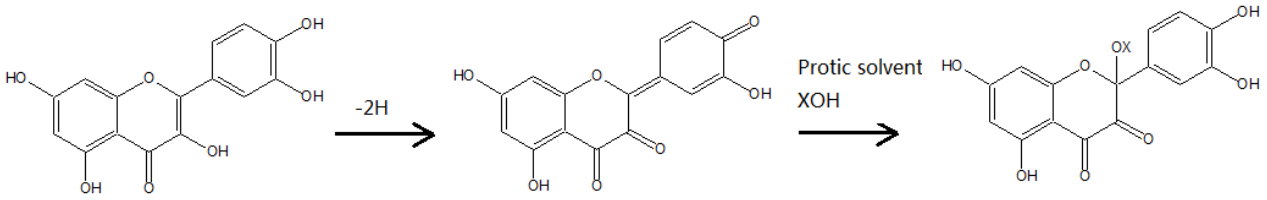

Figure 2.88 Pathway of oxidative changes in quercetin reaction with DPPH radical in protic solvents (Goupy *et al*., 2003).

a)

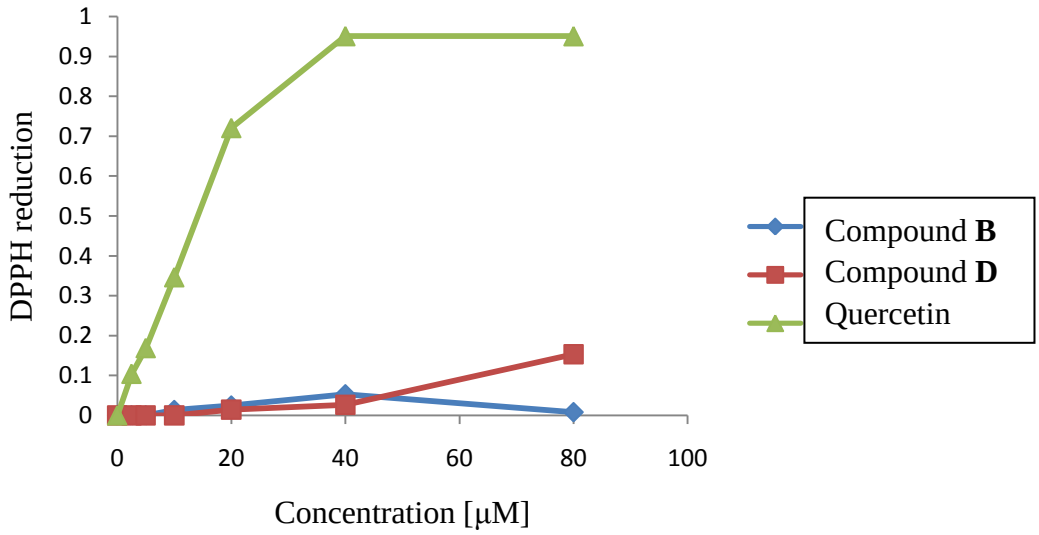

b)

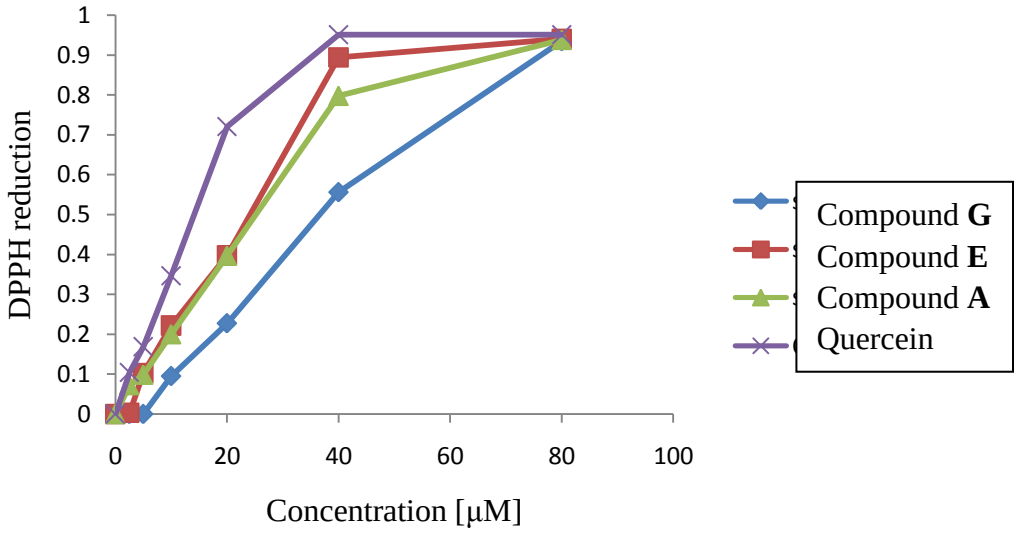

c)

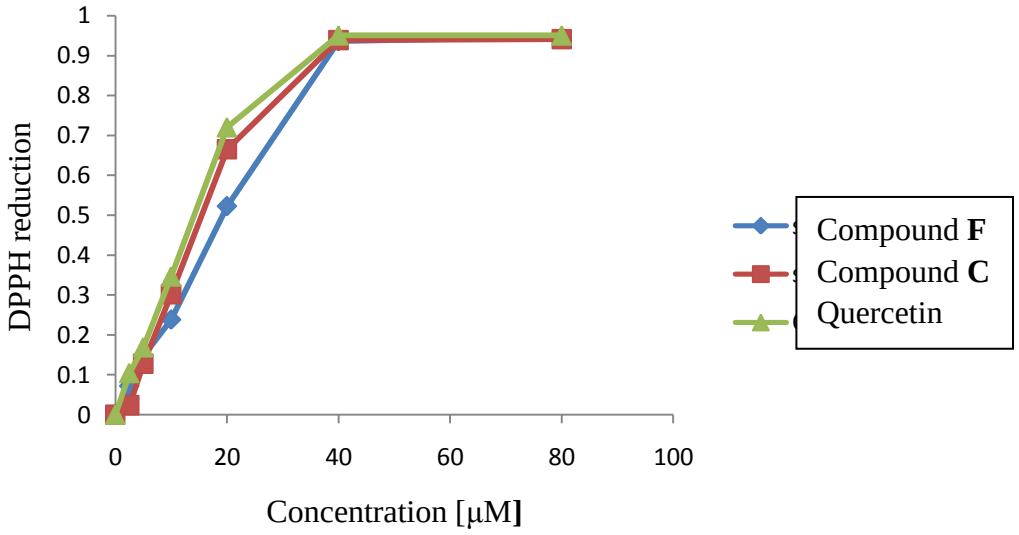

Figure 2.89 Scavenging activity on DPPH radical of compounds **A** to **G**.

2.3.5. Antimicrobial activities of compounds **A-G**

The antimicrobial testing of compounds **A-G** is shown in Table 2.7. There are some weak activities.

Table 2.7 Antimicrobial activities of compounds **A-G**.

MIC values (mg/ml)				
	E. coli ATCC 8739 (mg/ml)	*S. aureus* ATCC 25923 (mg/ml)	*K. pneumoniae* ATCC 13883 (mg/ml)	*E. facealis* ATCC 29212 (mg/ml)
Schotia brachypetala aril MeOH extract	0.50	16.00	8.00	8.00
Compound **A**	0.13	0.25	0.13	0.13
Compound **B**	0.63	0.31	0.37	0.31
Compound **C**	0.33	0.50	0.66	0.33
Compound **D**	0.63	0.21	0.42	0.42
Compound **F**, Compound **E***	0.25	0.25	0.13	0.13
Compound **G**	0.63	>1.63	0.81	0.81
culture control	>16.0	>16.0	>16.0	>16.0
negative control	>16.0	>16.0	>16.0	>16.0
ciprofloxacin control (μg/ml)	0.63	0.30	0.12	0.63

*Fraction containing mainly compounds **E** and **F**.

2.3.6. Antimalarial activities of compounds **A-G**

Compound **A** (3-*O*-methylquercetin 7-*O*-*β*-glucopyranoside) and the new compound **C** (3-*O*-methylquercetin 7-*O*-[*β*-D-6″(*E*-*p*-coumaroyl)glucopyranoside)] have weak activities in the antimalarial test (Table 2.8). Compound **B** was not tested since the quantity of compound **B** was small, but the fraction containing it (as major product) (Figure 2.5) was inactive (>50 μg/ml) (Table 2.6).

Table 2.8 Antimalarial activities of compounds **A**-**G**.

	Final mean % parasite growth at 50 μg/ml			Mean IC_{50} (μg/ml)		
	%	s.d.[a]	n[b]	IC_{50}	s.d.[a]	n[b]
Compound **A**				7.81	0.27	3
Compound **B**						
Compound **C**				5.18	1.09	4
Compound **D**				19.09	1.32	3
Compound **E**	110.95	9.00	3	> 50		3
Compound **F**				47.39	10.74	4
Compound **G**	108.50	12.07	3	> 50		
Quinine				0.023	0.004	5
Chloroquine				0.057	0.001	5
Pyrimethamine				0.023	0.004	4

a, standard deviation; b, number of tests.

2.4. ***Colophospermum mopane***

2.4.1. Fractionation of the methanol extract of the premature seeds

The methanol extract of *Colophospermum mopane* premature seeds showed distinct activities in the antimicrobial test (*E. facealis* ATCC 29212), in acetylcholinesterase inhibition, together with an interesting activity in the antimalarial test. Bioactivity-guided fractionation was thus performed on this extract.

The extract was first fractionated by HSCCC. The chromatogram is not shown due to lack of chromophore in the extract.

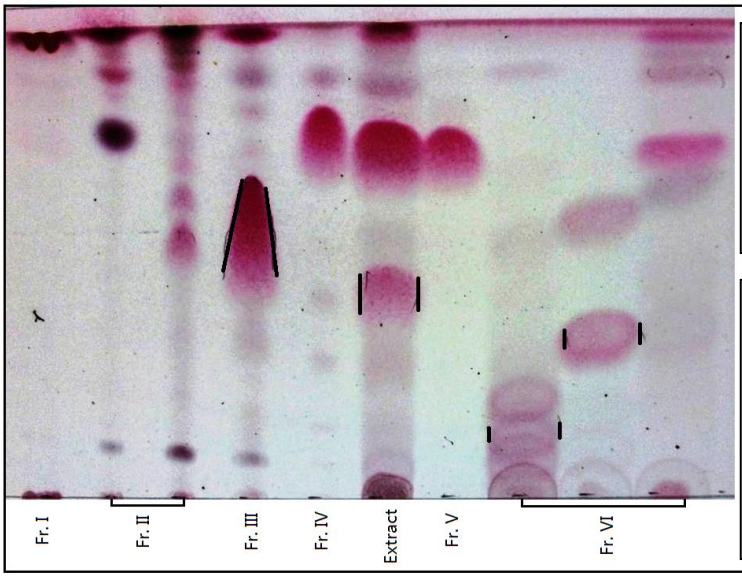

TLC: $CHCl_3$: MeOH 20 : 1
Detection:
(1) UV at 254 nm "( )"
(2) Reagent: 0.5% vanillin in 90% H_2SO_4 in H_2O

HSCCC conditions
Solvent system: MeCN : Heptane 1 :1
Mobile phase: upper phase.
rpm: 1500.
Flow rate: 3 ml/min.
Sample amount: 500 mg.

Figure 2.90 TLC chromatogram of the HSCCC fractions of the heptane part of the heptane-methanol partition of the methanol extract of the premature seeds of *Colophospermum mopane*.

Table 2.9 Antimicrobial activities of the HSCCC fractions of the heptane part of heptane-methanol partition of the methanol extract of the premature seeds of *Colophospermum mopane*.

MIC values (mg/ml)				
	E. coli ATCC 8739	*S. aureus* ATCC 25923	*K. pneumoniae* ATCC 13883	*E. facealis* ATCC 29212
Colophospermum mopane premature seeds MeOH extract	0.08	0.06	3.13	0.06
Colophospermum mopane premature seeds MeOH ext.--> MeOH partition	1.56	0.23	N.T.	0.16
Colophospermum mopane premature seeds MeOH ext.--> heptane partition	0.04	0.08	0.08	0.04
Fr. I	>12.50	>12.50	>12.50	3.13
Fr. II	6.25	0.02	1.56	2.63
Fr. III	6.25	0.60	N.T.	0.02
Fr. IV	0.35	0.25	3.13	0.30
Fr. V	0.04	0.02	1.56	0.08
Fr. VI	0.20	0.20	1.85	0.31
culture control	>16.0	>16.0	>16.0	>16.0
negative control	>16.0	>16.0	>16.0	>16.0
ciprofloxacin control (μg/ml)	0.63	0.30	0.12	0.63

N.T.: not tested.

2.4.2. Isolation of the pure compounds

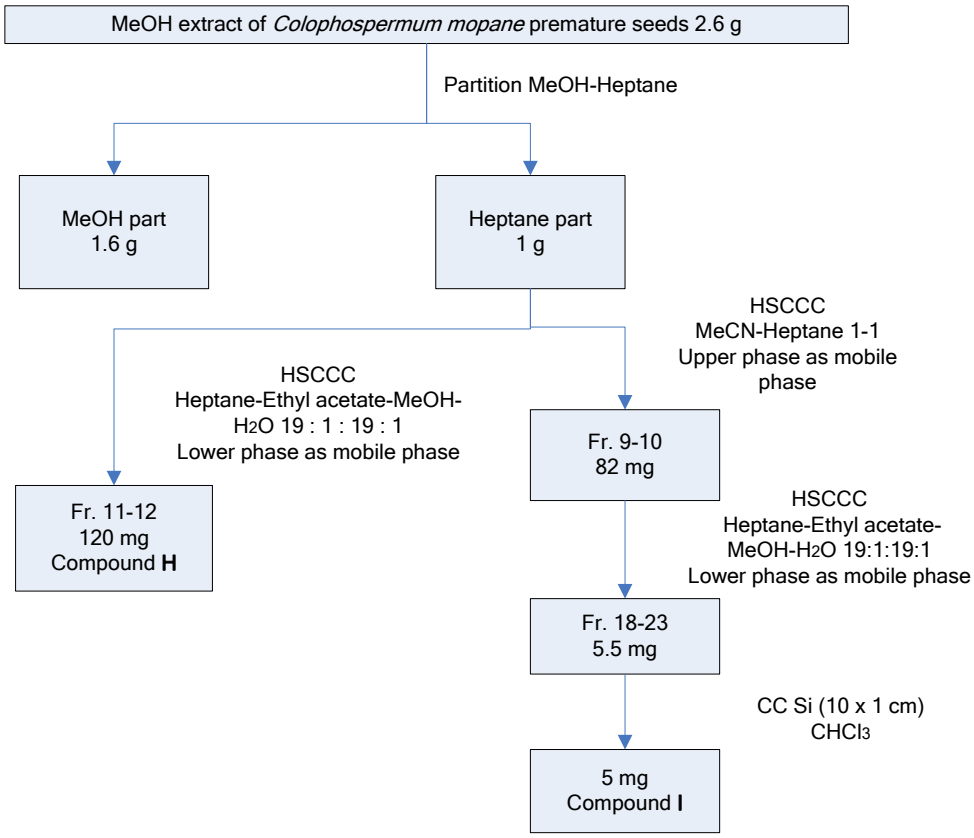

Figure 2.91 Isolation scheme of compounds **H** and **I** from the MeOH extract of *Colophospermum mopane* premature seeds.

2.4.3 Structure determination of pure compounds

2.4.3.1 Compound **H**

Compound **H** was isolated as a colorless oil. The positive LRESIMS showed a pseudomolecular ion at *m/z* 323 $[M + H]^+$ and the negative LRESIMS a pseudomolecular ion at *m/z* 321 $[M - H]^-$. The former ion analyzed for $C_{20}H_{35}O_3$ (Figure 2.92). Together with the ^1H and ^{13}C NMR spectra, a molecular formula of $C_{20}H_{34}O_3$ was deduced. Comparing the ^1H and ^{13}C NMR data with literature values (Mebe, 2001), suggested compound **H** to be dihydrogrindelic acid, which was previously isolated from the $CHCl_3$ extract of seeds and bark of *Colophospermum mopane*. Recently, however, Englund *et al.*, (2009) reported the isolation of two epimers, a new

8(*S*),13(*S*)-dihydrogrindelic acid and the previously described (Mebe, 2001) 8(*S*),13(*R*)-dihydrogrindelic acid from the ether extract of seeds of *Colophospermum mopane*. The presence of the two epimers was deduced from the ^{13}C NMR, based on the appearance of pairs of peaks of unequal intensities (Englund *et al.*, 2009). However, in the present work, the heptane fraction obtained by partition of the methanol extract between heptane and methanol did not give pairs of peaks in the ^{13}C NMR spectrum, suggesting only one epimer to be present (Figure 2.93).

The connectivities of compound **H** were further confirmed by standard 2-D NMR techniques (gCOSY, gHSQC, and gHMBC). The relative stereochemistry of compound **H** was deduced from studies of the NOESY spectrum, the correlations in which are shown in Figure 2.98. The NOE correlations revealed the fact that H-20 methyl, H-11, H-19 methyl, and H-17 methyl were on one side of the molecule, and H-5 on the other axial side, while the H-18 methyl and H-8 were in the equatorial-positions. The assignment of stereochemistry at C-13 was achieved by observing a NOESY correlation between H-16 methyl and H-8 and confirmed by a second NOESY correlation between protons at C-14 and C-1β. Thus, compound **H** was determined as 8(*S*),13(*S*)-dihydrogrindelic acid.

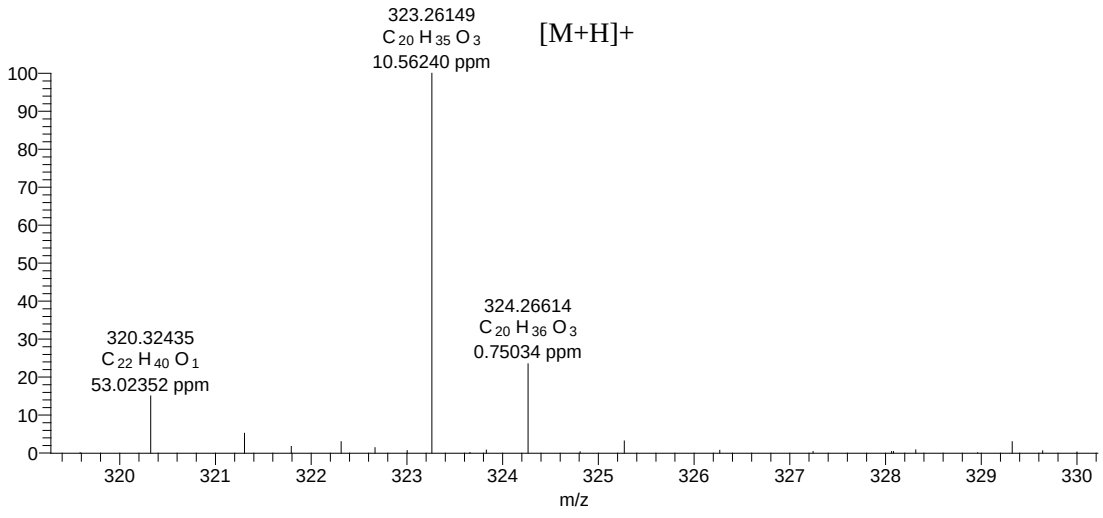

Figure 2.92 HRESIMS spectrum of compound **H.**

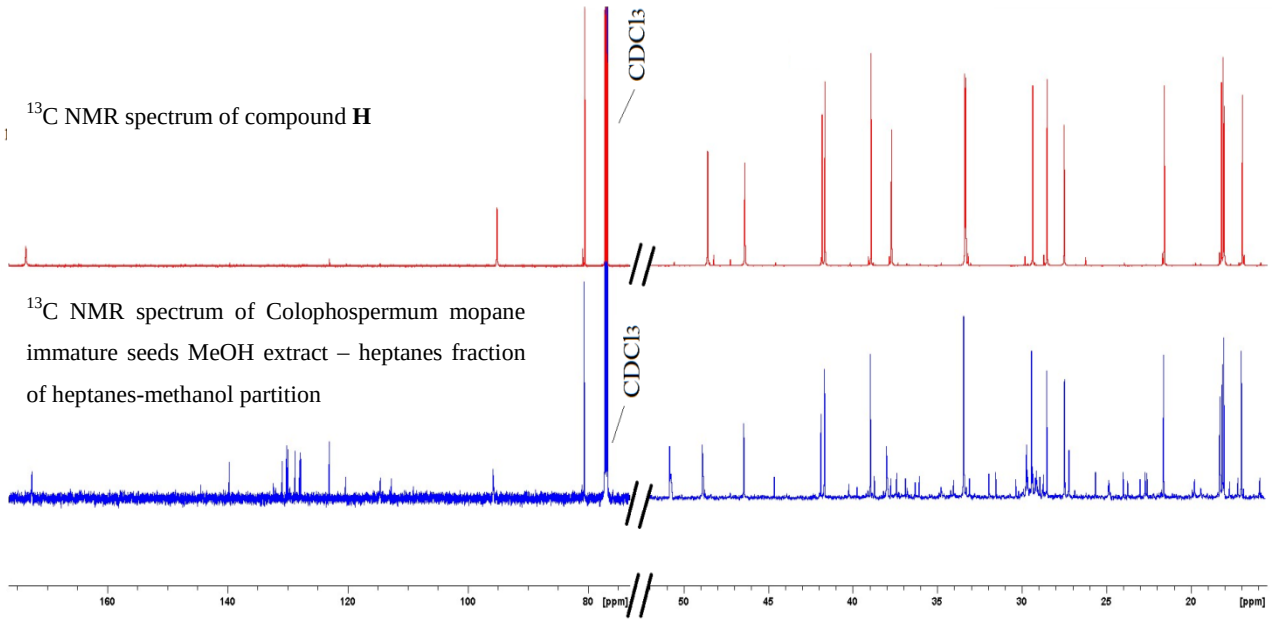

Figure 2.93 Comparative ^{13}C NMR spectra (150 MHz, $CDCl_3$) of compound **H** and *Colophospermum mopane* immature seeds MeOH extract – heptane fraction of heptane-methanol partition.

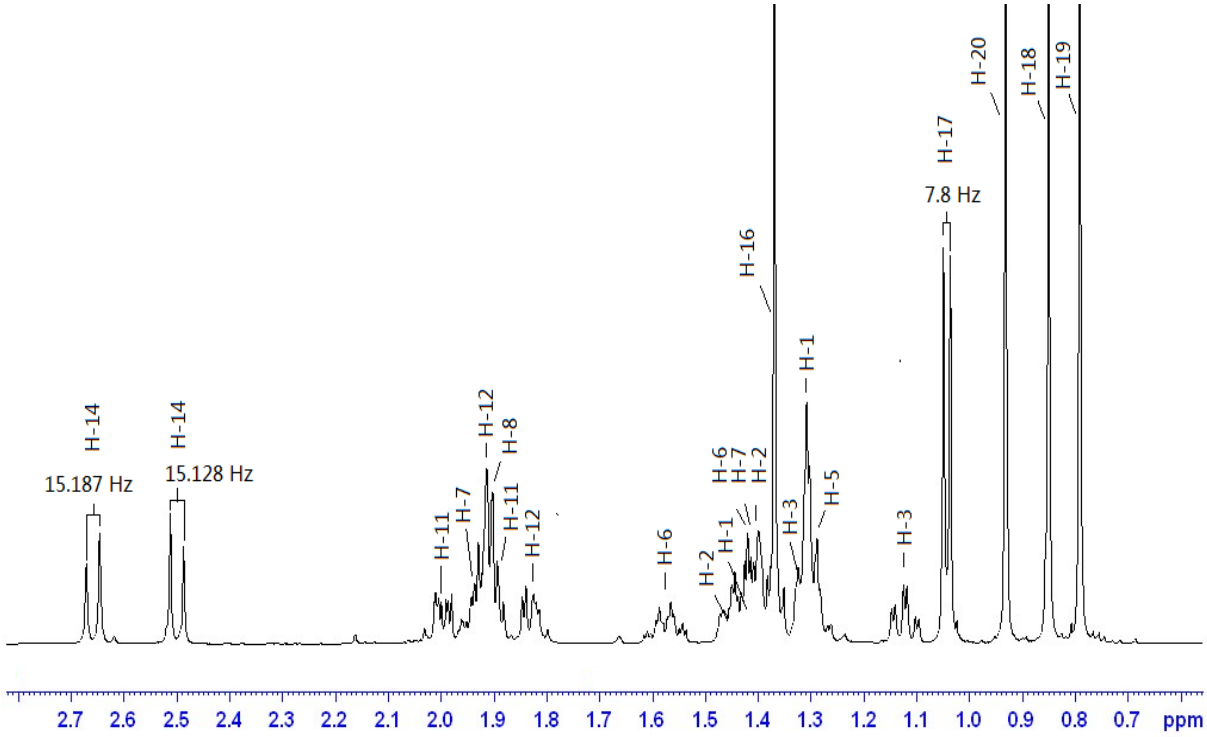

Figure 2.94 ^{1}H NMR spectrum (600 MHz, $CDCl_3$) of compound **H**.

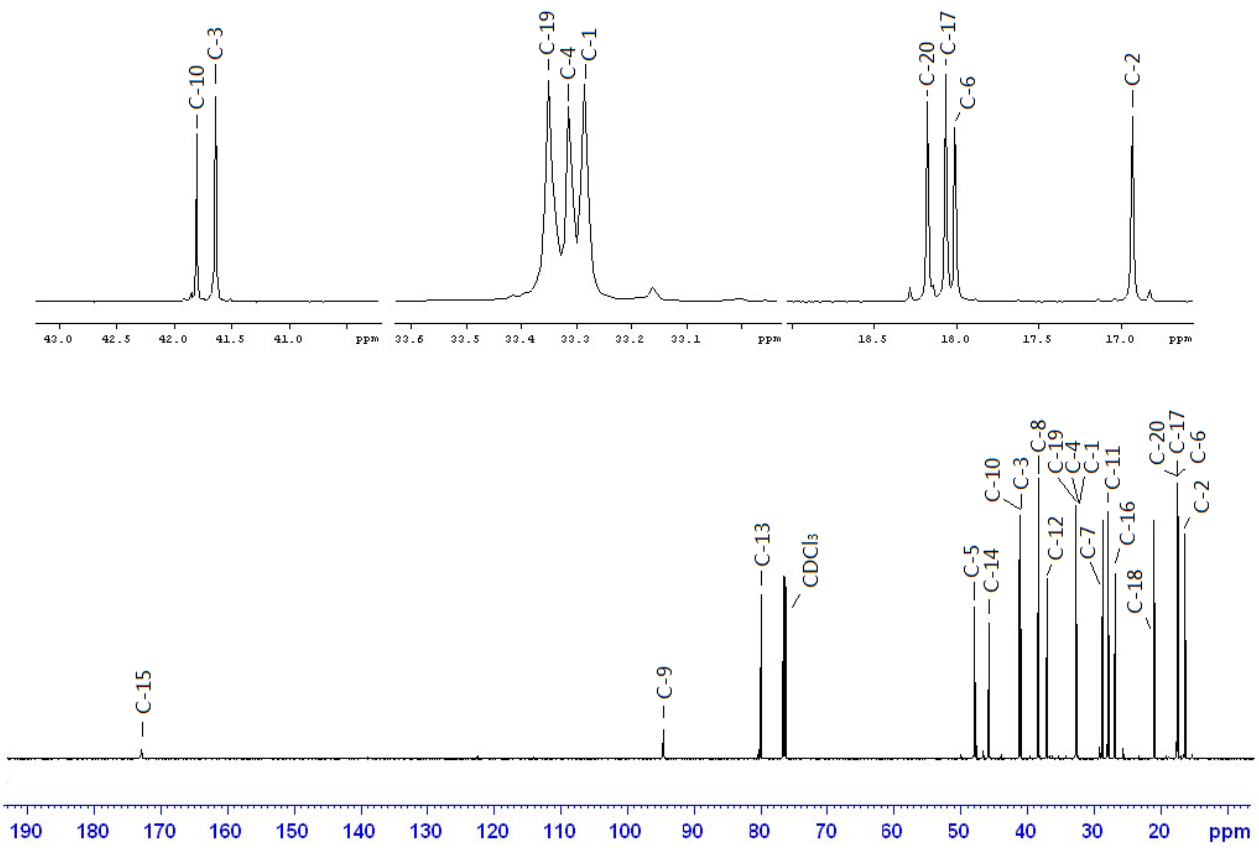

Figure 2.95 ^{13}C NMR spectrum (150 MHz, $CDCl_3$) of compound **H**

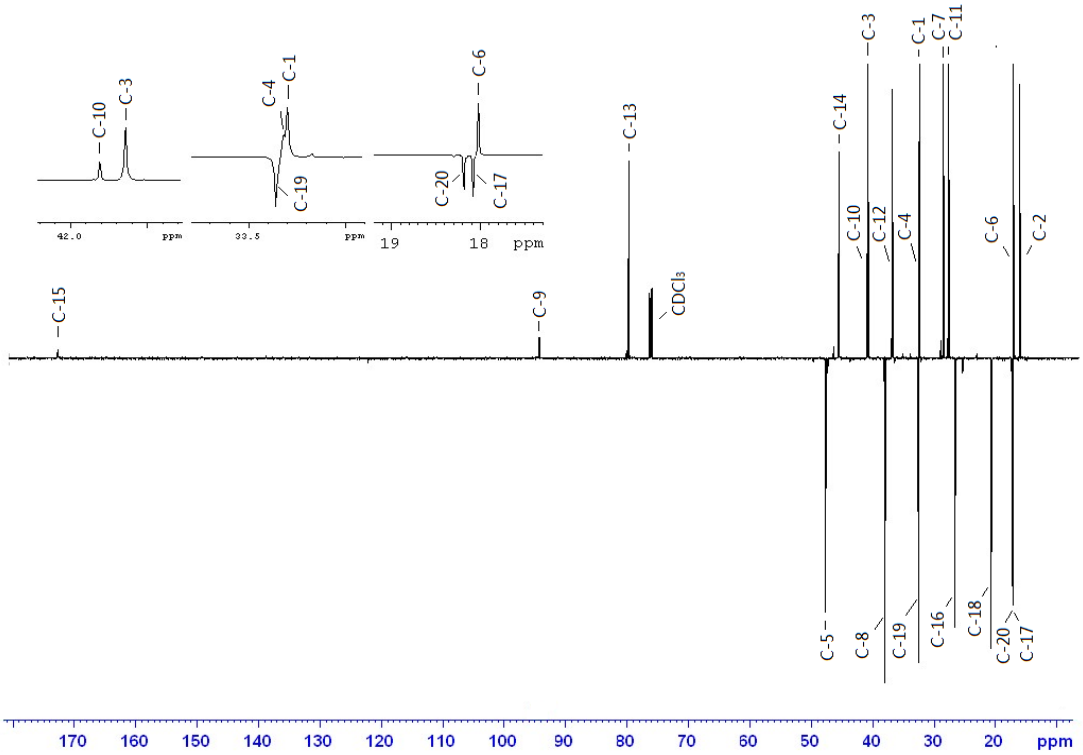

Figure 2.96 APT spectrum (150 MHz, $CDCl_3$) of compound **H**.

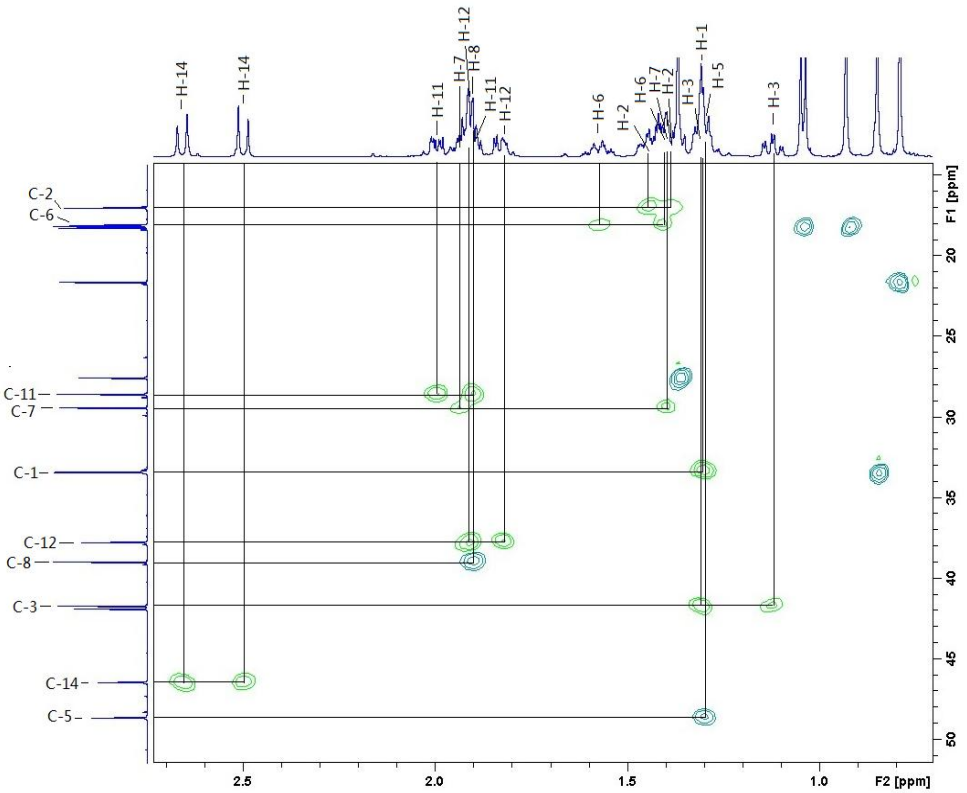

Figure 2.97 HSQC spectrum of compound **H**.

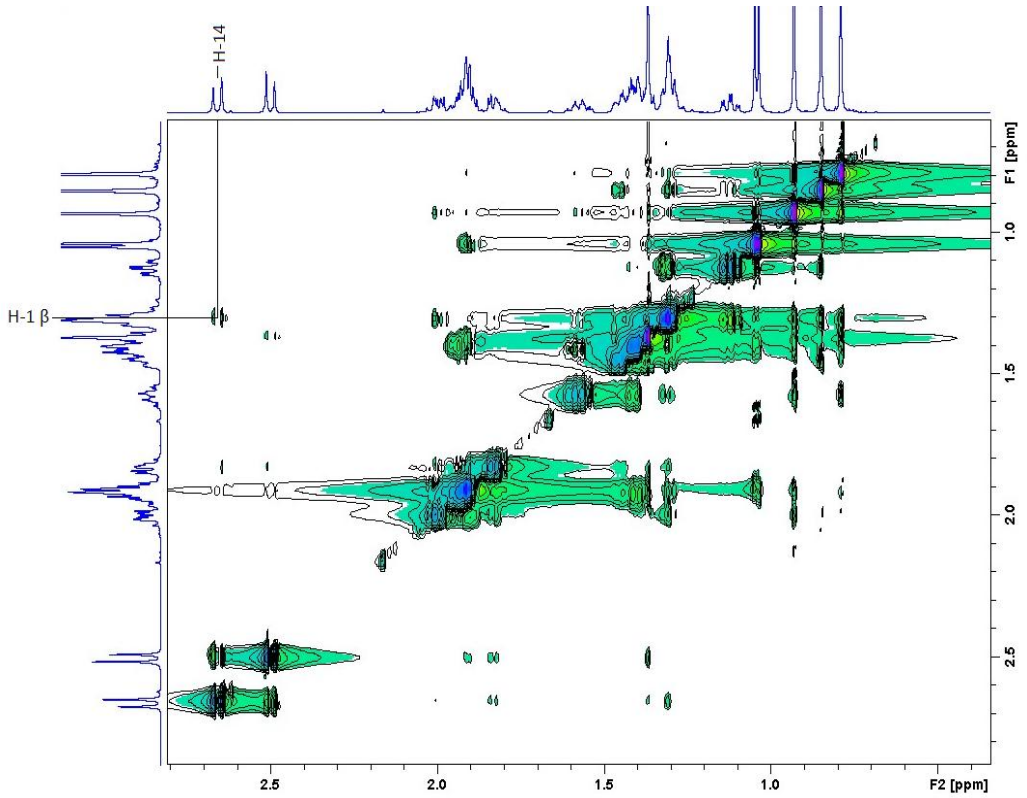

(a)

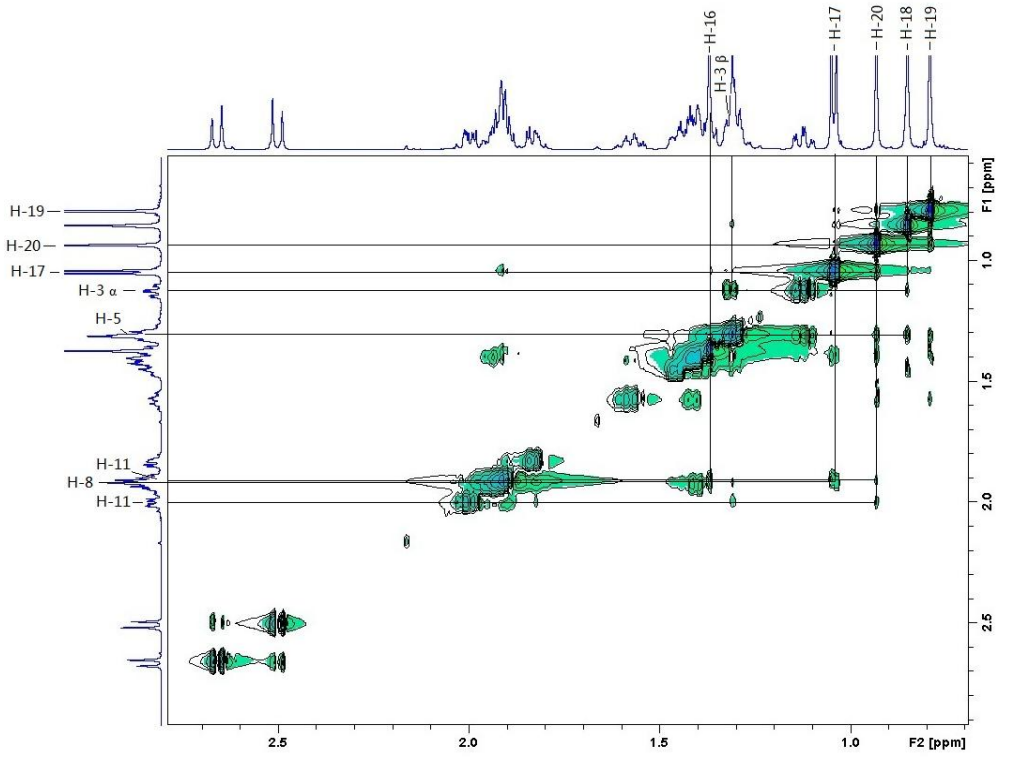

(b)

Figure 2.98 NOESY spectrum of compound **H**, (a) with more dense spots, (b) with less dense spots.

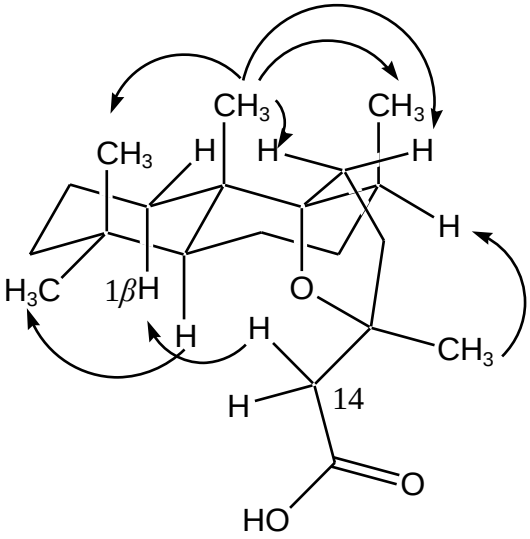

Figure 2.99 Significant NOEs observed for compound **H**

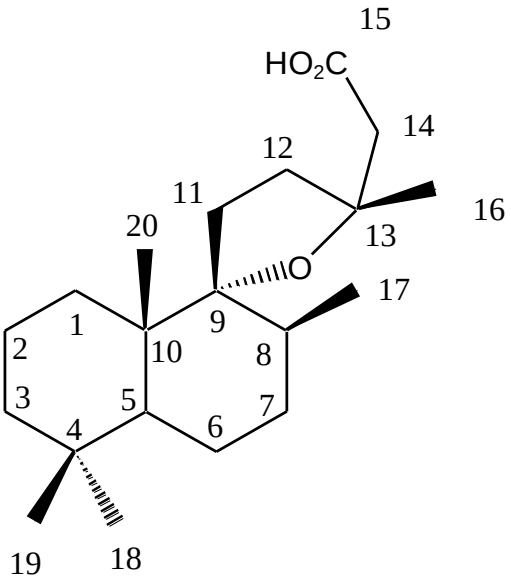

Compound H

2.4.3.2 Compound **I**

Compound **I** was obtained as colorless oil. The UV-inactive compound showed a pink color reaction on TLC with vanillin detection.

By comparison of its ^{1}H and ^{13}C NMR data with the literature (Choudhary *et al.*, 2006) and confirmation of the molecular formula $C_{15}H_{24}O$ by HRAPCIMS, compound **I** was identified as caryophyllene oxide.

The relative stereochemistry of compound **I** was deduced. From the ^{1}H NMR spectrum, the coupling constant of H-1 (J = 9.6 Hz) and H-9 (J = 9.6 Hz) suggested that H-1 and H-9 have a *trans* configuration, which was further evidenced by lack of a NOE interaction between them (Figure 2.106). The relative stereochemistry of H-1 and H-4 was deduced by COSY. C-1 is arbitrarily assumed to be *R*. H-1 couples more strongly to the *anti* H-2 *R* (1.42 ppm), whereas H-2 *S* is likely to be *syn* (1.65 ppm). H-2 *R* couples more strongly to one H-3 (0.96 ppm) than to the other (2.09 ppm), the stronger coupling being due to the *anti* configuration, so 0.96 ppm is assigned to H-3 *R* and 2.09 ppm to H-3 *S*. H-3 *S* is far downfield compared to H-3 *R*, the effect of a probable interaction with epoxide O. The lone pair shielding is a through-space effect, so C-4 is *R*. Thus if C-1 is *R*, C-4 is *R*, and *vice versa* (C-1 and methyl-12 are *trans* related). The NOE interaction between H-5 and H-3 *R* and no NOE interaction between H-5 and methyl-12, suggested that H-5 and methyl-12 are *trans*. Thus compound **I** was further elucidated as *β*-caryophyllene oxide. The most stable conformations of both *α*-caryophyllene oxide and *β*-caryophyllene oxide were modeled by MM2 (minimize energy) calculations (Figure 2.105). The NOE interactions of H-5 and H-1, and H-9 and H-13 in the NOESY spectrum of compound **I** agreed with the conformation of *β*-caryophyllene oxide, and were impossible from the calculated conformation of *α*-caryophyllene oxide (Figure 2.105).

No attempt was made to determine the absolute configuration of compound **I**. Of the two enantiomers of *β*-caryophyllene oxide, (-)-*β*-caryophyllene oxide is commercially available from *Sigma-Aldrich*, the other one is not.

This is the first time that *β*-caryophyllene oxide has been isolated from *Colophospermum mopane*.

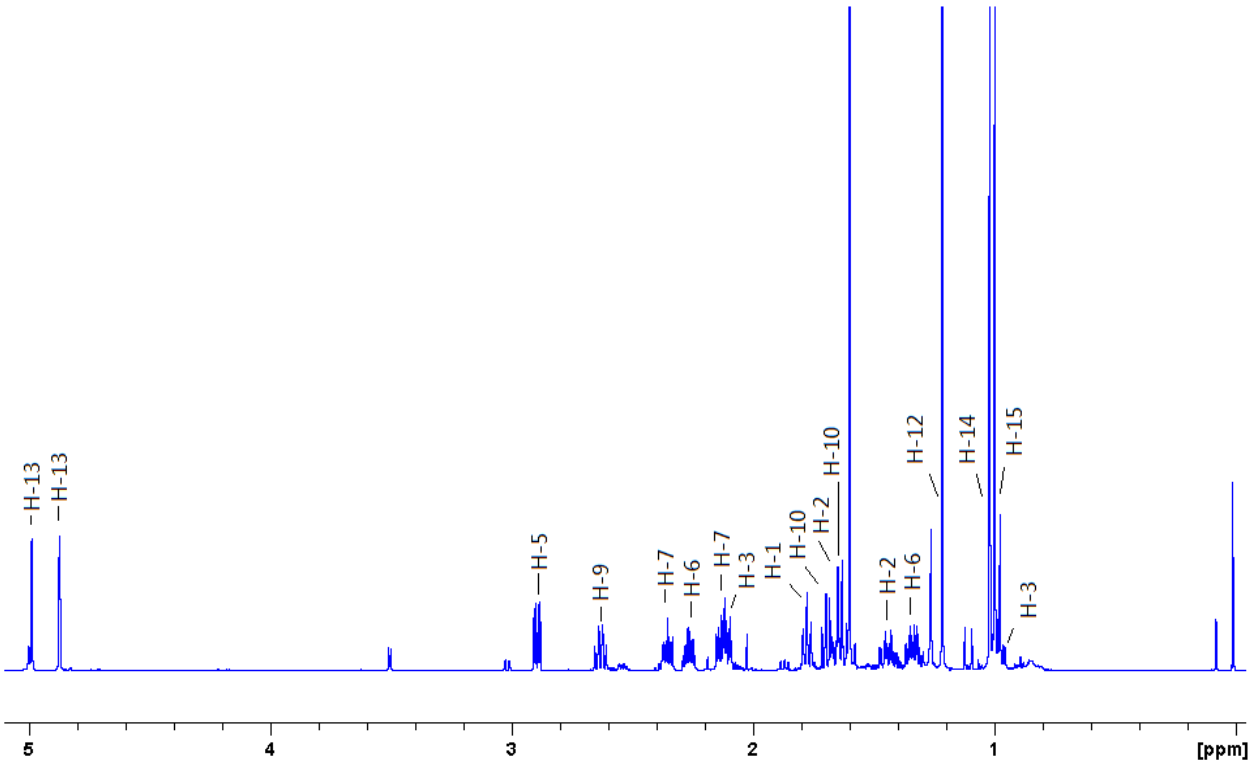

Figure 2.100 ^{1}H NMR spectrum (600 MHz, $CDCl_3$) of compound **I**.

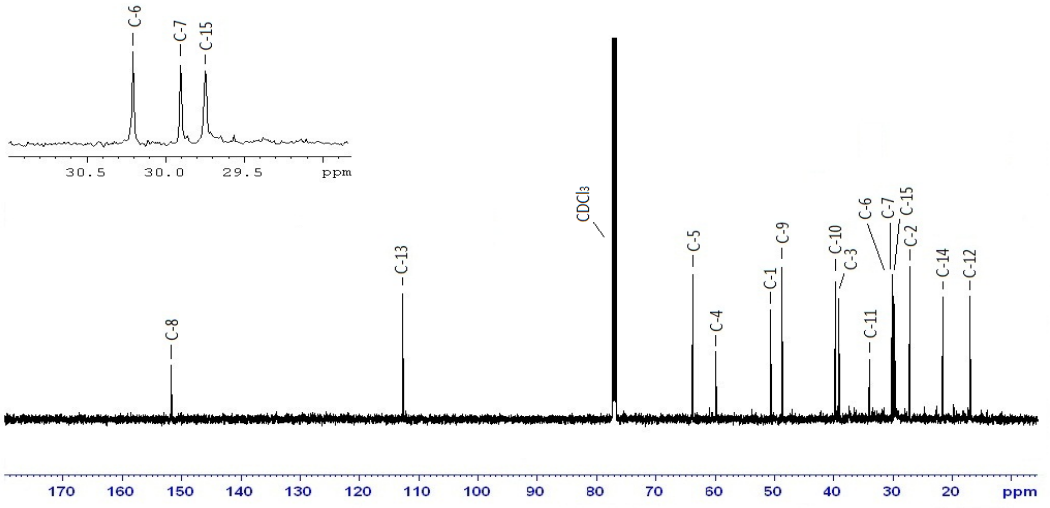

Figure 2.101 ^{13}C NMR spectrum (150 MHz, $CDCl_3$) of compound **I**.

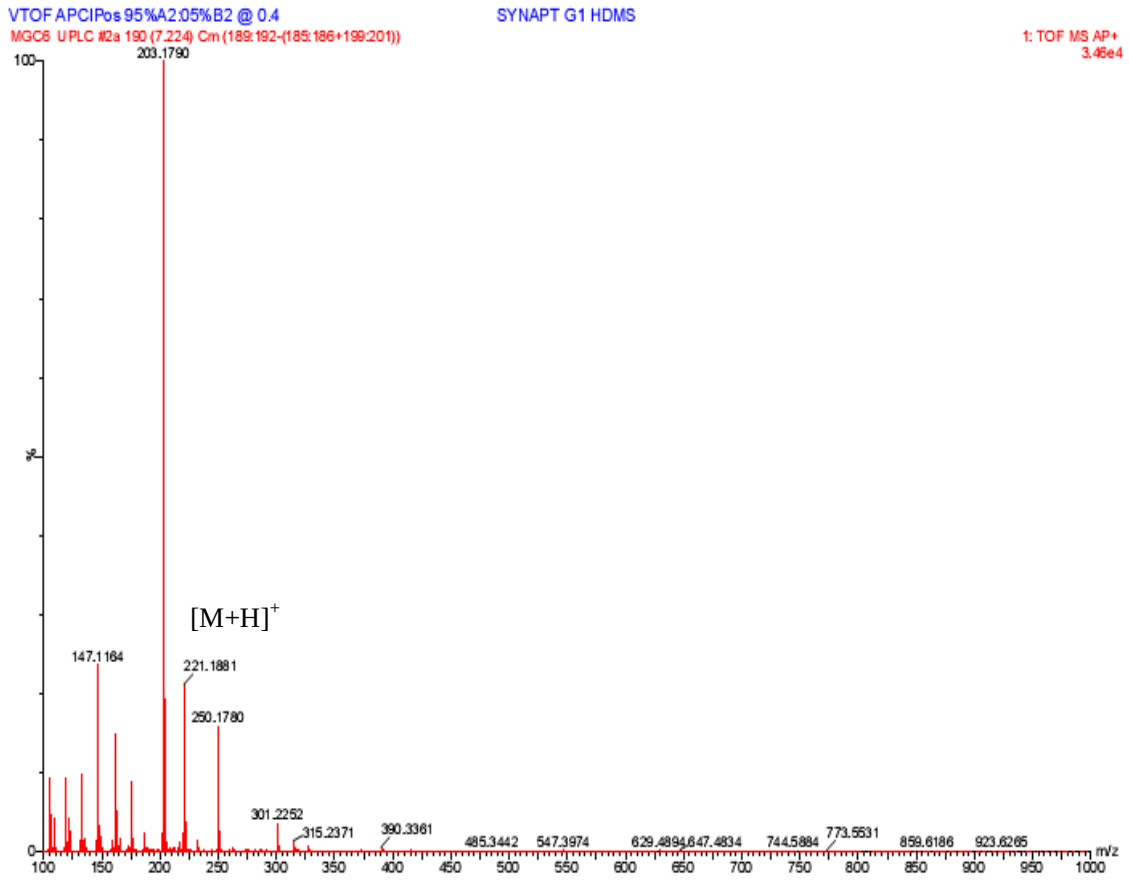

Monoisotopic Mass, Even Electron Ions
18 formula(e) evaluated with 1 results within limits (up to 10 closest results for each mass)
Elements Used:
C: 10-40 H: 1-100 O: 0-5

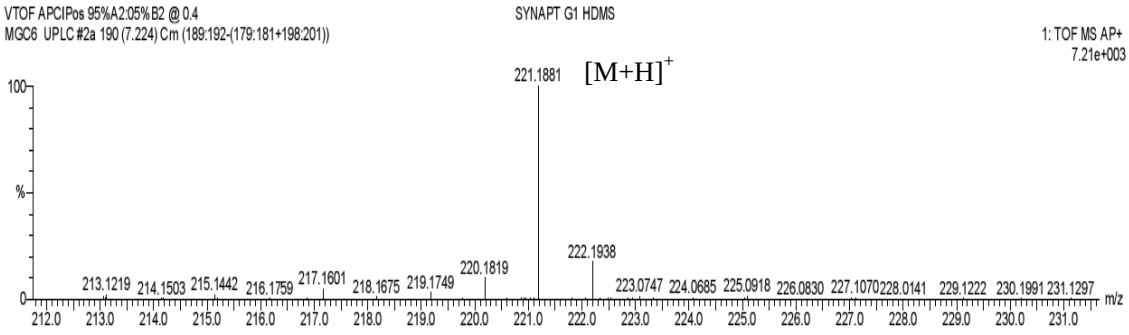

Minimum:	80.00				0.0			
Maximum:	100.00		5.0	10.0	50.0			
Mass	RA	Calc. Mass	mDa	PPM	DBE	i-FIT	i-FIT (Norm)	Formula
221.1881	100.00	221.1905	-2.4	-10.9	3.5	155.4	0.0	C15 H25 O

Figure 2.102 HRAPCIMS spectrum of compound **I** .

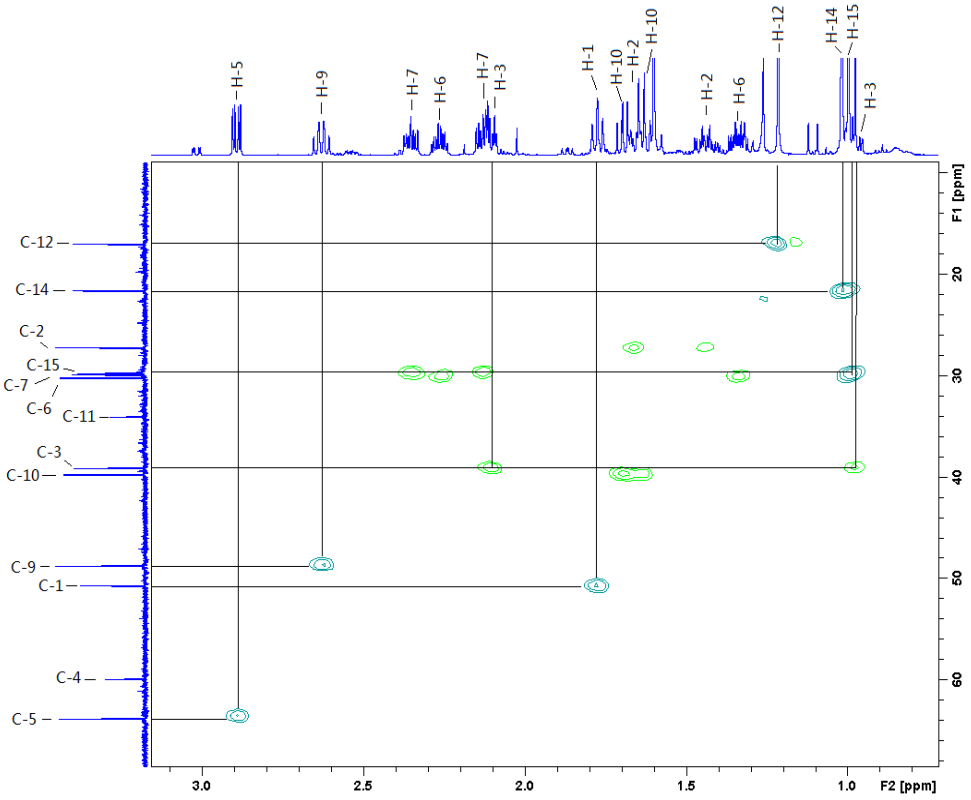

Figure 2.103 HSQC spectrum of compound **I**.

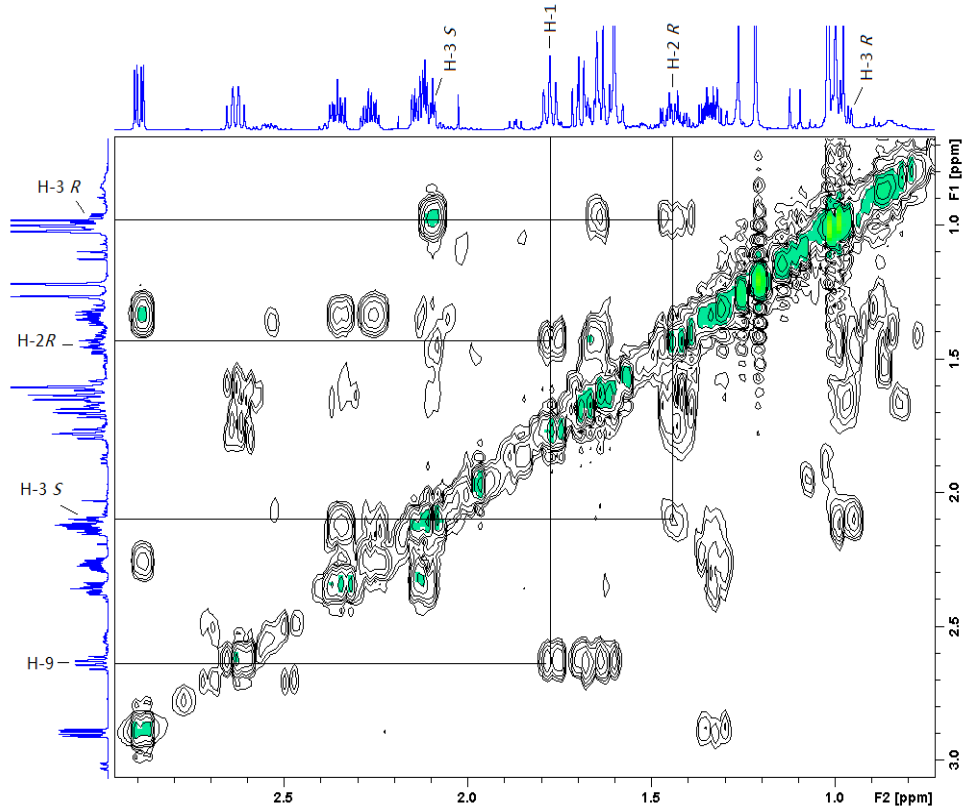

Figure 2.104 COSY spectrum of compound **I**.

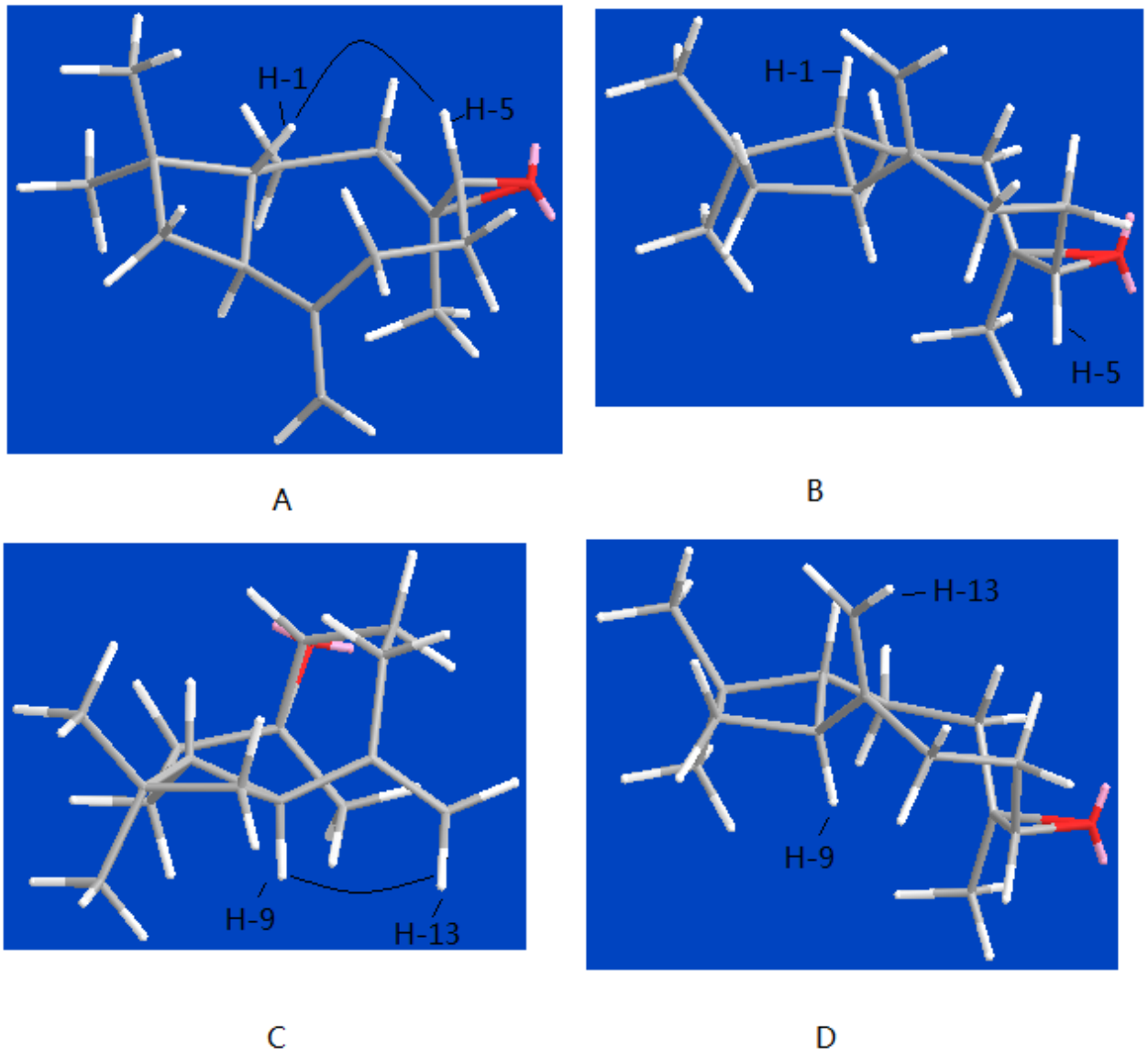

Figure 2.105 MMR calculations for caryophyllene oxide. A and C show the calculated conformation of *β*-caryophyllene oxide, B and D show the calculated conformation of *α*-caryophyllene oxide. The NOE interactions between H-1 and H-5, H-9 and H-13 are possible for *β*-caryophyllene oxide, but are impossible in *α*-caryophyllene oxide.

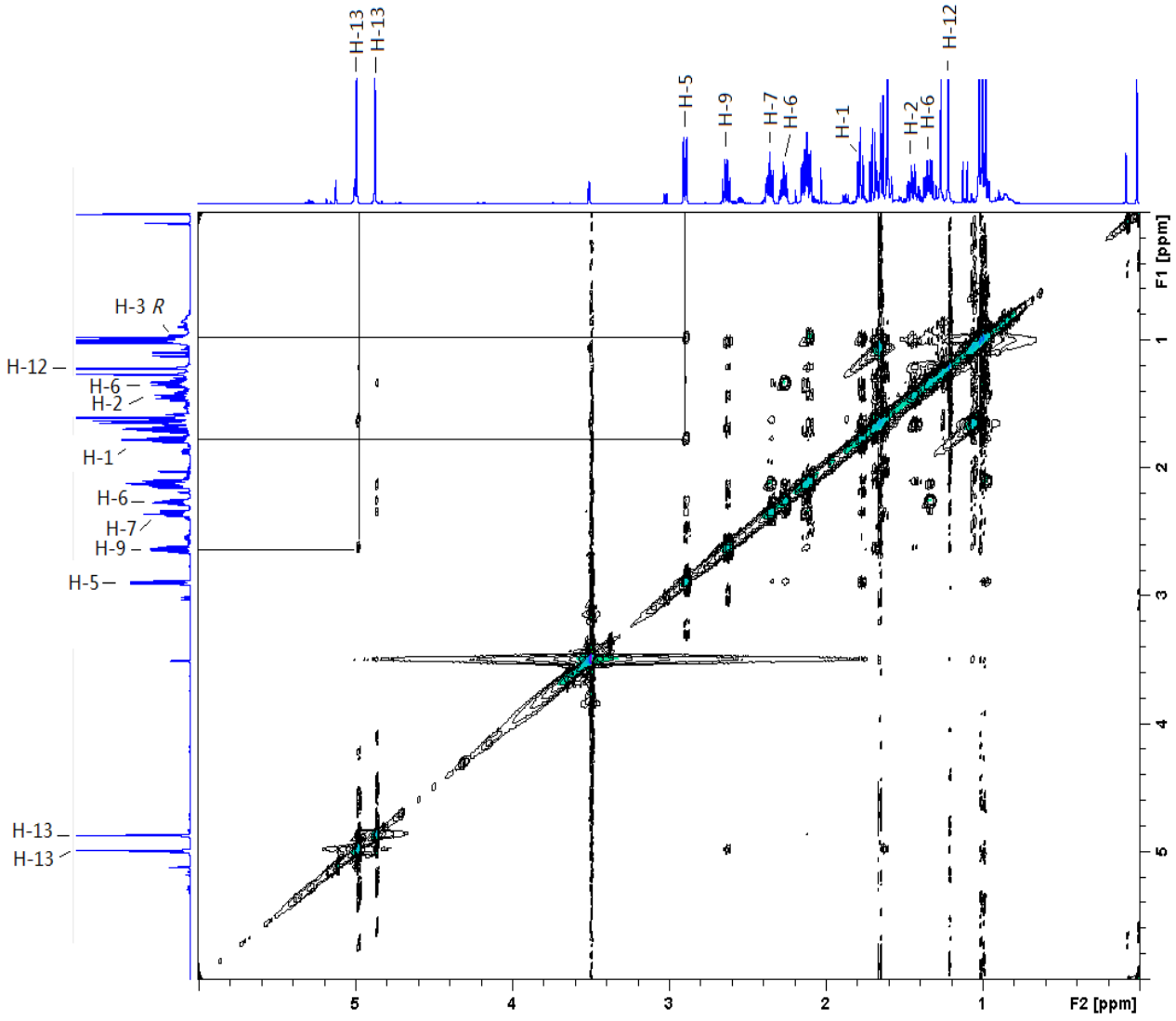

Figure 2.106 NOESY spectrum of compound **I**.

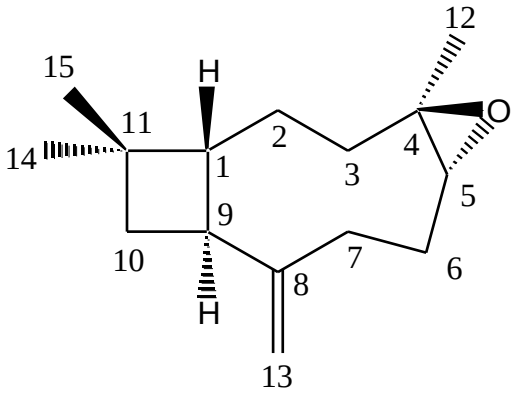

Compound I

2.4.4. Biological activities of compounds **H** and **I**

Compound **H** is 50 times less active than the reference compound (ciprofloxacin) against *E. facealis* ATCC 29212 (Table 2.10), but this is worth further investigation.

Table 2.10 Antimicrobial activities of compounds **H** and **I**.

MIC values (μg/ml)				
	E. coli ATCC 8739	*S. aureus* ATCC 25923	*K. pneumoniae* ATCC 13883	*E. facealis* ATCC 29212
Compound **H**	50.0	30.0	50.0	30.0
Compound **I**	600.0	230.0	200.0	450.0
culture control	>16.0	>16.0	>16.0	>16.0
negative control	>16.0	>16.0	>16.0	>16.0
ciprofloxacin control (μg/ml)	0.63	0.30	0.12	0.63

Compound **H** inhibited acetylcholinesterase in the TLC assay (Marston *et al*., 2002) at 1μg, while compound **I** was inactive at 10 μg.

Compound **H** was weakly active in the antimalarial test, with IC_{50} of 36.28 μg/ml (reference compound Quinine has IC_{50} 0.023 μg/ml). Due to lack of material, the antimalarial activity of *β*-caryophyllene oxide has not been reported.

3. CONCLUSION AND PERSPECTIVES

A total of 29 seed extracts, originating from 25 different plant species from South Africa were prepared. Extraction was with methanol, to minimize the quantity of oil obtained. The disadvantage of extraction with methanol is that the sample obtained may contain a lot of sugars or tannins. Tannins may affect bioassays by interacting non-specifically with protein biological targets due to hydrogen bonding (Wall *et al.*, 1996). The methanol extracts should thus be subsequently partitioned between n-butanol and water to concentrate sugars and tannins in the water phase, and potential bioactive compounds in the n-butanol phase.

The extracts were screened for activity as radical scavengers, inhibitors of acetylcholinesterase, antimicrobials and antimalarials.

On the basis of the activities observed and the limited knowledge of their phytochemistry, the seeds of two species were chosen for study: *Schotia brachypetala* Sond. (Leguminosae) and *Colophospermum mopane* (J. Kirk ex Benth.) J. Kirk ex J. Leonard (Leguminosae).

The methanol extract of the aril of *Schotia brachypetala* showed radical scavenging activity in a TLC assay and antimalarial activity. Fractionation furnished 7 flavonoids: 3-*O*-methylquercetin 7-*O*-*β*-glucopyranoside (**A**), 3,4′-di-*O*-methylquercetin 7-*O*-*β*-glucopyranoside (**B**), 3-*O*-methylquercetin 7-*O*-[*β*-D-6″(*E*-*p*-coumaroyl)glucopyranoside] (**C**), 3,4′-di-*O*-methylquercetin 7-*O*-[*β*-D-6″(*E*-*p*-coumaroyl)glucopyranoside] (**D**), quercetin 7-*O*-*β*-glucopyranoside (**E**), (*2R*, *3R*)-dihydroquercetin 7-*O*-*β*-glucopyranoside (**F**) and quercetin 3-*O*-[2-*O*-*β*-xylopyranosyl-6-*O*-*α*-rhamnopyranosyl]-*β*-glucopyranoside (**G**) . Among them, **E** and **F** are new compounds. Five of the flavonoids had radical scavenging activity (compounds **A**, **C**, **E**, **F** and **G**) and 2 flavonoids were weakly active principles in the antimalarial test (compounds **A** and **C**) (Table 2.8). The presence of the 4′-hydroxyl functional group was necessary for the radical scavenging properties since the 4-methoxyl analogue was devoid of such activity. There are some minor products in the seed extracts of *Schotia brachypetala* and these will be the subject of further investigation.

Glycosylation of the hydroxyl groups of quercetin derivatives results in an increase of its hydrophilicity. This change in character from lipophilic to hydrophilic is very significant in plants for glycosidic derivatives of quercetin, which are cytosol-soluble, can be easier transported to various parts of the plant and stored in vacuoles (Rice-Evans *et al*., 1997; Williams and Grayer, 2004).

The methanol extract of the immature seeds of *Colophospermum mopane* showed inhibition of acetylcholinesterase in the TLC autobiographical assay, as well as antimalarial, and antimicrobial activities. Fractionation furnished *β*-caryophyllene oxide (**I**), and one diterpenoid, the structure of which was established as 8(*S*),13(*S*)-dihydrogrindelic acid (**H**). This gave inhibition of acetycholinesterase at 1 μg in the TLC bioassay and antimicrobial activity against *E. coli*, *S. aureus*, *K. pneumoniae* and *E. faecalis*. The interesting antimicrobially active fraction from *Colophospermum mopane* will be further investigated.

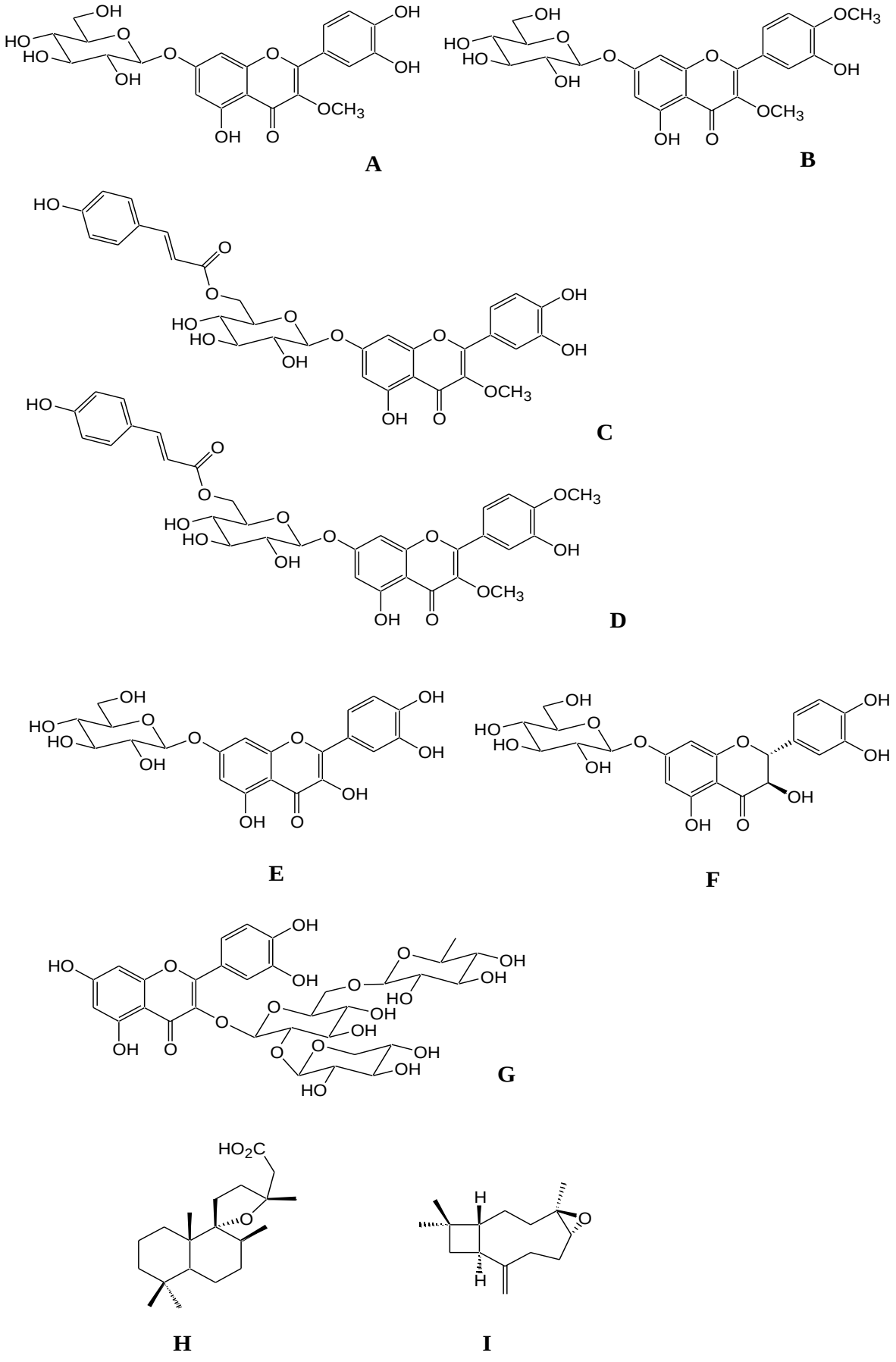

Figure 3.1 Compounds isolated from the seeds of *Schotia brachypetala* and *Colophospermum mopane*.

High-speed countercurrent chromatography was the main chromatographic technique employed. Gel filtration on Sephadex LH-20 and silica gel column chromatography were also used. Structure elucidation was achieved using various spectroscopic and spectrometric methods (UV, MS, 1D- and 2D- NMR - ^{1}H, ^{13}C, APT, COSY, HSQC, HMBC, TOCSY) as well as circular dichroism (CD) to determine the absolute configuration of compound **F**. Some chemical methods (acidic and basic hydrolysis) were also used to assist the structure determination.

The present work illustrates that seeds of South African herbs and woody plants are useful sources of bioactive metabolites. Further studies will be undertaken with the aim of isolating bioactive natural products from the other extracts which have been prepared.

Table 4.1 Seeds collected for study

Family	Col nr	Species	Col date	Locality	Description	Deliv date	NMB
Anacardiaceae	4505	*Lannea edulis* (Sond.) Engl. var. *edulis*	30/11/2009	Blyde Canyon	Ripe seeds	31/5/2010	23433
Anacardiaceae	4507	*Searsia dentata* (Thunb.) F.A. Barkley	30/11/2009	Blyde Canyon	Ripe seeds	22/1/2010	23442
Anacardiaceae	4509	*Searsia pyroides* (Burch.) Moffet var. *pyroides*	30/11/2009	Blyde Canyon	Ripe seeds	22/1/2010	25214
Burseraceae	4704	*Commiphora* cf *pyracanthoides* Engl.	12/3/2010	Lephalale	Ripe&green fruits	29/4/2010	
Burseraceae	4706	*Commiphora glandulosa* Schinz	12/3/2010	Lephalale	Green fruits	29/4/2010	
Burseraceae	4706(b)	*Commiphora glandulosa* Schinz	12/3/2010	Lephalale	Ripe fruits	29/4/2010	
Combretaceae	4693	*Terminalia prunioides* M.A.Lawson	9/3/2010	Vhembe	Ripe fruits	29/4/2010	25174
Combretaceae	4718	*Combretum apiculatum* Sond. subsp.*apiculatum*	20/5/2010	Lephalale	Ripe seeds	2010/3/8	
Cucurbitaceae	4417	*Acanthosicyos naudinianus* (Sond.) C.Jeffrey	27/05/2009	Kgalagadi TFP	Ripe fruits	3/2009	
Cucurbitaceae	No voucher	*Citrillus lanatus* (Thunb.) Matsum. & Nakai	7/2009	Kgalagadi TFP	Ripe fruits	2009	
Cucurbitaceae	No voucher	*Cucumis africanus* L.f.	7/2009	Kgalagadi TFP	Ripe fruits	2009	
Ebenaceae	4520	*Diospyros mespiliformes* Hochst. ex A.DC.	2/12/2009	Manyeleti	Ripe seeds	22/1/2010	22800
Ebenaceae	4525	*Euclea divinorum* Hiern	3/12/2009	Manyeleti	Green fruits	22/1/2010	25162
Ebenaceae	4712	*Diospyros lycioides* (Desf.) subsp.	20/4/2010	Winburg	Ripe fruits	29/4/2010	
Fabaceae	No voucher	*Acacia haematoxylon* Willd.	7/2009	Kgalagadi TFP	Ripe seeds	2009	
Fabaceae	No voucher	*Acacia erioloba* E. Mey.	7/2009	Kgalagadi TFP	Ripe seeds	2009	
Fabaceae	4742	*Afzelia quanzensis* Welw.	22/7/2010	Manyeleti	Ripe fruits	2010/3/8	23370
Fabaceae	4510	*Peltophorum africanum* Sond.	30/11/2009	Blyde Canyon	Ripe seeds	31/5/2010	25163
Fabaceae	4687	*Xanthocercis zambesiaca*(Baker) Dumaz-le-Grand	9/3/2010	Vhembe	Ripe fruits	26/3/2010	25171
Fabaceae	4700	*Schotia brachypetala* Sond.	11/3/2010	Vhembe	Ripe seeds	26/3/2010	25185
Fabaceae	4688	*Colophospermum mopane* (J.Kirk ex Benth.) J.Kirk ex J.L éonard	9/3/2010	Vhembe	Premature (green) seeds	29/4/2010	25172
Fabaceae	4688	*Colophospermum mopane* (J.Kirk ex Benth.) J.Kirk ex J.L éonard	9/3/2010	Vhembe	Mature (red) seeds	29/4/2010	25172
Fabaceae	4702	*Cassia abbreviata* Oliv. subsp. *beareana* (Holmes) Brenan	11/3/2010	Vhembe	Ripe fruits	29/4/2010	
Fabaceae	4714a	*Tylosema fassoglense* (Schweinf.) Torre & Hillc.	20/5/2010	Lephalale	Pericarp	31/5/2010	25189
Fabaceae	4714b	*Tylosema fassoglense* (Schweinf.) Torre & Hillc.	20/5/2010	Lephalale	Ripe seeds	31/5/2010	25189
Meliaceae	4533	*Trichilia emetica* Vahl subsp. *emetica*	5/12/2009	Manyeleti	Green fruits	22/1/2010	25216
Rhamnaceae	4695	*Berchemia discolor* (Klotzsch) Hemsl.	9/3/2010	Vhembe	Ripe fruits	29/4/2010	25176
Sapotaceae	4508	*Englerophytum magalismontanum* (Sond.) T.D.Penn.	30/11/2009	Blyde Canyon	Green fruits	22/1/2010	25155

NMB: Internationally accredited herbarium accession number.

4. EXPERIMENTAL

4.1. Plant material

The seeds were collected on the dates shown in Table 4.1. The plants were collected and identified by Dr. Pieter Zietsman, National Museum, Bloemfontein, South Africa. Voucher specimens are deposited in the National Museum, Bloemfontein, South Africa. The collection date, location and voucher specimen number (Col. nr.) are shown in Table 4.1. The delivery date is the date the sample was received in the Chemistry Department, UFS.

4.2. Extraction of seeds

The air dried plant material (40 g) was ground and then extracted with MeOH (150 ml) (the proportion of plant material to solvent was 1:3.75 w/v). The extraction was carried out at room temperature and under stirring overnight (24 h) three times. The mixture was filtered, and the filtrates were combined, evaporated and lyophilized to obtain MeOH extracts.

4.3. Chromatographic methods

4.3.1. Thin-layer chromatography (TLC)

TLC was carried out on silica gel 60 F_{254} precoated aluminium sheets (Merck). The solvent systems used were $CHCl_3$-MeOH-H_2O, heptane-ethyl acetate, $CHCl_3$-MeOH in different proportions.

After development, TLC plates were first observed under UV light (254 nm and 366 nm) for locating chromophoric compounds. Further detection was achieved by spraying with 0.5% vanillin in 90% sulphuric acid in H_2O. The sprayed plates were heated to about 100 °C during 5 min. Spots of different colors developed according to the nature of the compounds.

4.3.2. Open column chromatography on silica gel

Open column chromatography was employed for final stage purifications. Silica gel 60 (0.040-0.063 mm) (Merck) was used. The eluent systems were determined with the help of TLC analyses (Hostettmann *et al*., 1998). Liquid introduction of sample was adopted in the case of final stage purification of compound **I**, because the sample was perfectly soluble in the eluent.

4.3.3. Gel filtration on Sephadex LH-20

Some fractionations and clean-up steps were achieved by gel filtration on Sephadex LH-20 (Sigma-Aldrich, St. Louis, MO, USA) (Hostettmann *et al.*, 1998). The eluent was usually analytical grade MeOH. The elution rate was about 1 ml/min, and slower when better resolution was required.

4.3.4. High performance liquid chromatography (HPLC)

Analytical high performance liquid chromatography was used for analyzing crude extracts and fractions, guiding separation and isolation, and checking the purity of the isolates. The HPLC system employed was an Agilent Technologies 1200 series, equipped with a diode-array detector (DAD) for UV detection.

The columns routinely used were Phenomenex C18 (110 Å) reversed phase columns (150 x 4.6 mm i.d., stationary phase particle size 5 μm). The mobile phase used was solvent A: distilled H_2O + 0.1% HCOOH; B: 70% MeOH/H_2O + 0.1% HCOOH, gradient 0-15 min; 10-30% B; 15-25 min; 30-70% B; 25-27 min; 70-100% B; 27-35 min; 100% B; 35-35.01 min; 100%-10% B; 35.01-45 min; 10% B; wavelength 254 nm, flow rate 1 ml / min.

4.3.5. Gas chromatography

Gas chromatography was employed for the determination of the configurations of the sugars

from the two new compounds **C** and **D**. Instrument: Shimadazu GC-2010, column: Agilent 5ms, (0.25 mm i.d. x 30.0 m, coated with 5% phenol polysiloxane, film thickness 0.25 μm). Column temperature: 200 °C, injection temperature 280 °C, carrier gas He at a flow rate of 50 ml/min.

4.3.6. High-speed countercurrent chromatography

Countercurrent chromatography was employed for separations. In this technique, the stationary phase and mobile phase are two immiscible solvents and no solid support is present.

The rotating coil hydrodynamic HSCCC instrument used in the present study was a Spectrum model (Dynamic Extractions, Slough, UK) multilayer coil-planet J-type centrifuge, equipped with two preparative coils connected in series (wrapped with polytetrafluoroethylene PTFE tubing, 1.6 mm i.d., 142 ml total volume). The inner β_r-value was measured to be 0.52 at the internal end of the coil and outer β_r-value was 0.86 ($\beta_r = r/R$, where r is the distance from the coil to the holder shaft, and R, the revolution radius or the distance between the holder axis and central axis of the centrifuge). The direction of rotation determined the *head* locations at the periphery of the two coils. Solvent was pumped with a model 305 pump (Gilson, Middleton, WI, USA) and monitoring of the effluent was achieved with a model 151 variable wavelength detector (Gilson, Middleton, WI, USA) at 254 nm. Fractions were collected with a model FC204 fraction collector (Gilson, Middleton, WI, USA). A manual sample injection valve with a 5.0-ml loop from Rheodyne (Rohnert Park, CA, USA) was used to introduce the sample into the column.

The solvent systems were chosen based on TLC analyses. Sample (5 mg) was dissolved in a mixture of 1 ml of the upper and 1 ml of the lower phase and 10 μL of each phase was deposited on a TLC plate. Solvent systems which afforded an even distribution of the analytes between upper and lower phase were chosen.

The coils of the chromatograph were first filled with stationary phase and then the mobile phase was pumped into the apparatus under rotation until conditions were stable and no more

stationary phase eluted. The sample was then dissolved in equal amounts of upper and lower phases and injected via a sample loop.

4.4. Physicochemical methods

4.4.1. Lyophilization

Crude extracts, fractions, as well as purified compounds, after evaporation, were further lyophilized to remove traces of solvents and/or water. The residues in flasks containing solvent traces were frozen at -40°C in water and then connected to a lyophilizer (Vacutec, FTS Systems, Stone Ridge, New York, USA) under high vacuum at a pressure of 10^{-1} – 10^{-2} mbar until completely dry.

4.4.2. Ultraviolet spectra (UV)

A single cell (Beckman Coulter Du 800, Fullerton, CA, USA) spectrophotometer was used. The UV spectra were measured in methanol in a quartz cell, with an appropriate concentration of sample. Shift reagents were prepared and used according to Markham (1982).

The intensity of absorption peaks in a spectrum was expressed by *log ε* (logarithmic molar absorptivity) in this study. The UV absorption is indicated in the following formula:

$A = \log (I_0 / I) = \varepsilon cl = \log (1/T)$

where I_0 is the initial incident intensity of light, I is the transmitted intensity of light through the sample, T is the transmittance, c is the sample concentration (in moles per liter) and L is the path length of the sample solution (in cm).

4.4.3. Microplate reader

The quantitative analysis for radical scavenging activity of compound **A**–**G** was done on a UV

microplate reader (Molecular Devices, SpectraMax M2, USA)

4.4.4. Mass spectra (MS)

4.4.4.1. Low resolution mass spectra of compounds **C**, **D**, **E** and **F** (Department of Chemistry, University of the Free State).

For compounds **C** and **D**, all the low resolution spectra were run on a Thermo Finnigan LXQ linear ion trap mass spectrometer in the ESI mode. Polarity switching was used to get simultaneous positive and negative spectra. Capillary temperature 200 ^{o}C, spray voltage 5kV, Capillary voltage 14V.

Mass spectra of compound **E** and **F** were obtained on a Sciex API 2000 triple-quadrapole mass spectrometer (Applied Biosystems/MDS SCIEX, Concord, Ontario, Canada), coupled with a APCI source. Biosystems/MDS SCIEX analyst software version 1.3.2 was used for data acquisition and processing. The operating conditions in the APCI source were as follows: nebulizer current, 2.0 μA; probe temperature, 450 ^{0}C; declustering potential 10 V. Nitrogen was also used as the nebulizer gas (15 units), curtain gas (60 units).

4.4.4.2. High resolution mass spectra of compounds **G** and **I** (Dr. Paul Steenkamp, CSIR, Pretoria)

4.4.4.2.1. General

All chemicals for UPLC-MS work were of ultra-pure LC-MS grade and purchased from Fluka (Steinheim, Germany) while ultra-pure solvents were purchased from Honeywell (Burdick & Jackson, Muskegon, USA). Ultra-pure water was generated from a Millipore Elix 5 RO system and Millipore Advantage Milli-Q system (Millipore SAS, Molsheim, France).

4.4.4.2.2. Instrumentation

A Waters UPLC coupled in tandem to a Waters photodiode array (PDA) detector and a SYNAPT G1 HDMS mass spectrometer were used to generate accurate mass data. Two analytical procedures were used to analyse the samples.

Chromatographic separation of the compound **G** was done utilising a Waters HSS T3 column (150 mm x 2.1 mm, 1.8 µm) thermostatted at 60 ^{0}C. A binary solvent mixture was used consisting of water (Eluent A) containing 10 mM formic acid (natural pH of 2.3) and methanol (Eluent B). The initial conditions were 95% A at a flow rate of 0.4 mL/min with a linear gradient to 0.5 %A at 6 minutes. The conditions were kept constant for one minute and then changed to the initial conditions. The runtime was 10 minutes and the injection volume was 1 µL. The PDA detector was scanned between 200 and 500 nm (1.2 nm resolution) and collecting 20 spectra per second.

The SYNAPT G1 mass spectrometer was used with V-optics and operated in the electrospray mode to detect compound **G**. Leucine enkephalin (50 pg/mL) was used as reference calibrant to obtain typical mass accuracies between 1 and 3 mDalton. The mass spectrometer was operated in positive and negative mode with a capillary voltage of 3.0 kV, the sampling cone at 30 V and the extraction cone at 4 V. The scan time was 0.1 seconds covering the 100 to 1000 Dalton mass range. The source temperature was 120 ^{0}C and the desolvation temperature was set at 450 ^{0}C. Nitrogen gas was used as the nebulisation gas at a flow rate of 450 L/h.

Chromatographic separation of compound **I** was done utilising a Waters HSS T3 column (150 mm x 2.1 mm, 1.8 µm) thermostatted at 60 ^{0}C. A binary solvent mixture was used consisting of water (Eluent A) containing 10 mM formic acid (pH 2.3) and acetonitrile (Eluent B). The initial conditions were 95% A at a flow rate of 0.4 mL/min with a linear gradient to 0.5% A at 6 minutes. The conditions were kept constant for one minute and thereafter changed to the initial conditions. The runtime was 10 minutes and the injection volume was 3 µL.

The SYNAPT G1 mass spectrometer was used in V-optics and operated in atmospheric pressure chemical ionisation mode (APCI) using the IonSabre probe to detect the compound **I**. Leucine enkephalin (50 pg/mL) was used as reference calibrant to obtain typical mass accuracies between 1 and 3 mDalton. The mass spectrometer was operated in positive mode using the "current mode" with a corona voltage of 3.0 kV, corona current at 20 μA and the extraction cone at 4 V. The scan time was 0.1 seconds covering the 100 to 1000 Dalton mass range. The source temperature was 120 ^{0}C and the probe temperature was set at 500 ^{0}C. Nitrogen gas was used as the nebulisation gas at a flow rate of 450 L/h.

The software used to control the hyphenated system and do all data manipulation was MassLynx 4.1 (SCN 704).

4.4.4.3. High resolution mass spectra of compounds **A**, **B, C**, **D**, and **H** (University of the Witwatersrand)

For compounds **A**, **B**, **C**, **D** and **H**, the accurate mass measurements were run on a Thermo Electron DFS magnetic sector mass spectrometer in ESI positive mode. Polyethyleneimide was used as reference material. Accurate mass measurements were acquired in electric scan and peak matching was used to predict elemental composition. Samples were introduced via a Rheodyne injector with a constant stream of reference via a syringe pump. Capillary temperature 240^{o}C, spray voltage 2.5V, capillary voltage 10V.

4.4.4.4. Mass spectrometry with multiple reaction monitoring (MRM)

4.4.4.4.1 Mass spectrometry

For the mass spectrometric determination of *p*-coumaric acid hydrolyzed from compounds **C** and **D** employing multiple reaction monitoring (MRM) in the negative ion mode, the mass spectra and fragmentation spectra of coumaric acid were determined during infusions directly into the mass spectrometer. This resulted in a mass spectrum from which a combination of precursor and

fragment ions could be selected for the MRM detection. Table 4.2 indicates the settings on the instrument used for this process.

Table 4.2: Mass spectrometer settings

Mass spectrometer settings	*p*-Coumaric acid
Precursor ion $[M - H]^-$ (m/z)	163
Product ion (m/z)	119
Declustering potential (V)	-11
Collision energy (eV)	-18
Nebulizer gas	60
Auxiliary gas	15
Curtain gas	40
Collision gas, N_2	5
Source temperature (^{0}C)	450
Nebulizer Current μA	-2.0

4.4.4.4.2 Chemicals and instrumentation used

HPLC grade (≥99.9 % purity) methanol and water were purchased from Merck (Darmstadt, Germany) and the reference standard (*p*-Coumaric acid) was purchased from Sigma-Aldrich (Steinheim, Germany). An API 2000 triple-quadrupole mass spectrometer (Applied Biosystems/MDS Sciex), coupled with an atmospheric pressure chemical ionization (APCI) source, was used. Biosystems/MDS SCIEX Analyst software version 1.4.2 was used for data acquisition.

4.4.4.4.3 Chromatography

The column used was a Phenomenex® C_{18} (15cm × 2.0mm, 5μm). The injection solvent and mobile phase consisted of water : methanol (10:90, v/v) acidified with formic acid (0.05%) and 20μL was loaded onto the column. The flow rate of the mobile phase through the analytical column was 200 μL/min.

4.4.5.Nuclear magnetic resonance spectra (NMR)

^{1}H and ^{13}C NMR spectra were obtained on a Bruker Avance 600 spectrometer (600 MHz for ^{1}H NMR and 150 MHz for ^{13}C NMR). Different deuterated solvents were used for various samples, the operating temperature was set to 25 ^{o}C. Tetramethylsilane (TMS) was used as internal standard for ^{1}H signals (0 ppm).

For advanced and two dimensional spectra including APT DEPT, COSY, NOESY, HSQC, HMBC, the standard pulse sequences and processing macros were employed as provided in the original software.

4.4.6. Circular dichroism (CD) analysis (Prof. D. Ferreira and Dr. C. Coleman at the University of Mississippi's Department of Pharmacognosy)

The CD spectra were recorded on an Olis DSM 20 instrument.

Circular Dichroism (CD) spectra for compound **F** (MW 464) were acquired at the following concentrations (0.25. 0.10, 0.05, 0.025, and 0.010 mM). All spectra were obtained at room temperature using high purity methanol as the solvent and a cylindrical quartz cuvette with a path length of 1 cm and a volume of 2.8 mL. Sample concentrations of 0.10, 0.05, an 0.025 mM provided the most representative CD spectra and all three of these concentrations gave an absorbance maximum at 290 nm. A 'Digital Filter' smoothing algorithm was applied to the raw data to correct for small amounts of noise and produce the molar ellipticity (θ) values.

4.5. **Chemical methods**

4.5.1. Acid hydrolyses of the sugars

Compounds **A**-**G** (5 mg each) were refluxed in 10% HCl-H_2O for 3 h. The reaction solution

was evaporated to dryness. The residue was dissolved in MeOH, and the sugars were identified by comparison with standard references on TLC.

4.5.2. Configuration of sugars by GC

The acid hydrolyzed solution of compounds **C** and **D** (same procedure as 4.5.1.) was evaporated under N_2 and lyophilized. The residue was dissolved in anhydrous pyridine (100 μL), 0.1 M L-cysteine methyl ether hydrochloride (200 μL) (Sigma-Aldrich) was added, and the mixture was warmed at 60^{o}C for 1 h. The trimethylsilylation reagent HMDS-TMCS (hexamethyldisilazane - trimethylchlorosilane-pyridine (3:1:9) (Supelco, USA) was added, and warming at 60^{o}C was continued for another 30 min (Ito *et al.*, 2004). The thiazolidine derivatives were subjected to GC analysis to identify the configuration of the sugars by comparison with the reference standard.

4.5.3. Basic hydrolysis of *p*-coumaric acid

Compounds **C** and **D** (1 mg each) were added to 4 N NaOH solution in H_2O (10 ml) at room temperature for 16 h. The reaction solution was extracted by EtOAc. This extract was subjected to mass analysis.

4.6. **Biological methods**

4.6.1. Acetylcholinesterase inhibition

The acetylcholinesterase inhibition test was conducted in the following manner: The samples were first migrated on 10 cm x 10 cm TLC plates, The TLC plates were dried well and then sprayed evenly with 5 ml of AChE solution (from a solution of 440 U AChE in 70 ml pH 7.8 Tris) (Sigma C3389). The plates were left for 5 min. A solution of α-naphthyl acetate (6 mg) in ethanol (2.5 ml and a solution of Fast Blue Salt B (25 mg) (Sigma D9805) in water (10 ml) were prepared and mixed together. The resulting mixture was sprayed onto the TLC plates and ca. 5 minutes waiting

time was necessary for full development of purple background on TLC plates. (Marston *et al.*, 2002)

4.6.2. Radical scavenging activity

The antiradical or free radical scavenging activities were tested using a stable free radical, 1,1-diphenyl-2-picrylhydrazyl (DPPH), which has a violet color and an absorption maximum at 517 nm. When DPPH was reduced by free radical scavenger, the violet colour disappeared. In practice, the TLC test was performed by spraying a DPPH solution in methanol at 3 mg/ml on TLC plates on which samples had been developed with suitable solvent system. The active zones were observed as yellow spots against a violet background after 30 min (Cuendet *et al.*, 1997).

The spectrophotometric dilution test was used to evaluate radical scavenging compounds quantitatively. It was carried out on 96-well microplates. A 0.022% DPPH solution (25 μl) in MeOH was added to a solution of the compound to be tested at different concentrations in MeOH (115 μL). Absorbance at 517 nm was measured after 30 min and the percentage of activity was calculated (Cavin *et al.*, 1998). The percentage of activity of each sample was calculated according to the following equation:

Activity % = A_{DPPH}-A_s / A_{DPPH}

where A_{DPPH} is the absorbance at 517 nm of the DPPH solution, and A_s is the absorbance at 517 nm of the sample preparation. All tests and analyses were run in triplicate and averaged.

4.6.3. Antimicrobial activity

Culture and media preparation: The National Committee for Clinical Laboratory Standards (NCCLS) (2003) guidelines were used to ensure that accurate microbiological assay and transfer techniques were followed. All stock cultures were obtained from the National Health Laboratory Services (NHLS). Authorization to keep and use cultures for research purposes was obtained from the Department of Health (reference: J1/2/4/16 NO1). Table 4.3 lists the cultures with

corresponding reference numbers used in this study. Stock cultures were retained at –20 °C, subcultured onto Tryptone Soya (Oxoid) agar, incubated at optimum temperatures and checked for purity. Isolated pure colonies were selected and transferred onto Tryptone Soya (Oxoid) agar and thereafter kept viable by subculturing weekly for stock culture maintenance. All media was prepared according to the instructions provided by the supplier i.e. weighed, dissolved in distilled water and autoclaved (Butterworth) at 121 °C for 15 min. After sterilization, all media was pre-incubated to confirm sterility before further use.

Minimum inhibitory concentrations (MIC): After preliminary screening by disc diffusion assay**,** the broth micro-dilution bioassay MIC was determined (Carson *et al*., 1995; Eloff, 1998a; NCCLS, 2003). All bacterial cultures were subcultured from stock agar plates and grown in Tryptone Soya (Oxoid) broth overnight. Negative controls (acetone in microtitre plate without antimicrobial) were included in each assay.

Table 4.3 Microbial organisms with corresponding reference numbers.

Test organisms
Escherichia coli (ATCC 8739)
Staphylococcus aureus (ATCC 25923)
Enterococcus faecalis (ATCC 29212)
Klebsiella pneumoniae (ATCC 13883)

Positive bactericidal controls i.e. ciprofloxacin (Sigma-Aldrich) at starting stock concentrations of 0.01 mg/mL were included in each assay to confirm the antimicrobial susceptibility. The ciprofloxacin stock solution was prepared aseptically with sterile water. The selection of ciprofloxacin as suitable reference controls is in support of the NCCLS guidelines (2003). All assays were run with micro-organism controls of the particular pathogen studied. A 0.4 mg/mL *p*-iodonitrotetrazolium violet (Sigma-Aldrich) solution (INT) was prepared and 40 µl transferred to all inoculated wells. The use of INT to determine the end point MIC value is based on the principle of detection of dehydrogenase activity where the metabolically active test organism reduces INT to a red-purple colour. The microtitre plates inoculated with bacteria were examined

after six hours to determine a colour change in relation to concentration of microbial growth. The lowest concentration having no colour change was defined as the MIC. Minimum inhibitory assays were done in triplicate.

4.6.4. Antimalarial activity

4.6.4.1 Parasite cultivation

The chloroquine-resistant Gambian FCR-3 strain of the malaria parasite *Plasmodium falciparum* was cultured *in vitro* according to the method described by Jensen and Trager (1976). Briefly, parasitized erythrocytes were suspended at a 5% haematocrit in RPMI-1640, supplemented with 10 mM D-glucose, 0.32 mM hypoxanthine, 50 mg/L gentamicin, 10% (v/v) heat inactivated human plasma and was buffered with 25 mM HEPES and 25 mM $NaHCO_3$. Cultures were maintained at 37°C with a gas mixture of 5 % CO_2, 3 % O_2 and the balance with N_2. Cultures were synchronized with 5% D-sorbitol when the parasites were in the ring stage (Lambros and Vanderberg 1979). The percentage parasitaemia and stages were assessed daily by microscopic examination of thin blood smears stained with Giemsa.

4.6.4.2 Extract preparation

A stock solution of 10mg/ml extract in DMSO was prepared, aliquoted out and frozen at -20 ℃ until required. An initial screen at 50 µg/ml for each extract was performed and for those extracts showing good inhibitory activity, seven 1:2 dilutions were prepared and plated out in triplicate wells.

4.6.4.3 Antiplasmodial screening

The antimalarial activity of the various extracts was determined using the tritiated hypoxanthine incorporation assay (Desjardins *et al*. 1979). The parasite suspension (200 µl),

consisting predominately of the ring stage, was adjusted to a 0.5% parasitaemia and 1% haematocrit and exposed to the extracts (25 µL) for a single cycle of parasite growth. All assays were carried out using untreated parasites and uninfected red blood cells as controls. Labelled ^{3}H-hypoxanthine (Amersham, 25 µL) was added after 24 h and the parasitic [^{3}H]-DNA was harvested on a Wallac® GFB-filtermat with a Titertek® cell harvester. The filtermats were dried, transferred to sample bags which were filled with scintillation cocktail and sealed before being counted in the Wallac® beta counter. For the active extracts, the concentration that inhibited 50% of parasite growth (IC_{50} value) was determined from the log sigmoid dose response curve generated by the Enzfitter® software. For the inactive extracts, the percentage parasite growth at 50 µg/ml was reported. Chloroquine and quinine were used as the reference antimalarial agents. At least three independent experiments were performed, from which the mean and standard deviation were determined.

4.6.4.4 Antimalarial test for pure compounds

A screen at 50 µg/ml was done first to ensure activity. If there was activity, seven one in 2 dilutions from 50-0.78 µg/ml were prepared to try and obtain a log sigmoid dose response curve from which the IC_{50} was obtained. If the curve was not optimal, the procedure was repeated at lower starting concentrations to ensure an optimal curve. Quinine, chloloroquine, pyrimethamine and cycloproguanil were used as the reference compounds.

4.7 Computational methods

The conformations of *α*-caryophyllene oxide and *β*-caryophyllene oxide were calculated by using Chembio 3D Ultra 12.0 (MM2, minimize energy, minimum RMS gradient 0.01) (CambridgeSoft, England).

4.8 Physical constants and spectral data for the isolates

Compound A

3-*O*-methylquercetin 7-*O*-*β*-glucopyranoside. $C_{22}H_{22}O_{12}$; MW 478; fine yellow needle crystals from TBME : MeCN : H_2O 2 : 2 : 3. UV λ_{max} (MeOH) nm (log ε): 254 (0.91), 265 *sh* (0.74), 356 (0.78), +NaOAc 260, 286 *sh*, 403; +NaOAc+H_3BO_3 259, 286 *sh*, 377; +NaOMe 245, 263, 397; +$AlCl_3$ 274, 296 *sh*, 441; +$AlCl_3$+HCl 267, 292 *sh*, 360, 401. HRESIMS: calc. for $C_{22}H_{23}O_{12}$ $(M+H)^+$, 479.11645; found, 479.12019. **^{1}H NMR** (600 MHz, CD_3OD, ppm): 7.65 (1H, *d*, *J* = 2.1 Hz, H-2′), 7.56 (1H, *dd*, ^3J = 8.5 Hz, ^4J = 2.1 Hz, H-6′), 6.91 (1H, *d*, *J* = 8.5 Hz, H-5′), 6.75 (1H, *d*, *J* = 2.1 Hz, H-8), 6.48 (1H, *d*, *J* = 2.1 Hz, H-6), 5.07 (1H, *d*, *J* = 7.2 Hz, H-1″), 3.95 (1H, *dd*, ^2J = 12.2 Hz, ^3J = 2.1 H, H-6″), 3.80 (3H, *s*, OCH_3), 3.74 (1H, *dd*, ^2J = 12.2 Hz, ^3J = 5.8 Hz, H-6″), 3.48-3.58 (3H, *m*, H-2″, H-3″, H-5″), 3.39-3.45 (1H, *m*, H-4″). **^{13}C NMR** (150 MHz, CD_3OD, ppm): 178.23 (C-4), 162.73 (C-7), 160.73 (C-5), 156.60 (C-2), 155.88 (C-9), 148.13 (C-4′), 144.47 (C-3′), 137.72 (C-3), 120.72 (C-1′), 120.52 (C-6′), 114.56 (C-2′), 114.44 (C-5′), 105.58 (C-10), 99.62 (C-1″), 98.76 (C-6), 93.76 (C-8), 76.36 (C-5″), 75.83 (C-3″), 72.7 (C-2″), 69.24 (C-4″), 60.44 (C-6″), 58.51 (OCH_3).

Compound B

3,4’-di-*O*-methylquercetin 7-*O*-*β*-glucopyranoside. $C_{23}H_{24}O_{12}$; MW 492; pale green crystals from TBME : MeCN : H_2O 2 : 2 : 3. UV λ_{max} (MeOH) nm (log ε): 253 (0.93), 263 *sh* (0.76), 351 (0.77), +NaOAc 254, 261 *sh*, 353; +NaOAc+H_3BO_3 254, 262 *sh*, 355; +NaOMe 265, 381; +$AlCl_3$ 267, 288 *sh*, 360, 402; +$AlCl_3$+HCl 265, 272 *sh*, 294 *sh*, 356, 398. HRESIMS: calc. for $C_{23}H_{26}O_{12}$ $(M+H)^+$, 493.1327; found, 493.1353. **^{1}H NMR** (600 MHz, CD_3OD, ppm): 7.67 (1H, *dd*, ^3J = 8.6 Hz, ^4J = 2.1 Hz, H-6′), 7.63 (1H, *d*, *J* = 2.1 Hz, H-2′), 7.08 (1H, *d*, *J* = 8.6 Hz, H-5′), 6.77 (1H, *d*, *J* = 2.0 Hz, H-8), 6.49 (1H, *d*, *J* = 2.0 Hz, H-6), 5.06 (1H, *d*, *J* = 7.2 Hz, H-1″), 3.94 (3H, *s*, OCH_3), 3.92 (1H, *dd*, ^2J = 12.2 Hz, ^3J = 2.1 Hz, H-6″), 3.81(3H, *s*, OCH_3), 3.71 (1H, *dd*, ^2J = 12.2 Hz, ^3J = 5.8 Hz, H-6″), 3.48-3.57 (3H, *m*, H-2″, H-3″, H-5″), 3.38-3.43 (1H, *m*, H-4″). **^{13}C NMR** (150 MHz, DMSO-d_6, ppm): 178.66 (C-4), 163.44 (C-7), 161.37 (C-5), 156.49 (C-2), 156.42 (C-9), 150.85

(C-4′), 146.82 (C-3′), 138.73 (C-3), 122.62 (C-1′), 120.93 (C-6′), 115.62 (C-2′), 112.39 (C-5′), 106.38 (C-10), 100.34 (C-1″), 99.71 (C-6), 95.02 (C-8), 77.61 (C-5″), 76.85 (C-3″), 73.57 (C-2″), 70.01 (C-4″), 61.07 (C-6″), 60.25 (OCH_3), 56.14 (OCH_3). **^{13}C NMR** (150 MHz, CD_3OD, ppm): 178.28 (C-4), 162.84 (C-7), 160.82 (C-5), 156.23 (C-2), 156.04 (C-9), 149.90 (C-4′), 145.75 (C-3′), 138.17 (C-3), 122.10 (C-1′), 120.33 (C-6′), 114.29 (C-2′), 110.38 (C-5′), 105.72 (C-10), 99.65 (C-1″), 98.82 (C-6), 93.81 (C-8), 77.61 (C-5″), 76.39 (C-3″), 75.86 (C-2″), 72.74 (C-4″), 69.27 (C-6″), 60.47 (OCH_3), 58.58 (OCH_3).

Compound C

3-*O*-methylquercetin 7-*O*-[*β*-D-6''(*E*-*p*-coumaroyl)glucopyranoside]. $C_{31}H_{28}O_{14}$; MW 624; yellow amorphous product. UV λ_{max} (MeOH) nm (log ε): 255 (0.82), 266 (0.77), 294 *sh* (0.78), 314 (0.92), 357 (0.64), +NaOAc 261, 292 *sh*, 314, 367, 416 *sh*; +NaOAc+H_3BO_3 260, 291, 313, 379; +NaOMe 242, 261, 365; +$AlCl_3$ 276, 297 *sh*, 309 *sh*, 443; +$AlCl_3$+HCl 275, 298, 312, 358, 401. LRESIMS positive mode *m/z*: $[M+H]^+$ 625, $[M+H+Na]^+$ 647; negative mode *m/z*: $[M-H]^-$ 623. HRESIMS: calc. for $C_{31}H_{29}O_{14}$ $(M+H)^+$, 625.1559; found, 625.1539. **^{1}H NMR** (600 MHz, CD_3OD, ppm): 7.62 (1H, *d*, *J* = 2.1 Hz, H-2′), 7.54 (1H, *overlapped*, *dd*, ^3J = 8.4 Hz, ^4J = 2.1 Hz, H-6′), 7.53 (1H, *overlapped*, *d*, *J* = 15.9 Hz, H-7‴), 7.19 (2H, *d*, *J* = 8.5 Hz, H-2‴, H-6‴), 6.87 (1H, *d*, *J* = 8.5 Hz, H-5′), 6.67 (1H, *d*, *J* = 2.0 Hz, H-8), 6.64 (2H, *d*, *J* = 8.5 Hz, H-3‴, H-5‴), 6.49 (1H, *d*, *J* = 2.0 Hz, H-6), 6.27 (1H, *d*, *J* = 15.9 Hz, H-8‴), 5.08 (1H, *d*, *J* = 7.2 Hz, H-1″), 4.62 (1H, *dd*, ^2J = 12.2 Hz, ^3J = 2.0 Hz, H-6″), 4.29 (1H. *dd*, ^2J = 12.2 Hz, ^3J = 8.1 Hz, H-6″), 3.86 (1H, *t-like*, *J* = 8.1 Hz, H-5″), 3.74 (3H, *s*, OCH_3), 3.55 (2H, *m* , H-2″, H-3″), 3.42 (1H, *m*, H-4″). **^{13}C NMR** (150 MHz, CD_3OD, ppm): 178.71 (C-4), 167.70 (C-9‴), 163.02 (C-7), 161.31 (C-5), 159.83 (C-4‴), 157.02 (C-2), 156.35 (C-9), 149.34 (C-4′), 145.66 (C-7‴), 145.23 (C-3′), 138.26 (C-3), 129.66 (C-2‴, C-6‴), 125.44 (C-1‴), 121.17 (C-1′), 120.95 (C-6′), 115.33 (C-3‴, C-5‴), 115.09 (C-2′), 115.00 (C-5′), 113.14 (C-8‴), 106.16 (C-10), 99.78 (C-1″), 99.30 (C-6), 94.15 (C-8), 76.40 (C-3″), 74.09 (C-5″), 73.15 (C-2″), 70.76 (C-4″), 63.41 (C-6″), 59.01 (C-OCH_3).

Compound D

3,4'-di-*O*-methylquercetin 7-*O*-[*β*-D-6''(*E*-*p*-coumaroyl)glucopyranoside]. $C_{32}H_{30}O_{14}$; MW 638; pale green amorphous product. UV λ_{max} (MeOH) nm (log ε): 254 (0.65), 267 (0.61), 293 *sh* (0.63), +NaOAc 254, 266, 290 *sh*, 316, 351; +NaOAc+H_3BO_3 254, 267, 290 *sh*, 315, 353 *sh*; +NaOMe 263, 361; +$AlCl_3$ 274, 297, 312, 362, 404; +$AlCl_3$+HCl 266 *sh*, 274, 297, 312, 354 *sh*, 398. LRESIMS positive mode *m/z*: $[M+H]^+$ 639, $[M+H+Na]^+$ 661; negative mode *m/z*: $[M-H]^-$ 637. HRESIMS: calc. for $C_{32}H_{31}O_{14}$ $(M+H)^+$, 639.1723; found, 639.1681. **^{1}H NMR** (600 MHz, CD_3OD, ppm): 7.64 (1H, *dd*, ^3J = 8.5 Hz, ^4J = 2.2 Hz, H-6′), 7.62 (1H, *d*, *J* = 2.2 Hz, H-2′), 7.54 (1H, *d*, *J* = 15.8 Hz, H-7‴), 7.19 (2H, *d*, *J* = 8.6 Hz, H-2‴, H-6‴), 7.01 (1H, *d*, *J* = 8.5 Hz, H-5′), 6.73 (1H, *d*, *J* = 2.2 Hz, H-8), 6.62 (2H, *d*, *J* = 8.6 Hz, H-3‴, H-5‴), 6.51 (1H, *d*, *J* = 2.2 Hz, H-6), 6.27 (1H, *d*, *J* = 15.8 Hz, H-8‴), 5.10 (1H, *d*, *J* = 7.2 Hz, H-1″), 4.66 (1H, *dd*, ^2J = 11.9 Hz, ^3J = 2.2 Hz, H-6″), 4.27 (1H, *dd*, ^2J = 11.9 Hz, ^3J = 8.2 Hz, H-6″), 3.93 (3H, *s*, OCH_3), 3.87 (1H, *td-like*, ^3J = 8.2 Hz, ^4J = 2.2 Hz, H-5″), 3.78 (3H, *s*, OCH_3), 3.55 (2H, *m* , H-2″, H-3″), 3.43 (1H, *m*, H-4″). **^{13}C NMR** (150 MHz, CD_3OD, ppm): 178.79 (C-4), 167.62 (C-9‴), 163.15 (C-7), 161.30 (C-4‴), 161.20 (C-5), 156.70 (C-2), 156.48 (C-9), 150.74 (C-4′), 146.69 (C-3′), 145.94 (C-7‴), 138.70 (C-3), 129.72 (C-2‴, C-6‴), 124.85 (C-1‴), 122.55 (C-1′), 120.64 (C-6′), 115.31 (C-3‴, C-5‴), 115.03 (C-2′), 112.55 (C-5′), 110.86 (C-8‴), 106.28 (C-10), 99.86 (C-1″), 99.52 (C-6), 94.13 (C-8), 76.44 (C-3″), 74.21 (C-5″), 73.14 (C-2″), 70.83 (C-4″), 63.44 (C-6″), 59.17 (C-OCH_3),54.95 (C-OCH_3).

Compound E

Quercetin 7-*O*-*β*-glucopyranoside. $C_{21}H_{20}O_{12}$; MW 464; buff-coloured amorphous product. UV λ_{max} (MeOH) nm (log ε): 254 (0.89), 371 (0.78), +NaOAc 257, 415; +NaOAc+H_3BO_3 258, 389; +NaOMe 244, 266, 290 *sh*, 426; +$AlCl_3$ 254 *sh*, 270; +$AlCl_3$+HCl 264, 362, 426. LRAPCIMS *m/z*: $[M-H]^-$ 463.3, $[M-H\text{-}Gluc]^-$ 301.2. **^{1}H NMR** (600 MHz, CD_3OD, ppm): 7.77 (1H, *brs*, H-2′), 7.67 (1H, *dd*, ^3J = 8.4 Hz, ^4J = 1.4 Hz, H-6′), 6.89 (1H, *d*, *J* = 8.4 Hz, H-5′), 6.74 (1H, *d*, *J* = 1.8 Hz, H-8), 6.45 (1H, *d*, *J* = 1.8 Hz, H-6), 5.05 (1H, d, *J* = 7.1 Hz, H-1″), 3.94 (1H, *dd*, ^2J = 12.2 Hz, ^3J = 1.8 Hz, H-6″), 3.74 (1H, *dd*, ^2J = 12.2 Hz, ^3J = 5.8 Hz, H-6″), 3.48-3.58 (3H, *m*, H-2″, H-3″, H-5″),

3.39-3.45 (1H, *m*, H-4″). **^{13}C NMR** (150 MHz, CD_3OD, ppm): 176.08 (C-4), 163.02 (C-7), 160.75 (C-5), 156.28 (C-9), 147.73 (C-2), 147.39 (C-4′), 144.89 (C-3′), 136.25 (C-3), 122.46 (C-1′), 120.49 (C-6′), 114.85 (C-5′), 114.68 (C-2′), 104.87 (C-10), 100.27 (C-1″), 98.77 (C-6), 94.14 (C-8), 76.96 (C-5″), 76.46 (C-3″), 73.34 (C-2″), 69.88 (C-4″), 61.06 (C-6″).

Compound F

(*2R, 3R*)-dihydroquercetin 7-*O*-*β*-glucopyranoside. $C_{21}H_{22}O_{12}$; MW 466; light beige amorphous product. UV λ_{max} (MeOH) nm (log ε): 284 (0.81), 319 (0.15), +NaOAc 285, 334; +NaOAc+H_3BO_3 285, 322; +NaOMe 286, 360; +$AlCl_3$ 310, 385; +$AlCl_3$+HCl 287, 306, 377. CD (*c* = 0.050 mM, MeOH): $[\theta]_{224}$ 28539, $[\theta]_{240}$ 1254, $[\theta]_{250}$ 5102, $[\theta]_{296}$ -26235, $[\theta]_{336}$ -3327, $[\theta]_{345}$ -3927. LRAPCIMS *m/z*: $[M+H]^+$ 467.2, $[M+H\text{-Gluc}]^-$ 305.0. **^{1}H NMR** (600 MHz, CD_3OD, ppm): 6.98 (1H, *d*, *J* = 1.6 Hz, H-2′), 6.86 (1H, *dd*, ^3J = 8.2 Hz, ^4J = 1.6 Hz, H-6′), 6.81 (1H, *d*, *J* = 8.1 Hz, H-5′), 6.24 (1H, *d*, *J* = 2.1 Hz, H-8), 6.21 (1H, *d*, *J* = 2.1 Hz, H-6),4.98 (1H, *overlapped*, *d*, *J* = 7 Hz, H-1″), 4.97 (1H, *overlapped*, *d*, *J* = 11.5 Hz, H-2), 4.57 (1H, *d*, *J* = 11.5 Hz, H-3), 3.88 (1H, *dd*, ^2J = 12.2 Hz, ^3J = 1.8 Hz, H-6″), 3.69 (1H, *dd*, ^3J = 12.2 Hz, ^4J = 5.8 Hz, H-6″), 3.43-3.5 (3H, *m*, H-2″, H-3″, H-5″), 3.37-3.42 (1H, *m*, H-4″). **^{13}C NMR** (150 MHz, CD_3OD, ppm): 197.89 (C-4), 165.89 (C-7), 163.34 (C-5), 162.82 (C-9), 145.79 (C-4′), 144.92 (C-3′), 128.24 (C-1′), 119.56 (C-6′), 114.68 (C-5′), 114.54 (C-2′), 102.08 (C-10), 99.87 (C-1″), 96.88 (C-8), 95.61(C-6), 83.88 (C-2), 76.84 (C-5″), 76.36 (C-3″), 73.21(C-2″), 72.40 (C-3), 69.72 (C-4″), 60.90 (C-6″).

Compound G

Quercetin 3-*O*-[2-*O*-*β*-xylopyranosyl-6-*O*-*α*-rhamnopyranosyl]-*β*-glucopyranoside. $C_{32}H_{38}O_{20}$; MW 742, amber-coloured amorphous product. UV λ_{max} (MeOH) nm (log ε): 255(0.49), 261 *sh* (0.46), 294 (0.22), +NaOAc 271, 321, 395; +NaOAc+H_3BO_3 259, 375; +NaOMe 270, 325, 402; +$AlCl_3$ 272, 296 *sh*, 428; +$AlCl_3$+HCl 268, 295, 359, 398. HRESIMS: calc. for $C_{32}H_{39}O_{20}$ $(M+H)^+$, 743.2035; found, 743.1956, calc. for $C_{32}H_{37}O_{20}$ $(M-H)^-$, 741.1879, found, 741.1882. **^{1}H NMR** (600 MHz, CD_3OD, ppm): 7.64 (1H, *overlapped*, H-2′), 7.63 (1H, *overlapped*, H-6′), 6.89 (1H, *d*, *J*

= 8.5 Hz, H-5′), 6.38 (1H, *br.s*, H-8), 6.19 (1H, *br.s*, H-6), 5.41 (1H, *d*, *J* = 7.6 Hz, H- 1″), 4.80 (1H, *d*, *J* = 6.54 Hz, H-1‴′), 4.52 (1H, *br.s*, H-1‴), 3.98 (1H, *dd*, ^{2}J = 11.6 Hz, ^{3}J = 7.8 Hz, H-5‴′), 3.82 (1H, *d*, *J* = 10.1 Hz, H-6″), 3.73 (1H, *t*, *J* = 8.8 Hz, H-2″), 3.58-3.65 (2H, *m*, H-2‴, H-3″), 3.5-3.55 (2H, *m*, H-4‴′, H-3‴), 3.37-3.48 (4H, *m*, H-5‴, H-2‴′, H-3‴′, H-6″), 3.3-3.35 (2H, *m*, H-5″, H-4″), 3.25-3.3 (2H, *m*, H-5‴′, H-4‴). **^{13}C NMR** (150 MHz, CD_3OD, ppm): 177.97 (C-4), 164.94 (C-7), 161.59 (C-5), 157.20 (C-2), 157.06 (C-9), 148.29 (C-4′), 144.53(C-3′), 133.51 (C-3), 122.13 (C-1′), 121.87 (C-6′), 116.09 (C-5′), 114.67 (C-2′), 104.16 (C-10), 103.72 (C-1‴′), 100.73 (C-1‴), 99.51 (C-1″), 98.61 (C-6), 93.49(C-8), 80.50 (C-2″), 76.79 (C-3″), 75.62 (C-5″), 75.44 (C-3‴′), 73.27 (C-2‴′), 72.48 (C-4‴), 70.81 (C-3‴), 70.69 (C-2‴), 69.95 (C-4″), 69.56 (C-4‴′), 68.30 (C-5‴), 66.68 (C-6″), 65.15 (C-5‴′), 16.45 (C-6‴).

Compound H

8(*S*),13(*S*)-dihydrogrindelic acid. $C_{20}H_{34}O_3$; MW 322; colorless oil. HRESIMS: calc. for $C_{20}H_{35}O_3$ $(M+H)^+$, 323.2509; found, 323.2614. **^{1}H NMR** (600 MHz, $CDCl_3$, ppm): 2.67 (1H, *d*, *J* = 16 Hz, H-14), 2.50 (1H, *d*, *J* = 16 Hz, H-14), 2.02 (1H, *m*, H-11), 1.94 (1H, *m*, H-7), 1.93 (1H, *m*, H-12), 1.93 (1H, *m*, H-8), 1.92 (1H, *m*, H-11), 1.84 (1H, *m*, H-12), 1.58 (1H, *m*, H-6), 1.45 (1H, *m*, H -2), 1.42 (1H, *m*, H-1), 1.42 (1H, *m*, H-6) 1.41 (1H, *m*, H-7), 1.39 (1H, *m*, H-2), 1.33 (1H, *s*, H -16), 1.31 (1H, *s*, H-3), 1.30 (1H, *m*, H-1), 1.29 (1H, *m*, H-5), 1.14 (1H, *m*, H-3), 1.05 (1H, *d*, *J* = 7.8 Hz, H-17), 0.94 (1H, *d*, H-20), 0.85 (3H, *s*, H-18), 0.78 (3H, *s*, H-19). **^{13}C NMR** (150 MHz, $CDCl_3$, ppm): 173.14 (C-15), 95.87 (C-9), 80.86 (C-13), 48.97 (C-5), 46.62 (C-14), 42.04 (C-10), 41.84 (C-3), 39.13 (C-8), 38.10 (C-12), 32.60 (C-19), 33.56 (C-4), 33.56 (C-1), 29.58 (C-7), 28.69 (C-11), 27.65 (C-16), 21.77 (C-18), 18.43 (C-20), 18.30 (C-17), 18.22 (C-6), 17.17 (C-2).

Compound I

β-caryophyllene oxide. $C_{15}H_{24}O$; MW 220; colorless oil. HRAPCIMS: calc. for $C_{15}H_{25}O$ $(M+H)^+$, 221.1905; found, 221.1881.**^{1}H NMR** (600 MHz, $CDCl_3$, ppm): 4.99 (1H, *br d*, *J* = 1.2 Hz, H-13), 4.87 (1H, *br d*, *J* = 1.2 Hz, H-13), 2.89 (1H, *dd*, *J* = 10.7, 4.4 Hz, H-5), 2.63 (1H, *dd*, *J* = 20.2, 9.6

Hz, H-9), 2.36 (1H, *ddd*, *J* = 2.9, 7.6, 4.5 Hz, H-7a), 2.25 (1H, *ddd*, *J* = 16.8, 8.4, 4.2 Hz, H-6a), 2.12 (2H, *m*, H-3a,7b), 1.78 (1H, *t*, *J* = 9.6 Hz, H-1), 1.61-1.72 (3H, *m*, H-10, 2a), 1.44 (1H, *m*, H-2b), 1.33 (1H, *m*, H-6b), 1.22 (3H, *s*, H-12), 1.02 (3H, *s*, H-14), 1.00 (3H, *s*, H-15), 0.97 (1H, *m*, H-3b). **^{13}C NMR** (150 MHz, $CDCl_3$, ppm): 151.83 (C-8), 112.79 (C-13), 63.80 (C-5), 59.91 (C-4), 50.68 (C-1), 48.74 (C-9), 39.74 (C-10), 39.13 (C-3), 34.04 (C-11), 30.21 (C-6), 29.90 (C-7), 29.75 (C-15), 27.20 (C-2), 21.62 (C-14), 17.01 (C-12).

6. BIBLIOGRAPHY

Adewusi, E.A., Moodley, N., Steenkamp, V. (2011). Antioxidant and acetylcholinesterase inhibitory activity of selected southern African medicinal plants. *South African J. Bot.* **77**，638-644.

Alqasoumi, S.I. (2009). Phytochemical study of the aerial parts of *Conyza discoridis* growing in Saudi Arabia. *Nat. Prod. Sciences* **15,** 66-70.

Arnold, T.H., de Wet, B.C. (1993). Plants of Southern Africa: Names and Distribution. Memoirs of the Botanical Survey of South Africa No 62. National Botanical Institute, Pretoria.

Borman, S. (2002). Organic lab sparks drug discovery, Sam Danishefsky helps create model for chemistry at a medical center-but he deplores media hype. *Chem. Eng. News*, **80**, Jan 14, p23-24.

Botha, J.J., Viviers, P.M., Young, D.A., Du Preez, I.C., Ferreira, D., Roux, D.G., Hull, W.E. (1982). Synthesis of condensed tannins. Part 5. The first angular [4,6:4,8]-triflavanoids and their natural counterparts. *J.C.S. Perkin Trans I*, 527–533.

Brophy, J.J., Boland, D.J., Van der Lingen, S. (1992). Essential oils in the leaf, bark and seed of mopane. *S. African Forestry* **161**, 23–25.

Bruneton, J. (1995). Pharmacognosy, Phytochemistry, Medicinal Plants. Lavoisier Technique & Documentation, Paris.

Burda, S., Oleszek, W. (2001). Antioxidant and anti-radical activities of flavonoids. *J. Agric. Food Chem.* **49**, 2774-2779.

Butler, D., Maurice, J., O'Brien, C. (1997). Time to put malaria control on the global agenda. *Nature* **386**, 535-536.

Carson, C.F., Hammer, K.A., Riley, T.V. (1995). Broth micro-dilution method for determining the susceptibility of *Escherichia coli* and *Staphylococcus aureus* to the essential oil of *Melaleuca alternifolia* (tea tree oil). *Microbios* **82**, 181-185.

Cavin, A., Hostettmann, K., Potterat, O. (1998). Antioxidant and lipophilic constituents of *Tinospora crispa*. *Planta Med.* **64**, 393-396.

Chagonda, L.S., Makanda, C., Chalchat, J.-C. (1999). Essential oils of four wild and semi-wild plants from Zimbabwe: *Colophospermum mopane* (Kirk ex Benth.) Kirk ex Leonard, *Helichrysum splendidum* (Thumb.) Less, *Myrothamnus flabellifolia* (Welw.) and *Tagetes minuta* L. *J. Ess. Oil Res.* **11**, 573–578.

Chang, Q., Wong, Y.S. (2004). Identification of flavonoids in Hakmeitau beans (*Vigna sinensis*) by high performance liquid chromatography-electrospray mass spectrometry (LC-ESI/MS). *J. Agric. Food Chem.* **52**, 6694–6699.

Chen, Y., Qiu, Y., Fu, W., Pei, Y., Dou, D., Xu, S. (2003). New medical application of total flavones of Opuntia and its preparation from Faming Zhuanli Shenqing Gongkai Shuomingshu, CN 1442146 A 20030917. Language: Chinese, Database: CAPLUS.

Choudhary, M.I., Siddiqui, Z.A., Nawaz, S.A. (2006). Microbial transformation and butyrylcholinesterase inhibitory activity of (-)-caryophyllene oxide and its derivatives. *J. Nat. Prod.* **69**, 1429-1434.

Cmelik, S.H.W. (1970). Sterols in the diet and various organs of caterpillars of the mopane moth *Gonimbrasia belina*. *Z. Physiol. Chem.* **351**, 365–372.

Cragg, G.M., Newman, D.J., Snader, K.M. (1997). Natural products in drug discovery and development. *J. Nat. Prod.* **60**, 52-60.

Cuendent, M., Hostettmann, K., Potterat, O. (1997). Iridoid glucosides with free radical scavenging properties from *Fragraea blumei*. *Helv. Chim. Acta* **80**, 1144-1151.

Cullen, J. (1997). The Identification of Flowering Plant Families, 4th Edition, Cambridge University Press, Cambridge, p.43.

Decosterd, L.A., Parsons I.C., Custafson, K.R., Cardellina II, J.H., McMahon, J.B., Cragg, G.M., Murata, Y., Pannell, L.K., Steiner, J.R., Clardy, J., Boyd, M.R. (1993). Structure, absolute stereochemistry, and synthesis of conocurvone, a potent novel HIV-inhibitory naphthoquinone trimer from a *Conospermum* sp. *J. Am. Chem. Soc.,* **115**, 6673-6679.

Desjardins, R.E., Canfield, C.J., Haynes, D.J., Chulay, J.D. (1979). Quantitative assessment of antimalarial activity *in vitro* by a semiautomated microdilution technique. *Antimicr. Agents and Chemother*. **16**, 710-718.

Dictionary of Natural Products 2008. Version 16.2. Chapman and Hall, London.

Dondorp, A.M., Nosten, F., Yi, P., Das, D., Phyo, A.P., Tarning, J., Lwin, K.M., Ariey, F., Hanpithakpong, W., Lee, S.J., Ringwald, P., Silamut, K., Imwong, M., Chotivanich, K., Lim, P., Herdman, T., An, S.S, Yeung, S., Singhasivanon, P., Day, N.P., Lindegardh, N., Socheat, D., White, N.J. (2009). Artemisinin resistance in *Plasmodium falciparum* malaria. *N. Engl. J. Med.* **361**, 455-467.

Doyle, J.J., Luckowm, M.A. (2003). The rest of the iceberg. Legume diversity and evolution in a phylogenetic contex. *Plant Physiol.* **131**, 900-910.

Drewes, S.E., Fletcher, I.P. (1974). Polyhydroxystilbenes from the heartwood of *Schotia brachypetala*. *J. Chem. Soc. Perkin Trans. I*, 961-962.

Drewes, S.E., Roux, D.G. (1965). Absolute configuration of mopanol, a new leucoanthocyanidin from *Colophospermum mopane*. *J.C.S. Chem. Commun.*, 500–502.

Drewes, S.E., Roux, D.G. (1966). Stereochemistry and biogenesis of mopanols and peltogynols and associated flavonoids from *Colophospermum mopane*. *J. C. S. (C),* 1644–1653.

Drewes, S.E., Roux, D.G. (1967). Isolation of mopanin from *Colophospermum mopane* and interrelation of flavonoid components of *Peltogyne* spp. *J. C. S. (C),* 1407–1410.

Du Preez, I.C. (1971). Mono- and polymeric flavanoids from *Acacia* and *Colophospermum* species, PhD Thesis, University of the Orange Free State, Bloemfontein.

Du Preez, I.C., Rowan, A.C., Roux, D.G. (1971). Hindered rotation about the sp2–sp3 hybridized C–C bond between flavonoid units in condensed tannins. *J.C.S. Chem. Commun.* 315–316.

Eloff, K. (1998). A sensitive and quick microplate method to determine the minimal inhibitory concentration of plant extracts from bacteria. *Planta Med.* **64**, 711-713.

Englund B.M., Griffeth, L., Clausen, T.P. (2009). A 9,13-epoxylabdane from *Colophospermum mopane*. *Phytochem. Lett.* **2**, 144–147.

Ferreira, D., Marais, J.P.J., Slade, D. (2003). Phytochemistry of the mopane, *Colophospermum mopane*. *Phytochemistry* **64**, 31–51.

Gaffield, W. (1970). Circular dichroism, optical rotatory dispersion and absolute configuration of flavanones, 3-hydroxy flavanones and their glycosides. Determination of aglycone chirality on flavanone glycosides. *Tetrahedron* **26**, 4093-4108.

Gericke, N. (2002). Plants, products and people: southern African perspectives, Advances in

Phytomedicine. *Ethnomed*. *Drug Discov*. **1**, 155-162.

Glasby, J.S. (1991). Dictionary of Plants Containing Secondary Metabolites. Taylor and Francis, London.

Goupy, P., Dufour, C., Loonis, M., Dangles, O. (2003). Quantitative kinetic analysis of hydrogen transfer reactions from dietary polyphenols to the DPPH radical. *J. Agric. Food Chem.* **51**, 615–622.

Gustafson, K.R., Cardellina II, J.H., McMahon, J.B., Gulakowski, R.J., Ishitoya, J., Szallasi, Z., Lewin, N.E., Blumberg, P.M., Weislow, O.S. (1992). A nonpromoting phorbol from the Samoan medicinal plant *Homalanthus nutans* inhibits cell killing by HIV-1. *J. Med. Chem.*, **35**, 1978–1986.

Graham, P.H., Vance, C.P. (2003). Legumes: importance and constraints to greater use. *Plant Physiol*. **131**, 872-877.

Guerin, P.J., Olliaro, P., Nosten, F., Druilhe, P., Laxminarayan, R., Binka, F., Kilama, W.L., Ford, N., White, N.J. (2002). Malaria: current status of control, diagnosis, treatment, and a proposed agenda for research and development. *Lancet Infect. Dis.* **2**, 564-573.

Hamburger, M., Marston, A., Hostettmann, K. (1991). Search for new drugs of plant origin. In Advances in Drug Research, Vol. 20, (Testa, B., ed.), Academic Press, London, pp. 167-215.

Haynes, R.K. (2006). From artemisinin to new artemisinin antimalarials: biosynthesis, extraction, old and new derivatives, stereochemistry and medicinal chemistry requirements. *Curr. Top. Med. Chem.* **6**, 509-537.

Hostettmann, K., Marston, A. (2007). The search for new drugs from higher plants. *Chimia* **61**, 322-326.

Hostettmann, K., Marston, A., Hostettmann, M. (1998). Preparative Chromatography Techniques, 2nd Edition, Springer Verlag, Berlin.

Hostettmann K., Gupta, M.P., Marston, A., Queiroz, E.F. (2008). Handbook of Strategies for the Isolation of Bioactive Natural Products, SECAB & CYTED, Colombia.

Hutchings, A., Scott, A., Lewis, G., Cunningham A. (1996). Zulu Medicinal Plants: An Inventory. University of Natal Press, Pietermaritzburg.

Ito, Y. (2005). Golden rules and pitfalls in selecting optimum conditions for high-speed counter-current chromatography. *J. Chromatogr. A* **1065**, 145-168.

Ito, A., Chai, H.B., Kardono, L.B.S., Setowati, F.M., Afriastini, J.J., Riswan, S., Farnsworth, N.R., Cordell, G.A., Pezzuto, J.M., Swanson, S.M., Kinghorn, A.D. (2004). Saponins from the bark of *Nephelium maingayi*. *J. Nat. Prod.* **67**, 201-205.

Iwashina, T., Ootani, S., Hayashi, K. (1984). Neochilenin, a new glycoside of 3-*O*-methylquercetin, and other flavonols in the tepals of *Neochilenia*, *Neoporteria* and *Parodia* species (Cactaceae). *Botanical Magazine* (Tokyo) **97**, 23-30.

Jain, A.K., Saxena, V.K. (1986). Isolation and characterization of 3-methoxyquercetin 7-*O*-*β*-D-glucopyranoside from *Trifolium pratense*. *Nat. Acad. Sci. Lett.* (India) **9**, 379- 380.

Jensen, J.B., Trager, W. (1976). Human malaria parasites in continuous culture. *Science* **193**, 673-675.

Johnson, H.E., Banack, S.A., Alan Cox, P. (2008). Variability in content of the anti-AIDS drug candidate prostratin in Samoan populations of *Homalanthus nutans*. *J. Nat. Prod.* **71**, 2041-2044.

Jurzysta, A. (1983). Flavonoids of leaves of some *Nicotiana* species. *Pamietnik Pulawski* **79**, 231-237.

Khafagy, S.M., Sabri, N.N., Abd El-Salam, N., Seif El-Din, A. (1978). Flavonoidal contents of *Carthamus glaucus* Bieb-Emend, Hanelt spp. *alexandrinus* Hanelt (Compositae). *Egypt. J. Pharm. Sci*. **19**, 307-312.

Kinghorn, A.D., Pan, L., Fletcher, J.N., Chai, H. (2011). The relevance of higher plants in lead compound discovery programs. *J. Nat. Prod.* **74**, 1539-1555.

Kitteringham, N.R., Jenkins, R.E., Lane, C.S, Elliott, V.L., Park, B.K. (2009). Multiple reaction monitoring for quantitative biomarker analysis in proteomics and metabolomics. *J. Chromatogr. B* **877**, 1229-1239.

Klayman, D.L. (1985). Qinghaosu (artemisinin): an antimalarial drug from China. *Science* **228**, 1049-1055.

Krungkrai, J., Imprasittichai, W., Otjungreed**,** S., Pongsabut, S., Krungkrai, S.R. (2010). Artemisinin resistance or tolerance in human malaria patients. *Asian Pacific J. Trop. Med.* **3**, 748-753.

Lambros, C., Vanderberg, P. (1979). Synchronisation of *Plasmodium falciparum* erythrocytic stages in culture. *J. Parasitol*. **65**, 418-420.

Lewis, G., Schrire, B., Mackinder, B., Lock, M. (2005). Legumes of the World, Royal Botanic Gardens, Kew, Richmond, Surrey, UK.

Li, Y., Huang, H., Wu, Y.L. (2006). Qinghaosu (artemisinin) – a fantastic antimalarial drug from a traditional Chinese medicine. In: Liang, X.T., Fang, W.S. (Eds.), Medicinal Chemistry of Bioactive

Natural Products. Wiley Interscience, Hoboken, pp.183-256.

Lou, H., Yuan, H., Yamazaki, Y., Sasaki, T., Oka, S. (2001). Alkaloids and flavonoids from peanut skins. *Planta Med.* **67**, 345-349.

Mandava, N.B., Ito, Y. (Eds.), (1988) Countercurrent Chromatography—Theory and Practice, Chromatographic Science Series, vol. 44, Marcel Dekker, New York.

Markham, K.R. (1982). Techniques of Flavonoid Identification, Academic Press, London.

Marston A., Hostettmann, K. (2006). Developments in the application of countercurrent chromatography to plant analysis. *J. Chromatogr. A* **1112,** 181–194.

Marston, A., Kissling, J., Hostettmann, K. (2002). A rapid TLC bioautographic method for the detection of acetylcholinesterase and butyrylcholinesterase inhibitors in plants. *Phytochem. Anal.* **13**, 51-54.

Masika, P. J., Afolayan, A.J. (2002). Antimicrobial activity of some plants used for the treatment of livestock disease in the Eastern Cape, South Africa. *J. Ethnopharmacol.* **83**, 129-134.

Materska, M., Perucka, I., (2005). Antioxidant activity of the main phenolic compounds isolated from hot pepper fruit (*Capsicum annuum* L.). *J. Agric. Food Chem.* **53**, 1750-1756.

Mathabe, M.C., Nikolova, R.V., Lall, N., Nyazema, N.Z. (2006). Antibacterial activities of medicinal plants used for the treatment of diarrhoea in Limpopo Province, South Africa. *J. Ethnopharmacol.* **105**, 286-93.

McGaw L.J., Jäger A.K., van Staden J. (2002). Isolation of antibacterial fatty acids from *Schotia brachypetala*. *Fitoterapia* **73**, 431-433.

Mebe, P.P. (2001). Diterpenes from the bark and seeds of *Colophospermum mopane*. *Phytochem*. **57**, 537–541.

Mulholland, D.A., Drewes S.E. (2004). Global phytochemistry: indigenous medicinal chemistry on track in southern Africa. *Phytochem*. **65,** 769–782.

Muller, K. (1992). Freie Radikale. *Dtsche Apoth*. *Ztg*. **132,** 1473-1482.

Muller, H. (2000). Natural products and their importance in drug discovery. In: Luijendijk T, de Graf P, Remmelzwaal A, Verporte R, editors. 2000 years of natural products research: past, present and future. Leiden: University of Leiden: L05.

NCCLS, 2003. Methods for dilution antimicrobial susceptibility tests for bacteria. Approved standard-Sixth edition ISBN-56238-486-4, USA.

Netshiungani, E.N. (1981). Notes on the uses of indigenous trees in Venda. *J. Dendrol*. **1**, 12-17.

Newman, D.J., Cragg, G.M. (2007). Natural products as sources of new drugs over the last 25 years. *J. Nat. Prod.* **70**, 461-477.

Nifant'ev, E.E., Koroteev, M.P., Kaziev, G.Z., Uminskii, A.A., Grachev, A.A., Men'shov, V.M., Tsvetkov, Yu.E., Nifant'ev, N.E., Bel'skii, V.K., Stash, A.I. (2006). On the problem of identification of the dihydroquercetin flavonoid, *Russian Journal of General Chemistry* **76**, 161-163.

Oksuz, S. (1977). Flavonoidal compounds of *Inula viscosa*. Part II. *Planta Med.* **31**, 270-273.

Palgrave, K.C. (2002). Trees of Southern Africa, C. Struik Publishers, Cape Town, pp. 268–269.

Palmer, E. (1981). A Field Guide to the Trees of Southern Africa, 2nd Edition, Collins, London and Johannesburg.

Patrick, G.L. (2005). Introduction to Medicinal Chemistry, 3rd Edition, Oxford University Press, New York, p 379.

Polhill, R.M. (1994). Classification of the Leguminosae and complete synopsis of Legume genera. In F.A.Bisby, J.Buckingham and J.B. Harbone (Eds.), Phytochemical Dictionary of the Leguminosae. Vol.1: Plants and their Constituents, pp 35-57. Chapman and Hall, London.

Potterat, O., Hostettmann, K. (1995). Plant sources of natural drugs and compounds. In Encyclopedia of Environmental Biology, Vol. 3, Academic Press, London, pp.139-153.

Pujol, J. (1993), Naturafrica-the Herbalist handbook. Jean Pujol Natural Healer's Foundation, Durban.

Reiter, E., Treadwell, E., Cederstrom, E., Reichardt, P.B., Clausen, T.P. (2003). Diterpenes from *Colophospermum mopane*: ''Missing links'' in the biogenesis of 9,13-epoxylabdanes. *J. Nat. Prod.* **66**, 30–33.

Rice-Evans, C. A., Miller, J., Paganga, G. (1997). Antioxidant properties of phenolic compounds. *Trends Plant Sci.* **2**, 152–159.

Rouhi, A.M. (2003). Rediscovering natural products, *Chem. Eng. News* **41**, 78-91.

Shu, Y.-Z. (1998). Recent natural products based drug development: a pharmaceutical industry perspective. *J. Nat. Prod.* **61,** 1053-1071.

Slade, D., Ferreira, D., Marais, J.P.J. (2005). Circular dichroism, a powerful tool for the assessment

of absolute configuration of flavonoids. *Phytochem*. **66,** 2177-2215.

Snow, R.W., Guerra, C.A., Noor, A.M., Myint, H.Y., Hay, S.I. (2005). The global distribution of clinical episodes of *Plasmodium falciparum* malaria. *Nature* **434**, 214-217.

Sprent, J.I. (2001). Nodulation in Legumes. Royal Botanic Gardens, Kew, Richmond, Surrey, UK.

Stafford, G.I., Pedersen, P.D., Jäger, A.K. and Van Staden, J. (2007). Monoamine oxidase inhibition by Southern African traditional medicinal plants. *S. African J. Botany* **73**, 384-390.

Strohl, W.R. (2000). The role of natural products in a modern drug discovery program, *Drug Discovery Today* **5**, 39-41.

Tiwari, K.P., Savitri, S., Srivastava, D. (1979). Pigments from the stem bark of *Dillenia indica*, *Planta Med.* **35**, 188-190.

Van den Bosch, K., Stacey, G. (2003). Advances in legume biology. *Plant Physiol.* **131**, 839.

Van Staden, J. (2008). Ethnobotany in South Africa. *J. Ethnopharmacol*. **119**, 329–330.

Venter, F., Venter, J.-A. (1996). Making the Most of Indigenous Trees, Briza Publications, Pretoria.

Wall, M.E., Wani, M.C., Brown, D.M., Fullas, F., Oswald, J.B., Josephson, F.F., Thornton, N.M., Pezzuto, J.M., Beecher, C.W.W., Farnsworth, N.R., Cordell, G.A., Kinghorn, A.D. (1996). Effect of tannins on screening of plant extracts for enzyme inhibitory activity and techniques for their removal. *Phytomed*. **3**, 281-285.

Wang, L., Tu, Y.Ch., Liam, T.W., Hung, J.T., Yen, J.H., Wu, M.J. (2006). Distinctive antioxidant and anti-inflammatory effects of flavonols. *J. Agric. Food Chem.* **54**, 9798-9804.

Watt, J.M., Breyer-Brandwijk, M.G. (1962). The Medicinal and Poisonous Plants of Southern and Eastern Africa. 2nd edition. Livingstone, London.

Webby, R.F. (1991). A flavonol triglycoside from *Actinidia arguta* var. *giraldii*. *Phytochem*. **30**, 2443-2444.

Weina, P.J. (2008). Artemisinins from folklore to modern medicine-transforming an herbal extract to life-saving drugs. *Parasitologia* **50**, 25-29.

Williams, C.A., Grayer, R.J. (2004). Anthocyanins and other flavonoids. *Nat. Prod. Rep.*, **21**, 539–573.

World Health Organization. (2001). Antimalarial drug combination therapy: report of WHO technical consultation. WHO, Geneva.

World Health Organization. (2008). World Malaria Report 2008. WHO, Geneva.

Yang, J.H., Kondratyuk, T.P., Jermihov, K.C., Marler, L.E., Qiu, X., Choi, Y., Cao, H.M., Yu, R., Sturdy, M., Huang, R., Liu, Y., Wang, L.Q., Mesecar, A.D., van Breemen, R.B., Pezzuto, J.M., Fong, H.H.S., Chen, Y.G., Zhang, H.J. (2011). Bioactive compounds from the fern *Lepisorus contortus*. *J. Nat. Prod.* **74**, 129-136.

Yang, Y., Wu, T., Yang, W.X., Aisa, H.A., Zhang, T.Y., Ito, Y. (2008). Preparative isolation and purification of four flavonoids from *Flos gossypii* by high-speed countercurrent chromatography. *J. Liq. Chromatogr. Relat. Technol.* **31**, 1523-1531.

Zhang, P.F., Li, C. (2008). Flavones from flowers of *Paulownia fortunei*. *Zhongguo Zhongyao Zazhi* (*Chinese Journal of Chinese Materia Medica*) **33**, 2629-2632.

OPSOMMING

Natuurlike produkte speel ‘n groot rol in die ontdekking van nuwe geneesmiddels en was in 2007 betrokke by meer as 52% van alle nuwe medisyne. In teenstelling met die willekeurige strukture beskikbaar van kombinatoriese chemie en met rekenaarmodulering, word natuurprodukte gekenmerk deur ‘n groter en intelligenter variasie in struktuur. Plante is ‘n potensiele bron van nuwe bioaktiewe verbindings met oneindige variasie. Suid Afrika is een van die lande met die rykste plantdiversiteit in die wêreld en dus ‘n ongelooflike bron van nuwe natuurprodukte.

Die chemiese verbindings in die saad van Suid-Afrikaanse plante is tot dusver redelik verwaarloos in vergelyking met verbindings uit ander plantdele. In die lig van hul funksie mag sade belangrike metaboliete bevat. Sade van twintig plantsoorte is versamel en ondersoek. Die keuse is beïnvloed deur tradisionele kennis en beskikbaarheid van saadmonsters. Bome het groter en makliker versamelbare sade. Metanol-ekstrakte is gemaak om die olieinhoud van die saadekstrak so laag as moontlik te hou. Dertig ekstrakte is vir biologiese aktiwiteit getoets.

Die metanol ekstrak van die ariel van *Schotia brachypetala* Sond. (Fabaceae) saad en onvolwasse saad van *Colophospermum mopane* (Kirk ex Benth.) J. Leonard (Fabaceae) het die mees belowende aktiwiteite getoon en is verder ondersoek.

Hoë spoed teenstroom chromatografie (HSCCC) is gebruik om die ekstrakte te fraksioneer en suiwer verbindings te isoleer. Aktiwiteits geleide fraksionering (Vry-radilaal inhibering, cholienesterase inhibering, antimikrobiale aktiwiteit en anti-malaria aktiwiteit) is gebruik om die bioaktiewe ekstrakte, fraksies en isolate verder te skei. Die strukture van suiwer verbindings is met spektroskopiese (UV, MS, KMR en SD) en chemiese metodes bepaal. ‘n Totaal van nege verbindings, waarvan twee nuwe verbindings, is geisoleer. Die verbindings verantwoordelik vir van die waargenome biologiese aktiwiteit in die fraksies is geidentifiseer.

Uit die metanolekstrak van die ariel van *Schotia brachypetala*, is sewe kwersitien glukosiede

geisoleer: 3-*O*-metielkwersitien 7-*O*-*β*-glukopiranosied (**A**), 3,4′-di-*O*-metielkwersitien 7-*O*-*β*-glukopiranosied (**B**), 3-*O*-metielkwersitien 7-*O*-[*β*-D-6″(*E*-*p*-kumaroiel) glukopiranosied] (**C**), 3,4′-di-*O*-metielkwersitien 7-*O*-[*β*-D-6″(*E*-*p*-kumaroiel) glukopiranosied] (**D**), kwersitien 7-*O*-*β*-glukopiranosied (**E**), (*2R, 3R*)-dihidrokwersitien 7-*O*-*β*-glukopiranosied (**F**) and kwersitien 3-*O*-[2-*O*-*β*-zylopiranosiel-6-*O*-*α*-rhamnopiranosiel]-*β*-glukopiranosied (**G**). Vyf van die verbindings het DPPH anti radikaal aktiwiteit. Een van die nuwe verbindings het die hoogste DPPH aktiwiteit gehad. Verbindings **A** en **C** het swak anti malaria aktiwiteit.

Uit die metanolekstrak van *Colophospermum mopane* onvolwasse saad is twee verbindings beskryf. Een was seskwiterpeen *β*-karofileen oksied (**I**) en die ander ‘n diterpenoied (**H**). Die stereochemie van **H** was met KMR spektroskopie, insluitende NOE eksperimente, bepaal. Die diterpenoied het anti- mikrobiale aktiwiteit en is ‘n potente asetielcholienesterase inhibeerder.

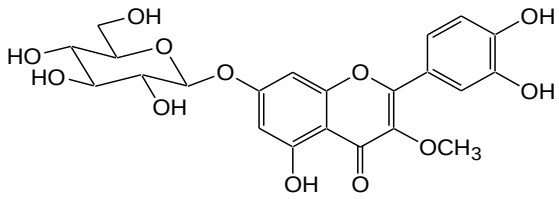

A

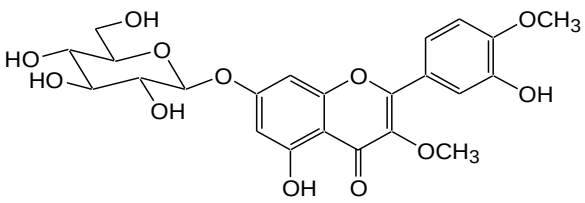

B

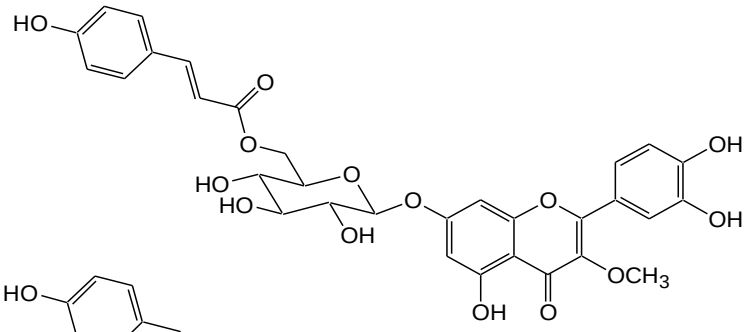

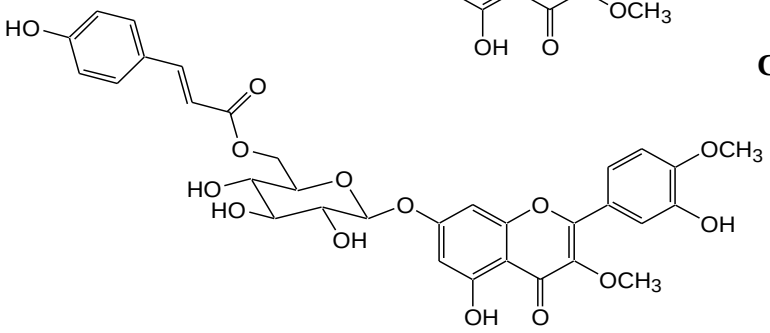

C

D

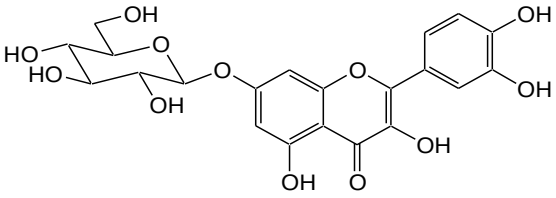

E

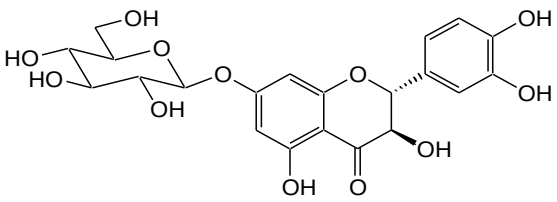

F

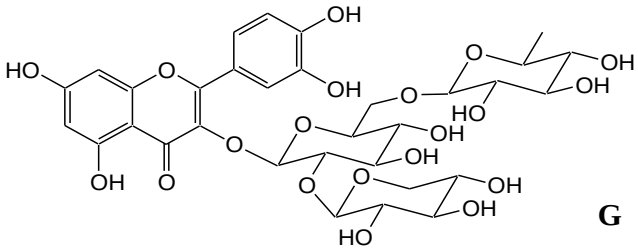

G

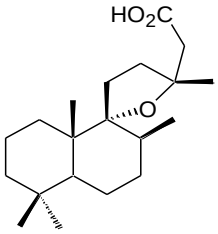

H

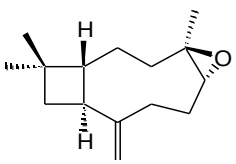

I